UTS UNIVERSITY OF TECHNOLOGY SYDNEY

Digitally Integrated Material Practice: Computational Methods of Engaging Non-Standardised Plantation Hardwood in Architecture

by Peter Charles Booth

Thesis submitted in fulfilment of the requirements for
the degree of

Doctor of Philosophy

under the supervision of

Professor Tim Schork, and
Dr. Mohammed Makki

University of Technology Sydney
Faculty of Design, Architecture and Building

December 2023

CERTIFICATE OF ORIGINAL AUTHORSHIP

I, Peter Charles Booth, declare that this thesis is submitted in fulfilment of the requirements for the award of Doctor of Philosophy, in the Faculty of Design, Architecture and Building at the University of Technology Sydney.

This thesis is wholly my own work unless otherwise referenced or acknowledged. In addition, I certify that all information sources and literature used are indicated in the thesis.

This document has not been submitted for qualifications at any other academic institution.

This research is supported by the Australian Government Research Training Program.

Signature: Production Note: Signature removed prior to publication.

Date: 1st December, 2023

ABSTRACT

As a material-based practice, architecture has an inherent relationship with both material understanding and its application within the built environment; however, this relationship has been truncated by the ubiquity of material elements and workflows introduced in the Industrial Revolution. The built environment's unprecedented growth to meet global demand has resulted in the construction industry becoming a lead contributor to climate change. This has triggered significant international initiatives to explore the use of timber in commercial construction as an alternative to resource-intensive, non-renewable materials.

While considered a highly renewable and carbon-positive resource, typical modes of engagement of timber in construction rely on industrialised processes of standardisation that remove the capacity for material irregularity to be considered as a positive characteristic. Critically, this results in significant volumes of plantation hardwood being disregarded as a viable construction material, due to an incapacity to capture and engage the intrinsically unique and heterogeneous material characteristics.

In this context, the practice-led, applied research of this thesis establishes Digitally Integrated Material Practices (DIMPs) that engage irregular heterogeneous materials within Computational Design Frameworks (CDFs). It investigates opportunities for Australian plantation hardwood, as a potential construction material, by engaging digital modes of material interrogation, computational simulation, optimisation, and design. In doing so, it establishes design-centric workflows that enable the integration of material irregularity and bespoke design outcomes, which utilise latent, renewable materials within construction.

The proposed DIMPs combine open and scalable methods of material capture and discretisation, computational modelling, material and performance-based optimisation, architectural design and timber fabrication. The research explores these methods through a series of investigative Design Probes and Prototypes, finding that bespoke, digitally enabled workflows can facilitate data-rich inventories for material irregularities that can be engaged as 'active' participants within architectural design and fabrication frameworks. These workflows acts as an intermediary between material supply chains and design applications that engage irregular and heterogeneous materials as viable materials of exploration, with the clear aim of reducing the built environment's reliance on non-renewable and unsustainable material practices.

COVID-19 IMPACT STATEMENT

The COVID-19 pandemic impacted nearly all global inhabitants to varying degrees. In the context of my PhD research, its arrival coincided with the final 14 months of my research program, which was intended to be a period of intense experimentation and productivity. Subsequently, the inability to travel, 'rolling lockdowns' and continued working from home requirements impeded the final stages of my research significantly.

While my doctoral study was undertaken at University of Technology Sydney, I am physically based In Tasmania. As an island, Tasmania closed is borders for a twenty-one-month period from March 2020 until December 2021. As I was unable to travel during this period, it was not possible to undertake the originally intended advanced fabrication-based research in Sydney at UTS. As a result, the two major Design Prototypes were reframed to minimise the intended cyber-physical investigations of irregular material engagement, and the experiments focused more centrally on the methods of computational and evolutionary optimisation required for the engagement of irregular materials in more abstract design environments.

The delay in access to fabrication facilities at the University of Tasmania during COVID-19 coincided with the School of Architecture & Design (in which the facilities are located) undergoing major construction works. During this time the pack of sample timber that had-been set aside for my research was relocated to another building, for long-term storage. This material had already been discretised as a part of the Design Probes (detailed in Chapter 3). The computational components of the Design Prototypes (Chapters 4 and 5) proceeded with this constrained inventory of material, as they required a large dataset to achieve evolutionary optimisation; however, the fabrication components were undertaken using a limited secondary supply of sample boards. For this reason, the physical demonstrator components within the experiments required workflow adjustments to utilise replacement materials. Subsequently, these physical artefacts should be considered as proof of workflow, rather than accurate outcomes of full material engagement.

These factors impacted the progress and execution of the initial PhD research scope significantly; yet, the methods and workflows developed within the design experiments proved flexible enough to accommodate these setbacks. They generated successful outcomes that demonstrate the capacity of design-oriented material processes, which employ computational methods of optimisation to utilise a constrained inventory of inherently irregular fibre-managed plantation hardwood.

ACKNOWLEDGEMENTS

First and foremost, I would like to thank Professor Tim Schork for his supervision over the duration of this research. His expertise, advice and guidance were been vital in providing freedom to explore unknown research avenues and opportunities. The ongoing support he provided has been pivotal in shaping me as a researcher and ensured my study had continuing relevance, over such a long period of time.

Similarly, I would like thank Dr. Mohammed Makki for joining my supervisory team halfway through my candidature. His expertise and guidance in re-shaping the experimentation focus was pivotal in defining the computational direction I was able to pursue. His forensic examination of the thesis itself was above and beyond what I had hoped for. Without his support and critical engagement my research would have remained a shadow of what it is today. I'm forever grateful.

Undertaking my research at University of Technology Sydney (UTS), while located at the University of Tasmania (UTAS), allowed me to engage with a range of colleagues and influences who have helped shape aspects of my research. I would therefore like to thank Dave Pigram, Max Maxwell and Tran Dang at UTS for their support, critical engagement, and advice. Similarly, I would like to thank Luke Dineen and Robin Green for their support in the UTAS workshop, and without whom my physical demonstrators would not exist; Georgia Lindsay for being physically in the building and a sound sounding board for all things research and academia-related; Jon Shanks for his friendship, critical engagement and advice on all things timber; Greg Nolan for his advice, support and generous supply of plantation timber for experimentation; and my academic colleagues for providing me with the space to complete my PhD, during the recent turbulent period.

I would also like to thank Richard Hough, Prof. Jennifer Loy, A/Prof. Teresa Vidal-Calleja, Dr. Stefan Lie, Prof. Sidney Newton, Dr. Elif Erdine, Prof. Paul Nicholas, and Prof. Anthony Burke each of whom reviewed my research and provided critical feedback at significant milestones through my candidacy.

Thank you to my parents for the support and love provided throughout my educational journey. Thank you to my in-laws for their support, understanding and child minding through the difficult times.

Thank you to Ari, Otis and Dante who put a smile on my face every time I walk in the door, regardless of how hard or long the day has been.

Finally, and most importantly, I thank Loren. I cannot express my gratitude enough for the love, support, tolerance and endless hours of critique and discussion she has provided over the past six years. Somehow she managed to do this while also bringing our children into the world. For as long as we have known each other at least one of has been undertaking a PhD - I can't wait to see what it is like when there isn't one in our lives. I am eternally grateful for the precious time that she has provided in supporting me and our family through my studies, it is a debt that I can never repay.

GLOSSARY OF ACRONYMS, TERMS AND ABBREVIATIONS

ABARES	Australian Bureau of Agricultural and Resource Economics and Sciences
Anisotropy	A material that exhibits different physical properties when measured along axes in different directions.
CDF	Computational Design Framework
CLT	Cross Laminated Timber
CT	Computer Tomography The process of digitally reconstructing multiple section-based image slices into three dimensional representations of the internal structure of an element.
Constrained Inventory	A limited library or catalogue of available material with which a design problem can be resolved.
Convergence	A scenario in which the fitness criteria are complementary to each other, potentially generating a single optimal solution. This does not represent an increase in fitness; rather, it suggests a decrease in variation of solutions.
CPS	Cyber-Physical System
Crossover	The exchange of genes between two evolutionary solutions.
Crossover Probability	The percentage of solutions in the generation that will be passed to the next generation
Design problem	The algorithmic relationship between 'Fitness Objectives', and 'genes' and their specification in the construction of the 'phenotype'.
DIMP	Digitally Integrated Material Practice
Discretisation	The extraction and extrapolation of data from raw image captures to generate a layered representation of material character for utilisation within computational workflows.
Divergence	A scenario in which the fitness criteria of an evolution simulation are at odds with each other, resulting in no single optimal solution; thus, generating greater variation in the range of solutions.
Engineered Wood Product	A composite material that has processed heterogeneous wood into higher-performing products suitable for the construction industry.
Fibre-managed	A method of forest management that promotes rapid growth of trees, while requiring minimal maintenance.
Fibres	Elongated cellulose cells of timber found in hardwood species.
Fitness Objective	The specified design objectives and goals that an evolutionary simulation will optimise towards, and against which phenotypes are evaluated.

Fitness Value	The empirical performance measure of each generated solution/ phenotype according to the evaluation results of the simulation.
Gene Pool	The unique genes used by the different solutions in the population.
Gene	A single parameter / variable that defines one part of an individual. In Grasshopper3D (the primary digital design environment within this research), and Wallacei (the evolutionary solver utilised in this research), this is represented by a numeric slider.
Generation	A single iteration of the evolutionary algorithm.
Generation Count	The number of generations (iterations) to be run within the evolutionary simulation.
Generation Size	Number of generated solutions/phenotypes within each evolutionary generation.
Genotype	All the genes that define a single solution/phenotype.
Glulam	Glue Laminated Timber
Heterogeneous material	A material comprising non-uniform composition that has differing physical and performance characteristics.
Homogeneous material	A material comprising uniform composition that has consistent physical and performance characteristics.
Hygroscopic	The capacity of a material to absorb moisture from the air.
Individual	A unit generated by the evolutionary simulation, represented by a genotype and a phenotype, that comprises the population.
Irregular/ity	The unpredictable occurrence of heterogenous material characteristics within an individual or group of elements.
LiDAR	Light Detection and Ranging. A laser scanning technique that determines object characteristics by targeting an object or surface with a laser and measuring the time taken for the reflected light to return to the receiver.
Lignin	A class of complex organic polymer found in the tissue of most plants that forms key structural materials.
LVL	Laminated Veneer Lumber
Mass timber	Solid timber construction elements that are composed of layers of wood joined together to form strong panels or beams (see CLT, LVL, Glulam).
MOEA	Multi-Objective Evolutionary Algorithm. A computational optimisation simulation comprising multiple Fitness Objectives that are to be considered and optimised independently from each other within the evolutionary simulation.

Mutation	A change in a gene within a genotype.
Mutation probability	The probability of a gene to mutate within a solution.
Mutation rate	The rate at which each gene will mutate.
Native forest	A forest consisting entirely of indigenous trees and plants.
Optimisation	The increase in fitness of a solution or population towards the 'best' value. In the context of Wallacei (see above), fitness refers to the minimum value.
Pareto front	A solution or solutions that cannot be improved without negatively impacting the rank of another solution.
Phenotype	The formal (numeric or geometric) representation of the solutions. The phenotype is the manifestation of the genotype.
Photogrammetry	A computational process that facilitates the extraction of three-dimensional measurements from a two-dimensional collection of two-dimensional images, allowing the reconstruction of a digital three-dimensional model.
Plantation forest	Intensively managed stand of trees of either native or introduced species, created by the regular placement of seedlings or seeds. Typically established for commercial wood production.
Population	All individuals generated by the evolutionary simulation across all generations.
Pulplog	A log harvested from a plantation or native forest stand that does not meet sawlog quality specifications and is designated to produce pulpwood.
Pseudocode	A description of the steps in an algorithm, using a mix of conventions of programming languages with informal, usually self-explanatory, notation of actions and conditions.
RGB capture	A two-dimensional capture process that records a combination of Red, Green, and Blue light, which is then combined to create a full-colour image. This is the most common method used in digital cameras, and other image capture devices.
RGB-D capture	A three-dimensional imaging method that captures both RGB (Red, Green, Blue) colour information and Depth information to create a three-dimensional representation of an object or scene. The depth information is typically recorded using a depth sensor, such as a time-of-flight or structured light sensor.
Sawlog (high and low quality)	Log used to manufacture sawn timber.; notably, a high-quality sawlog meets specified size and grade specifications. Low-quality sawlogs are those that do not meet high-quality sawlog specifications.

Search space	All the possible solutions that can be explored by the evolutionary algorithm.
Silviculture	The art and science of growing and cultivating forests for production purposes, based on a knowledge of silvics.
Simulation	A complete single algorithmic run of the evolutionary solver.
SOEA	Single-Objective Evolutionary Algorithm. A computational optimisation simulation comprising a single fitness objective.
Solution	A unit generated by the evolutionary simulation, represented by a genotype and a phenotype, that comprises the population.
Timber	Sawn and or processed wood that has been converted into products for use within the Australian construction industry.
Tracheid	A very long, elongated cell of timber found in softwoods species, making up over 90% of the volume of the wood.
Viscous elasticity	The capacity of a material to deform when a force is applied and subsequently return to its original shape when the force is removed, with the extent of deformation known as deflection.
Wood	The structural fibrous material the makes up a tree. Wood is the fibrous, structural material that comprises and supports the growth and stability of a tree, prior to harvesting (cf. timber - see above).

TABLE OF CONTENTS

Certificate of Original Authorship ii
Abstract iv
COVID-19 Impact Statement vi
Acknowledgements viii
Glossary of Acronyms, Terms and Abbreviations x
Table of Contents xvi
List of Figures xxii
List of Tables xxviii

1 INTRODUCTION 1
1.1 Overview 2
1.2 Research Context 3
1.2.1 Material Sustainability 4
1.2.2 Timber in Construction 5
1.2.3 Digitally Integrated Material Practice 6
1.3 Hypothesis 7
1.4 Objectives and Research Questions 8
1.4.1 Research Aims 8
1.4.2 Research Questions 8
1.4.2.1 Primary Research Question 8
1.4.2.2 Secondary Research Questions 8
1.5 Methodology 9
1.5.1 Research Instrument One: Literature Review 10
1.5.2 Instrument Two: Design Experimentation 11
1.5.2.1 Design Probes 11
1.5.2.2 Design Prototypes 12
1.6 Contributions to Knowledge and Research 12
1.6.1 Primary Contribution 13
1.6.2 Secondary Contributions 13
1.7 Thesis Structure 14

2 LITERATURE REVIEW 17
2.1 Introduction 18
2.2 Material Sustainability 21
2.2.1 Environmental Challenges 21
2.2.2 Historic Understanding of Material 23
2.2.3 Standardisation of Architecture 25
2.2.4 The Development of Standardised Materials 27
2.3 Timber as a Construction Medium 30
2.3.1 Timber in Australia 31
2.3.1.1 Plantation Timber 32
2.3.1.2 Plantation Softwood 34
2.3.1.3 Plantation Hardwood 35

2.3.2 Material Properties of Wood . . . 37
2.3.2.1 Anisotropy . . . 38
2.3.2.2 Viscous Elasticity . . . 39
2.3.2.3 Hygroscopicity . . . 39
2.3.3 Timber as a Heterogeneous Material . . . 40
2.3.4 Understanding Timber Heterogeneity . . . 41
2.3.4.1 Feature Typologies . . . 42
2.3.4.1.1 Warp . . . 42
2.3.4.1.2 Wane and Want . . . 43
2.3.4.1.3 Checks and Splits . . . 43
2.3.4.1.4 Knots, Clusters and Groups . . . 43
2.3.4.1.5 Structural Grade Classification . . . 45
2.3.5 Applications . . . 46
2.4 Digitally Integrated Material Practice . . . 48
2.4.1 The Digital Turn in Architecture . . . 48
2.4.2 Computational Materiality . . . 51
2.4.2.1 Cyber-Physical Approaches to Engagement . . . 52
2.4.2.2 Capturing Material Irregularity . . . 56
2.4.2.2.1 RGB-D . . . 56
2.4.2.2.2 LiDAR . . . 58
2.4.2.2.3 Computer Tomography . . . 60
2.4.3 Constrained Material Inventories . . . 61
2.4.4 Computational Optimisation . . . 66
2.5 Discussion . . . 69

3 DESIGN PROBES . . . 73
3.1 Introduction and Chapter Structure . . . 74
3.1.1 Timber Orientation . . . 76
3.2 Probe 1: RGB-D Scanning . . . 77
3.2.1 Introduction . . . 77
3.2.2 Probe Context . . . 77
3.2.3 Probe Workflow . . . 77
3.2.4 Summary . . . 80
3.3 Probe 2: RGB and Constrained Inventories . . . 82
3.3.1 Introduction . . . 82
3.3.2 Probe Context . . . 82
3.3.3 Probe Workflow . . . 85
3.3.3.1 Multi-face Image Capture . . . 85
3.3.3.2 Feature Detection . . . 86
3.3.4 Summary . . . 88
3.4 Probe 3: Architectural Panel . . . 89
3.4.1 Introduction . . . 89
3.4.2 Probe Context . . . 90

3.4.2.1 Acoustic Absorption 91
3.4.2.2 Acoustic Diffusion 93
3.4.3 Probe Workflow 94
3.4.3.1 Design Strategy 94
3.4.3.2 Material Supply 95
3.4.3.3 Panel Lamination 95
3.4.3.4 Design Workflow 97
3.4.3.4.1 Material Capture 98
3.4.3.4.2 Acoustic Absorption Design 99
3.4.3.4.3 Acoustic Diffusion Design 100
3.4.3.4.4 Fabrication 101
3.4.4 Summary 104
3.5 Probe 4: Evolutionary Optimisation 106
3.5.1 Introduction. 106
3.5.2 Probe Context 106
3.5.3 Probe Workflow 108
3.5.3.1 Virtual Material 108
3.5.3.2 Panel Specification 109
3.5.3.3 Evolutionary Optimisation 110
3.5.4 Summary 113
3.6 Discussion. 115

4 DESIGN PROTOTYPE 1: ACOUSTI-SIM 119
4.1 Introduction 120
4.2 Prototype Context 120
4.3 Experiment Setup 122
4.3.1 Stage 1: Acoustic Simulation and Performance Determination 123
4.3.1.1 Acoustic Simulation of Existing Conditions 124
4.3.1.2 Acoustic Measurements 124
4.3.1.3 Acoustic Simulation Parameters 126
4.3.1.4 Evolutionary Approach to Acoustic Intervention Typology. 129
4.3.1.4.1 Room Panelisation 130
4.3.1.4.2 Acoustic Material Properties Specification. 132
4.3.1.4.3 MOEA Fitness Objectives 133
4.3.1.4.4 MOEA Iteration Configuration 133
4.3.1.5 Hybridisation of Fittest Solutions 136
4.3.1.6 Results. 142
4.3.2 Stage 2: Material Discretisation 145
4.3.2.1 Material Discretisation 145
4.3.2.2 Results. 148
4.3.3 Stage 3: Material Distribution. 148
4.3.3.1 Selection of Subject Panels 149
4.3.3.2 MOEA Approach to Material Distribution 152

4.3.3.3 MOEA Fitness Objectives and Genes 153
4.3.3.4 Results 157
4.3.4 Stage 4: Augmentation Design 159
4.3.4.1 Multi-Performance Augmentation Generation 160
4.3.4.2 Acoustic Performance and Augmentation Correlation 165
4.3.4.3 Results 169
4.3.5 Stage 5: Physical Demonstrator 170
4.3.5.1 Material Discretisation, Distribution, and Panel Lamination 171
4.3.5.2 Augmentation Adaptation 173
4.3.5.3 Fabrication Process 175
4.3.5.4 Results 178
4.4 Discussion 187

5 DESIGN PROTOTYPE TWO: MAT-TRUSS 191
5.1 Introduction 192
5.2 Prototype Context 193
5.3 Experiment Setup 196
5.3.1 Stage 1: Material Discretisation 199
5.3.1.1 Subdivision Scale 200
5.3.1.2 Segmentation 201
5.3.1.3 Inventory Dataset Extrapolation 201
5.3.1.3.1 Board Character Classification 201
5.3.1.3.2 Correlation of Feature Significance and Buffer . . 203
5.3.1.3.3 Identification of Physical Connection Zones 204
5.3.1.4 Results 205
5.3.2 Stage 2: Multi-Objective Evolutionary Algorithm 205
5.3.2.1 Iteration of Potential Board Connection Points 206
5.3.2.1.1 Point A Determination 208
5.3.2.1.2 Point B Determination 209
5.3.2.2 Generating a Truss 211
5.3.2.2.1 Inventory Selection 212
5.3.2.2.2 Truss Top Chord 214
5.3.2.2.3 Truss Web Segments 215
5.3.2.2.4 Truss Bottom Cord 217
5.3.2.2.5 Geometry Transfer 219
5.3.2.3 Structural Simulation: Finite Element Analysis 221
5.3.2.3.1 Simulation Parameters 222
5.3.2.3.2 Material Specification 224
5.3.2.3.3 Truss Displacement 226
5.3.2.3.4 Elemental Analysis of Axial Stress 226
5.3.2.3.5 Features Distribution in Compression Elements 227
5.3.2.4 Results 227
5.3.3 Stage 3: Selection of Fittest Solution 235

5.3.3.1 Boundary and Duplicate Solutions 235
5.3.3.2 Displacement Threshold 238
5.3.3.3 Span Differential 238
5.3.3.4 Bottom Chord Differential 239
5.3.3.5 Board Character Matching 240
5.3.3.6 Material Features in Compression Zones 243
5.3.3.7 Subjective Assessment and Results 244
5.3.4 Stage 4: Material Recovery and Inventory Consolidation 245
5.3.4.1 Offcut Generation 246
5.3.4.2 Results 248
5.3.5 Stage 5: Physical Demonstrator 250
5.3.5.1 Truss Detailing 251
5.3.5.2 Fabrication Process 254
5.3.5.3 Results 258
5.4 Discussion 260

6 CONCLUSION 265
6.1 Introduction 266
6.2 Restatement of Research Aims 266
6.3 Answering the Research Questions 267
6.4 Restatement of Contributions 273
6.4.1 Primary Contribution 273
6.4.2 Secondary Contributions 274
6.5 Limitations and Future Perspectives 276
6.5.1 Plantation Hardwood Resources 276
6.5.2 Scalability of Probes and Prototypes 276
6.5.3 Notions of Material and System Performance 277
6.6 Concluding Remarks 278

7 REFERENCES 279

LIST OF FIGURES

Figure 1.1 Fields of research 4

Figure 1.2 Iterative Praxis-Exegesis research model (adapted from Marshall, 2010; Swann, 2002) 10

Figure 2.1 Literature review map illustrating intersections between the fields of material sustainability, timber in construction and digitally integrated material practice 19

Figure 2.2 Identification of sections of curved wood within tree branch segments required for specific components of traditional timber ship building (From 'Encyclopédie Méthodique: Plate 103', 1797. In the public domain). 24

Figure 2.3 Energy consumption of major construction materials in Australia (From Tasmanian Timber, 2019. Copyright 2019 Tasmanian Timber. Reproduced with permission). 30

Figure 2.4 Fossil fuel consumption in the production process of major construction materials in Australia (From Tasmanian Timber, 2019. Copyright 2019 Tasmanian Timber. Reproduced with permission). 31

Figure 2.5 Atmospheric carbon credentials of major building materials in Australia (From Tasmanian Timber, 2019. Copyright 2019 Tasmanian Timber. Reproduced with permission). 31

Figure 2.6 Australian plantation inventory regions 2019-20 (From Legg et al., 2021 CC BY 4.0). . 33

Figure 2.7 Hardwood and softwood plantations by state (From Legg et al., 2021 CC BY 4.0). . . . 33

Figure 2.8 Australian plantation log availability forecast (From Legg et al., 2021 CC BY 4.0). 33

Figure 2.9 Irregular features on sample *E. nitens* sawn boards 36

Figure 2.10 Cellular structure of hardwood (left) and softwood (right) (From Walker et al., 1993. Copyright 1993. Taylor & Francis Informa UK Ltd - Books. Reproduced with permission). 37

Figure 2.11 The three primary axes of wood in relation to tree formation 38

Figure 2.12 Warp based timber feature typologies: Cup (a), Bow (b), Spring (c), and Twist (d). . . . 44

Figure 2.13 Wane and want feature typologies. 44

Figure 2.14 Checks and splits in timber boards. 44

Figure 2.15 Knot based features in timber boards. 45

Figure 2.16 Knot cluster (a) and grouping (b) typologies. 45

Figure 2.17 Forest to Fabricator workflow indicating the three industry silos. 47

Figure 2.18 Landesgartenschau Exhibition Hall (From Schwinn & Menges, 2015, Copyright 2015 John Wiley & Sons - Books. Reproduced with permission). 53

Figure 2.19 The Sequential Roof (From Apolinarska et al., 2016. Copyright 2016 Taylor & Francis Informa UK Ltd - Books. Reproduced with permission) 54

Figure 2.20 Robotic Pavilion: House 4178 (From Eversmann, 2017. Copyright 2017 Springer. Reproduced with permission). 55

Figure 2.21 Adaptive robotic wood carving with material force feedback (From Brugnaro & Hanna, 2018. Copyright 2018 Springer. Reproduced with permission). 55

Figure 2.22 The Woodchip Barn tree fork discretisation and design distribution (From Self, 2017. Copyright 2016 Taylor & Francis Informa UK Ltd - Books. Reproduced with permission) 57

Figure 2.23 RGB-D assisted material capture and robotic placement (From Wu & Kilian, 2018. Copyright 2018 Springer. Reproduced with permission) 58

Figure 2.24 LiDAR scan of open forest canopy distinguishing between woody (red) and non-woody (blue) tree materials (From Newnham et al., 2015. CC-BY-4.0, Reproduced with permission) 59

Figure 2.25 LiDAR scanning for fabrication precision of complex mass timber elements (From Svilans et al., 2020. CC-BY-4.0, Reproduced with permission) 59

Figure 2.26 Umeå 01 (RawLam 3): Allocation of timber boards within bespoke structural glulam beams (From Svilans, 2021b. Copyright 2021 CITA. Reproduced with permission) . . . 61
Figure 2.27 Reuse of steel elements from electrical pylons within a new roof structure using the Phoenix plugin (From Brütting, Desruelle, et al., 2019. CC-BY-NC-ND-4.0, Reproduced with permission) . . . 64
Figure 2.28 Suspended remnants – allocation of timber elements to closest matching structural location (From Baber et al., 2020. Copyright 2020 Springer Nature. Reproduced with permission) . . . 65
Figure 2.29 Hypothetical design problem with conflicting objectives . . . 66
Figure 3.1 Design Probe field of inquiry: Material understating, Material optimisation, and Material fabrication domains; and Method development and Design integration Typologies. . . . 75
Figure 3.2 Board orientation axes within Cartesian coordinate system . . . 77
Figure 3.3 *E. globulus* sample boards (Tasmanian Blue Gum) used for testing . . . 79
Figure 3.4 Knots in timber boards. Live (left) and dead (right) . . . 79
Figure 3.5 Long range (left) and short range (right) RGB-D experiment setup. . . . 80
Figure 3.6 Knot identification and board sorting workflows. . . . 80
Figure 3.7 RGB-D raw data captured from timber board, displayed as coloured voxels (left) and with dead knot detection enabled (right) . . . 81
Figure 3.8 Post-capture RGB-D data processing. Dead knot isolation (left) and usable length output in green (right) . . . 81
Figure 3.9 Whole timber board post-capture RGB-D data processing . . . 81
Figure 3.10 Grouping of five timber boards for image high resolution RGB capture . . . 86
Figure 3.11 Examples of wane (top) and spring (bottom, top left corner) features in *E. nitens* sawn boards.. . . . 88
Figure 3.12 Initial feature detection of *E. nitens* boards. RGB image capture (top), Bradley threshold filter applied (middle), and curve geometry of detected features (bottom). 88
Figure 3.13 Overlay of detected features (top) from board front (red) and rear (green). Consolidated features (bottom).. . . . 88
Figure 3.14 Natural timber features: (clockwise from top left) dead knot and colour variation; live knot; grain variation; surface checking . . . 96
Figure 3.15 End grain of timber boards arranged to oppose the natural cupping force. . . . 97
Figure 3.16 Demonstration panel lamination process for Probe 3 . . . 98
Figure 3.17 The Probe 3 demonstration panel (900x2200x35mm) . . . 98
Figure 3.18 Panel feature detection . . . 99
Figure 3.19 Simplification of feature geometry . . . 100
Figure 3.20 Weighted perforations in panel based on half-tone image processing . . . 101
Figure 3.21 Surface deformation for acoustic diffusion . . . 102
Figure 3.22 Fabrication simulation – roughing process . . . 104
Figure 3.23 Fabrication simulation - parallel finishing process . . . 104
Figure 3.24 Hybrid acoustic panel physical demonstrator . . . 105
Figure 3.25 Sample of generated virtual boards . . . 109
Figure 3.26 Wall panel specification indicating structural zones (green) and openings (blue) . . . 110
Figure 3.27 Random distribution of virtual boards overlaid across a wall panel . . . 110
Figure 3.28 Probe 4: Evolutionary workflow pseudocode . . . 112

Figure 3.29 Statistical representation of the fitness values generated by the simulation. 113
Figure 3.30 Probe 4 pareto front solution {87;0} 114
Figure 4.1 Design Prototype 1: Acousti-SIM workflow division of into five stages 123
Figure 4.2 Test room used for acoustic simulation. 124
Figure 4.3 Acoustic simulation setup of virtual room. Single point source (shown as red), single receiver location (shown as blue), and primary acoustic reflection rays 129
Figure 4.4 Acoustic treatment determination: Evolutionary simulation pseudocode 131
Figure 4.5 Test room wall and ceiling subdivision 132
Figure 4.6 Panel subdivision into timber segments 132
Figure 4.7 Parallel coordinate plot of fitness values of each solution 136
Figure 4.8 Statistical analysis of each Fitness Objective 138
Figure 4.9 K-means clustering of 45 Pareto solutions – geometric acoustic panel variations. . . 140
Figure 4.10 Hybridisation of Pareto front solutions into a single panel 142
Figure 4.11 Hybridisation of 91 Pareto solutions represented as geometric room panels 144
Figure 4.12 Board subdivision with discretised features shown in brown. 147
Figure 4.13 Discretisation of timber boards at 5mm resolution 149
Figure 4.14 Nine panels selected for experimentation 151
Figure 4.15 Acoustic material distribution: Evolutionary simulation pseudocode 153
Figure 4.16 Material distribution of timber segments across 9 panels 157
Figure 4.17 Statistical analysis of evolutionary solutions 158
Figure 4.18 Augmentation design workflow 161
Figure 4.19 FlowL vector field methods. (L to R) Equipotentiality, streamline, and vortex 163
Figure 4.20 Parameter input requirements of the FlowL plugin within Grasshopper 164
Figure 4.21 3D Curve generation from vector field influence 164
Figure 4.22 Intersection detail between detected material feature (red) and generated field geometry 165
Figure 4.23 A range of CNC cutter head profiles. 167
Figure 4.24 Impact of ball-end cutting tool at varying depths 168
Figure 4.25 19mm round nose, double flute cuter head with a 32.5mm cut depth 168
Figure 4.26 Curve distribution generated for augmentation of Panel 87 169
Figure 4.27 Demonstrator Panel (2300x1080mm) 173
Figure 4.28 Feature detection of demonstrator panel. 174
Figure 4.29 Augmentation field origin points 174
Figure 4.30 Vector field augmentation curve generation 175
Figure 4.31 Panel positioned in the CD zone of the CNC router. 177
Figure 4.32 Machining process simulation generated by VisualCAD/CAM 178
Figure 4.33 Top view of fabricated demonstration panel 180
Figure 4.34 Perspective view of fabricated demonstration panel 182
Figure 4.35 Detail of demonstration panel, showing augmentation and perforation of surface . 184
Figure 4.36 Detail of demonstration panel, showing surface augmentation and material tear-out 186
Figure 5.1 Design constraints for floor truss generation. 198

Figure 5.2 Division of experiment workflow into five stages 199
Figure 5.3 Detected features (black outline) with subsequent discretisation (dark brown) employing a 30mm resolution 201
Figure 5.4 Discretisation of boards 53 (top) and 68 (bottom), representing the lowest and highest featured areas 203
Figure 5.5 Extent of non-connection buffer zone around features of different dimension in the X-axis of a sample board 205
Figure 5.6 Geometrically establishing zones of potential connection 205
Figure 5.7 Truss generation: Evolutionary simulation pseudo code 207
Figure 5.8 Iterations of connection point location and impact on geometry 209
Figure 5.9 Iterative location of connection Point A as demonstrated on Board 60 209
Figure 5.10 Relocation of connection point A when initially within board end threshold zone . . 210
Figure 5.11 Selection of boards from the constrained inventory demonstrating a range of varying connection zone scenarios 210
Figure 5.12 Positioning of connection Point B as demonstrated on Board 60 212
Figure 5.13 Truss generation logic 215
Figure 5.14 Top chord of truss (solution 122;68) 216
Figure 5.15 Web segment intersection arcs & point/element generation (solution 122;68) 217
Figure 5.16 Bottom chord segmentation (solution 122;68) 218
Figure 5.17 Highest rank bottom chord differential (FO.3) in comparison with other objectives. 221
Figure 5.18 Geometric representation of truss solution 122;68 transferred to MOEA structural simulation, simple (above), and complex (below) 221
Figure 5.19 Structural simulation loading conditions 224
Figure 5.20 Material parameter specification within the Karamba3D simulation environment . 226
Figure 5.21 Displacement of truss solution 122;68. Colour intensity represents amount of displacement on the Z-axis 227
Figure 5.22 Internal axial stress of each segment within truss solution 122;68 228
Figure 5.23 Location of material features within truss segments demonstrating compression-based axial loading within truss solution 122;68. Circles indicate areas within compression segments that should be free of material feature. 228
Figure 5.24 Parallel coordinate plot of valid solutions, categorised by Fitness Objective on the X-axis 231
Figure 5.25 K-means clustering of Pareto solutions into nine groups 231
Figure 5.26 Statistical analysis of each Fitness Objective 232
Figure 5.27 Five Evolutionary Objectives, ranked by fittest solution 234
Figure 5.28 Selection filter interrogation workflow 236
Figure 5.29 Truss displacement fitness value plot FO1: 237
Figure 5.30 Truss displacement fitness value plot with two invalid solutions culled 237
Figure 5.31 FO1: Truss displacement fitness value plot with 200 invalid solutions culled 238
Figure 5.32 Parallel coordinate plot of 11,050 valid evolutionary solutions 238
Figure 5.33 Solutions remaining after displacement filter 240
Figure 5.34 Solutions remaining after span differential filtering 240
Figure 5.35 Solutions remaining after bottom chord differential assessment 241
Figure 5.36 Solutions remaining after material character match assessment 241

Figure 5.37 Geometric manifestation of 29 solutions remaining after implementation of five levels of selection filtering 242
Figure 5.38 Geometric representation of truss solutions 122;68 (above) and 133;02 (below) . . . 244
Figure 5.39 Solutions remaining after assessment of features within compression sensitive truss segments 245
Figure 5.40 Geometric representation of truss solution 122;68 to be considered for material recovery and fabrication 246
Figure 5.41 Overlay of connection points and board utilisation within truss solution 122;68 . . . 248
Figure 5.42 Geometric representation of truss 2 solution 133;51, geometric representation (top), and board representation (bottom) 250
Figure 5.43 Staggering of truss web diagonals to minimise thickness. Blue elements are on front face of top and bottom chords, red elements are positioned at the rear 254
Figure 5.44 Assembly logic of top chord intersection with web truss diagonals 254
Figure 5.45 Drilling 12mm clearance holes for M10 blot fixing 257
Figure 5.46 Docking of board to required length at specified angle 258
Figure 5.47 Rebating connection shoulder at each end of board 258
Figure 5.48 Demonstration of shoulder cut stages 259
Figure 5.49 Pneumatic clamp arrangement in place for fabrication 259
Figure 5.50 Alternate fixing method at intersection nodes 260
Figure 5.51 Truss layout during assembly process 261
Figure 5.52 Physical demonstrator of truss fabrication 264
Figure 5.53 Physical workflow demonstrator overlaid with digital truss representation 264

LIST OF TABLES

Table 3.1 Sample of live and dead knot location dataset. 81
Table 3.2 Survey of commonly available perforated panel products in Australia 92
Table 3.3 Probe 4: Gene pool specification 111
Table 3.4 Probe 4: Evolution algorithm parameters 111
Table 4.1 Speech Transmission Index (STI) classifications 126
Table 4.2 Test room panelisation dimensions 131
Table 4.3 Absorption coefficient of material types over frequency range (% energy absorbed) 132
Table 4.4 Diffusion coefficient of material types over frequency range (% non-specular reflected energy) 132
Table 4.5 Acoustic treatment determination: Evolutionary algorithm parameters 134
Table 4.6 Acoustic treatment determination: Gene pool specification 134
Table 4.7 K-means clustering of 45 Pareto solutions – geometric acoustic panel variations . . 136
Table 4.8 Comparison of STI and T60 results from acoustic simulation 142
Table 4.9 Subdivision resolution and feature classifications (board_ID_20) 147
Table 4.10 Acoustic Fitness Objectives 151
Table 4.11 Hybrid performance targets 151
Table 4.12 Acoustic Material distribution: Chromosome specification 153
Table 4.13 Acoustic Material distribution: Evolutionary algorithm parameters 155
Table 4.14 Impact of generation relationship size on optimisation fitness and calculation time 155
Table 4.15 Material distribution results 156
Table 4.16 Augmentation geometry depth classification 175
Table 4.17 Fabrication times of the physical demonstrator 177
Table 5.1 Truss generation: Genotype specification 207
Table 5.2 Truss generation: Evolutionary algorithm parameters 207
Table 5.3 Top chord board selection (solution 122;68) 215
Table 5.4 Truss diagonal web segments board selection (solution 122;68) 216
Table 5.5 Correlation of iterated bottom chord segments and ordered inventory (solution 122;68) 218
Table 5.6 Results of search matching segment length with remaining inventory elements (solution 122;68) 219
Table 5.7 Inventory items for truss solution 122;68 221
Table 5.8 Material parameters required by Karamba3D 224
Table 5.9 MOEA Fitness Objective results 228
Table 5.10 Fitness objective values of remaining truss iterations 244

Unless specifically credited otherwise, all photographs, tables, graphics and figures are by the author.

1 INTRODUCTION

1.1 Overview

The construction industry typically uses standardised materials and products in the assembly of architectural space (Ramsgaard Thomsen et al., 2019). These elements are readily available, easy to work with and easily adaptable to different building types and scenarios. They are produced in large quantities through known manufacturing processes and present a cost-effective option for the construction industry; however, the ubiquity of standardised elements, materials, and systems has resulted in an increase in application of generic detail solutions and material specification within architectural design. This creates a misalignment between architectural intent and material realisation, which limits the capacity for architects to explore the full ambition of their designs, from both sustainability and performance-based perspectives.

Perhaps more importantly, the reliance on standardised solutions in architecture and design has given rise to a preference in the construction industry for materials that present regular characteristics, both from a performance and aesthetic point of view. In utilising standardised solutions, architecture is (by proxy) reliant on materials that are heavily manufactured and contain significant embodied energy (Amtsberg et al., 2022). This poses a significant problem, with many countries striving for net zero emissions by 2050, those in the construction industry must examine current practices and shift to a more sustainable method of operating. As one of the heaviest polluters in terms of emissions, the construction industry cannot continue to engage with the materials, systems and processes it has relied on during the 20th century, if it is to meet its global sustainability obligations (as urged by the UN Sustainable Development Goals) (United Nations, 2015) and The Paris Agreement (United Nations Framework Convention on Climate Change, 2016).

The 21st century has seen the beginning of a shift in architectural practices that demonstrates a preference for the bespoke rather than the standardised solutions prevalent in the 20th century (Beorkrem, 2017; Kolarevic, 2003a; Kolarevic & Klinger, 2008). This shift is being fostered by the adoption of computational methods of design, *simulation* and fabrication within architectural practice (Iwamoto, 2009; Jenny et al., 2022; Sheil et al., 2020); however, the synergy between innovative modes of computational design and digital fabrication is yet to result in a widespread rethink regarding material usage. The base materials of bespoke architectural solutions are still reliant on the same manufacturing processes that result in standardised, *homogeneous* base materials.

The increasing value of bespoke architectural solutions presents an opportunity to explore design and fabrication methods that reset

material expectations from a manufacturing perspective. The potential for integration between innovative performance-orientated material engagement and fabrication processes, coupled with materials that are overlooked or unavailable to the construction industry, affords consideration of a wider range of material potentials. Irregular and under-utilised materials become a viable option for architectural investigation through the extension of these innovative workflows.

The findings of this research specifically consider the engagement of *fibre-managed* plantation hardwood as a plentiful resource of under-valued timber that currently has little uptake by the construction industry. The consideration of *fibre-managed* plantation hardwood within construction is coupled with the adoption of sustainable and responsible material methods that address wider contextual sustainability issues across the industry.

This Chapter is divided into seven sections. This first section is the overview. The second declares the hypothesis for the research. The third describes the research's context and places it within fields of investigation. The fourth specifies the research objectives and states the questions this study pursues. The fifth establishes the employed research methodology. The sixth provides an overview of the main contributions and significance of the research. The final section describes the structure of the research and details the experimental design investigations undertaken as a part of the study.

1.2 Research Context

This study is a practice-led investigation primarily situated in the field of architectural design within the construction industry. It aims to increase sustainable material practices by focusing on Australian plantation hardwood as a potentially viable material for tailor-made design outcomes. In doing so, it challenges the means in which architecture and construction considers *irregularity* within heterogeneous materials, shifting away from highly engineered, manufactured, and standardised elements that are the established industry norms. It does this by developing integrated computational approaches to material discretisation, material optimisation and tailor-made design outcomes that place inherent material irregularities centrally within the workflow. Therefore, within the broad field of architectural design, this study is concerned with Material

Sustainability, Timber as a Construction Medium, and Digitally Integrated Material Practice (DIMP), and where they overlap, as shown in Figure 1.1.

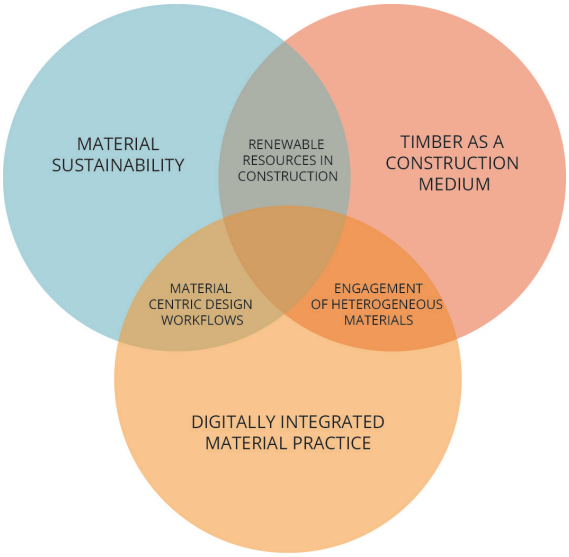

Figure 1.1 Fields of research

1.2.1 Material Sustainability

In industrialised countries, construction and the built environment is responsible for approximately 40% of material consumption, 39% of energy consumption, and 40% of all waste (Ness & Xing, 2017; Shooshtarian et al., 2022; United Nations: Environment Program, 2022). In the context of the projected urbanised population growth of 1.75 billion people over the next 25 years (United Nations: Department of Economic and Social Affairs, 2022), the demand on resources required to accommodate this growth within the built environment is unparalleled in human history. Without significant and immediate large-scale interventions across the construction industries, the traditionally materially-intense paradigms will reach a breaking point, resulting in irreversible damage to Earth's ecosystems.

The interventions required will see a significant shift in both the manner in which we build and what we build with. While it is unlikely that material consumption will reduce given that the global population is expanding, the availability of contemporary materials within the industry will eventually become scarce, fostering a shift towards renewable materials that have a higher level of sustainability. Subsequently, a re-evaluation of the materiality and design workflows within of the built environment

is necessary to ensure that the industry rapidly adopts more sustainable modes of materialisation and construction.

1.2.2 Timber in Construction

Globally, the use of timber as a construction material is rapidly expanding. Kreig et al. (2016) note timber is a highly renewable resource, has a positive carbon footprint and extremely low embodied energy, is fully recyclable and biodegradable, demonstrates exceptional structural strength in relation to its weight, and is widely available throughout the world. As a naturally occurring, heterogeneous material, trees (timber) adapt to local environmental constraints and opportunities during their growth. Consequently, the construction grade material extracted from forests is highly irregular and variable, even when sourced from plantation environments, when compared with other construction materials, such as steel or concrete.

The use of timber in the built environment within developed countries relies on predominantly softwood *plantation forests* and requires significant industrialised processes of standardisation to ensure the material suitable for construction. These processes standardise the irregular, naturally occurring heterogeneous character of timber into a consistent and predictable homogeneous medium that can more easily be employed within construction. However, as global warming increases, many of the plantation forests that historically produced softwood timber will no longer be viable, with productive regions being limited to areas of higher altitudes and cooler average temperatures (Krieg et al., 2016). This will have a greater impact of softwood forests, as hardwood species demonstrates a higher tolerance to warmer conditions (T. H. Booth, 2013).

This is significant in Australia as approximately 60% of plantation resources are softwood species (Australian Bureau of Agricultural and Resource Economics and Sciences, 2022a) and are currently grown in cooler to temperate climate zones (Bureau of Meteorology, 2001). This represents a potential under supply of construction grade timber from softwood plantation resources that correlates with global warming.

The end use of timber products in Australia is dominated by sawn timber boards, which account for approximately 65% of forest consumption (ABARES, 2022), with the remaining 35% being utilised within pulp, chip and veneer based products. The construction industry accounts for consumption of 83% of all sawn timber, with 89% being used in residential construction and 11% being used in commercial application (ABARES, 2022; Nolan et al., 2005; Ximenes & Gardner, 2005). The demand for sawn timber boards within Australia is intrinsically linked to the construction of the built

environment and will continue to grow due to population growth. However, as the viability of softwood plantations diminishes due to global warming (Krieg et al., 2016), the industry must consider the potential of currently disregarded fibre-managed plantation hardwood as a viable construction material. To realise the potential of this resource as a construction material the building/architectural industry needs to reconsider how it engages with timber across the supply and design chains.

1.2.3 Digitally Integrated Material Practice

Architecture is fundamentally a material practice (Kolarevic & Klinger, 2008) and primarily concerned with the creation of spatial environments through the precise manipulation of material objects. While the choice of materials available today is extensive, the construction industry relies heavily on standardised materials that are graded, engineered, and manufactured to known physical and performance standards (Stanton, 2010), as has been the case for much of the 20th and 21st centuries. Despite the ongoing technological advances, the construction sector has favoured materials that are cheaper and faster to work with, overlooking the potential and unique properties that natural and raw materials exhibit, disregarding them as suitable media for construction (Vasey & Menges, 2020). However, this preference for standardised materials has led to stagnation in architectural innovation, limiting the industry's capacity to envisage new material processes in design and construction (Sheil & Ramsgaard Thomsen, 2020).

The privileging of standardisation within architecture and construction has reduced materiality to a set of technical and aesthetic variables that are typically subservient to form (Thomas, 2007), an ideology that will continue to increase the construction industries impact on climate change due to the heavily industrialised modes of material extraction and manufacturing. For this scenario to be reversed, the material applications and design workflows that currently exist must shift, to place modes of sustainable material engagement at the core of architectural ideation.

Achim Menges (2008) postulates that computational material systems that foster a deep understanding of material potentialities should be populated throughout the architectural design cycle, thereby acting as "generative drivers" (Menges, 2008, p. 196) of the design process, rather than by products of standardised building systems and elements. This challenges the traditional linearity within architectural design cycles, promoting an overlap between design intent, material heterogeneity, performance, simulation and optimisation, fabrication, and construction (Ramsgaard

Thomsen et al., 2021), which would allow an interplay of parameters throughout the design process.

The cultural change brought about by the implementation of complex computational modes of material engagement within the construction industry will bring about new understandings of materiality, performance, and knowledge-sharing between the currently siloed disciplines. A Digitally Integrated Material Practice (DIMP) that adopts the data-driven principles and technologies of Industry 4.0 (Karmakar & Delhi, 2021; King, 2017; Sawhney et al., 2020), can engender a greater level of material engagement within the design cycle, promoting an iterative understanding of the intersections between materialisation, communication, simulation, and fabrication.

A DIMP promotes the consideration of digitally-rich materiality to be integrated across scales and disciplines within the construction industry. As such, it increases the efficiency of engaging irregularity and material complexity within the design and fabrication cycle, providing opportunities for the reduction of non-renewable material consumption and carbon footprint of the construction industry.

1.3 Hypothesis

Heterogeneous materials of irregular characteristics and performance capacities present significant complexities and challenges when considered within common, current design methodologies. This highlights the need to enable a materially aware, digitally augmented material practice that addresses the environmental and material resource challenges that the global construction industry currently faces. A DIMP extends traditional perceptions of the architectural design space to encompass methods of material understanding, engagement of irregularity within design workflows, and adaptive fabrication processes. These methods enact integrated computational workflows that adopt tailored outcomes that engage materials that are considered low-value, which would otherwise be disregarded within the construction industry.

In this context, this research hypothesises that material irregularity (as present in fibre-managed hardwood timber plantations) can be interrogated within performance-based Computational Design Frameworks (CDFs) to maximise material utilisation, and thus has potential to reduce the

construction industry's environmental impact through the increased adoption of sustainable practices and renewable material alternatives.

1.4 Objectives and Research Questions

1.4.1 Research Aims

This research aims to establish methods of engagement that employ irregular *heterogeneous materials* within an architecturally focused CDF. It considers the capacity of fibre-managed Australian plantation hardwood as a potential construction material through coupling digital modes of material interrogation and computational simulation, optimisation and design. This establishes innovative scenarios to exploit the indeterminate qualities of low-grade, naturally occurring irregular materials;. This subsequently shifts the onus of material understanding away from primary producers and incorporates it within a design focused environment, encouraging a closer engagement with material character. This integration provides opportunities for irregular materials to become active participants within architectural design and fabrication processes, generating greater material sustainability within the construction industry.

1.4.2 Research Questions

1.4.2.1 Primary Research Question

This research is focused on two primary fields:

- the utilisation of heterogeneous materials of irregular character within architecture (sustainable material practice); and
- the application of innovative computational workflows to engage indeterminacies as integral design agents (DIMP).

Accordingly, each chapter addresses the first, and key, Research Question:

1. **To what extent does the intersection of material irregularity and digitally integrated design workflows establish a platform for the engagement of low-value materials within architecture?**

1.4.2.2 Secondary Research Questions

Secondary to the above, specific questions are structured to address the domains of *material sustainability* and *digitally integrated material practices*. In the domain of *material sustainability,* pertaining to modes of material engagement and digital representation that seek to extend

our understanding of heterogeneous materials at differing scales, the following two questions are posed:

2. **How far can the current paradigms within architectural design and fabrication converge to extend beyond the use of standardised materials?**
3. **To what extent can Australian fibre-managed plantation hardwood be exploited within innovative architectural design environments?**

In the domain of *digitally integrated material practice*, in which heterogeneous materials within architectural design and fabrication are utilised (specifically with the intent to increase the capacity for innovative design outcomes and material integration) digital and physical realms of production, a fourth and final question is posed:

4. **What mechanisms within computational design frameworks can mediate material irregularity and notions of precision?**

1.5 Methodology

This research employs a practice-led, applied research methodology that places the act of design experimentation central to knowledge generation and employs traditional modes of literature review to locate the experimentation contextually within the field of research. With its origin closely aligned with Frayling's notion of 'research through design' (1993), Muratovski (2021) suggests an applied research methodology aims to generate 'culturally novel' knowledge and outcomes that are new to the field of design itself, rather than being positioned in relation to a particular designer or client. To this effect, applied research emphasises *processes* rather than *products* or *artefacts*, a view identified by Candy (2006) as being practice-led.

In the 30 years since Frayling (1993) first proposed his notions of design-based research, there has been a wide adoption of his methods across creative fields, including visual art, architecture, industrial design and theatre. Downton (2003, 2004) embraces Frayling's modes of design research, arguing that the act of design is a valid mode of enquiry and knowledge development and discovery in the creative fields of endeavour; however, modes of engagement within the creative industry (and subsequently design-based research) have shifted significantly in the last 30 years (Cross, 2007), partly due to technological advances and the corporatisation of the creative sectors. Frayling's premise is seen as taking an empiricist and pragmatic approach (Koskinen et al., 2013), that

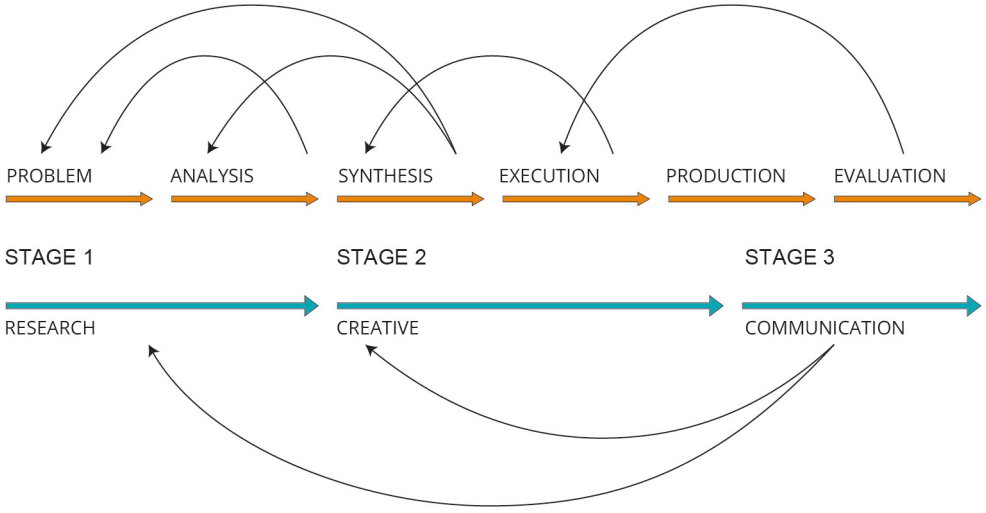

Figure 1.2 Iterative Praxis-Exegesis research model (adapted from Marshall, 2010; Swann, 2002)

sometimes falls short of being adaptable to the shifting landscapes of design practice today.

Marshall (2010) argues for an interlinked mode of design research methodologies, which she refers to as the Praxis-Exegesis model. This entails a cyclical loop that shifts between the creation of artefact and critical observation or reflection (Figure 1.2). The reflexive, practice side of the research (praxis) initiates activities that emphasise creation, reflection and responding, which directly link to the exegesis (written) components of observe, describe, and analyse. Critically, the relationship between praxis and exegesis is both iterative and non-linear, a view supported by Swann's (2002) investigation into action-based methodologies within applied research. This iterative approach (Figure 1.2) provides a mechanism for research to be reflective and critical of itself, forcing a return to earlier stages of the research cycle to introduce newly acquired knowledge and subsequently directing the path of investigation into an augmented direction.

The research methodology employed within this research follows a practice-led mode of applied research, and appropriates Marshall's (2010) non-linear Praxis-Exegesis model. Within this framework, two parallel research instruments are applied allowing iteration within the research model. These instruments are discussed in the following sections.

1.5.1 Research Instrument One: Literature Review

The review of literature undertakes an in-depth engagement with significant literature and texts, and relevant case studies in the fields of material

sustainability, timber as a construction medium and computational design. As such, it includes reviews of the following subtopics:

- material understanding,
- standardisation,
- fibre-managed plantation hardwood in Australia,
- material irregularities,
- parametric design,
- digital fabrication,
- computer vision, and
- evolutionary optimisation in architectural workflows.

In addition to the literature review (Chapter 2), other forms of contextual review are contained within each of the design based investigations contained within Chapter 3 (Design Probes), Chapter 4 and Chapter 5 (Design Prototypes). These smaller contextual studies are specifically focused on the adjacent fields of endeavour employed within each of the experiment workflows.

1.5.2 Instrument Two: Design Experimentation

Research Instrument Two employs a series of experimental investigations, testing the hypothesis and four Research Questions (see Section 1.4.2). These projects each realise a designed artefact that enables opportunity for observation and reflection, thereby enabling a self-critical research loop. The knowledge generated from these experiments informs the direction of the research, in both future experiments and the contextual literature review. The designed artefacts that are outcomes of these projects take on a range of mediums including physical objects, virtual or simulation outcomes, and workflows and approaches to *design problems*. Two modes of design experimentation are employed within this research and are discussed in the following sections.

- Design Probes, and
- Design Prototypes.

1.5.2.1 Design Probes

Design probes are developed as computational techniques that are foundational to the research, as a means of generating digitally augmented

workflows that can be built upon in subsequent investigations. Four design probes are outlined in Chapter 3.

- *Probe 1: RGB-D scanning* is a computer vision-based method that integrates RGB and depth-based scanning to identify material irregularities in timber boards.
- *Probe 2: RGB and Constrained inventorie*s develops a high-resolution workflow that can identify timber irregularities and generates a *constrained inventory* of discretised materials.
- *Probe 3: Architectural panel* considers material irregularity within a design and fabrication workflow through the development of a physically fabricated demonstrator panel.
- *Probe 4: Evolutionary algorithms* develops a innovative method of evolutionary optimisation that correlates material irregularities within a bespoke design environment.

1.5.2.2 Design Prototypes

The two Design Prototype used this research establish material-centred workflows within tailor-made CDFs that engage material indeterminacies and datasets. *Design Prototype 1: Acoustic-SIM* (Chapter 4) and *Design Prototype 2: Mat-Truss* (Chapter 5), apply the techniques developed by the Design Probes within their design workflows. Additionally, they employ innovative modes of material discretisation, material optimisation and distribution, performance-based simulation and analysis and bespoke fabrication workflows. As this research investigates heterogeneous materials, the design-centred workflows require innovative modes of generation, optimisation, and selection to address the near-infinite variation in design outcome. As a result, each Prototype investigation employs evolutionary methods of computation to negotiate this complexity.

1.6 Contributions to Knowledge and Research

The research outcomes of this practice-led study, and its contributions, have two levels of significance, noted here and discussed in the following sections.

a) the primary contribution of the thesis itself; and

b) the secondary contributions of each of the three contextual domains – material sustainability, timber in construction, and DIMP.

1.6.1 Primary Contribution

The primary contribution of the findings of this study is centred on the engagement of material irregularity within design-based computational workflows. This material practice extends the architectural design territory beyond traditional modes of material standardisation and specification, pushing it into an environment that re-evaluates currently latent materials within architecture and construction. In doing so, it establishes opportunities for abundant renewable resources (specifically fibre-managed plantation hardwood) to be considered as highly viable options for material exploration within architectural design. The framework comprises divergent notions of material engagement within the fields of material capture, material optimisation, and material fabrication, each of which occur (but not necessarily lineally) at different stages of the architectural design cycle.

In the domain of material capture, this thesis documents innovative digitally enabled methods of capturing material irregularities and characteristics that occur within fibre-managed plantation hardwood timbers. Further, it establishes methods of material discretisation, thereby establishing a constrained inventory of material that can support the articulation of irregularity within a design workflow.

In the domain of material optimisation, the thesis documents methods of computational simulation and optimisation that employ multi-objective evolutionary algorithms to correlate design opportunities with the inherent complexity of naturally occurring characteristics of a highly variable material medium. The material fabrication domain contributes computationally augmented modes of contemporary digital fabrication, which engage material engagement as an active agent of mediation between performance orientated design objectives and material manipulation.

1.6.2 Secondary Contributions

The secondary contributions are more specific to each of the three contextual domains:

a) In the domain of *material sustainability*, the main contribution is the development of proof-of-concept techniques for material capture (*Probe 1: RGB-D scanning*) and cataloguing (*Probe 2: RGB and Constrained Inventories*) that bridge the supply chain-data gap between the material suppliers, and the construction industry. This provides opportunities for the re-evaluation of out-of-grade and waste materials that present irregular and unpredictable material characteristics and performance, and

which are currently latent within higher-value applications, such as construction.

b) In the domain *of timber in construction*, the research contributes to the development of engagement modes that promotes fibre-managed plantation hardwood to be considered as a potential material of value within the construction industry. The techniques within this field utilises those developed within the previous domain to establish fabrication-based workflows (namely, *Probe 3: Architectural Panel, Prototype 1: Acousti-SIM*, and *Prototype 2: Mat-Truss*), which are responsive to the naturally occurring material characteristics. Further, the intersection of material character and digital fabrication is executed using commonly available digital fabrication equipment, indicating that the methods developed have potential for adoption by industry stakeholders, without additional financial burden.

c) In the domain of *digitally integrated material practice* this research contributes innovative methods of material engagement that remain present throughout the design workflow, enabling a non-linear approach to correlation between material, discretisation, design intent, optimisation, and fabrication. The material optimisation workflow developed (*Probe 4: Evolutionary Algorithms*) investigates both Single and *Multi-Objective Evolutionary Algorithms* (MOEA) to generate a *population*-based method of material optimisation that facilitates the pairing of a practically infinite material variations with a complex combination of multiple design objectives. These methods form core components within *Prototype 1: Acousti-SIM*, and *Prototype 2: Mat-Truss*, fostering innovative computational means of engaging a constrained material inventory, material distribution, performance simulation, and solution selection that is scalable to larger applications within industry.

1.7 Thesis Structure

This thesis comprises six chapters.

Chapter 1: The first chapter introduces the study and the thesis by establishing the research context and stating its hypothesis. In addition to detailing the research objectives, it states its primary Research Question, which incorporates three secondary questions. It defines the research methodology as being a Praxis-Exegesis mode of applied research. The

impact of the research is detailed through a discussion of its contribution and significance within the field. Finally, it provides the structural framework of the thesis by outlining each chapter's context.

Chapter 2: The second chapter is a contextual literature review within which this research is located within. It first discusses material sustainability within the built environment, establishing that new modes of material engagement within architecture are required to meet the significant environmental challenges over the next 30 years. Second, it surveys the re-emergence of timber as a viable material in the construction industry and identifies fibre-managed plantation hardwood as a potential material for the construction industry to consider, as it shifts towards a more sustainable future. Finally, it considers the affordances that a computationally integrated material practice offers material-centric design and fabrication workflows within the construction industry. Specifically, it investigates industry's capacity to engage materials of irregular and unknown character, as found in heterogeneous material sources, such as plantation hardwood.

Chapter 3: The third chapter comprises four *Design Probes* developed as initial investigations into the current capacity of irregular material engagement within a design-based environment. The first Probe develops an *RGB-D* computer vision-based workflow that detects naturally occurring irregular features in timber boards. The second Probe identifies a high-resolution method of material capture and promotes the development of an inventory of available materials. The third Probe investigates the capacity of design and fabrication workflows to be responsive to material irregularities. The final Probe develops an optimisation workflow that employs a MOEA to integrate material irregularities within a bespoke design scenario.

Chapter 4 and Chapter 5: Building on the methods developed in Chapter 3, this chapters details two *Design Prototypes* that establish integrated material practices and which interrogate a constrained inventory of available material through the employment of advanced computational methods.

Chapter 4 develops a material discretisation method that engages material irregularities and material distribution through an evolutionary approach to performance optimisation of a bespoke acoustic surface.

Chapter 5 considers element irregularities in the evolutionary generation of a series of non-standard trusses. Both Chapters 4 and 5 result in a physical prototype demonstrating the developed workflows.

Chapter 6**:** The final chapter summarises the findings the accomplished work, addresses each of the research questions, outlines specific contributions of the findings and suggests directions for future research.

2 LITERATURE REVIEW

2.1 Introduction

This chapter is structured around the objective of understanding contemporary modes of a new material practice in architecture. These modes aim to generate greater material sustainability by engaging irregular, heterogeneous materials through CDFs. As such, an in-depth review of existing literature was undertaken, and summaries are presented to establish the following:

- an understanding of material sustainability in modern day architectural practices;
- the state of timber within the construction industry, to establish a threshold between existing and latent timber resources; and
- current developments in architectural design methods, and how they are being informed by new notions of material practice.

The review of literature explores the notion of material irregularities and unknown performance capacities that are common in Australian plantation hardwood resources, and which are not currently engaged within the architecture, or more broadly within the construction industry. Additionally, the presented review identifies existing methods of digital engagement that underpin a greater utilisation of these irregularities, enabling sustainable resource chains to become viable options for design exploration.

Accordingly, Chapter 2 is divided into three domain-related sections: the intersection between the fields of *material sustainability*, *timber in construction* and *digitally integrated material practice* forms the primary focus of the literature review (see Figure 2.1). These domains are discussed the following sections, but outlined as follows:

Section 2.2 *Material sustainability*, identifies the current pressures facing the construction industry, at a global scale.

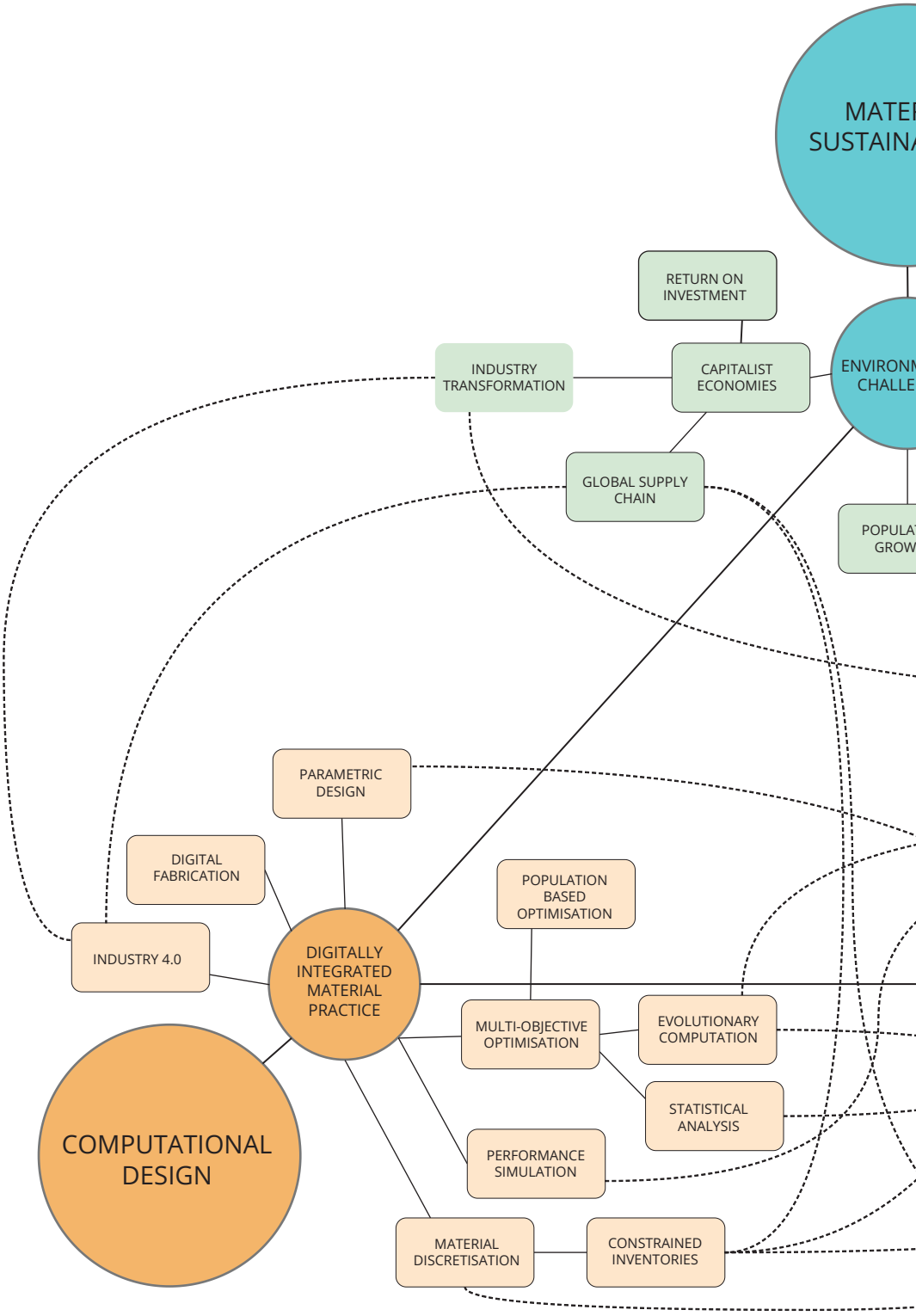

Figure 2.1 Literature review map illustrating intersections between the fields of material sustainability, timber in construction and digitally integrated material practice

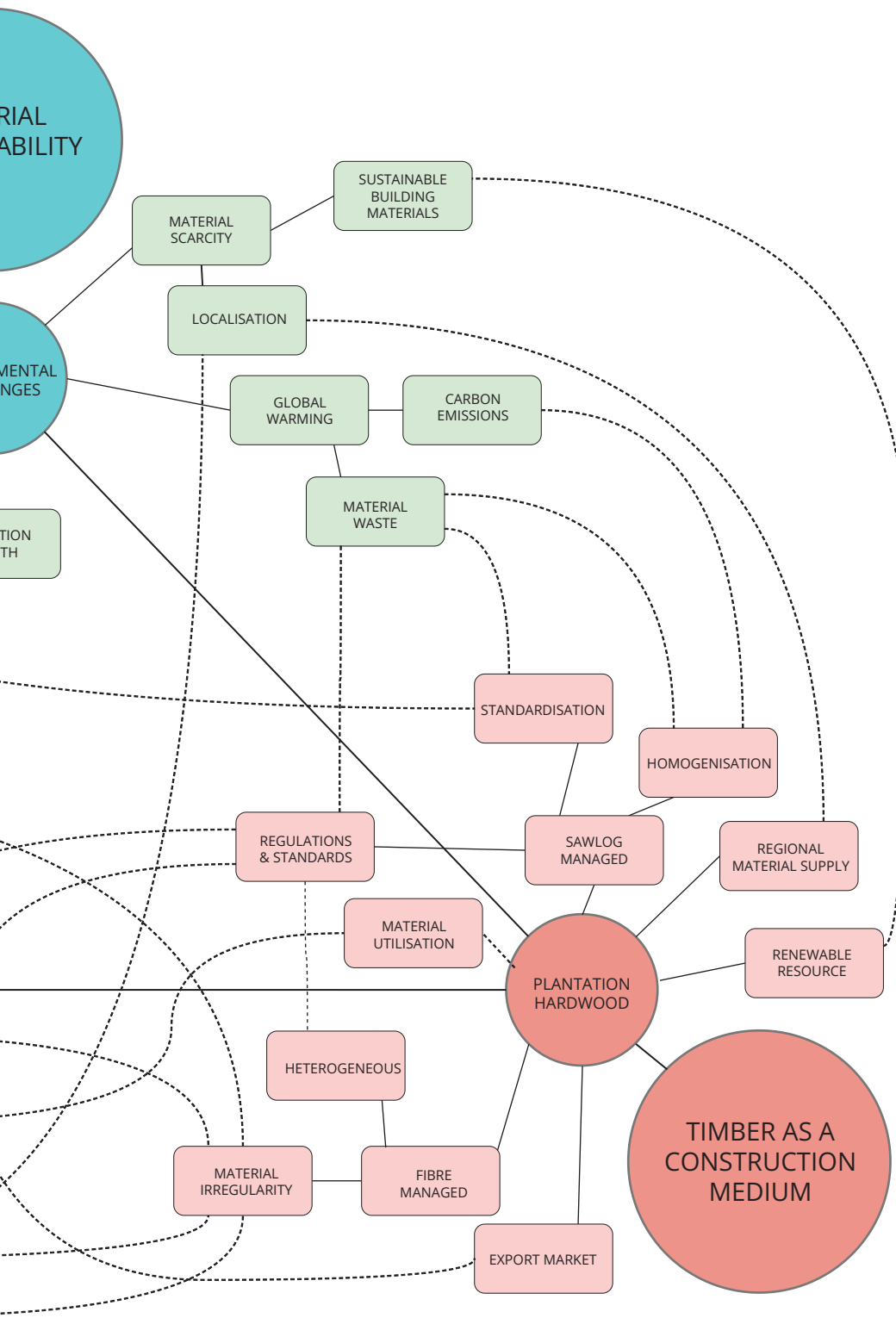
RIAL
ABILITY
MENTAL
NGES
TION
TH
SUSTAINABLE BUILDING MATERIALS
MATERIAL SCARCITY
LOCALISATION
GLOBAL WARMING
CARBON EMISSIONS
MATERIAL WASTE
STANDARDISATION
HOMOGENISATION
REGULATIONS & STANDARDS
SAWLOG MANAGED
REGIONAL MATERIAL SUPPLY
MATERIAL UTILISATION
RENEWABLE RESOURCE
PLANTATION HARDWOOD
HETEROGENEOUS
TIMBER AS A CONSTRUCTION MEDIUM
MATERIAL IRREGULARITY
FIBRE MANAGED
EXPORT MARKET

Section 2.3 *Timber as a construction medium*, provides a review of the relevance of timber as a re-emerging material for construction, and outlines the significant growth in application across the industry;

Section 2.4 *Digitally integrated material practice*, considers opportunities that modes of design computation might provide to the engagement of irregular materials in the architecture and construction industries.

2.2 Material Sustainability

2.2.1 Environmental Challenges

While the relationship between architecture and the environment was historically in a state of an equilibrium, the transformation that the Industrial Revolution introduced severed this balance. Vernacular architecture relied on materials that could be sourced locally and manipulated by hand, using non-mechanical means (Langenbach, 2020), with minimal environmental impact as a result. Conversely, since the first Industrial Revolution (1760-1840), humans have caused an increasing strain on the environment, by consuming resources at a rapidly increasing rate, with little regard for environmental impact.

Modern mechanisation and automation processes have created a dramatic increase in the quality of human life (coupled with an intense period of economic growth) (Ghavami, 2020). This growth intensified during the 20th Century, resulting in a construction industry largely reliant on non-renewable resources and energy intensive manufacturing processes.

Materials used for construction of the built environment (within Australia) account for approximately 50% of all material consumption and contributes nominally 50% of landfill globally through the construction and demolition processes (Pickin et al., 2020). Additionally, it is estimated that 39% of energy consumption and 43% of carbon emissions globally are a direct result of the operation of buildings that already exist (United Nations: Environment Program, 2022). These percentages will increase over the next 30 years, as urban population growth is projected to increase by 1.75 billion people by 2050 (United Nations: Department of Economic and Social Affairs, 2022).

Prior to the COVID-19 pandemic, the UN noted that the construction sector moved away from the goal of 2% mean temperature increase set within the 2015 Paris Agreement of 2015, rather than towards it (United Nations: Environment Program, 2022). It reported a 1% increase in CO_2 emissions (United Nations: Environment Program, 2022), with energy consumption

by the industry to manufacture and transport materials for construction as the primary contributing factor.

If the demand for new buildings (due to an expanding population) is met with contemporary modes of construction, additional pressure will be placed on material supply chains. Availability of the raw minerals required for core building materials utilised in current modes of construction will become limited (Harper et al., 2015; United Nations Environment Programme, 2014) driving the cost of building significantly higher and continuing irreversible damage to the environment.

While the shift towards renewable and sustainable materials will undoubtedly contribute greatly to reducing the impact of the built environment from a climate change standpoint, there is debate around the consequences of large-scale utilisation of naturally occurring, biologically based materials. It is widely accepted there is a finite extractable volume of minerals (Valero & Valero, 2010), and the impact of harvesting circular and renewable material resources, such as timber, is somewhat contested (Ramsgaard Thomsen & Tamke, 2022). The forests that cover much of Earth's landmass are critical to the process of photosynthesis that makes the planet habitable and, as with all resources, forests are finite. The energy balance within our ecosystems dictates there is a limit to forests' photosynthetic capacity: effectively, more trees cannot be grown than the global environmental systems allow. This will also be negatively impacted by a slowly warming planet. While a significant volume of *native forests* is protected in most of the developed countries, the widespread clearing of plantation forests and questionable forest practices in many developing countries has potentially catastrophic consequences for the environment, globally (Adhikari & Ozarska, 2018; Hill, 2019; Mishra et al., 2022). Accordingly, the ongoing stewardship of existing forests, world-wide, is vital.

It is clear that any industry shift towards bio-based materials needs to be considered beyond its direct impact on the built environment and that a significant change is required in resource production and allocation and disposal of waste used in and generated by the construction industry (Ramsgaard Thomsen et al., 2019). Architectural practice, and the construction industry more broadly, must employ a new approach, towards a material practice that encompasses a higher integration with modes of responsibly managed sustainable materiality. Ramsgaard and Tamke (2022) make a timely suggestion: the endeavour must be "build[ing] smarter with less" (p. 2).

Contemporary modes of material practice within architecture rely on industrialised methods that focus on obsolete paradigms of standardisation

and mass production, which are centred around particular material processes. These processes typically convert raw material resources into abundant and predictable material elements that can be easily specified by architects, and easily manipulated by builders. This is at the expense of many other, more sustainable materials that are too difficult to fit within conventional manufacturing processes. The conventional paradigms of standardisation and mass production in the construction sector must evolve towards applications that see material as "hyper-specific and functionally graded" (Ramsgaard Thomsen et al., 2019, p.485) in order to develop methods that utilise more sustainable materials in lesser quantities, in a more intelligent manner.

As a renewable material, timber is experiencing a resurgence in popularity within the construction sector (Menges et al., 2017, Rainer, 2014) and is increasingly identified as a viable solution for moderating the impacts of an expanding construction sector on the global environment (Martin et al., 2021). Since 2000, architectural practitioners have adopted wood-based products as a viable medium for a variety of construction scales, due to the development of new material configurations, manufacturing systems and fabrication processes (Menges et al., 2017). Yet, most *Engineered Wood Products* currently available within the construction industry subscribe to the 'one size fits all' paradigm, in which they are manufactured from higher-grade raw material that present a greater level of homogeneous quality (Svilans 2020, p8) (despite the inherently heterogeneous nature of wood). The manufacturing processes employed also consume large amounts of energy, generate significant volumes of waste and often contain synthetic toxins (in the form of glues and adhesives), all of which contribute detrimentally to the environment.

Timber that is currently unable to be easily graded, classified, standardised, or re-packaged is currently deemed unusable by the construction industry. This is particularly evident in timber sourced from Australia's plantation hardwood forests. While there are potential applications within developing mass timber construction markets, these only account for a small portion of the commercial construction sector (Cusp, 2022; Evison et al., 2018). Adoption within residential construction sector would require a massive shift in the established practices currently used; however, a re-evaluation would present significant opportunity for a more sustainable approach to material engagement within the built environment.

2.2.2 Historic Understanding of Material

The discipline of architecture grew from the role of the master builder (Kolarevic, 2003c) in Mediaeval times, in which case a single master builder was responsible for the design and oversight of a structure and its

construction. A master builder was an artisan who possessed a mastery of the material and tools at their disposal, enabling an immediate connection between thought and design realisation (Ruan et al., 2021). This was due to the Mediaeval reliance on naturally occurring materials and limited capacity to pre-process these materials into predictable elements. This relationship between designer/maker/artisan/builder and material was not unique to construction, with most traditional forms of craft and construction having a similar connection (see Figure 2.2).

Figure 2.2 Identification of sections of curved wood within tree branch segments required for specific components of traditional timber ship building (From 'Encyclopédie Méthodique: Plate 103', 1797. In the public domain).

Construction during the same period was a highly localised endeavour: a building project was constructed from materials sourced from its surrounding area, due to availability and ease of transportation. The scale and volume of construction during this period was comparatively small due to the smaller settlements and slower population growth. The master builder had an intimate knowledge of each material available in their local area, in addition to an intimate knowledge of its properties. This allowed the selection of materials and construction techniques to be matched on a case-by-case basis to ensure that the maximum economic value was being extracted (Carpo, 2017, p. 50). Higher quality and valuable materials were used where they would be seen; hidden or low-performance sections of a structure had lower value materials utilised.

This continued into the Renaissance, with Leon Battista Alberti, the Italian humanist author, artist, architect, poet, priest, linguist, philosopher, and cryptographer, generally credited as being pivotal in differentiating the

role of architects and artists as having a higher level of intellectual rigour to that of the previous master builders and craftsmen (Kolarevic, 2003c). Benay Gürsoy and Mine Özkar (2015) note that, as the role of the architect emerged, it simultaneously became removed from the material and material-making process, reinforcing the separation between the fields of architecture and making.

As the segregation of design ideation and realisation accelerated during the Industrial Revolution, the connection between design intent and material understanding was further weakened. With the mastery of material diminished, new modes of representation were required that instructed others as to how to build. Evans (1997) identifies the new medium of representation and communication as being almost always a drawing; establishing is as the primary tool of architectural communication.

The contemporary exchange between architect and builder represents the communication and interpretation of intent. Mario Carpo (2011) proposes that the nature of architecture is allographic; that is, being mediated and executed through a set of drawn instructions. Architects communicate with a level of detail and precision that ensures there is sufficient clarity from which a builder to work; however, the communication process, in general, has been greatly simplified by the development of standardised building practices and construction materials. There is a shared relationship between building complexity and the detail of communication; when modes of standardisation give preference to elemental geometry, rather than the intrinsic materiality (Thomas 2007).

Achim Menges suggests that while digital design and communication tools have been widely adopted within the common workflows of architecture, the underlying conception and logic of established processes remains largely unchallenged, in that computerised drawing plays the same role as manual drawing, which has resulted in a "computerised extension of the well-known" forcing materials to remain a static rationalisation of digitally generated form (Menges 2016, p. 78).

2.2.3 Standardisation of Architecture

Standardisation in the construction industry was developed, as noted, during the Industrial Revolution and successive periods of mechanised development (such as Fordism). Mass-manufacturing was quickly appropriated by other work practices, such as those in the automotive industry. In the 20th Century, the rapid development of new material

processes shifted manufacturing well away from a craft-based pursuit, towards a factory style production line.

The production of munitions and vehicles, for example (in the volume required during World War 1 by the military) subsequently accelerated this approach (Caneparo, 2014). As industrialisation continued into the second half of the 20th Century, standardised materials and processes were largely seen as playing a positive role in architecture and construction. By extracting the resources and establishing manufacturing processes that standardised the appearance, performance and character of new material configurations, the built environment was no longer limited to the traditional and vernacular modes of construction and design. The adoption of standardised materials and processes greatly enhanced the safety, quality, performance, energy efficiency and cost-effectiveness of construction, now expected on building sites.

However, the reliance on standardised and reputable tools of communication also started to reinforce a reliance on standardised materials and manufacturing processes, which reduced aspects of architecture to a mere process of arrangement and assembly (Carpo, 2014, p. 43; Migayrou, 2014, p. 23): that is, a 'kit of parts' approach.

At the time of writing, commonly available construction materials are reduced to a mix of generic single units, sheets, slabs and stick based elements that are cut and formed as required. Fure (2011) indicates a standardised and narrower material scope is also strongly connected with, and on occasion based on, industrial manufacturing, contemporary construction methods and digital fabrication processes. He suggests this practice reflects the dominant, top-down approach of architecture ideation and creation, in which an artefact is produced that most closely matches the drawings from which it originates. Consequently, innovation in the built environment is centred on how to best optimise engagement with, and the performance of, a pre-determined and standardised material palette.

Traditionally, the character of a natural material (such as wood) was elaborated (or exploited) during construction (Carpo, 2017; Monier et al., 2013), with the unique geometry and character of individual material elements being paired with specific tasks that maximised the potential of the component (Rainer, 2014). As the scale and volume of construction increased, the viability of matching unique properties with specific performance diminished. The adoption of engineered and manufactured construction materials dramatically increased in the early 20th Century,

influenced heavily by the international Modernist movement, which generally advocated,

> *... the replacing of natural materials by artificial ones, of heterogeneous and doubtful materials by homogeneous and artificial ones (tried and proved in the laboratory) and by products of fixed composition [and] natural materials, which are infinitely variable in composition, must be replaced by fixed ones* (Le Corbusier, 1970, p. 232).

This practice continued through the 20th Century, with the current, global construction industry relying heavily on materials that are engineered and manufactured. This has established an expectation that materials will always be homogeneous and demonstrate predictable properties; both favourable characteristics for design, construction efficiencies and economies. Since then, architects have preferred to reject the unknown and irregular, favouring instead the determined and calculable (both time and budget saving attributes). This, in turn, has limited the need for the exploration of new modes of engagement that could potentially consider irregular material geometries and performance capacities. This is particularly significant in terms of the utilisation of natural materials.

2.2.4 The Development of Standardised Materials

The period between the First and Second World Wars saw a continued growth in industrialised manufacturing, despite western economic downturn. The end of this period gave rise to capitalist-based consumerism, particularly in these western countries. As part of this capitalist economic framework, the focus was on the efficiencies and volume of production that mass-manufacturing provides (a focus that has persisted). This transition resulted in products becoming increasingly generic and component based, with globally distributed elemental production. These methods of production provided economic gains at the cost of a gradual de-skilling of the labour market, leaving little room for traditional notions of bespoke craft-based manufacture, as such.

Standardisation, which was initially aimed at increasing the efficiency and cost-effectiveness of manufacturing, meant the creation of homogeneous materials could be more easily integrated within construction processes. Critically, these homogeneous materials could be mass manufactured to a high level of consistent, matching accuracy, allowing for their adoption in national and global markets (due to an intensification of export-based transportation networks). This has intensified since the 1950's to a point where the heavily industrialised processes of standardisation and mass-

transportation are now considered a major contributor to the global warming crisis (United Nations: Environment Program, 2022).

In terms of the construction industry, standardisation has similarly resulted in the development of 'manufactured' or 'engineered' materials that are available for architects to specify. As noted, until the 19th century, construction consisted predominantly of raw material elements (typically earth, stone and timber). The emergence of new materials in the 20th Century, coincided with the separation of existing professional specialisations within the built environment, in which a division in responsibilities formed between architects, engineers, material specialists and builders. This led to an increase in the specification of standardised materials and processes, as they were easily communicated between allied professions.

There is a tendency by many architectural practitioners to create buildings that fit to, and within, the realms of standardised materials, which relates to the economics of construction. Non-standard and natural, raw materials can be seen as complex, requiring a higher level of calculation and consideration at the time of design. They also present challenges in an increased difficulty in the procurement of material, longer construction times on-site and a higher level of skill and labour to assemble them. As these things all contribute to a higher overall cost, the construction industry tends to favour materials and processes that are easier to shape, are more predictable, require less labour-intensive processes and are cheaper.

Architectural practice and construction have continued to adopt standardised processes and materials to rationalise design intent and generate cost-effective solutions. This process enables materials to be treated equally, simplifying the computation, engineering, fabrication and assembly processes significantly. The paradox of this approach is that, as the opportunity for formal complexity of architectural design intent has recently increased through the adoption of computational processes, the understanding and utilisation of material complexity has decreased.

The methods of material standardisation rely on energy intensive modes of secondary processing and manufacturing to turn what is a naturally occurring heterogeneous material (such as wood), into a manufactured homogeneous one. The energy consumption and waste generated by these industrialised processes have considerable impact on the global environment and its resources. The emergence of manufactured materials during the Industrial Revolution saw the creation of homogeneous and predictable elements for construction as paramount (Stanton, 2010). The technological advancements in manufacturing established during the 20th Century brought the widespread adoption of these materials. More

recently, computer numerically controlled (CNC) fabrication equipment has allowed the generation of mass-produced components and standardised building materials (Pfeiffer, 2017). As global warming continues to increase and the availability of non-renewable construction materials decreases, the construction industry must critically re-evaluate its material processes and consumption. The development of new modes of assessment, design and fabrication workflows (that can better utilise heterogeneous materials with minimal processing) is key to the long-term sustainability of the construction industry.

While most industries have evolved over the past few decades to situate product and methodologies-based innovations at the core of their business model, the construction sector has remained relatively stagnant, failing to keep pace with technological opportunities offered by the Information Age (which is characterised by a rapid shift from traditional industries to an economy centred on IT) (Maskuriy et al., 2019). By doing so, the construction industry is heavily reliant on labour-based processes that are fragmented, resource heavy and lack the levels of industrialised efficiencies that other sectors had readily, and much earlier, embraced.

Architectural practice has progressively severed its intrinsic link with local materials and place, shifting towards a rigorously controlled and generic stasis (Buri & Weinand, 2011). Many factors contribute to this, including legal risk, speed and economics; however, when assessed broadly, Carpo (2017) suggests it is the result of a (capitalistic) desire for materials to be predictable, homogeneous and, significantly, calculable. The common methodologies within architecture require materials that are 'known'; that is, they enable the accurate prediction of material performance within a building, based on proven methods of calculation. An increase in material complexity significantly intensifies the computation required to calculate the performance of a design, beyond what is practical within established workflows.

This homogenisation of material and mechanical processes has led architectural design to an industrialised 'kit-of-parts' approach, in which the performance and character of material is pre-determined and predictable, while fabrication becomes a process of forming known materials into a prescribed design. These systems significantly reduce the potential for naturally occurring materials of heterogeneous irregularity and unknown character to be utilised within architectural design.

This is especially the case with 'grown' materials, such as timber, that present characteristics that are intrinsically unique to the specific piece. Timber is influenced by the environment (and the processes) in which it is grown, significantly transforming its quality of material, bestowing a

unique character to each piece. The process of homogenisation seeks to classify unique materials into predictable groups that can be deployed across multitudes of uses, stripping the potential of the innate character from the material. Timber, in its raw, heterogeneous state, is difficult to work with using current design and fabrication methodologies (that predominantly require parameters to be known at the outset). The challenge for heterogeneous materials within architectural practice is the development of design models that accommodate and engage material irregularities within a design outcome, in addition to developing new modes of fabrication that allow for variable and indeterminate material characteristics.

2.3 Timber as a Construction Medium

Timber offers a compelling opportunity for the construction sector to intensify its engagement with materials that fall outside the normal range of manufactured and standardised options, while presenting significant benefit from a sustainability perspective. It is renewable, has low-embodied energy, a positive carbon footprint, is fully recyclable, has a comparatively high strength to weight ratio and is regionally available (Krieg et al., 2016).

In comparison with other major construction materials used in Australia, timber consumes significantly less energy in converting forest resources to finished products (Figure 2.3), has much lower embodied energy (Figure 2.4), and demonstrates a excellent capacity to store atmospheric carbon (Figure 2.5).

For the construction industry to adapt to more sustainable practices, wider adoption of timber as a base material, as opposed to steel or concrete, is a necessity. This shift requires the revaluation of timber resources, along with the way they are utilised within the construction sector.

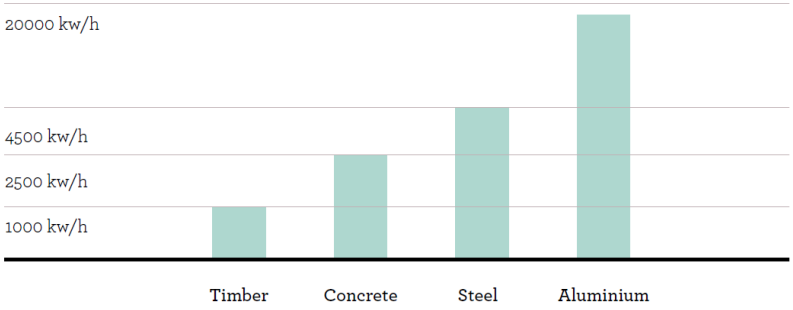

Figure 2.3 Energy consumption of major construction materials in Australia (From Tasmanian Timber, 2019. Copyright 2019 Tasmanian Timber. Reproduced with permission).

Material	Fossil fuel energy (Mj / Kg)	Fossil fuel energy (Mj / M³)
Rough Sawn timber	1.5	750
Steel	35	266000
Concrete	2	4800
Aluminium	435	1100000

Figure 2.4 Fossil fuel consumption in the production process of major construction materials in Australia (From Tasmanian Timber, 2019. Copyright 2019 Tasmanian Timber. Reproduced with permission).

Material	Carbon released (kg/t)	Carbon released (kg/m³)	Carbon stored (kg/m³)
Rough Sawn timber	30	15	250
Steel	700	5320	0
Concrete	50	120	0
Aluminium	8700	22000	0

Figure 2.5 Atmospheric carbon credentials of major building materials in Australia (From Tasmanian Timber, 2019. Copyright 2019 Tasmanian Timber. Reproduced with permission).

2.3.1 Timber in Australia

Timber in the Australian construction industry is predominantly harvested from plantation forests and transformed into a standardised material, as either sawn-boards or sheet-based products. Sawn timber accounts for approximately 65% of timber production from Australian forests, of which 85% is consumed by the residential construction in the form of structural framing, flooring, decking, and joinery (ABARES, 2018). Additionally, relatively new mass timber applications, including Cross Laminated Timber (CLT) and Glue Laminated Timber (GLT), are gaining popularity in the commercial construction sector. The remaining 27% of construction timber is found in sheet-based materials, such as plywood, particle board and Medium Density Fibreboard (MDF). These standard timber products predominantly use softwood-based plantation timbers in their manufacture. This process of using standardised timber elements has proven highly successful, due to capacity to create predictable and homogeneous elements that are cost-effective and easy to manipulate on-site. Subsequently, the construction industry has had minimal incentive for re-evaluating timber as a medium for construction, beyond the optimisation of existing products and processes; however, there is significant environmental and economic incentive for its position to be re-evaluated as a construction medium.

ABARES states that traditional timber supply in Australia had been met by harvesting native old-growth forests. Eucalypt species (75%), with Acacia (8%), Melaleuca (5%) and minor rainforest species (3%) have proven to be the most useful (ABARES, 2018). With constant harvesting since colonisation, Australia's old-growth native forest reserves are all but

exhausted, with most of the remaining forests either protected within conservation areas or excluded from timber production.

Outside of the protected and reserved forests there remains 5.5 million hectares of mixed species (hardwood and softwood), accounting for approximately 14% of Australia's forests available for harvest. On a national basis, 1.4% of this available forest is harvested annually, accounting for approximately 77,000 hectares (4.3 million cubic metres). 50% of this harvest supplies the high value hardwood and softwood sawlog and veneer purposes, catering for 80% of the total Australian structural and appearance-grade timber market. 46% of the annual harvest is destined for pulplog markets, either for woodchip export or domestic paper production (Legg et al., 2021). While the majority of harvested timber is utilised and provides an economic return, the pulplog material returns a lower profit margin and has potential for a re-evaluation of alternate uses of higher value.

With depleting reserves and an increasing awareness of the political, social and environmental impact of harvesting Australia's native forests, the national production yield has decreased steadily since 2020, a trend that is expected to continue into the future (ABARES, 2022b). As a result, the forest industry has refocused on using plantation timber as the primary sustainable business model moving forward. This has had a significant impact on the timber available in the construction sector, with reliance now solely on plantation timbers.

2.3.1.1 Plantation Timber

Australia has 135 million hectares of forests, covering 17% of its total land mass (ABARES, 2018). The majority of this resource is native forest, with only an approximate 1.3% being commercial plantations. These plantations account for approximately 1.8 million hectares, predominantly spread across the eastern and south-western regions (see Figure 2.6). Of these plantations, approximately 60% is softwood forests with the remaining 40% comprising hardwood resources.

As shown in Figure 2.7, Australia's plantation forests are spread across the country; however, the comparative resource value and utilisation does not correlate with the plantation distribution. Australia's softwood plantation is almost exclusively managed for high value sawlog production, 82% of hardwood plantations are managed for pulplog purposes, reducing the potential export value by an estimated 50% in comparison with sawn boards from the same resource (ABARES, 2018). This is a particular issue for Tasmania and Western Australia, which have a significantly higher proportion of hardwood forests within their plantation inventory. Tasmania

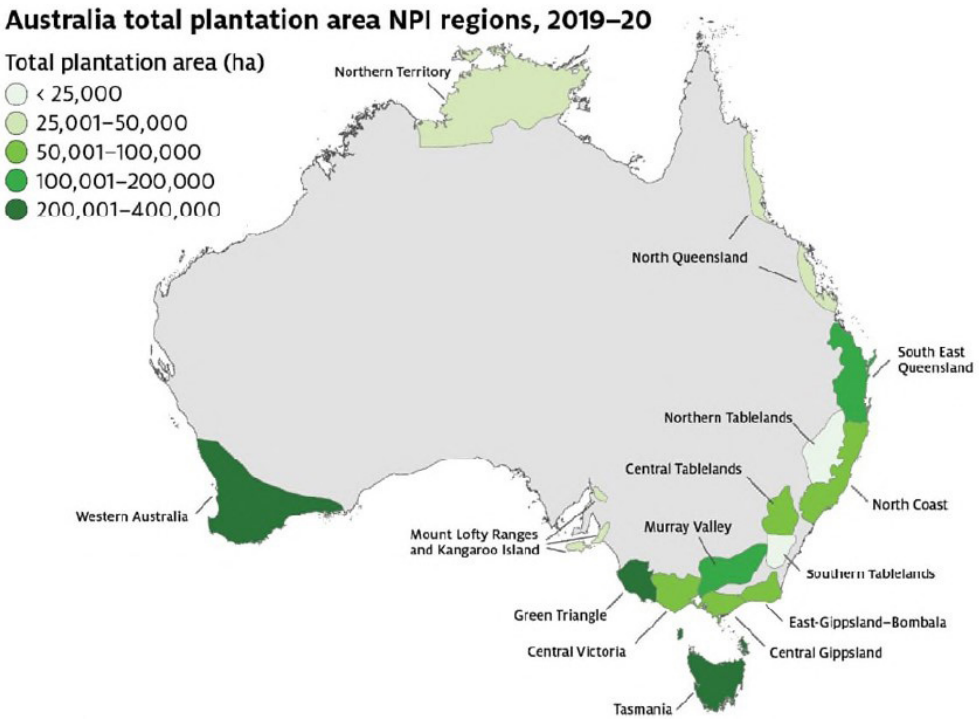

Figure 2.6 Australian plantation inventory regions 2019-20 (From Legg et al., 2021 CC BY 4.0).

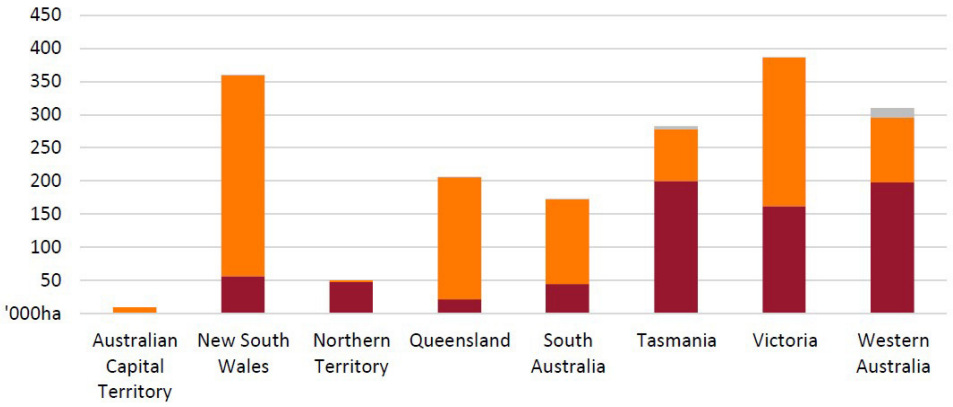

Figure 2.7 Hardwood and softwood plantations by state (From Legg et al., 2021 CC BY 4.0).

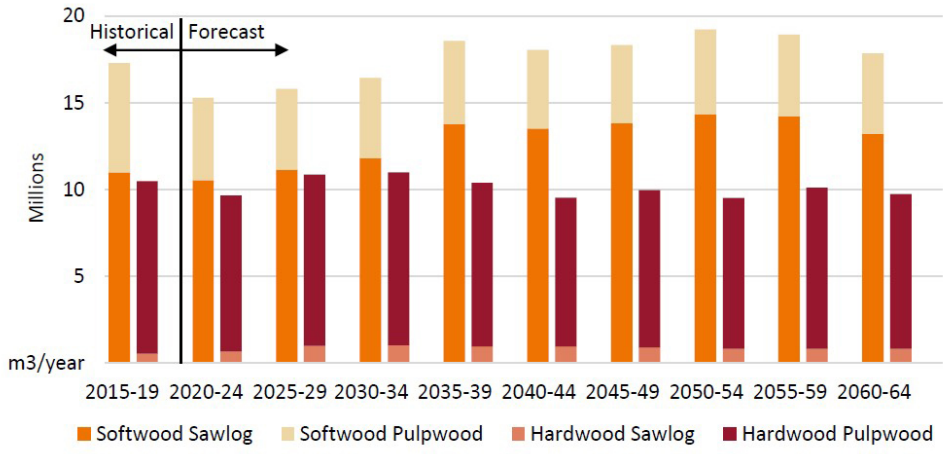

Figure 2.8 Australian plantation log availability forecast (From Legg et al., 2021 CC BY 4.0).

has 0.9% of Australia's total land mass, and a 28% share of Australian hardwood plantation, so there is significant economic and political interest in maximising this resource commercially beyond a pulp-based export market at a state level. However, this predicament is not limited to a Tasmanian, or indeed Australian, context. There are an estimated 22.57 million hectares of *Eucalyptus* spp. hardwood plantations spread across at least 90 countries globally (Ferreira et al., 2019; Zhang, 2021), of which approximately 93% is considered fibre-managed (Forrester et al., 2010).

In comparing the future availability of plantation timber in Australia over the next 40 years (see Figure 2.8), it is evident that the volume of hardwood logs will experience only minor fluctuations, and that the major proportional volume of plantation hardwood harvested remains consistent throughout this period, correlating with the harvest cycles and expected maturation of existing plantation forests. It is also evident that while most of the timber from softwood plantations is destined for high value sawlog grade outcomes, almost all plantation hardwood is forecast to be used in the low-grade pulplog markets. (Section 2.3.1.2 and Section 2.3.1.3 explore the characteristics of softwood and hardwood plantations in more detail).

2.3.1.2 Plantation Softwood

Australia's plantation softwood forests predominantly comprise three exotic species: *Pinus radiata* ('Radiata' (or 'Monterey') Pine, 75%), with *Pinus elliottii* (Slash Pine) and *Pinus caribaea* Caribbean Pine), a combined 15%; with a selection of minor and exotic species completing the national softwood plantation inventory (ABARES, 2022a). 98% of this resource is managed for sawlog grade timber and serves approximately 70% of all demand for softwood production in Australia.

Plantation softwood forests have short harvest cycles that can reach maturity in as little as 25 to 30 years, when grown for sawlog timber (England et al., 2013). When managed for pulplog timber, typical harvest cycles are twelve to 15 years. The nature of plantation softwood species tends towards taller and straighter trees, resulting in a more regular and predictable material, while remaining heterogeneous. The lighter mass of softwood makes the material more suitable for manual construction

methods, both in prefabrication and on-site environments. Softwood is predominantly utilised in the high value construction markets of:

- stick-based structural framing (sawn boards);
- engineered solid timber products, including CLT, LVL and Glu-lam beams; and
- engineered sheet-based products, including plywood, particle board and OSB (oriented strand board).

This trend has led to substantial transformations within the softwood market sector. The industrialised processes of harvesting, sawing and grading of softwood materials has undergone significant advancements, with high levels of automation currently present within established supply chains. This has been facilitated by the economic advantages provided by the demand for large volume of softwood to meet market demands within Australia.

2.3.1.3 Plantation Hardwood

The majority of Australia's plantation hardwood reserve consists of two native species; *Eucalyptus globulus* (Tasmanian Blue Gum), 52.7% and *Eucalyptus nitens* (Shining Gum), 25.2%; with the remaining 22.1% comprising a mixture of minor species (Legg et al., 2021). As these reserves are primarily managed for pulplog (81%), the timber produced from the forests is generally considered unsuitable for high value markets. As such, most of the plantation hardwood within Australia is destined for lower-value high-volume industries, such as paper and fibre, rather than higher-value lower-volume markets, which includes the construction industry.

In comparison with softwood, hardwood has significantly longer harvest cycles, reaching maturity at a slower rate. Most plantation hardwood forests within Australia were developed from the late 1990s onwards and, as such, are yet to reach maturity for sawlog production. In comparison, re-growth native forests in Australia are typically harvested at between 60 to 100 years of age (England et al., 2013). However, fibre-managed hardwood plantations reach maturity at 15 to 20 years of age (Derikvand et al., 2016), representing a harvest cycle similar to that of fibre-managed softwood plantations.

As a fibre-managed resource grown with the intention of being exported as a low-value woodchip commodity, a plantation is generally left to grow in a state that is termed 'un-thinned and unpruned'. This strategy sees minimal intervention applied during the life cycle of the plantation, reducing the labour cost in managing and maintaining the plantation resource. Subsequently, the trees are allowed to grow in natural competition with

each other and naturally develop irregular branch structures, which affects the quality of the timber that can be produced. This results in timber that is generally unsuitable to be used in higher-value construction markets, as it cannot be graded effectively using current methodologies, due to the presence of irregular, unpredictable features (as shown in Figure 2.9).

Figure 2.9 Irregular features on sample *E. nitens* sawn boards

Unlike the softwood industry, which benefited from importation of tree species, automated grading methods and new standards into Australia, the hardwood supply chain has not undergone a significant technological advancement in decades. This is due, in part, to the combination of a range of factors: a decrease in hardwood log supply in the late 20th Century, the high economic costs of handling and processing, the small scale and dispersed nature of hardwood sawmills in Australia and the establishment of commercial quantities of plantation softwood (Davis et al., 2017).

While automated grading methods can be applied to hardwood resources, they are not currently widespread within the Australian timber industry, largely due to the high cost of implementation and the low volume of hardwood material harvested for structural purposes. As such, the existing methods of grading hardwood timber in Australia (as outlined in *AS 2082-2007: Timber - Hardwood: Visually stress-graded for structural purposes - Standards Australia*, 2007), remains predominantly a labour intensive, manual process of visually inspecting boards for the presence of material irregularities that are considered defects (that potentially reduce the capacity of the timber). Further, the highly irregular material characteristics of plantation pulplog timbers discounts it as a resource for grading for this purpose, at any significant scale.

While the construction industry demonstrates significant growth in the adoption of new mass timber products that primarily utilise Australian softwood plantations, there are currently very few commercially available products that utilise fibre-managed plantation hardwood in high value markets. As these softwood plantations have begun to reach maturity, an

interest in both structural and non-structural construction applications has developed, including products/processes such as:

- sawn timber boards (Farrell et al., 2012);
- plywood (Blackburn et al., 2018) and laminated veneer lumber (LVL); and
- mass timber applications (Derikvand, 2019; Ettelaei, Taoum, Shanks, et al., 2022).

Derikvand et al. (2016) also suggest that the development of new workflows and construction systems are intrinsic to the sector's capacity to adopt this resource in higher value markets.

2.3.2 Material Properties of Wood

Within an Australian context, the raw material that originates from a tree is referred to as wood. Wood is fundamentally a composite material comprising different types of elongated cellulose cells, called *tracheids* in softwoods, or *fibres* in hardwood (see Figure 2.10). Hardwood fibres are arranged in parallel lines in the wood and are bonded by a matrix of *lignin*, which holds the fibres in place. The fibres within a tree are orthotropic, in that they are oriented primarily along its long axis and are symmetrical about two or three mutually perpendicular planes (McMullin & Price, 2017), which gives wood its characteristic strength and stiffness (Hoadley, 2000). The cellulose fibres are surrounded by a layer of cells (the 'cell wall') that made up of several layers of cellulose and other polysaccharides, as well as lignin (Miller, 2012). The cell density and thickness of cell walls contribute to the structural capacity of the wood and its resistance to water. From a structural perspective, the long cells are strong in tension, while the matrix of lignin is comparatively strong in compression (Deplazes, 2005).

The composite and cellular nature of wood has a significant impact on the behaviour and capacity of the resulting timber used as a construction material. Wood's naturally occurring *anisotropy*, *viscous elasticity*, and

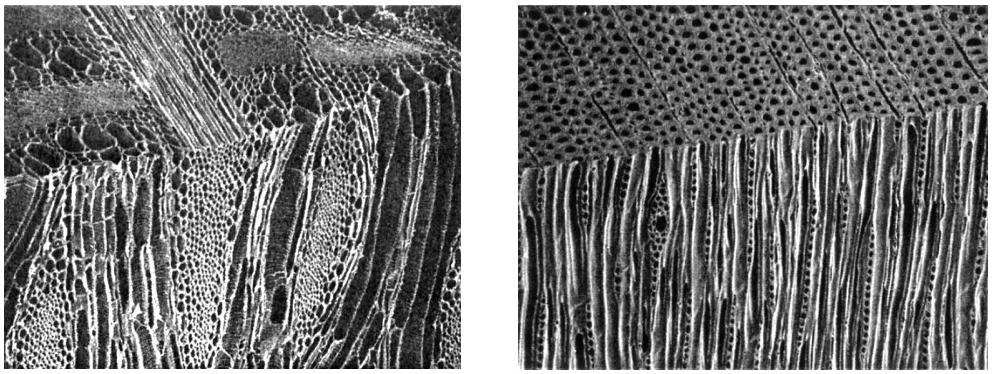

Figure 2.10 Cellular structure of hardwood (left) and softwood (right) (From Walker et al., 1993. Copyright 1993. Taylor & Francis Informa UK Ltd - Books. Reproduced with permission).

hygroscopicity (each discussed in the following sections) are the primary characteristics that affect the capacity and suitability of a piece of timber, in a construction system.

2.3.2.1 Anisotropy

Anisotropy refers to the character of a material that has different physical properties when measured in different directions. Wood has three main axes of orientation as it grows within a tree structure – longitudinal, radial, and transverse (see Figure 2.11) – that are typically treated as being perpendicular to each other. As the elongated cells of the wood are arranged in parallel to the longitudinal axis of growth, its anisotropic character presents fundamentally different mechanical properties across each of the axes (Dinwoodie, 2017). For example, wood is generally stronger and stiffer in the longitudinal axis, as it follows the direction of the grain, demonstrating a higher capacity compared with when it is loaded transversely to the grain (McMullin & Price, 2017). Further, the grain direction is rarely consistent within a log as a tree will adapt to external environmental and mechanical forces as it grows, resulting in varied fibre within the wood. This behaviour impacts how timber is extracted from raw tree logs and subsequently determines the size and orientation of timber elements within construction (Desch & Dinwoodie, 1996).

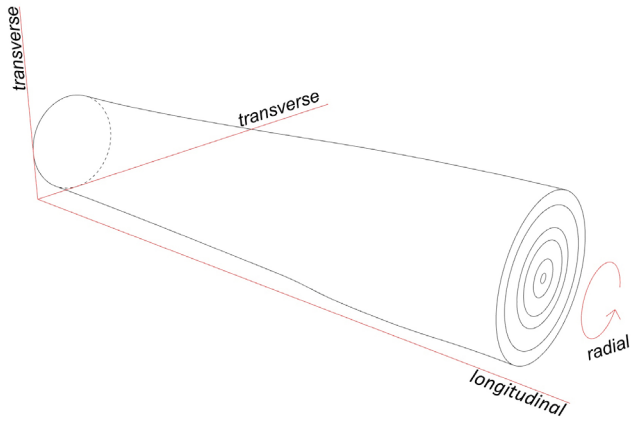

Figure 2.11 The three primary axes of wood in relation to tree formation

Anisotropy can also affect the density of wood, which is determined by the cell wall thickness within it, as well as the arrangement of the cells. Wood density can vary greatly between hardwood and softwoods, in addition to the species of tree and the location of the tree from which the wood is taken. Typically, the heartwood located at the centre of the tree is denser than the sapwood wood found in the outer layers of the tree. Timber that

is sourced from the heartwood will generally have a higher structural capacity compared with sapwood.

2.3.2.2 Viscous Elasticity

Viscous elasticity describes the capacity of a material to deform when a force is applied and subsequently return to its original shape when the force is removed, with the extent of deformation known as deflection. This property is significant in many engineering applications, including the design of structural elements such as timber beams and columns. While most materials exhibit some degree of elasticity, the arrangement of cellular fibres within wood, in conjunction with the lignin matrix, provides a higher capacity to return to its original state during short term loading periods; however, as the lignin bond is not completely elastic, long-term loading of timber elements will cause the cellulose fibres to relax and re-settle into their new physical state. While this causes permanent deformation, the element maintains the majority of its bearing capacity, allowing continued serviceability of structural applications (McMullin & Price, 2017).

2.3.2.3 Hygroscopicity

The naturally hygroscopic character of wood allows it to absorb and release moisture from the air, until it reaches an equilibrium with the humidity of the external environment. Moisture that is held within a wood cell displaces the cellulose, in turn engorging the cell and leading to the swelling and expansion of the timber element due to the increase in moisture content. Conversely, as the moisture content is reduced, the wood cells shrink reducing the physical size of the timber element. This dynamic physical change is in constant flux in untreated timber and affects its mass, density, and physical and performance characteristics. As with other characteristics of wood, its elongated cellular structure and anisotropy influence how this swelling and contracting physically occurs. As such, the radial and tangential axes of wood are more susceptible to swelling and contraction due to moisture content than the longitudinal axis. This characteristic causes dimensional instability within the wood, in which the size of the timber changes over time due to variations in moisture content. This can cause problems with fit and function, as well as deformations and cracks in the timber.

The drying process of timber is also greatly affected by its hygroscopic nature. While this is more evident in softwood timber species, plantation hardwood timbers are also particularly prone to hygroscopic degradation through the harvesting and sawmill processes due to their rapid growth and young age at the time of harvesting (Ananías et al., 2014). Freshly

harvested wood has a high moisture content, and once sawn and dried, will lose moisture rapidly and shrink in size. This shrinkage can cause deformation and warping of the timber boards, especially if the drying process is not carefully controlled. There are several factors that can affect the degree of deformation during drying, including the initial moisture content of the timber, the drying rate, and the final moisture content. Timber with a higher initial moisture content will have a greater tendency to deform during drying. A slower drying rate can also reduce deformation, as it allows more time for the moisture to redistribute within the timber and cause stresses that can lead to warping (Yang & Liu, 2018).

2.3.3 Timber as a Heterogeneous Material

The environment in which a tree is grown directly impacts the character and quality of the timber; a complex integration of physical and biological elements. The genetics of a tree help to shape it to uniquely adapt to varying physical conditions, such as solar radiation, precipitation, air quality, soil structure and quality, and topographic conditions. The biological variables include fungus, animals, soil micro-organisms and other trees competing for available resources (Fowells & Means, 1990). The complex interaction of these variables ensure that no two trees are identical, even when they originate from the same genetic origin. While the topology of a tree can be somewhat predicted, its final form and intrinsic characteristic is always indeterminate. This is exacerbated when timber is sourced from fibre-managed plantations at multiple stages throughout the supply chain including, harvest cycle times, management strategies, sawing and drying methods, and grading.

Trees harvested from native forests within Australia typically grow in diverse ecosystems that have evolved over many centuries. The largest of these trees provide canopy coverage for other vegetation communities and were historically sought for construction timbers, due to their size, density and straightness of trunks. In comparison, fibre-managed hardwood plantations typically reach maturity in 15 to 20-year rotations (Balasso et al., 2021), as the volume of recoverable timber is more critical than its quality.

In a fast-growing species, such as *E. nitens*, this time frame represents the point at which growth in the plantation density begins to slow, providing an opportune time for an economic return on the investment (Acuna et al., 2017). As trees grow rapidly during this time frame they develop significant internal stresses that can not be equalised effectively until the material density increases in later stages of growth. This increases the relative proportion of internal and external defects, and dimensional instability within the tree, and subsequently extracted timber boards (Shelbourne

et al., 2002; Yang & Liu, 2018). As a consequence, the potential recovery rate of sawn boards from the log is reduced, which in turn diminishes the economic viability of the product when harvested within 15 to 20 years.

As fibre-managed hardwood plantations are not regularly maintained beyond three years with routine silvicultural practices (including thinning and pruning) the lower stems of trees are prone to dense lateral branching, which can result in a significant increase in knot-based features (Derikvand et al., 2018). Although the grading standards in *AS 2082-2007: Timber - Hardwood: Visually stress-graded for structural purposes* can be applied to fibre-managed plantation hardwood containing diverse timber characteristics, they rely on the presumption that the visually identifiable characteristics of timber (including knots, checking and 'wane and want'), directly correlate to the structural capacity. While this correlation exists within timber from Australian native forests for which it was originally developed, it is less reliable for plantation hardwood sources as the correlation is not present (Balasso et al., 2021).

To date, the highly variable character of plantation hardwood has limited its application within the architectural and construction sectors; however, this limitation is based on long-held industry expectation that materials should be homogeneous and defect free. Fibre-managed plantation hardwood has a specific set of material properties and characteristics, just as other materials have their own intrinsic nature. Rather than this heterogeneity forcing it to be disregarded, a more intimate understanding of these specificities is required to unlock the full material potential of the timber, liberating it from being classed as defective or unsuitable for the construction sector. For irregular materials to be incorporated within contemporary practice, the notion of what constitutes a 'defect' or 'error' needs to be reconsidered.

2.3.4 Understanding Timber Heterogeneity

Within Australia, *AS 2082-2007: Timber Hardwood-Visually stress-graded for structural purposes* (Standards Australia, 2007) is used by the timber industry in relation to the visual grading of sawn hardwood timbers for structural applications. It is intended to be read in conjunction with *AS /NZS 4063: Characterisation of structural timber, Determination of characteristic values* (Standards Australia, 2010) and *AS 1720.2-2006: Timber Structures & Properties* (Standards Australia, 2006), as a means of linking material grade identification, structural classification and structural timber design as a complementary progression. While not specifically stating that the detailed visual grading methods are not applicable to plantation hardwood timbers, *AS 2082-2007: Timber Hardwood-Visually stress-graded for structural purposes* suggests that the accuracy of correlation between

species, structural grade, and strength group stress grade (F-rating) is not reliable (Balasso et al., 2021). This is due to the long-standing application in commercial hardwood production sourced from mature native forests, and most of its strength groups and stress grades being derived from historic datasets of clear timber samples from European species. Early stage research is unveiling some correlation between visual characteristics and structural performance in sawn timber sourced from sawlog managed plantation hardwood through the application of destructive testing methods (Derikvand et al., 2018), and non-destructive predictive methods (Derikvand et al., 2020; Ettelaei, Taoum, & Nolan, 2022; Pangh et al., 2019). However, as fibre-managed plantation hardwood typically presents a significantly higher level of material character variation the correlations are not applicable to the material used within this study.

Although methods of visual grading (as outlined in *AS 2082-2007: Timber Hardwood-Visually stress-graded for structural purposes*) are not suitable for application to both sawlog and fibre-managed plantation hardwood timber, characteristics that it details as significant to impact performance have relevance within this research. While there is variation in the size, regularity, density, and occurrence of material features between native and plantation hardwood, the typology of features remains relatively consistent. Both timber sources are subject to naturally occurring irregularities that are a result of the geographic environment in which they are grown. As such, the material features identified in *AS 2082-2007: Timber Hardwood-Visually stress-graded for structural purposes* (Standards Australia, 2007), and *AS /NZS 4491:1997 Timber-Glossary of terms in timber-related Standards* (Standards Australia, 1997) that are applicable to the plantation timber used in this study are discussed following.

2.3.4.1 Feature Typologies

The feature typologies defined in *AS 2082-2007: Timber Hardwood - Visually stress-graded for structural purposes* (Standards Australia, 2007) are derived from the glossary of terms detailed in *AS/NZS 4491: Timber - Glossary of terms in timber-related Standards* (Standards Australia, 1997). The relevant material characteristics of timber (specified within *AS 2082-2007: Timber Hardwood-Visually stress-graded for structural purposes*) that are specifically related to the potential performance of sawn hardwood boards are warp, wane and want, checks and splits, knots, knot clusters, and knot groups. These characteristics are discussed in the following sections.

2.3.4.1.1 Warp

Warp is typically identified as a generally regular physical distortion of either part or all of a timber board and manifests as curvature either on a

face or within the length. It includes physical deformations including cup, bow, spring, twist, or any combination of these (see Figure 2.12).

2.3.4.1.2 Wane and Want

Wane and want are characterised by the absence of timber on a face, or along the corner edge of a sawn timber board (see Figure 2.13). Wane is identifiable in situations where presence of the original under-bark surface is exposed, potentially with bark intact. Want is classified as all other situations. Both classifications are also applicable where sapwood is exposed during the sawing process.

2.3.4.1.3 Checks and Splits

Checks and splits are easily identifiable as cracks appearing on one or more faces of a sawn timber boards (Figure 2.14). Checks are the separation of fibres radially across the growth rings of a board and along the grain. This causes a fracture to develop, but does not extend through the element from front to back. Checks can be present on a surface, which is easily detected, or limited to the interior of the board. This makes detection difficult using visual methods of grading, unless exposed at the end.

Splits are a longitudinal separation of wood fibres extending through a board, and are predominantly found in sawn timber. As opposed to checks, splits extend through the board typically from front to back. As the wood fibre direction determines the grain of a timber board, the separation is commonly split non-linearly through the board following the grain direction from the point of rupture. Splitting commonly occurs at the end of a board due to the release of internal forces within the timber during the drying process.

2.3.4.1.4 Knots, Clusters and Groups

Knots are caused by a section of a branch being embedded within a tree trunk, and are defined by their location on a board's cross section or their appearance on a board's surface. Depending on the size and location, a knot can have significant impact on the structural capacity of the tree, and subsequently the capacity and appearance of sawn boards. Visually, knots commonly present as darkened areas of timber with a significant shift in grain direction around a central circular-like core. *AS/NZS 4491: Timber - Glossary of terms in timber-related Standards* specifies twenty-two variations of knots, including tight or loose; sound or unsound; intergrown or not; round or oval; single or in clusters; and knot holes (Standards Australia, 1997). However, *AS 2082-2007: Timber - Hardwood: Visually stress-graded for structural purposes* (Standards Australia, 2007) groups these into type

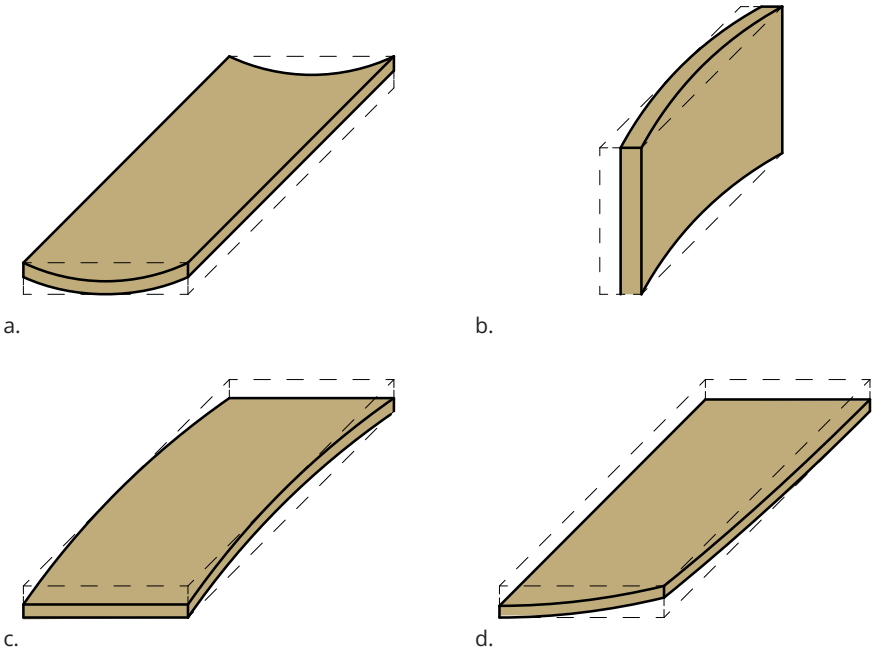

Figure 2.12 Warp based timber feature typologies: Cup (a), Bow (b), Spring (c), and Twist (d).

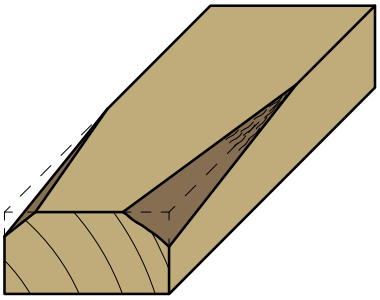

Figure 2.13 Wane and want feature typologies.

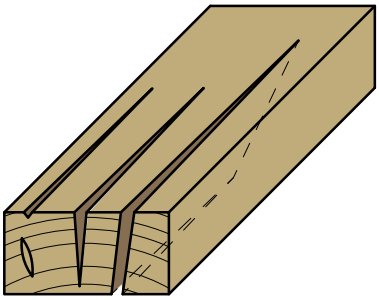

Figure 2.14 Checks and splits in timber boards.

distinct types for the purposes of measurement: those that intersect an arris (a sharp edge formed by the meeting of two curved or flat surfaces) of the sawn board, and those that do not. The measurement techniques for both varieties are shown in Figure 2.15.

Knots are often found near each other and are classified as either knot clusters or knot groups (see Figure 2.16). Knot clusters are when two or more knots are grouped together as an entity and the grain of the timber board is deflected around the entire entity. In contrast, a knot group is identified as two or more knots grouped together where the timber grain passes between them.

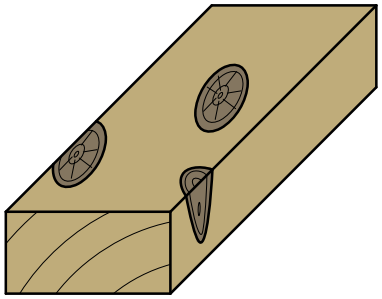

Figure 2.15 Knot based features in timber boards.

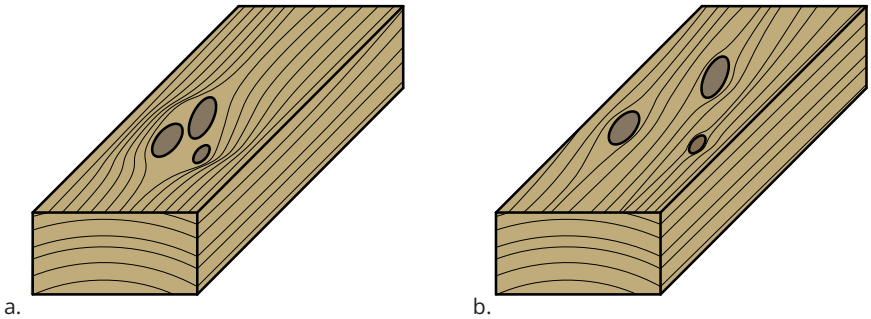

Figure 2.16 Knot cluster (a) and grouping (b) typologies.

2.3.4.1.5 Structural Grade Classification

In addition to the identification and classification of material features, *AS 2082-2007: Timber - Hardwood: Visually stress-graded for structural purposes* describes methods for categorising the likely performance of a board into one of four structural classifications. By detailing the occurrence and severity of material features on a graded scale, in addition to other properties including species, density, and seasoned strength group *AS 2082-2007: Timber - Hardwood: Visually stress-graded for structural purposes* can determine a stress grade for a seasoned board ranging from F7 (having the least structural capacity), through to F34 (which demonstrates the highest structural capacity). *AS 2082-2007: Timber - Hardwood: Visually*

stress-graded for structural purposes also notes that locally sourced *E. nitens* can be graded in the F11 through to F22. However (as discussed in Section 2.3.4) the correlation of these classifications within plantation hardwood (especially when fibre-managed) is tenuous. Despite not grading the timber specifically for structural purposes in this study, there is value in acknowledging the potential capacity of the highest quality timber of the same species.

2.3.5 Applications

While the feature identification methods (discussed in Section 2.3.4.1) are primarily applied to sawn timber boards from native forests, there is inherent value in understanding the material character sets within current industry practices. The three primary considerations are:

a) transferability to plantation timber resources;

b) potential for computerisation; and

c) automation and scalability.

With regards to transferability, the visual identification of material features is relevant to plantation hardwood timber resources. Irrespective of native or plantation forest origin, hardwood species harvested for timber production will contain a set of material characteristics that are consistent. While differing origins and tree species will demonstrate varying intensities and irregularity of naturally occurring material characteristics, they will all be within those specified by *AS 2082-2007*. Additionally, as this identification methodology is widely employed within industry, it supports the potential for scalability with existing workflows. Subsequently, the visual methods of identification and classification are transferable to plantation hardwood timber.

The potential for the computerisation and automation methods of visual classification amongst plantation hardwood is significant. Non-destructive methods of visual grading - processes have significantly impacted its expansion and profitability since the 1980s - are widely used within the plantation softwood industry. While current demand for hardwood within the construction industry is focused on non-structural application, the adoption of Industry 4.0 digital-augmented workflows offers the capacity for both the automation of existing processes and the value-adding of new resource opportunities within the sector.

Finally, the visual identification methods investigated are scalable, in terms of both material volume and size of automation process. As demand for plantation hardwood increases, the method of material character identification will remain consistent. The capacity of an automated

systems to be easily configurable and calibrated allows the workflow to be adjusted to suit natural variation presented by differing timber species and geographic origin, for example. Additionally, the workflows that are developed in smaller scale installations (which employ more cost-effective digital solutions) can be scaled up to larger scenarios by increasing material throughput and specification of industry grade digital hardware. This scalability is critical in developing and demonstrating new modes of DIMPs, which have the potential to be adopted within larger existing industrial settings.

Two points within a DIMP are relevant to the engagement of material data in relation to Australian plantation hardwood. The first requires timber to be catalogued at the point of primary production, resulting in material being graded and data captured within a sawmill as the log is being converted into sawn boards (see Figure 2.17). This data would be tagged to the individual timber element and made available to designers and fabricators, resulting in a level of material data and design control that is greater than that currently available within the industry. This scenario would provide a big-data approach to timber that allows designers to specifically procure and design within the bounds of known features and irregularities of a particular source of material. Yet, this supply-chain intervention requires a significant shift to current timber industry practices, and suggests that an increase in digital means of data acquisition and management are required across multiple industrialised processes (such as, plant botany, silviculture, harvesting, milling and grading), and that the digital data chain is available at the point of supply to fabricators. While this would bring about significant change within the forestry industry, the impact on the architectural and construction industries would remain largely unchanged due to existing lineal modes of procurement within the sector.

The second point of material engagement suggests that material capture can be obtained at the point of design and fabrication. This scenario reduces the impact of widespread change within the existing timber industry, by focusing on capacities of engagement at a smaller scale that is relevant to bespoke architectural outcomes (see Figure 2.17). This setting implies

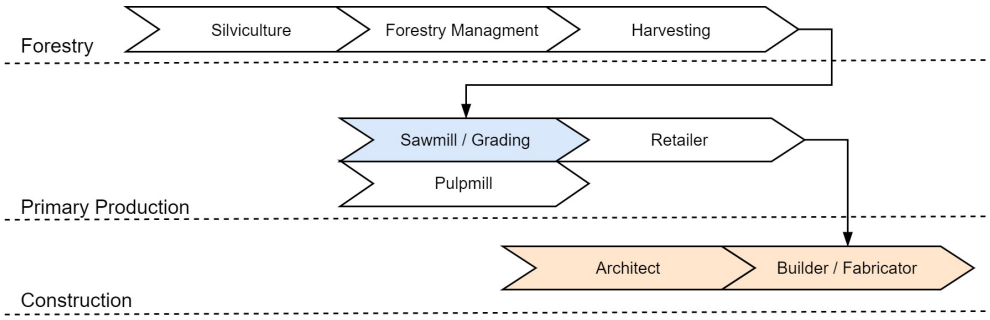

Figure 2.17 Forest to Fabricator workflow indicating the three industry silos.

that timber would be procured from suppliers with minimal information regarding its unique material character, necessitating the design and fabrication workflow to mediate the material data capture and resulting project parameters. This shift in workload may initially seem an extra burden on the comparably smaller scale of architectural practice; however, it presents opportunities for design. Compared with the standardised approaches to grading taken by the forestry industry, this approach fosters a greater capacity for architectural engagement of material irregularities within bespoke environments. Further, as the adoption of Industry 4.0 expands within the architecture and construction sectors, the tools and methods required for this level of innovative material engagement will become more widely available.

While adoption of the first scenario would be beneficial to the architectural and construction industries, it is highly focused on transforming the existing modes of practice within the forestry sector. As such, the second scenario (adopting material engagement within the design and fabrication cycle), is highlighted as the primary point of engagement in this study. The methods developed are aimed at exploiting and adding value at the design and fabrication end of the supply chain. In doing so, they demonstrate that larger shifts within the forestry and primary-production supply-chains have merit from both economic and sustainability perspectives.

2.4 Digitally Integrated Material Practice

2.4.1 The Digital Turn in Architecture

Historically, the practice of architecture has been a manual, labour-intensive endeavour, both in the office and on the construction site. Until the 1980s, a typical architectural practice comprised a room full of architects and technicians laboriously generating precise, hand-drawn representations of a building and its details. However, even the implementation of computers and Computer Aided Design (CAD) systems within architectural practice did not initially alter this method of production. Early applications of CAD were primarily digital reflections of the manual processes they were designed to replace (Leach, 2009, p. 34). The effort required to create a drawing initially did not alter significantly, and the capacity to make subsequent adjustments and reproductions did. While the ability to edit, cut, copy, and paste elements within drawings saved time, it led to an ease in duplication that enabled a new wave of standardised approaches to the detailing of materials and construction systems that were a “computerised extension of the well-known” (Menges, 2016, p. 78).

The development of spline-based drawing tools during the late 1980s and early 1990s was the first major change within CAD software that shifted

it from the traditional hand drawn methods embedded within practice. The precise control of continuous free-form curves was available to designers for the first time. Significantly, the ease of generation, accuracy of evaluation, and capacity to approximate complex shapes promoted utilisation without the need for the designer to have a background in mathematics or computation (Crolla, 2018, p. 29). As CAD software matured, the capacity for the representation of complex curvature extended into three-dimensions through the application of surface-based geometries, giving rise to a curvature and smoothness in built form that was unprecedented. Greg Lynn (1998) first described this stylistically as the 'blob' aesthetic, and it became synonymous with the first age of 'digital architecture' (Carpo, 2017, p. 4; Kolarevic, 2003b, p. 27).

The rapid adoption of this process by the 'digital avant-garde' brought about a fundamental shift in the way architects communicated and understood the design, development, fabrication, and assembly of buildings. Kolarevic and Klinger (2008) note this was a result of the re-emergence of complexity in architectural ideation that could not be adequately conveyed to, or fabricated by, contractors. Early adopters of complex architectural aesthetics relied heavily on digital tools borrowed from allied professions, such as the aeronautics, automotive, and engineering domains. These software tools had a closer relationship with the techniques of design and communication, and the processes used to manufacture them (Kolarevic, 2003a).

Computer-aided design (CAD), engineering (CAE), and manufacturing (CAM) tools that had been available in other industries for many years, were readily embedded into architectural and construction workflows, enabling the realisation of form and materiality otherwise unavailable (Iwamoto, 2009). This flow of information through the design-construction project cycle allowed complex outcomes to be realised with an unprecedented level of execution and precision, which was a direct result of the rise of computer numerically controlled (CNC) fabrication within the construction industry (Dunn, 2012).

While the adoption of these production methods had been typically slow within the construction industry, the benefits were quickly apparent. The physical manifestation of complex digital forms during the 1990s demonstrated that file-to-factory workflows could be applied to architecture and construction, paving the way for adoption across both industries. These integrated methods of CAD and CAM shifted the capacity of architectural tools beyond the use of standardised modes of

construction, allowing the exploration of new systems and materials as cost-effective solutions for buildings.

The underlying means of exploring these systems were parametric and associative-based design frameworks. Providing a fundamental shift from the (previously prevalent) representational nature of architectural design and communication, parametric and associated methods engaged the geometric and numerical relationships between elements as part of a larger system. Branko Kolarevic describes 'parametric' as allowing for an 'infinite number of similar objects, geometric manifestations, of a previously articulated schema of variable dimensional, relational or operative dependencies' (2003b, p. 25). These systems allowed for the efficient communication, and subsequent fabrication, of complex designs that comprised a multitude of unique components, representing a shift away from the modes of standardisation that had been favoured through the 20th Century.

In the twenty years since the emergence of digital modes of design and fabrication as a valid means of architectural exploration, the construction industry has remained relatively stagnant. The adoption of these technologies has typically been implemented as an augmentation layer applied to existing modes of fabrication and construction, akin to Menges' (2016) observations in relation to the adoption of CAD being a digital replacement of manual processes. However, the adoption of Industry 4.0 by the construction industry posits a shift in manufacturing from the automation of generic, labour-intensive and repeated tasks towards the establishment of reciprocal interactions between physical processes and increasingly aware and intelligent computational decision-making strategies. Industry 4.0 (first proposed in 2011 as a mechanism for advancing the German economy) (Lu, 2017), is aimed at achieving higher levels of operational efficiency, productivity, and automation. Stepping beyond the introduction of automation and computing technologies of the third Industrial Revolution (the digital revolution), Industry 4.0 sees the decentralisation of production that emphasises smaller scale and localised management of processes and smart objects through an interlinked supply chain (Erboz, 2017). While the business world is quickly embracing Industry 4.0 as the next phase in the revolution of the manufacturing and processing industries, the construction sector is cautious in this adoption (Maskuriy et al., 2019).

The economic gains that Industry 4.0 will potentially provide might see the manufacturing and production industries the first to widely adopt it as a new way of working (Colella & Fallacara, 2019). In the context of architecture and the built environment Industry 4.0 promotes the re-evaluation of

digital information chains within the design process, incorporating material procurement and specification, design conceptualisation and simulation, and the manufacture and construction of buildings and their constituent elements.

Pivotal to Industry 4.0 is the reciprocal connection between the virtual and physical worlds (Akanmu et al., 2013), commonly referred to as a Cyber-Physical System (CPS). CPS is defined by objects that incorporate technological devices that enable the collection of unique data (using elements, such as sensors) and the transmission of this information to other objects via a network referred to as the Internet of Things (IoT) (Colella & Fallacara, 2019). Critically, the data that is collected at object and process levels is active: it can influence other entities within the overall operation.

The interoperability of data and action paves the way for production to move beyond the linear methodologies of existing supply chains; towards a reactive environment that is alive and adaptive to both internal and external influences. Consequently, this allows industry to embrace manufacturing processes that present highly flexible modes of production that shift away from mass-production, towards unique production cycles, tailored to real-time consumers and economic and environmental needs. Rather than measuring success through productivity efficiencies, as seen in previous industrial revolutions, Industry 4.0 focuses on 'best fit' – customised, demand-based solutions (Colella & Fallacara, 2019).

2.4.2 Computational Materiality

As a material practice, architecture is centred around the notion that materials and making are intrinsically embedded in the design process, both in terms of conceptualisation and realisation. Professor Katie Loyd Thomas suggests that the privileging of form over material is deeply entrenched within architecture practice, and that "material is rarely examined beyond it aesthetic or technological capacities to act as a servant to form" (2007, p. 2). A reversal of this dichotomy is required to examine computational means of engagement within architecture through a material lens. Similarly, Menges (2008) notes that the development of computational material systems should be considered "not so much as derivatives of standardised building systems and elements, but rather generative drivers in the design process" (p. 197). Both views imply that a deep understanding of material character and performance should be populated *throughout* the architectural design cycle.

As industry shifts beyond modes of standardisation in architectural materiality, the overlap between design intent, material character,

performance, simulation and optimisation and fabrication must converge. However, this holistic approach is in contrast with the more sequential modes that both traditional and a significant proportion to which contemporary practice is accustomed (Tamke et al., 2013).

The interrelation of these design parameters requires them to be conceptualised as an interweave of data, resulting in a design 'space' that inherently benefits from computational generation and algorithmic processing of information (Terzidis, 2006). In this regard, material systems can be seen as the computational interaction of a defined system, its external and internal data, and its performative capacity against a set of design criteria or objectives (Menges, 2008). Within such a computational system, material is no longer an understudy to a predetermined form or style; rather, it is an active agent or architectural design. Accordingly, Menges observes that "computation is not limited to processes that operate only in the digital domain. Instead, it has been recognised that material processes also obtain a computational capacity – the ability to physically compute form" (2016, p. 78).

In the context of material applications and performance within CDFs, the power of a DIMP lies in its interactivity and interconnectivity. The capacity for the interplay between design variables is readily available within visual programming platforms, such as Grasshopper3D (Robert McNeel & Associates, 2022) and Dymano (Autodesk, 2021). The process of designing an architectural outcome routinely has multiple inputs and constraints that can be varied to different degrees; however, as the number of design inputs and data sources increase, the opportunity for new, revealable architectural potentialities exponentially expands. Although access to an endless pool of design solutions may appear to be a positive outcome, there is an underlying complexity to the problem. In an ideal world, the complex interactions of design variables would neatly converge to a single solution. Unfortunately, the nature of design is almost always divergent in that the variables, data and objectives are at odds with one another; ever in a state of conflict.

2.4.2.1 Cyber-Physical Approaches to Engagement

The use of computational modelling and simulation in architectural design has historically been employed in digital or physical methodologies. These methodologies have seldom been applied as an integrated workflow to enact an architectural design process or outcome; that is, in architecture,

generally the digital remains digital, and the physical articulation of materiality is a layer of information applied at a later stage.

Contemporary computational techniques, including parametric and algorithmic design processes with physical outputs via computer numerically controlled (CNC and robotic) fabrication strategies, can enact limited machine-based material processes that assume that material and machine are constant. There is little capability for material or machine to augment or be augmented by each other. Within this realm, materials remain homogeneous, and machines are linear processes, excluded from the potential of integrated digital design topologies. An early key example of this method within timber design and construction is the *Landesgartenschau Exhibition Hall* (2014), developed by the ICD Stuttgart (see Figure 2.18). The lightweight segmented timber plate shell was realised using agent-based design tools that mediated multiple constraints including structural capacity, material size, material geometry, connection methods and robotic fabrication limitations (Krieg et al., 2015; Schwinn et al., 2013; Schwinn & Menges, 2015). Although the computational method employed was behavioural, the material engagement and robotic fabrication processes utilised a lineal prefabrication methodology.

Figure 2.18 Landesgartenschau Exhibition Hall (From Schwinn & Menges, 2015, Copyright 2015 John Wiley & Sons - Books. Reproduced with permission).

Similarly, Gramazio Kohler Architects' *Sequential Roof* (2014) in Zurich, (Figure 2.19) applied large scale robotic CNC fabrication methods in the production of a complex, non-standard spatial fame constructed from over 14,000 individual timber elements. The developed CDF negotiated element size, position, structural capacity, fixing details, fabrication constraints, and functional and aesthetic preferences to generate the prefabricated trusses (Apolinarska, Bärtschi, et al., 2016; Apolinarska, Knauss, et al., 2016; Willmann et al., 2016).

Both of these key projects mediate standard and pre-determined materials through computational design, simulation and fabrication, and establish

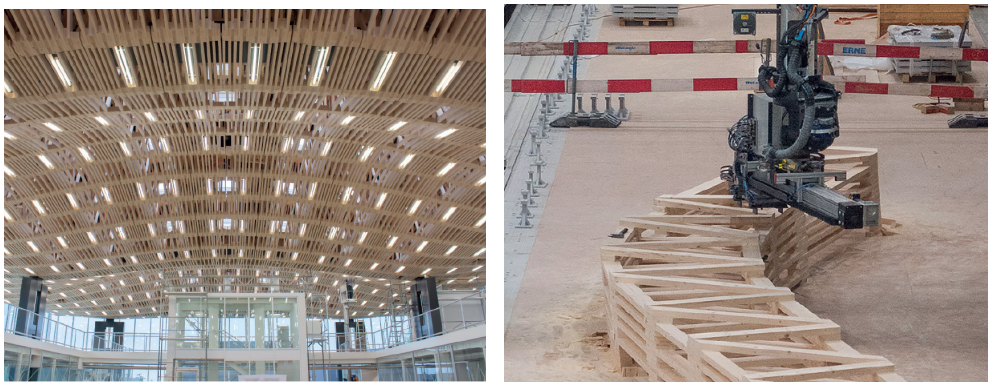

Figure 2.19 The Sequential Roof (From Apolinarska et al., 2016. Copyright 2016 Taylor & Francis Informa UK Ltd - Books. Reproduced with permission)

a lineal file-to-factory workflow that facilitates complex geometries and fabrication methods.

However, integration of machine and material processes support a capacity for reciprocal digital agency: Menges (2015) suggests that as architectural fabrication systems gain increased capacity for sensing, processing and interaction, design and materialisation will converge. This technological leap will afford fabrication systems the capacity to capture their environments and adjust production processes in real-time. The introduction of cyber-physical frameworks (CPF) within architecture presents fertile ground for the uptake of irregular and unknown materials within design.

CPFs provide an integrated environment for digital and physical processes to be integrated throughout a design/fabrication process. The creation of live feedback loops within a CFP establishes a reciprocal relationship between the physical (such as the material, events, processes and fabrication) and digital (which includes computations, structure and form) environments (Vasey & Menges, 2020). The consolidated material practice promotes a scenario that allows design to be emergent to material and fabrication constraints, and *vice-versa*, in a real-time environment (Ramsgaard Thomsen et al., 2020).

A key demonstration of this cyber-physical feedback loop facilitating the engagement of non-standardised timber materials is demonstrated by *House 4178* (2016) (Figure 2.20). Utilising geometrically irregular timber shingles, the layout and assembly of the façade was determined by the physical properties of the material in real-time during construction. Coupling computer vision and robotic assembly methods allowed a predetermined logic to optimise and adjust the placement of individual singles, with regards to underlying structural form (Dell'Endice et al., 2017; Eversmann et al., 2017) and the knowledge of previous shingle placement. In this mode of fabrication, the final organisation of the cladding is unknown until the workflow in complete. The aesthetic quality

Figure 2.20 Robotic Pavilion: House 4178 (From Eversmann, 2017. Copyright 2017 Springer. Reproduced with permission).

and general characteristic of the façade is pre-determined, but the details are a mediation between material availability and immediate localised requirements (Eversmann, 2017). A similar methodology was utilised by Craney & Adel (2020) in their wood shingle façade system studies.

In shifting material irregularity from a geometric constraint to an inherent material property, Giulio Brugnaro's research into adaptive robotic carving (see Figure 2.21) established a cyber-physical workflow that can adapt its fabrication processes in terms of how the carving tool is physically removing material (Brugnaro, 2021). The project utilised a complex subtractive manufacturing process intrinsically linked with traditional craft, coupling trained Artificial Neural Networks (that is, biologically inspired computational networks) with material force feed-back to create an adaptive design and fabrication workflow that was responsive to the inherent heterogeneous material qualities of timber.

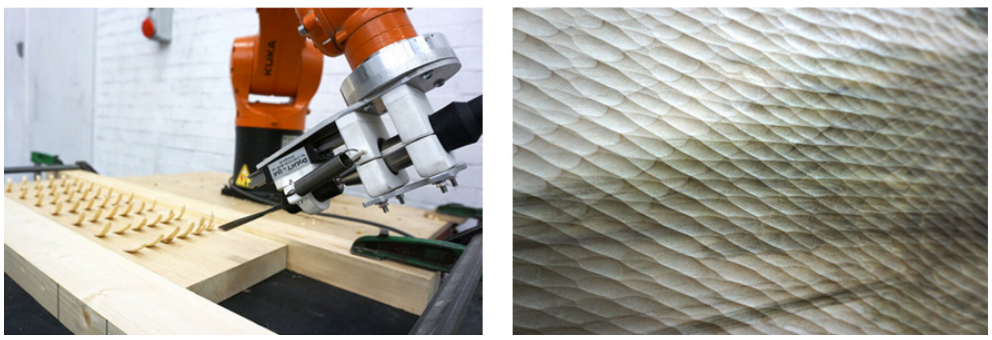

Figure 2.21 Adaptive robotic wood carving with material force feedback (From Brugnaro & Hanna, 2018. Copyright 2018 Springer. Reproduced with permission)

These modes of cyber-physical material and workflow engagement enforce a strategy contrary to current norms; one that requires design to be described and communicated in a responsive manner. A design will have end goals and parameters, but a DIMP determines how materials can be engaged and optimised to meet those objectives, taking into consideration conditions, such as design intent, geometry, structure, construction, economics and sustainability. This premise heralds a new interdisciplinary approach to the relationships between design, material, and fabrication.

2.4.2.2 Capturing Material Irregularity

2.4.2.2.1 RGB-D

RGB and *RGB-D* scanning techniques have been utilised in the context of both increasing yield and improving production line efficiency. It is common for proof-of-concept studies to utilise off-the-shelf hardware solutions, such as the Microsoft Kinect platform (Microsoft, 2022) used to capture data for assessment of product quality. Roii Spoliansky *et al* (2016) and Malcolm McPhee *et al* (2017) utilised this platform to collect real-time data in the livestock industry, for example. These studies couple RGB-D scanning with digital image processing and machine learning to establish a method of assessing the physical characteristics cattle in the livestock industry. As is the case in other modes of computer vision-based material capture (see Section 2.4.2.2.2 and Section 2.4.2.2.3), the introduction of RGB-D based computer vision in this scenario aims to increase the value, efficiency, and yield of existing production processes.

The application of RGB-D methods in the forestry industry has been investigated as a means assessing and monitoring of trees within a plantation (Fan et al., 2018; Hyyppä et al., 2017; Talbot & Astrup, 2021); however, consumer level RGB-D devices (such as Kinect) have been found to be restricted by daylight sensitivity and scan range (Brouwer, 2013). This suggests that RGB-D based scanning techniques are more suited to a controlled, indoor environment.

Applications of RGB-D based computer visions within architectural and fabrication environments have been investigated widely, particularly within smaller scale and tailored applications. The designers of built projects at the Architectural Association's Hooke Park have employed Kinect as a means of capturing naturally occurring three-dimensional tree forms to assess their structural suitability within a building, in addition to the

capacity for robotically controlled modes of digital fabrication (Devadass et al., 2016; Self, 2017).

The Wood Chip Barn (2015), at Hooke Park, employed both RGB-D and *photogrammetry* computer vision methods in the selection of suitable trees for harvesting, and the detailed capture for design and robotic fabrication (Figure 2.22). This approach focused on a high level of material sustainability, as the design outcome was matched exactly with material availability, minimising material wastage.

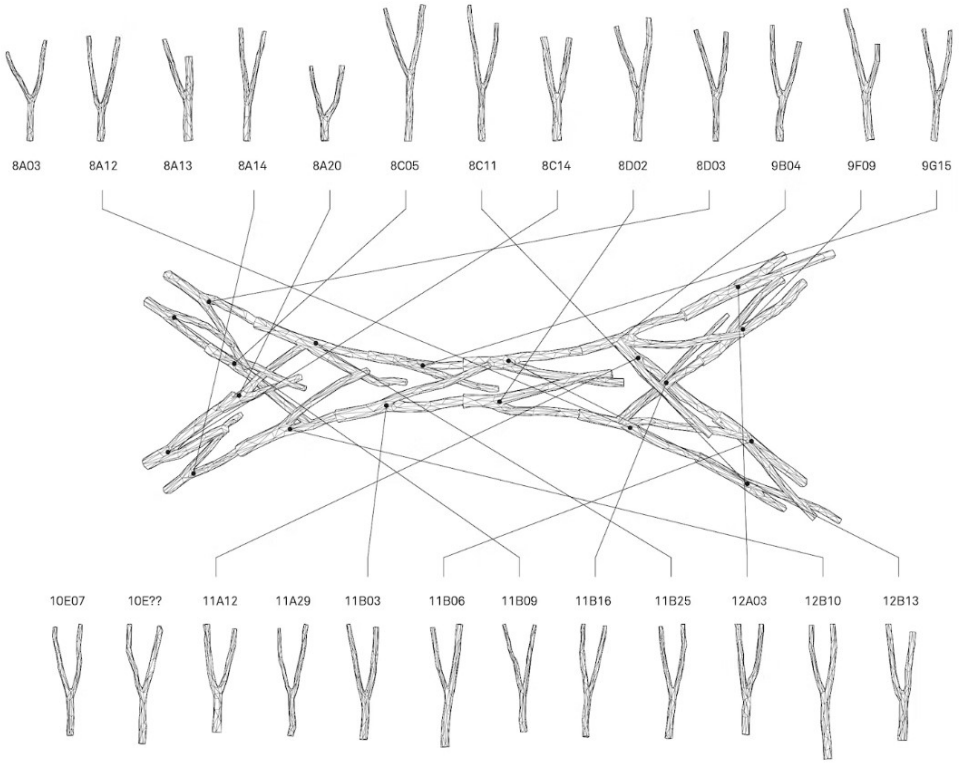

Figure 2.22 The Wood-chip Barn tree fork discretisation and design distribution (From Self, 2017. Copyright 2016 Taylor & Francis Informa UK Ltd - Books. Reproduced with permission)

A similar approach to computer vision enabled waste minimisation is taken by Wu and Kilian (2016), in their investigation of the utilisation of material offcuts within the fabrication process. As opposed to the Wood Chip Barn (Figure 2.22), this experiment did not pre-determine or optimise the arrangement of irregular elements prior to fabrication; rather, it assessed the material and calculated its location once the assembly process had begun. As such, the digital capture of elements on-the-fly is dependent on the creation of an unknown structure that performs within a set of design goals. This methodology was adapted in their investigation into the assembly of complex structures using irregular timber logs (Wu & Kilian, 2018) (Figure 2.23).

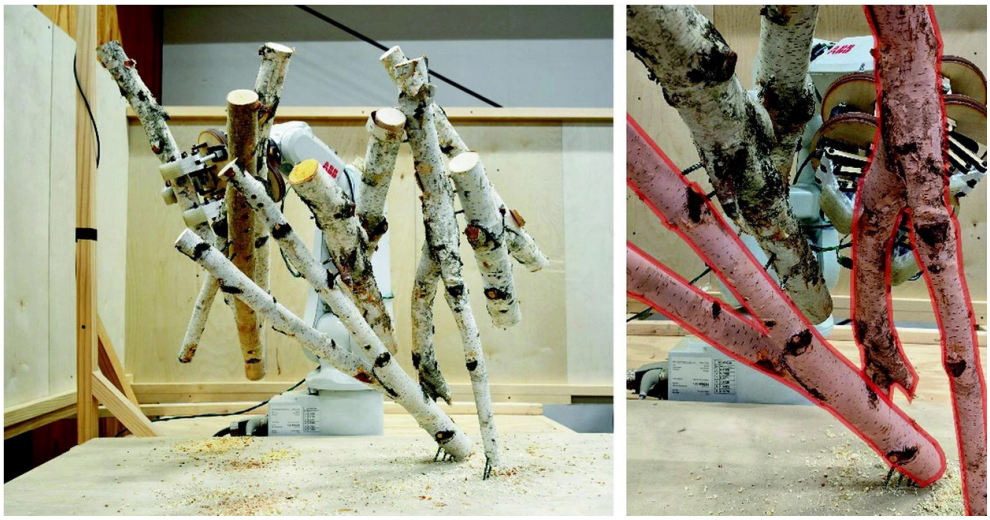

Figure 2.23 RGB-D assisted material capture and robotic placement (From Wu & Kilian, 2018. Copyright 2018 Springer. Reproduced with permission)

2.4.2.2.2 LiDAR

LiDAR (*Light Detection and Ranging*) is a technology that uses laser beams to measure the distance between a sensor and objects in the environment. First conceptualised in 1920 by Edward Synge (Synge, 1930) the invention of the laser (*light amplification by stimulated emission of radiation*) in the late 1950s saw its development and adoption in environmental science and military applications (Wandinger, 2005). Its technological development has continued to advance during the latter part of the 20th Century, with its development into LiDAR scanning, which is used in a wide variety of commercial applications, including autonomous vehicles, geology, mining, robotics, surveying and agriculture.

The management of plantation forests is also undertaken using LiDAR systems to monitor the growth, health, and yield of the trees during their lifecycle, prior to harvest. Coupled with GPS enabled land and airborne based systems, LiDAR has the capacity to scan large, forested areas and calculate land topography, distribution of plant canopies, volume of recoverable timber and likely vegetation structural characteristics (Lefsky et al., 2002; Wotherspoon, 2008). This facilitates predictions regarding the maturity of the forest, potential yield and suitable strategies for further management and harvesting (Guo et al., 2021; C. Xu et al., 2018) (Figure 2.24). While these conclusions can be drawn using traditional field work and analyses, there are significant economic advantages in utilising digital system of material capture at a forest scale (Means et al., 2000). These methods contribute to the decision-making process about when a forest is ready to harvest, which subsequently impacts the economic return of the investment.

LiDAR scanning techniques have also been adopted in architectural design and fabrication workflows that require a high level of precision between

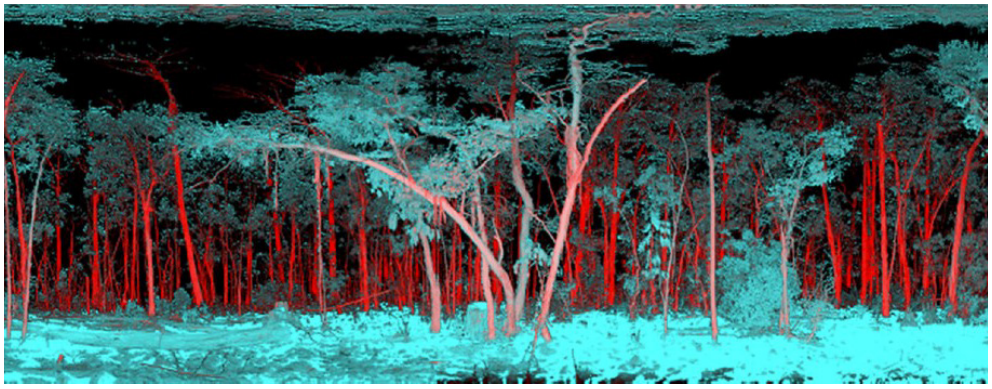

Figure 2.24 LiDAR scan of open forest canopy distinguishing between woody (red) and non-woody (blue) tree materials (From Newnham et al., 2015. CC-BY-4.0, Reproduced with permission)

irregular materials and tolerance within fabrication processes. At the material capture end of the workflow Aagaard and Larsen's investigations demonstrate the capacity of LiDAR scanning to capture the irregularity of crooked tree logs for use in innovative design and fabrication environments (Aagaard & Larsen, 2020; Larsen et al., 2020; Larsen & Aagaard, 2020). Similar methods can be utilised within mass-timber fabrication to assess the accuracy of complex, curved Glulam banks prior to fabrication (Svilans et al., 2019), in addition to validating the precision of fabricated elements against the digital models (Svilans et al., 2020) (see Figure 2.25).

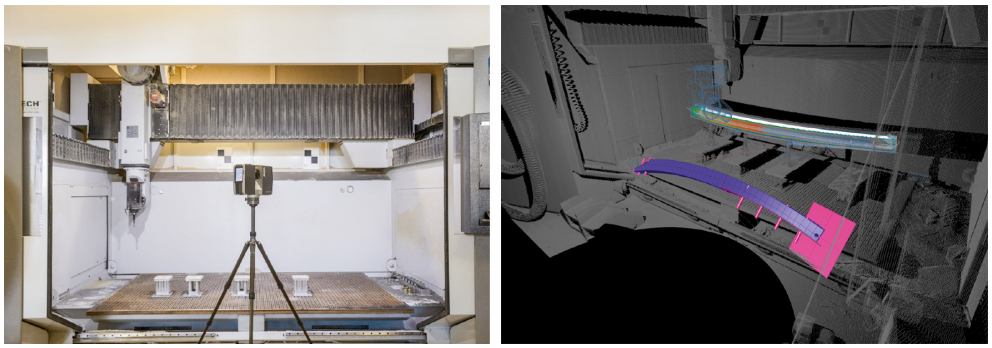

Figure 2.25 LiDAR scanning for fabrication precision of complex mass timber elements (From Svilans et al., 2020. CC-BY-4.0, Reproduced with permission)

In addition to the validation of fabricated elements within production environments, LiDAR scanning is emerging as a method of live material capture on construction sites as it can inform the assembly logics of structures. For example, building upon earlier RGB-D based experiments undertaken in controlled indoor environments (Furrer et al., 2017; Johns & Anderson, 2019; Liu et al., 2021), early experiments by Johns et al. (2020) relate to developing methods that couple the real-time LiDAR scanning with a robotically controlled excavator to construct dry-stacked stone walls with materials that are unknown prior to the commencement of assembly. The LiDAR methods employed enable terrain mapping, material localisation and digitisation, and assembly planning and automation, in real time, as a means of engaging materials of irregular character in a

structural assembly that would traditionally be required to be executed by skilled stonemasons.

2.4.2.2.3 Computer Tomography

Once a forest reaches maturity and is harvested, the application of computer vision methods can be applied at the sawlog processing stage. It is increasingly common for larger sawmills (particularly in the North America and Europe) to employ *Computer Tomography* (CT) scanning as a means of optimising sawing strategies to increase recoverable yield (Fredriksson, 2014; Rais et al., 2017; Ursella, 2021). CT scanning techniques can be enhanced through machining learning and Artificial Neural Networks in order to increase the accuracy and reliability of feature detection within a sawlog (Nordmark, 2002).

Andreas Rias et al. (2017) found that CT and machine learning techniques could increase recovery yield by up to 20% through the optimisation of log positioning and rotation prior to sawing. When coupled with non-destructive mechanical testing methods, computer vision can provide a complementary assessment of potential material performance and grading (Hashim et al., 2015; Mitsuhashi et al., 2008).

While these applications demonstrate CT scanning can identify material features within an industrialised sawmill environment, the datasets are rarely passed down the supply chain (Martin et al., 2021), as the current (standardised) approach to timber grading is the basis of material specification within the architecture, engineering and construction industries. As a result, data-rich material explorations are unlikely to occur without the re-capturing and assessment of timber boards at the point of design and fabrication.

The RawLam series of experiments undertaken by Tamke et al (2021), demonstrates the opportunities of integrating sawmill-based CT imagery within architectural design processes. Tamke et al (2021) employed industrial CT scanning of whole timber logs as a means of enhancing the persistence of the material data chain from forest to production (Martin et al., 2021). The high-resolution material data allows the timber to be sawn and subsequently allocated to the specific structural, assembly and fabrication performance demands of a non-standard glue laminated structure (Figure 2.26). This methodology challenges traditional notions of material utilisation as it integrates the discrete engagement of a unique material inventory and optimises its utilisation in non-standard design scenarios.

With highly automated modes of computer vision being limited to industrial sawmills (due to the scale of operation and subsequent financial

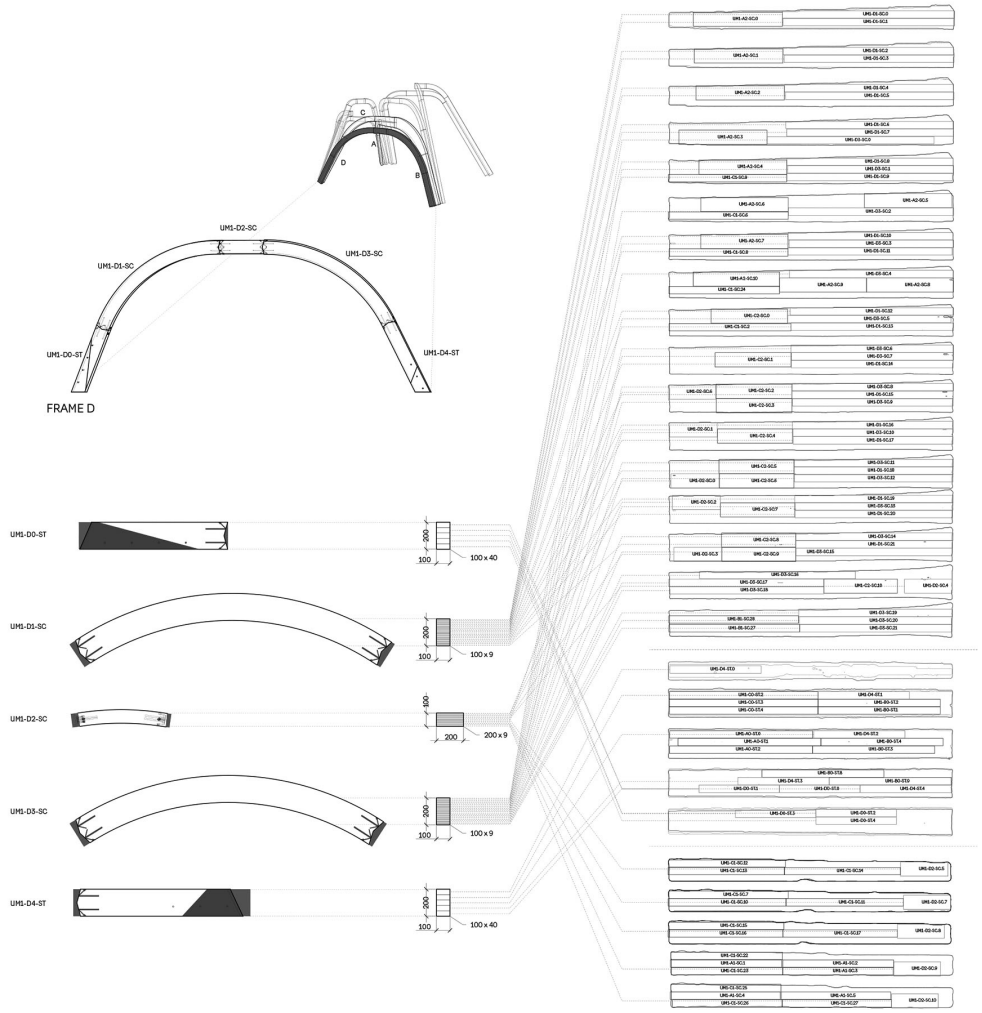

Figure 2.26 Umeå 01 (RawLam 3): Allocation of timber boards within bespoke structural glulam beams (From Svilans, 2021b. Copyright 2021 CITA. Reproduced with permission)

burden), is it unlikely that these more advanced techniques will be scalable to smaller-use case scenarios. This highlights the need for investigations pertaining to innovative digital processes, positioned *outside* the primary processing environment of industrialised sawmills, that integrate semi-automated modes of feature identification and material capture. There is an opportunity for computer vision methods to be integrated at the point of design and fabrication, and utilising consumer level scanning technologies as a methodology for the classification of feature rich timber boards that originate from fibre-managed hardwood plantations.

2.4.3 Constrained Material Inventories

The success of an DIMP is highly dependent on the quality of the data on which it is built. By using common, standardised building materials, the dataset is typically known and predictable: the dataset will include (amongst others) specific physical dimensionality, defined performance properties, and demonstrate a predictable level of aesthetic variation. While these

traits are relatively constant within commonly used construction materials, they present quite differently within naturally occurring materials.

In the case of construction grade timber, Svilians (2020, p. 70) suggests that even the clearest and featureless timber boards contain unique properties that are not captured, and states that material heterogeneity needs to be encoded in order to optimise computational modes of material representation and interfacing (Svilians, 2020, p. 143).

While fibre-managed plantation timber presents the same typology of material characteristics, the scale of irregularity is significantly larger. As such, innovative methods of material encapsulation and encoding are required to ensure material properties are accurately represented within the digital design environment. In essence, CDFs require an inventory of classifications to optimise material application within a design workflow.

The consideration of construction material as an inventory in architectural practice is not new, with existing cataloguing and communication methods limiting availability to a narrow field of options, commonly based around the methods of standardisation in the manufacturing process. For example, a sheet of plywood could be specified as having a particular size, thickness, structural rating, appearance grade, glue type or timber species. While each configuration of these properties would result in a different sheet of plywood, it is still a sheet of plywood with known homogeneous characteristics. In shifting to irregular materials that demonstrate heterogeneous characteristics, the idea of a catalogue of options is no longer applicable. As each element within the catalogue is unique, the inventory becomes constrained, and it is no longer a case of selecting an option and ordering fifty of them; rather, it establishes a scenario that dictates that design must be responsive to the material that is directly available and optimised to each element's unique characteristics.

The notion of working within a constrained inventory of materials for design and construction is also not new. Significant research and project examples that incorporate the use of waste products, reclaimed materials, and those with naturally occurring irregularities, have been explored since 1990 (Gorgolewski, 2008; Monier et al., 2013; Stanton, 2010). However, there are several other significant projects that have coupled constrained inventories of irregular materials with CDF, and which shift beyond single irregularities and top-down approaches to material engagement.

An early example of developing a constrained inventory of irregular material is Klinger's SmartScrap collaboration with the Indiana limestone industry (c. 2005), which investigates the material capture of irregular stone slabs for reuse (Klinger, 2007). The cutting of stone generates significant volumes of potentially reusable pieces that, without an accurate

inventory of their properties, have no effective method of reuse. In this project the physical shape and dimension of each offcut, in addition to the appearance and texture information, was recorded. The resultant data, documented in an Excel spreadsheet, was employed in a subsequent virtual demonstrator project that matched a mosaic layout with material character in a parametric software environment (Klinger, 2008, p. 33). Although employing the material in non-performative manner, Klinger inadvertently established one of the earliest architectural applications of a constrained digital inventory of irregular materials.

The strength of digital inventories, such as that established by Klinger's selection methods, is now recognised in the discipline as an opportunity for engaging waste and disregarded materials more effectively. Carpo, for instance, argues that the strength of databases is that they enable the search of inventories, rather than simply the sorting or organising of data (2017, p. 23). By allowing the classification of elements across categories or characteristics, data can be recalled based on searching for a series of descriptors; rather than looking in a single location for the best matching piece. This factor is an invaluable tool in the cataloguing and recalling of discrete material elements.

It is evident the engagement of constrained material inventories is inherently linked with sustainability-based objectives, including the minimisation of waste through reclamation and redeployment. Fivet and Brütting (2020) demonstrate the computational methods of engaging constrained inventories through the reuse of deconstructed elements in structural applications (see Figure 2.27). Through their series of investigations (Brütting et al., 2018; Brütting, Senatore, et al., 2020; Brütting, Vandervaeren, et al., 2020), a particular focus on repurposed steel elements in truss-based structural configurations becomes evident.

Their work culminated in the development of the industry-focused Phoenix plugin (Warmuth et al., 2021) for the Rhino/Grasshopper3D (Robert McNeel & Associates, 2021) environment. This plugin offers two methods of stock-controlled design Mixed-Integer Linear Programming and Best-fit Heuristic, which both allow for the inclusion of reused and new elements within the processes.

Further, the inclusion of life-cycle analysis and configurability for either steel or timber materials provides the capacity for assessment of environmental saving, through the reuse of materials (Warmuth et al., 2020). While these investigations support the comprehensive engagement of a constrained inventory of material, they also continue to treat the material inventory

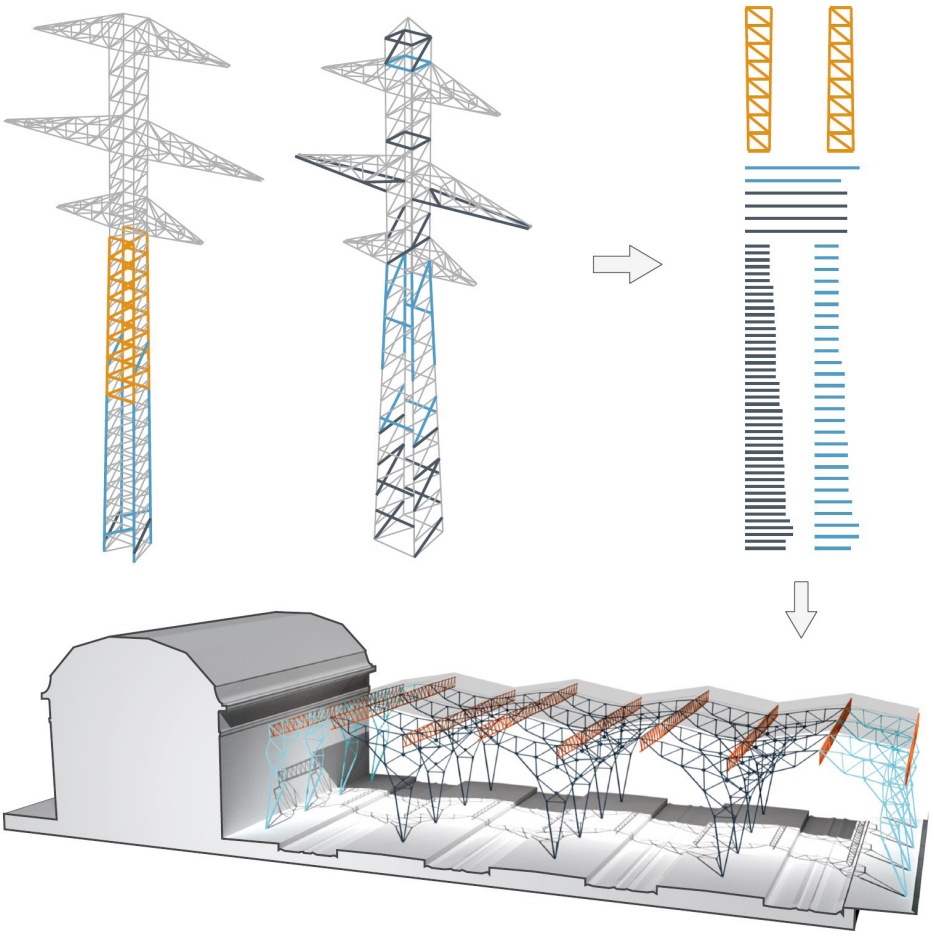

Figure 2.27 Reuse of steel elements from electrical pylons within a new roof structure using the Phoenix plugin (From Brütting, Desruelle, et al., 2019. CC-BY-NC-ND-4.0, Reproduced with permission)

as a dimensionally varied entity, which has a pre-determined structural capacity.

In shifting the notion of constrained digital inventories to timber, the researchers of several recent projects are exploring a restricted supply of material as a method of digital material practice. Bukauskas et al investigations into the structural applications of a constrained inventory of dimensionally varied whole tree logs (Bukauskas et al., 2017b, 2017a), and employed search strategies employ heuristic methods of combinatorial optimisation (Bukauskas, 2020) to correlate physical and predictive material data against a range of structural scenarios.

As noted in Section 2.4.2.2.1 the *Wood Chip Barn* (2016) employs evolutionary methods of optimisation to engage material variation and determine material placement within a semi-prescribed spatial geometry (Mollica, 2016; Self & Vercruysse, 2017). While these methods leverage the irregularities of whole timber logs as a viable material for construction, they

do not address the most common form of timber within the construction industry; namely, the sawn board.

Exemplars of the engagement of sawn timber, within constrained inventories through computational methods, are limited for two reasons:

a) Sawn timber salvaged from the demolition of buildings is typically redeployed in its existing form, or cut to size to fit design requirements.

b) Out of grade timber and offcuts generated through the milling process are typically converted to low-grade commodities (such as woodchip or solid fuel) as quickly as possible to minimise the cost of additional processing and storage (Asa et al., 2022).

The designers of the Suspended Remnants project (2019) employed a constrained inventory of below-grade softwood offcuts to negotiate the designed form of a funicular structure (Baber et al., 2020). The inventory of materials provided length variation of timber elements as a basis for a Heuristic distribution method, and they sought to optimise the location of inventory elements throughout the structure by assessing its capacity to accommodate the curvature of individual segments required within the base form (Figure 2.28).

The designers also employed a structural relaxation method that negotiated the rigidity of the base structure with the closest approximation of material placement (Baber et al., 2019). While this method did not provide a fully material led design application, it is representative of a computational

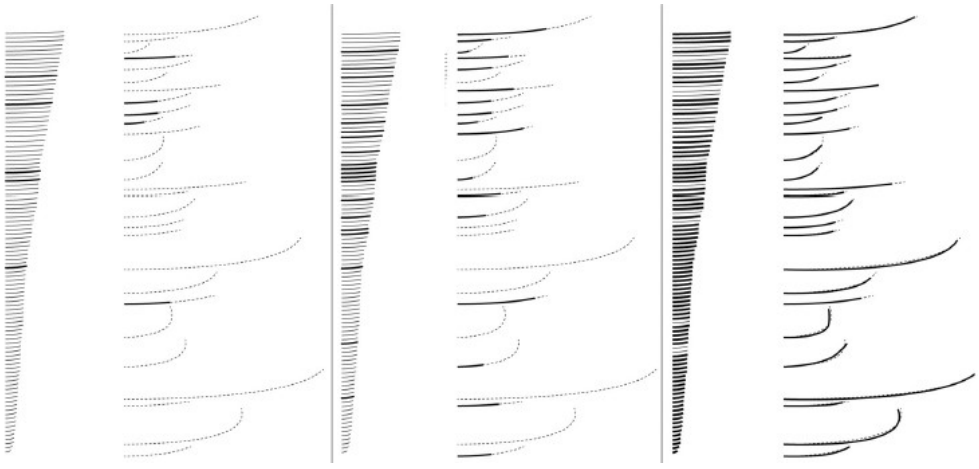

Figure 2.28 Suspended remnants – allocation of timber elements to closest matching structural location (From Baber et al., 2020. Copyright 2020 Springer Nature. Reproduced with permission)

mediation of material, form, structure, and design intent that successfully places a digital-augmented material processes within a design workflow.

2.4.4 Computational Optimisation

It is evident from the precedents discussed in Sections 2.4.3 and 2.4.4 that explorations of heterogeneous materials and constrained material inventories demonstrate an increased use in methods of optimisation to mediate the complexities of indeterminate material characteristics and complex design objectives. This reflects both the wider accessibility of computational tools that integrate optimisation methods within architectural design, and the significance of optimisation as a method of negotiation between complex variables.

The complexity associated with negotiating a set of competing design objectives and a multitude of variables is intrinsically embedded within the generation of architectural design. At its core, architectural design remains a process of manual adjustment of a set of variables, with the aim of finding the best (or most optimised), solution for a predetermined set of design objectives. As noted in Section 2.2.3, the adoption of standardised practices in the construction industry has negated this complexity by reducing the number of variables available from which architects can choose. However, even scenarios with a single design objective can produce millions of potential solutions, governed by the number of initial input variables. It is impossible for traditional modes of design generation to test and select the single best option from an extremely large pool of potential solutions.

This complexity is significantly amplified with the introduction of multiple conflicting design objectives and material irregularity. An example of conflicting design objectives is the hypothetical design problem (Figure 2.29), which requires a material to be selected for a structural application with three design objectives: *use the lightest, strongest, and cheapest material*

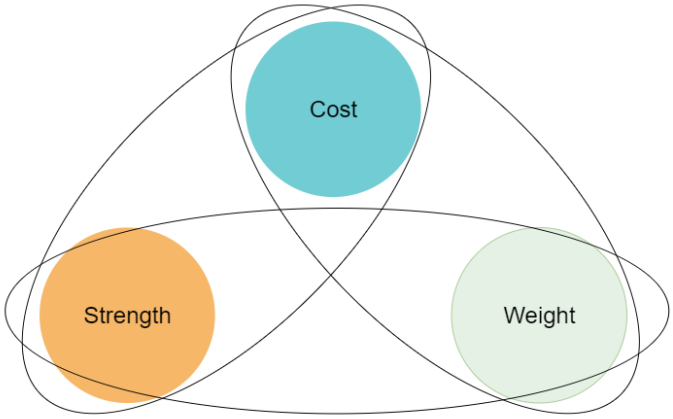

Figure 2.29 Hypothetical design problem with conflicting objectives

for the structural purpose. While intentionally abstract, it is evident that a potential solution can only meet two of the three objectives – it can be:

- strong and lightweight, but expensive;
- strong and cheap, but heavy; or
- cheap and lightweight, but structurally inadequate.

This scenario necessitates a preference-based decision to be undertaken within the design process; an approach that results in the selected solution heavily influenced by subjective personal preference, rather than objective optimisation. As the number of design objectives increases, the capacity for a subjective process to be effective in selecting an optimal solution decreases rapidly.

The introduction of irregular materials into the design problem results in an infinite number of potential solutions to be generated, which eliminates the possibility of subjective design testing. In the hypothetical design problem (Figure 2.29), the singular input variable was the specification of a standardised material that had homogeneous performance characteristics. While substituting this with a constrained inventory of material, such as fibre-managed plantation hardwood, would result in a single material variable being specified, every available element would be unique, resulting in an infinite number of potential material configurations that would be impossible to find an optimised solution for. As such, the complexity of a design problem with multiple design objectives and a large pool of input variables necessitates computational optimisation methods to be employed within the integrated design workflow. This is apparent in recent explorations with irregular materials that have been integrating optimisation methods within their workflows.

Many methods of computational multi-objective optimisation have been utilised in design problems, and include:

- the Genetic Algorithm (Holland, 1962);
- Evolutionary Strategies (Rechenberg, 1965);
- Ant Colony Optimisation (Drigo, 1996); and
- Particle Swarm Optimisation (Kennedy & Eberhart, 1995).

Conversely, Makki (2019) observes that computational optimisation techniques are not limited to those originating from the biological paradigms of the natural world. Methods such as Simulated Annealing (Kirkpatrick et al., 1983), Hill Climbing (Ackley, 1987), and Random Optimisation (Rastrigin, 1963) are examples of such alternatives. In both biological and non-biological paradigms of optimisation, the utilisation of

population-based methods allows for the examination of design problems that comprise multiple conflicting objectives and variables, negating the need for subjective based preference between design criteria. This population-based approach is critical to the simultaneous and independent optimisation of multiple objectives, a process that has been extensively explored through MOEAs, specifically through the integration of *Pareto front* optimality within the algorithmic framework that ensures solutions are selected based on optimisation, as well as variation.

In the context of architectural design and construction, the application of evolutionary optimisation methods, specifically MOEAs, has gained momentum since 2010. This is in part due to their integration within the Grashopper3D (Robert McNeel & Associates, 2022) visual scripting environment through the Biomorpher™ (Harding, 2022), Octopus™ (Vierlinger, 2018), DeCodingSpaces Toolbox™ (Abdulmawla et al., 2017) and Wallacei™ (Makki et al., 2022) plugins. The intuitive interface provided by Grasshopper3D's interface affords architects the opportunity to optimise complex multi-objective, design-based problems using methods that would otherwise be well beyond their mathematical capacity.

The application of optimisation within a design context requires three key stages to be identified:

1. Design problem formation;
2. algorithm selection; and
3. analysis of the results for the purposes of selection.

Stage 1 requires the methodical and delicate interplay between three key metrics:

a) The input variables that inform the morphology (genes);

b) the morphological characteristics that are being generated (*phenotypes*); and

c) the *Fitness Objectives* that are being optimised towards.

Using the hypothetical design problem (see Figure 2.29), the genes would be specified as the constrained inventory of irregular material, the phenotype correlates with the structural arrangements of elements, and the Fitness Objectives comprise numerical simulation of the cost, weight, and strength of the phenotype.

Stage 2 requires the selection of an evolutionary algorithm to optimise the inherent design problem. Many differing MOEAs have been developed over the past twenty years, each with varying degrees of optimisation success and efficiency (Huang et al., 2019; Nedjah & Mourelle, 2015). Of

those surveyed within these studies, the NSGA-2 algorithm developed by Deb et. al. (2000) is widely accepted as an efficient MOEA that facilitates the interrogation of large pools of Fitness Objectives and variables, while requiring relatively low computational capacity.

Additionally, of the currently available optimisation algorithms available within Grasshopper3D, the NSGA-2 is the most widely employed, as it presents a significant advantage in its integration within design workflows.

Stage 3 is related to the selection method employed to reduce the algorithmically generated pool of solutions down to the most highly optimised solution; however, as MOEA design problems usually contain conflicting objectives, the selection method will most likely result in a small pool of the fittest, compromise solutions. These solutions form part of the *Pareto solution* front, which represents the most optimised solutions generated by the MOEA.

Depending on the size of the solution pool, the number of Pareto solutions can vary widely, with larger quantities resulting in a more complex selection process for the designer. A greater conflict between design objectives will typically result in a greater diversity in the Pareto solution set, requiring a rigorous analytical approach to selection, and as such, the selection approach is critical to the capacity to rationalise the algorithmic output of a MOEA.

Within the context of this research, the Wallacei plugin (Makki et al., 2022) is employed to generate both single and multi-objective design problems for three reasons.

a) It employs the widely accepted NSGA-2 algorithm as its evolutionary solver.

b) It incorporates several methods of analysis to assist in rationalising the generated solution sets.

c) Its integration within the Grasshopper3D environment provides the capacity to engage MOEA processes, in addition to other methods of data capture and simulation relevant to constrained inventories of fibre-managed plantation hardwood and DIMPs.

2.5 Discussion

As discussed in Section 2.2 the construction industry's impact on the environment, and its subsequent contribution to global climate change, is undeniable. The standardised manufacturing processes, introduced during by the Industrial Revolution and promulgated by economic capitalism, contribute to most of the current elemental based material systems within

the built environment. These energy-intensive manufacturing processes rely on the consumption of non-renewable resources that will eventually deplete, as the global population increases by a predicted 2.5 billion people by 2050 (United Nations: Department of Economic and Social Affairs, 2019). Additionally, export markets facilitate the global distribution of mass-produced construction materials, placing increased demand on localised resources for the economic gains available in other countries.

These methods of material procurement and utilisation are a relatively recent phenomenon; established during the Industrial Revolution and optimised in the second half of the 20th Century. Prior to this, the relationship between material, design and construction was closer, with a single 'master-builder' controlling all aspects of creating a building. This is evident in vernacular architecture typically constructed from locally sourced heterogeneous materials, such as stone and timber. Unfortunately, this approach has been diminished by the 'siloing' of specialisations and responsibilities within architecture and construction since the early 1900s. Accordingly, if the architectural industry intends to address its impact on the material world it must re-evaluate its relationship with both renewable and sustainable sources of material, and its role in the interdisciplinary nature of the construction industry.

Of the renewable materials available for construction, timber offers significant opportunity for the construction sector to intensify its engagement with materials that sit outside of the widely available standardised palette (Section 2.3). Already widely used in construction applications in developed countries, plantation softwood transformed the residential construction industry in the second half of the 20th Century, by offering a renewable resource with low-embodied energy, having a positive carbon footprint, being fully recyclable, having comparatively high strength to weight ratio, and can be easily manipulated on the construction site. Now, as climate change impacts the viability of plantation softwoods forests across the globe, there is the opportunity for the forestry industry to supplement the short fall with plantation hardwood timber products.

In the Australian context (Section 2.3.1), approximately 40% of plantation forests are hardwood species. Unfortunately, 81% of this resource is managed to produce material suitable for fibre markets (pulp and chip), resulting in timber that is currently unsuitable for contemporary construction purposes. A similar predicament is present globally with an estimated 93% of the 22.57 million hectares of plantation hardwood being fibre-managed. While there are opportunities for this resource to be used in the construction sector in developing mass timber markets, the current manufacturing processes mostly relies on similar wasteful standardisation

methods. Further, the knowledge gained from when the forestry industry engages digital modes of material assessment and processing is siloed, eliminating potential for the persistence of rich material data to be passed along the supply chain to designers and fabricators. For fibre-managed plantation hardwood to be widely adopted as a sustainable construction material, new modes of engagement are required that accommodate heterogeneous and irregular materials within architecture and construction.

The technological transformation (Section 2.4) embedded in the adoption of Industry 4.0 across the construction industry has potential to afford the capacities required to engage material irregularity with design and construction workflows. Material supply-chains are set to be transformed, by employing new modes of material capture and discretisation that (when paired with models of performance prediction) allow intrinsic material data to be accessible within the design process at an elemental level.

Material-aware design workflows will allow the interplay of heterogeneity, performance, and design intent to become active agents of design generation through the application of computational simulation and optimisation (Section 2.4.3).

These innovations have the potential to transform the industry, significantly reducing its impact on carbon emissions and climate change, and in turn ensuring that the built environment has a sustainable future. While it is evident that the adoption of transformative technologies is required to address some of the construction sector's environmental shortcomings, it has been historically slow and resistant to substantial change (Maskuriy et al., 2019). Without proven applications of new materials and processes, (especially in relation to economic viability) it is unlikely there will be a rapid realignment within the industry.

In Chapter 3, Chapter 4 and Chapter 5 of this practice-led research a series of investigations and design experiments are developed that examine tailored implementations of digitally enabled material practice. The workflows generated demonstrate that material-led processes are viable options for design intervention. Chapter 3 comprises a series of investigative Probes that develop workflows informed by four key technology innovations identified by the literature review, namely:

- RGB computer vision methods that enable the capacity to differentiate knot typology within plantation hardwood boards;
- high resolution material feature recognition and discretisation of timber board defects, and the development of a constrained material inventory;

- a design and fabrication workflow that is responsive to material irregularity in the generation of an architectural panel with acoustic performance properties; and
- a innovative mass timber workflow that employs a multi-objective optimisation process to correlate the distribution of highly featured timber boards with the specific localised performance requirements of a laminated timber panel

Chapter 4 and Chapter 5 apply these Probes as digitally integrated design and fabrication workflows within two Design Prototypes.

3 DESIGN PROBES

3.1 Introduction and Chapter Structure

The design-centred component of this study focuses on computational interventions and workflows, which encompass design and fabrication environments as a means of engaging the heterogeneous material qualities of fibre-managed plantation hardwood, as a valid medium of architectural exploration. The engagement of material irregularities at the juncture of architectural design and fabrication reduces the integral changes that the primary production stages of the timber industry need for performance endurance. This study's experimentation thus assumes that material is available for use in sawn board form of varying physical character and performance, with minimal data specific to the boards themselves.

This chapter details four investigative Probes that establish methods of material engagement and, as such, this chapter is divided into four parts:

1. Probe 1: RGB-D scanning;
2. Probe 2: RGB and constrained inventories;
3. Probe 3: Architectural panel; and
4. Probe 4: Evolutionary optimisation.

The Probes are envisaged as developmental precursors to the larger material-centric design explorations undertaken in Chapters 4 and 5. The four Probes fall into three key domains (the relationships between each are illustrated in Figure 3.1):

Figure 3.1 Design Probe field of inquiry: Material understating, Material optimisation, and Material fabrication domains; and Method development and Design integration Typologies.

- Material understanding;
- Material fabrication; and
- Material optimisation.

Further, two Probe Typologies are investigated:

- *Method development*, comprising Probes 1 and 2, are standalone investigations that develop techniques of material characterisations, capture and cataloguing; and
- *Design integration*, comprising Probes 3 and 4, aimed at to embedding the methods within small design related contexts.

Material understanding-based Probes develop methods that enable the discretisation of physical material, allowing it to be engaged in design-based scenarios. These Probes seek to identify visually identifiable timber characteristics including warp, wane and want, checks and splits, and knots, as outlined in Section 2.3.4. Two Probes are investigated within this domain and are detailed in Sections 3.2 and 3.3;

- *Probe 1: RGB-D scanning* (Section 3.2) investigates an RGB-D based method of material capture that can identify material features and differentiate physical three-dimensional deformation on the surface of a timber board; and
- *Probe 2: RGB and constrained inventories* (Section 3.3) investigates a high-resolution optical capture method and detection that generates a constrained inventory of available timber boards in a digital environment.

The material fabrication domain contains *Probe 3: Architectural panel* (Section 3.4) and investigates a method of digital fabrication that can be driven by material irregularities. This Probe identifies and engages material features as design generators for material augmentation within an architectural hybrid acoustic panel. In doing so, this Probe considers the practicality of utilising lower grade materials within DIMPs.

Finally, the material optimisation domain comprises *Probe 4: Evolutionary Algorithms* (Section 3.5), which employs a Multi-Objective Evolutionary Algorithm (MOEA) to optimise the distribution of irregularly featured boards within a laminated panel. It seeks to correlate knot-based timber features with areas of the panel that have specific performance requirements. In doing so, this Probe seeks to develop a computational optimisation

workflow that negates the need for the manual selection and placement of boards within laminated panel-based products.

The investigative Probes in this Chapter generate a set of discrete computational methods and demonstrators that have capacity the to engage with the intrinsic character of irregular materials, at differing stages of the design workflow cycle. As such, they are intended to be scalable to suit combined and hybrid applications within the Design Prototypes (as undertaken in Chapters 4 and 5).

3.1.1 Timber Orientation

Within the Probes and Prototypes of this study, the axial planes of a sawn timber board are referenced in accordance with the Cartesian coordinate system (Figure 3.1). The length, thickness and width of a board is nominally aligned with the X-axis, Y-axis and Z-axis respectively. The origin (0, 0, 0) of the board resides at the intersection of these axes.

A sawn board has a front face (a), which aligns with the XZ-axis, and a back face that sits on the opposing side. Within a face, the grain of the timber will be visible and run lengthwise along the XY-axis of the board. The edges of the board also run lengthwise, are narrower than the faces, and has a top (b) and bottom designation. The ends of the board (c) are formed by cutting using a saw, align with the YZ-axis, and display a cross section of the grain.

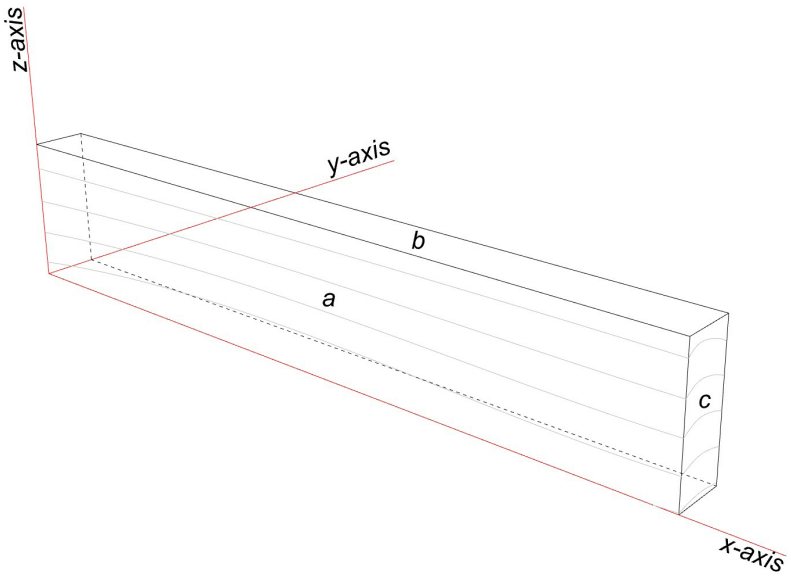

Figure 3.2 Board orientation axes within Cartesian coordinate system

3.2 Probe 1: RGB-D Scanning

3.2.1 Introduction

Probe 1 explores live computer vision methods for the assessment of visible surface features of fibre-managed plantation hardwood. It employs RGB image scanning with 3-dimensional depth detection to determine the location, typology, and size of knot-based timber features. The addition of depth scanning capacity allows the physicality of sawn timber boards to be captured beyond planar measurements, in addition to providing capacity to differentiate between live and dead knot features within the timber board. The differentiation between live and dead knots is significant, as it can impact the structural performance of a timber board in a different manner, allowing alternative engagement strategies within larger timber construction systems (Kretschmann & Hernandez, 2006). Rather than expecting feature classification to be undertaken within the forestry sector, Probe 1 seeks to develop detection methods within a designer/fabricator environment. As such, it incorporates a consumer level RGB-D capture method, which allows intuitive integration within a design-based software environment.

3.2.2 Probe Context

It was identified in Section 2.4.2.2.1 that the application of RGB-D capture techniques is suitable for the real-time material sensing and environment awareness that is particularly specific to a single project or material palette, with a high level of accuracy. The investigations discussed in Section 2.4.2.2.1 demonstrate that RGB-D's strength lies at is capacity to rapidly capture the three dimensionality of complex objects and spaces as a means of gathering data to inform other processes within a given scenario; whether it be the potential yield from a plantation forest or the effect that a fabrication process has had on a material element. Additionally, RGB-D offers a cost-effective entry point into computer vision that can easily be integrated into any number of unique use cases.

However, there are few examples of these methods of RGB-D scanning being employed to capture large inventories of material for use in multiple design applications. Accordingly, this study seeks to determine the suitability of RGB-D methods of capture that are scalable to large inventories of irregular materials within a design and fabrication context.

3.2.3 Probe Workflow

The sample material used within this investigation comprised a range of short offcuts from a pack of *Eucalyptus globulus* that exhibited a typical

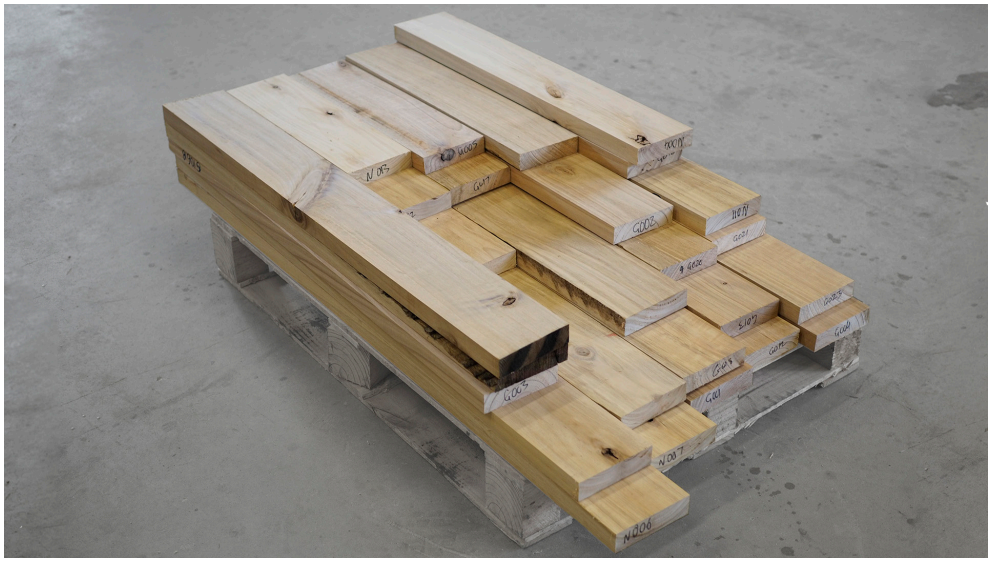

Figure 3.3 *E. globulus* sample boards (Tasmanian Blue Gum) used for testing

Figure 3.4 Knots in timber boards. Live (left) and dead (right)

range of features common to fibre-managed plantation hardwood, including clear wood, gum vein, live and dead knots (see Section 2.3.4.1). Twenty boards were chosen from the pack of dressed 140x35mm stock at random lengths between 450mm and 2100mm (see Figure 3.3). This investigation focused on the identification of live and dead knots (see Figure 3.4). The primary difference between the two types is that live knots remain engaged within the timber and have structural integrity, while dead knots create a hole within a board due to becoming loose and falling out creating a structural void (As et al. 2006, Cao et al. 2019). A void in a board can be differentiated from its surface through the application of RGB-D scanning.

Kinect (Microsoft, 2022) was the RGB-D sensor used in the investigation. This sensor was widely available at the time and chosen due to its ease of integration within multiple hardware and software platforms, low cost, and high configurability. Significantly, these factors indicate that Kinect is both well-suited for development within innovative workflows, and scalable to larger applications within the industry. Kinect integrates a RGB camera sensor (1920x1080, 30 fps) and 512x424 pixel infrared sensor with a 0.5-4.5m range (Diaz et al., 2015; Lachat et al., 2015).

Using Kinect as a proof of concept allows for transition to larger scale applications as it shares sensor methodologies with many other high-quality and specialised components suitable for production environments. The sensing workflow was integrated into Rhino®/Grasshopper® and

employed the Tarsier library plugin (Newman, 2019) as a point cloud importation platform. This choice was vital for developing a scalable application, as it provides capacity for captured data to be directly processed and integrated within a design and fabrication workflow.

This mode of the experiment was tested in two scenarios: a 600mm short-range scan, and a longer-rage 3000mm scan (see Figure 3.5). This provided the opportunity for comparison of the Microsoft Kinect's® RGB-D fidelity and resolution in different applications. The short-range scanning configuration is more suitable within a production environment as it provides a higher capture resolution. It also has the capacity to be scaled to larger application through further development as part of a lineal scanning workflow, with the benefit of being able to accommodate longer lengths of timber for material capture.

Figure 3.5 Long range (left) and short range (right) RGB-D experiment setup.

The first stage of Probe 1 controlled the RGB-D scanning and identified feature location and typology. It included a parsing filter and compared RGB and Depth data streams to establish which features are live knots (intact) or dead knots (voids) within the sample. The second stage compiled the collected data and entered it into a database for use within a design and fabrication workflow. The Grasshopper workflow for the scanning process is illustrated in Figure 3.6.

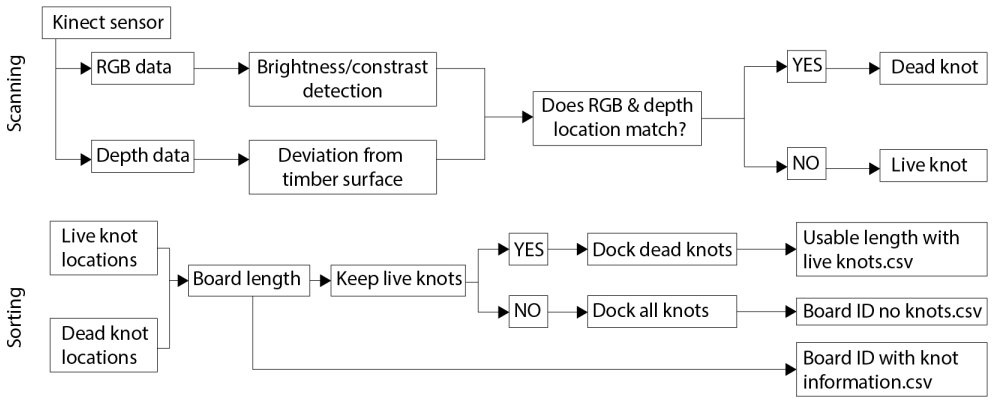

Figure 3.6 Knot identification and board sorting workflows

The raw RGB-D data captured from Kinect (see Figure 3.7), showed the dead knot being identified as having both a darker colour, and a dimensional deviation from the intended flat board surface. Capacity for calibration of the scan was formed as part of the workflow, allowing fine adjustment of the depth range, scan density (resolution), smoothing and frequency (frame rate). Live knots were detected in relation to the overall depth and compared against the thickness of the board. A depth threshold of 5mm was set, with any voxels having a greater depth identified as potential dead knots and grouped together. The processing of the detected dead knot group and resulting usable timber is shown in Figure 3.8. Additionally, sets of points that were within a proximity threshold were grouped together and treated as dead knots.

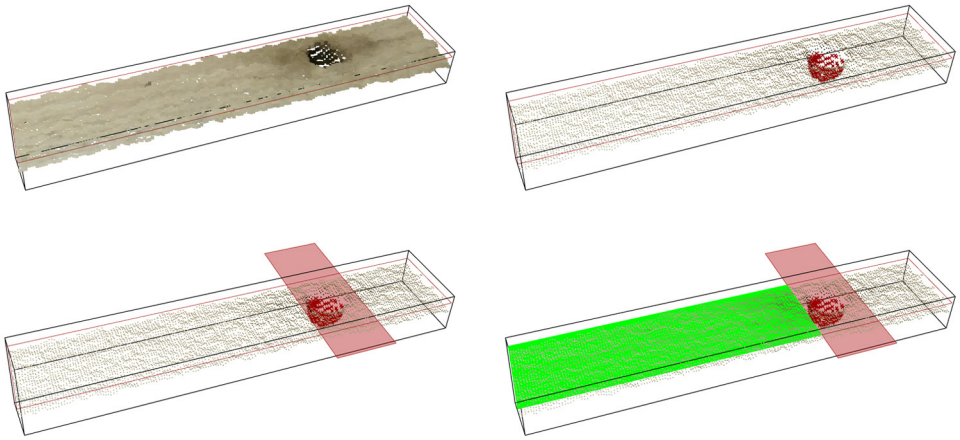

Figure 3.7 RGB-D raw data captured from timber board, displayed as coloured voxels (left) and with dead knot detection enabled (right)

Figure 3.8 Post-capture RGB-D data processing. Dead knot isolation (left) and usable length output in green (right)

3.2.4 Summary

Typical results obtained from the long-range scans from the Mode A configuration are shown in Figure 3.9. After RGB and depth comparisons, the red zones indicate dead knot locations, and the blue zones are linked with live knots. The green areas identify usable lengths within the board between knots, while the uncoloured areas were lengths that were shorter than the specified minimum-length. These short lengths were designated as waste material. The dataset was stored in a text-based dataset for future reference (see Table 3.1).

Figure 3.9 Whole timber board post-capture RGB-D data processing

Sample ID	Length	Live knot pos/s	Dead knot pos/s	Usable lengths
N001	465	159, 316	62	-
N002	614	249, 401	560	594
N003	1072	227, 602	-	1072
N004	820	260	-	820
...	...	...	...	...
N019	2100	714	1997	1980
N020	2100	-	601	1450, 580

Table 3.1 Sample of live and dead knot location dataset

The long-range tests demonstrated that knot detection was successful in long sample timber boards; however, the distance between the scanner and sample limited the capacity for finer resolution capture. Within the twenty-board sample size Kinect had a 17% failure rate in differentiating between live and dead knots consistently. In comparison, the short-range tests were able to detect much smaller features in the timber samples and demonstrated a higher level of correlation between RGB and depth data in the determination of live and dead knots, with a 5% failure rate; while, the short-range tests limited the maximum length of board that could be scanned due to the restricted field of capture at closer distances.

The techniques within Probe 1 present methods that enable the acquisition of timber board data using RGB-D capture methods. Critically, it demonstrates that Kinect could collect data in real time, demonstrating this workflow could be used in either passive or active environments within a design and fabrication ecosystem. The adoption of readily available computer vision hardware within material capture workflows provides opportunities to bridge the current information gaps in timber supply chains. This introduces a persistence of data between forest and design application with the potential to engage the material heterogeneity and irregularity, which currently eliminates the consideration of plantation hardwood as a viable material for high value application within the built environment.

Unfortunately, the shortcomings in relation to board length and scan resolution indicate that other modes of material capture are required to remove the limitations found within this experiment. Subsequently, alternative methods of material capture were investigated (detailed in

Section 3.3) to enable the efficient generation of large material libraries of plantation hardwood timber for use within design workflows.

3.3 Probe 2: RGB and Constrained Inventories

3.3.1 Introduction

Probe 2 investigates a method of material capture that addresses the limitations of the techniques identified in Probe 1 (Section 3.2). Probe 2 develops a high-resolution RGB method of capturing both sizes of a timber board that facilitates a computational technique to extrapolate detected surface features and forecasts their impact internally. It employs a two stage scanning processes that initially assesses timber boards for physical deformation (in the form of spring and wane) and proceeds to identify and capture the locations of knot-based features significant within the board's physical presentation.

Additionally, the higher resolution capture method employed in Probe 2 found that zones of fibre abnormality and discolouration often occurred around detected features, suggesting that the knot impacted the performance of the board beyond its physical dimensions. Finally, Probe 2 utilised a large volume of *E. nitens* sawn boards, which warranted the establishment of detailed inventory of data that could be cross-referenced with the physical elements. This would allow an abstract representation of a material data chain to potentially connect the forestry and construction industries.

3.3.2 Probe Context

A variety of industrial scale imaging technologies currently used within the timber industry, including image based RGB, CT, and laser scanning are commonly coupled with traditional timber testing techniques, either as manual or automated processes, such as the following, to predict the capacity of timber elements:

- Visual grading;
- Modulus of Elasticity (MoE);
- Modulus of Rupture (MoR); and
- Acoustic wave velocity, and CT scanning.

As discussed in Section 2.3.1.1, these technologies are already implemented in many sawmills, and they enable a higher yield and economic value to be extracted from a sawlog within a large volume environment; however,

the implementation of these technologies is not practical at a smaller scale given the significant financial and infrastructure requirements.

New, emergent modes of data-rich computation have the capacity to augment more accessible modes of material capture, extending their capacity within a performance-based design and fabrication system (Tamke et al., 2018). Extending the methods developed in Probe 1 (to include multi-face scanning provides a suitable volume of data to be captured), enables the prediction of internal structure of sawn timber elements, and establishes an extrapolation model that can determine areas within a timber board that have a high probability of containing full-thickness features such as knots. This factor influences both their structural capacity and machinability within design and fabrication.

By precisely locating full thickness features, design processes can be developed to use these irregularities appropriately. The inclusion of machining learning with the scanning workflow provides an increased level of material intelligence within a tailored design and fabrication environment. Subsequently, this increases opportunities for the inclusion of low-grade, fibre-managed plantation hardwood within architectural design workflows. 3D scanning techniques generate large volumes of data that can be stored in many ways, as documented in a range of studies, including the following:

- RGB capture generates image files that contains colour and brightness information at the scale of a pixel (Hittawe et al., 2015; Pölzleitner & Schwingshakl, 1992).
- Adding depth to RGB (RGB-D) encapsulates data into a 3-dimensional point cloud at the scale of a voxel (3D pixel) (P. Booth et al., 2017).
- Laser scanning is commonly used within sawmill for the grading of softwood (Füssl et al., 2019; Lukacevic et al., 2019).
- X-ray scanning creates a single grey scale image file (Couceiro et al., 2016).
- CT scanning expands this into a complex 3-dimensional array of RGB images (Bucur, 2003; Chubinskii et al., 2014).
- Photogrammetry extrapolates a collection of images into a textured 3D mesh topology (Guindos & Ortiz, 2013).

These data storage methods can be represented in numerical, geometric, or image-based means, usually within a database. It is critical to consider

how this information can be represented at a suitable level of specificity for the intended purpose within material capture and design applications.

The level of material detail required for different tasks can vary substantially. In structural and lamination processes, such as Cross Laminated Timber (CLT) and Glulam, refined characteristics such as grain direction become critical (Svilans, 2020). In design scenarios, where structural performance is of less concern, aesthetic considerations, such as colour variation and repetition, become more significant. In the context of this research, areas of natural feature were key to the design process, as they had an impact on material placement, fabrication capacity and subsequent performance of the designed artefact.

The RGB scanning workflow developed in Probe 1 provides information on a single side of a timber board; however, timber features, such as grain direction and knots, are not limited to a single surface or face, as they operate within the three dimensions of the board. While they have a general directionality, their exact nature is subject to the growth of the tree.

When tree logs are processed in a sawmill they are sawn into long, rectangular boards that slice through the intrinsic grown formations of the tree. The external faces of the resultant timber boards present only a cross section of features; yet these surface features can be captured through multi-face RGB scanning and offer an insight into the internal structure of the element. Carpo (2019), Morel (2019) and Svilans (2020) suggest that a scalable approach to the discretisation of material representation is required to allow these considerations to be accessible to a variety of design workflows.

In scanning multiple faces of a timber board, correlations can be made that provide an understanding of the significance of features. For example, a knot-based feature present on the front face and has a tight alignment with a similar feature on the rear of the board has a high probability of being continuous through the thickness of the element. Equally, a feature that appears on the rear face, but has no corresponding feature on the front is likely to be a shallow depth feature that has less significance within the element. Within the context of this research, the differentiation between featured and non-featured internal board areas provides opportunity to use the material with greater specificity within design environments.

3.3.3 Probe Workflow

3.3.3.1 Multi-face Image Capture

Shifting beyond the single board and face methods investigated in Probe 1, boards were captured in groups of five (Figure 3.10). This allowed the front face to be captured with the left-hand edge of each board aligned on the *y-axis*, relative to their front face. To capture the rear face, the boards were rotated 180 degrees around their *y-axis*, and re-aligned on the left-hand edge. It was critical that the boards were all rotated in the same manner to ensure the sequencing and orientation of final images could be correlated and automated. Each set of five boards was subsequently captured in a pair of matching 40-megapixel JGP files, using an Olympus OMD-EM5 mk2 digital camera with a fixed 17mm lens (35mm equivalent) at f/22, 1/3sec, ISO200.The second process of the image capture method split the JPG images into separate files in accordance with single boards, and cross referenced between the front and rear captures. An image processing script was used to extract five full width slices from each image at a height of 90 pixels in the location of each board within the image.

Figure 3.10 Grouping of five timber boards for image high resolution RGB capture

A third process employed a global colour balance on each slice to eliminate colour and light differentiation, in addition to cropping out the white background areas of the capture, leaving only the timber board section. A final imaging process was applied to the rear face captures that mirrored the captured image on the y axis, ensuring that the image orientation matched that of the front face.

While these processes did not optimise the material capture to the level available within industry, it was anticipated they would offer a greater level of immediacy to material information within later design experimentation workflows. This was critical in enabling the subsequent stages of the study

to be undertaken, as the material datasets originating from the timber industry are not readily available within the design process.

The automated image processing scripts contained in this stage of the experiment increased the speed at which material datasets could be captured and processed, while being embedded within future design workflows. As noted in Section 2.3.4, similar datasets are currently captured within the forestry industry, but are not available to architects and fabricators, who rely on traditional methods of grading and standardisation to make performance-based decisions. Ideally, this dataset would be available to the construction industry, negating the need of this processes to undertaken in future design workflows.

3.3.3.2 Feature Detection

The feature detection techniques employed in Probe 1 engaged computer vision processes designed for generic applications across a broad range of applications. These methods detected material features with relative success; however, the resolution at which they extracted information was not adequate for the Design Prototypes in the later stages of this study. A higher level of discrete material data was required to be employed within Probe 1's embedded workflow. Additionally, a higher level of automation was necessary, as a larger quantity of material was to be used within the Design Prototypes.

The feature detection methods employed within Probe 1 utilises the Aviary™ plugin (Mans, 2017) for Grasshopper. Aviary offers a number of advanced imaging methods that are built on the Accord.NET Learning Framework™ (Souza, 2014). This plugin provides a robust set of tools that enable the creation of production-grade computer vision applications with embedded machine learning capacities, including classification, regression, and clustering.

Due to typical timber processing and drying methods, a significant amount of variation is common in plantation hardwood board stock, with dimensional variation being a frequent irregularity. The first stage of the feature detection workflow determined which of the 96 boards did not have significant dimensional deformation, thus they were suitable for use within Design Prototypes. The features detected within this process were spring (board curvature) and wane (portion of board face missing along an edge due to being sawn from the external part of a log). Both present relatively long features (Figure 3.11) that are aligned along the board in the direction of the timber grain (the X-axis). These features were subsequently found to be readily identifiable using computer vision methods.

Figure 3.11 Examples of wane (top) and spring (bottom, top left corner) features in *E. nitens* sawn boards.

Aviary's threshold detection filter was applied to extract curve based geometric outlines of identified timber features present within the board. The dimensions of the feature curves were measured (along the grain, as compared with across the grain) and converted to a co-efficient by dividing the two values. The inventory of 96 boards was filtered using a threshold value that determined if the detected features had either spring, or wane characteristics, with twelve being identified as potentially having physical irregularities. Manual verification was undertaken and confirmed that the twelve boards did have the identified physical irregularities, subsequently eliminating them from future consideration within the workflow, with the remaining 84 boards being deemed suitable.

With the inventory of boards free of dimensional variation, the significance of detected features needed to be determined. The second feature detection stage identified the location and size of timber features on the front and rear faces individually, subsequently merging them into a single representation. Aviary's 'Bradley' threshold filter was applied to convert detected features to curve based geometry, as it generates the most consistent results in test scenarios, as shown in Figure 3.12.

Figure 3.12 Initial feature detection of *E. nitens* boards. RGB image capture (top), Bradley threshold filter applied (middle), and curve geometry of detected features (bottom).

A sample of ten boards was taken from the material inventory to determine an understanding of feature dimensions and their relative significance within the board; this represented approximately 10% of the available boards. Features that presented an area of less than 250mm^2 on either face were found to not be significant (that is, they did not have a corresponding feature on the opposing face) in 94% of cases. Any features that fell below this threshold value were ignored in subsequent stages of the discretisation process, as shown in Figure 3.13.

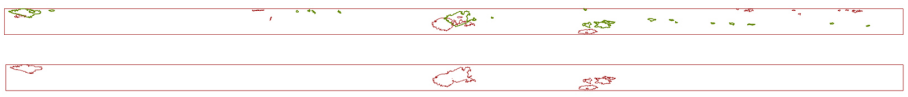

Figure 3.13 Overlay of detected features (top) from board front (red) and rear (green). Consolidated features (bottom).

Once the features were determined to be above the significance threshold, the front and rear board faces were merged. This process considered their significant features and determined if there was positional overlap between them on the opposing faces. Where features overlapped (or were in close proximity) the outline geometry was consolidated into a single entity, as it is highly likely that the feature is continuous through the board. The consolidation of the feature boundary representations allows them to be considered as having higher significance in later experiments. The outcome of removing insignificant features and consolidated front and rear features is shown in Figure 3.13 (bottom).

A by-product of the manual verification process was a secondary observation in relation to the impact of a knot-based feature on the area of board surrounding it. It was found that the irregular range of knots within a board affected the directionality and density of the timber grain immediately surrounding it and, in some cases, significant colour variation. Additionally, correlation was evident between the size of the knot and the affected area, ranging from between 25mm on smaller significant knots, through to 125mm on the larger knots. The variation of timber fibres within these regions is likely to affect the structural profile and an increase in the density of timber in the immediate area, as the natural growth of the tree would have likely been required to reinforce areas where lateral branches required support (Guindos & Ortiz, 2013). While additional physical testing of this phenomenon was not undertaken, it is anticipated that the integrity of the timber within these regions is compromised and has potential impact on construction systems that rely on mechanical fixings within these zones. As such, the size range of 25-125mm is noted for future reference.

The capture and feature detection of 96 boards established a digital catalogue of material specific data that can be used as a constrained inventory of irregular materials within subsequent design workflows. The dataset for each board was primarily encapsulated using a geometric representation, within a minimal text-based ID code, allowing for the data to be stored within a relatively simple structure and providing the capacity for easy data recall and interrogation in future design-based workflows. Additional numeric data was not required to be recorded as specific information relating to the board dimension; feature locations and sizes could be extracted from the geometric dataset.

3.3.4 Summary

The method developed in Probe 2 provide a greater resolution of captured material character to be stored within a (constrained) material inventory. Engaging a high-resolution image-based capture method, which considered multiple board faces, provided the capacity for a digitally

enabled, predictive technique of forecasting the internal structure of a timber board. The increased resolution of capture, coupled with a static data stream allowed for the detection of finer features unobtainable using methods employed in Probe 1. While image-based methods of material capture are currently available in the timber industry, the manner in which this Probe translates and stores data in numerical and geometrical representations within a constrained inventory provides an immediate accessibility for architects with which to engage, in design workflows.

While the notion of a constrained material inventory is established at the point of design and fabrication within the scope of this study, it is scalable to industry applications. Yet, significant shifts would be required in the commercial distribution supply chains and procurement of timber within construction for data-rich material inventories to be established at a scale suitable to supply the construction industry. The hardwood forestry industry would be required to increase its digital capacity to include automated material testing and capture, in addition to ensuring the persistence of data and physically storing timber until it was required within a project.

From an architectural standpoint, the procurement of timber would need to occur much earlier in the design and construction process, to ensure that the dataset used within design remained persistent with material that was available.

These two major shifts have the potential to provide timber end-use products with a set of unique performance characteristics of all individual timber boards within a pack, allowing each of them to be deployed based on their specific capacity, rather than the standardised grade to which they may that they may adhere. In turn, this would generate a closer interrelation between material and application, which would promote a greater level of material sustainability.

3.4 Probe 3: Architectural Panel

3.4.1 Introduction

Probe 3 seeks to validate the established material capture workflows in a contained design experiment that will leverage material character in the design and fabrication of a hybrid, architectural acoustic panel. The investigations and methods undertaken with Probes 1 and 2 outlined the identification and classification of material irregularities of fibre-managed plantation hardwood using computer vision methods including RGB-D scanning (Probe 1), and established a constrained material inventory of discretised boards at a high resolution (Probe 2). While these investigations

established successful workflows, their scalability and application within design problems requires validation.

The Design Prototypes in Chapters 4 and 5 have a higher level of complexity, and success with smaller workflows would be difficult to gauge amongst the other operations and processes. Accordingly, a validation design problem needed to be small enough to successfully test the capacity of the workflows in a controlled context. As such, this experiment expands the scale from a single timber board to consider a larger architectural panel as a potential end use for the use of fibre-managed plantation hardwood, in a laminated arrangement. As such, it adapts the high-resolution scanning technique developed in Probe 2 to discretise material features. The captured features become design drivers inherently linked with fabrication and performance criteria. Specifically, it engages knot-based timber features as the design driver for perforation and surface deformation.

Significantly, the primary objective of Probe 3 was to explore the potential of utilising heterogeneous plantation hardwood in an architectural panel that would otherwise use high-grade material. An integrated parametric method was developed that interrelates design, performance, and fabrication parameters. The design and fabrication workflow of Probe 3 used naturally occurring features as aesthetic focal points, which influenced the design of a tailored architectural acoustic panel that hybridised indicative absorption and diffusion characteristics commonly only present as separate products in the construction industry.

3.4.2 Probe Context

Architectural lining products that integrate acoustic control properties are widespread in the built environment, and are used in internally where the augmentation of ambient noise is required to provide an acceptable a comfort level for occupants. There are many products available on the market that provide either absorption or diffusion acoustic control characteristics; however, these characteristics are rarely combined within a single element or product. Further, the available panels typically provide generic acoustic performance characteristics, as they are considered 'off-the-shelf' products.

Current products are typically manufactured from homogeneous materials, whether it be foam, plasterboard or timber. Timber-based acoustic panels are commonly constructed from plywood or veneered composite board, utilising high-grade appearance quality materials. While these products demonstrate an efficient use of material from a production point of view, they rely on high value timbers as a material resource. Conversely, there

are currently no known products available within this sector that utilise highly irregular fibre-managed plantation hardwood as a material.

From a material perspective, Probes 1 and 2 presented workflows that enabled a level of material capture and understanding employable within digital design workflows; however, a specific understanding of how these material characteristics can be correlated with unique design problems needed to be explored in order to engage heterogeneous materials within innovative workflows.

Accordingly, Probe 3 is employed to investigate the physical qualities of acoustic panel products used in architectural applications as design drivers, as a means of discovering potential opportunities for material irregularity to be paired with typical acoustic augmentation typologies. It considers the physical differences between acoustic absorption and diffusion, and the effects of material, shape, and size on their efficiency. It quantifies the variables found in existing products to establish a point of reference for the design workflow, within Probe 3.

3.4.2.1 Acoustic Absorption

Acoustic absorption is commonly used to control or mitigate the amount of noise within a room. The use of mineral wool insulation, in its raw form within wall and ceiling cavities for porous absorption is ubiquitous. As a dense porous material, it traps sound waves within its material volume, reducing their capacity to reflect and reverberate around a room.

As this material is regularly installed within walls or ceilings, it must be considered prior to, and installed at, the time of construction. As an after-market solution, higher density fibre products can be positioned discretely within a room, on walls or a similar plane. In both types, material thickness impacts the absorption capacity, and is effective for reducing mid-to-high frequency sound transmission (Cox & D'Antonio, 2017).

In order to attenuate low frequency sound waves, porous absorption materials can be exploited within an acoustic resonance configuration by placing a sheet of perforated material in front of a porous absorbent (Sakagami et al., 2011). This type of acoustic device is known as a *Helmholtz absorber*, and forms the functional basis of perforated acoustic panels (Cox & D'Antonio, 2017). This panel configuration has the advantage of concealing the absorptive material, while maintaining an aesthetically acceptable level of finish for architectural application.

Perforated, sheet based acoustic products are also commonly used in architectural projects and are normally integrated within the building surfaces (Negro et al., 2010). As such, they are often made from

plasterboard or plywood in a range of sheet sizes with a limited range of regular perforation patterns. The performance of this type of panel is subject to the relationship between the size and density of perforation, the percentage that is perforated, thickness and type of absorptive material concealed behind, and material finish (Kłosak, 2020; X. Xu et al., 2018).

A survey of commonly available perforated plasterboard and plywood products is provided in Table 3.2. The products surveyed demonstrated a variety of configurations with varying hole and spacing size, which affected the subsequent percentage open area of the panel. It should be noted that all of the standard products available offer a repetitive perforation or slotted pattern.

Panel dimensions have been omitted from this survey as there was a wide variation in sheet sizes across the sample set. Independent of material, perforated products were found to offer an open area of between 7.2%

Product	Perf. Size (mm)	Perf. Spacing (mm)	Open Area
Gyprock Standard 6mm Round	6	15	8.3%
Gyprock Gyptone 12mm Square	12	25	16%
Gyprock Rigitone Galaxy	8, 15 & 20	unspecified	10%
Gyprock Rigitone Matrix 8mm Round	8	18	15.5%
Gyprock Rigitone Astral	12 & 20	33	19.6%
Boral Echostop 6mm hole	6	Unspecified	8.5%
Boral Echostop 13.5mm hole	13.5	unspecified	16%
Austral Perforated Plywood 4mm	4	16	4.6%
Austral Perforated Plywood 6mm	6	16	10.4%
Austral Perforated Plywood 8mm	8	16	18.4%
Austral Perforated Plywood 10mm	10	32	7.2%
Austral Slotted Plywood 8mm	8	30	22%
Austral Slotted Plywood 10mm	10	30	27%
Austral Slotted Plywood 12mm	12	30	24.5%

Table 3.2 Survey of commonly available perforated panel products in Australia

and 19.6%; slotted products provided a greater open area of between 22% and 27%. Perforation size was found to impact the spacing and overall open area of a panel, with larger perforations resulting in wider spacing and greater open area. While it is unknown why this is so, it is assumed it has correlation with material strength around perforations and the overall visual aesthetic of the product.

The regularity of perforations within the surveyed products is due to the capacity of manufacturing constraints. Plasterboard based products are fabricated using a die-based perforation process that allows multiple holes to be punched simultaneously, increasing the speed of manufacturing. Similarly, the perforations and slot dimensions in plywood-based products correlate to standard CNC drill sizes, allowing manufacturing speed increases using multi head/drill CNC machines. The use of standardised perforation size and spacing dictates the necessity to use standard and determinate materials, as methods of mass fabrication do not lend themselves to irregular and unpredictable materials. While this is advantageous to manufacturers, it limits the capacity of architectural exploration in which irregular materials are engaged with material indeterminacies.

Customisation of perforated panels is often used as a visual device within architectural design. The capacity to vary perforation size and spacing is often employed as an opportunity to create customised patterns. This capacity informs processes including image sampling, which allows the encapsulation of a photograph or graphic in a single or multi-panel arrangement. Customisation brings with it increased manufacturing times and associated costs. As there is potential for a wide variation in perforation size in a single panel, each perforation is required to be cut individually on a CNC router. In most cases, the perforation variation is a result of an aesthetic choice, as opposed to a specific performance requirement relating to acoustic control and material properties.

3.4.2.2 Acoustic Diffusion

Acoustic diffusers are control devices designed to reflect and scatter sound waves in different directions within an internal space. They are installed within a room to mitigate Reverberation, specular reflections and flutter echoes that cause audible acoustic artefacts (Dessi-Olive & Hsu, 2019). They are particularly important in music performance environments where there is a requirement to maintain acoustic integrity between the source and multiple locations within the audience zone (Koren & Muller, 2017). In these scenarios, controlling the spread of acoustic energy favours

diffusion treatments, rather than absorption, which reduces energy transfer (Walker, 1990)

Contrary to the common two-dimensionality of absorptive panels, diffusing panels have a three-dimensional form that increases the relative surface area, and hes the capacity to reflect sound waves in different directions. The material choice for diffusion devices is a much wider range than for absorption. As the surface is required to reflect sound waves, it can be constructed from a range of non-porous materials, including timber, hard expanded polystyrene, masonry or plasterboard. Acoustic diffusers are commonly employed as an after-market solution that are installed post-construction. As with 'off-the-shelf' absorption solutions, diffusion products possess comparable limitations in their material, performance, and aesthetic properties.

Significant opportunities exist for tailored diffusion solutions within the architectural industry. The limitations of the generic nature of commercially available products can be alleviated by coupling specific panel design with desired performance characteristics. The intrinsic three-dimensionality of tailored diffusion panels lends itself to intensive manufacturing methods, and would encourage the revaluation of innovative methods of engagement with fibre-managed plantation hardwood.

3.4.3 Probe Workflow

3.4.3.1 Design Strategy

As discussed in Section 3.4.2, most acoustic panel products currently available are manufactured from homogeneous materials (such as plasterboard and plywood) and rarely combine both acoustic absorption and diffusion performance characteristics. This experiment considers an alternative approach that utilises a solid timber panel, laminated from 90x35mm sawn fibre-managed plantation hardwood. This offers a compelling alternative to traditional products, as it engages a material that demonstrates a high level of natural character and creates the capacity for a more sustainable use of low-grade timber in tailored construction environments.

The timber panel used in this experiment was laminated from fibre-managed plantation hardwood boards that would otherwise be used for pulp. Additionally, the timber retains all the irregular natural features found in the boards, a scenario uncommon in current construction materials. The

panels are considered an 'off the shelf' material that utilises minimum manufacturing steps and maximises material usage.

This experiment seeks to retain natural timber features within each panel, by engaging design and fabrication strategies that highlight and emphasise the unique characteristics as a basis for design generation. RGB-based image detection is utilised to identify locations of high feature that can be used as points of focus within the design. These focal points are used as drivers for the varying density and size of perforations, as well as the surface deformation profiling. Further, the employed surface machining strategy generates small scale deformation in localised areas, controlled by a combination of tooling selection and machining time.

3.4.3.2 Material Supply

The boards used within Probe 3 were dressed 90x35mm *E. globulus*, with a length of between 2300mm and 2700mm, and were sourced from uncompromised offcuts of an unrelated destructive structural loading experiment. The selected timber exhibited a moderate level of variation across the boards and a variety of irregular natural features, including knots, colour variation, grain variation, and surface checking, in addition to clear straight grained areas, (see Figure 3.14). The timber features contained within the selected boards are representative of the sawn timber originating from Australian fibre-managed plantation hardwood forests and correlate with the material that could be used within industry to manufacture a similar panel product.

Figure 3.14 Natural timber features: (clockwise from top left) dead knot and colour variation; live knot; grain variation; surface checking

3.4.3.3 Panel Lamination

At the time of writing, there are few commercially available timber panel products that utilise fibre-managed plantation hardwood; however, the market is being moved forward by Tasmanian based Cusp Building Solutions (Cusp, 2022), the only certified manufacturer of plantation hardwood mass timber products in the world. Its made-to-order product range includes mass timber engineered products (such as cross laminated timber and

Glulam structural elements) and 'appearance'-grade panels. Yet, prior to its manufacturing process, significant irregular material features have already been removed, during material supply and processing. Subsequently, Probe 3 investigated the fabrication of a laminated panel that includes irregular material features, as a means of testing design capacity with a material that has a smaller processing requirement.

The demonstration panel was fabricated using a traditional lamination method found in joinery manufacture. The selected 90x35 *E. globulus* boards were laid out to form a 900x2200mm panel and distributed without material bias to ensure natural feature was spread relatively evenly across the panel face. When using solid timber in this manner, an understanding of grain direction at the end of each board is notable as it affects the dimensional stability of the laminated panel (Walton, 1990). As the timber will naturally cup tangentially across the predominate end grain conditions, it is important to lay boards with opposing end grain direction to the adjacent boards to minimise cupping (Jackson & Day, 2005) (Figure 3.15), while ensuring face grain directionality is consistent across the panel. Within the demonstration panel, individual boards were visually inspected and manually flipped or rotated to accommodate end grain direction, in addition to ensuring a non-uniform spread of timber features across the panel face.

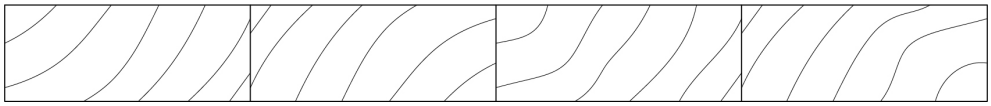

Figure 3.15 End grain of timber boards arranged to oppose the natural cupping force.

The boards were edge laminated using Titebond® II Premium cross-linking PVA adhesive, which is recommended by the manufacturer for edge-gluing operations. Figure 3.16 shows the boards arranged to create an oversized panel, which would be subsequently trimmed to the prescribed size after glue adhesion was complete. There were no internal dowel or biscuit alignments used in the lamination, and this reduced the machining preparation and processing required. Additionally, the absence of internal alignment dowels eliminates the possibility of them being exposed during the CNC fabrication process (later in this investigation).

The panel was clamped using 1200mm clamps for 24 hours. The clamps were positioned at nominally 300mm centres from opposing sides of the panel to minimise the introduction of additional cupping forces. The panel was trimmed using a table saw, with the final arrangement shown in Figure 3.17.

Figure 3.16 Demonstration panel lamination process for Probe 3

Figure 3.17 The Probe 3 demonstration panel (900x2200x35mm)

3.4.3.4 Design Workflow

The design workflow was split into four stages:

1. Material capture;
2. Acoustic augmentation design – absorption;
3. Acoustic augmentation design – diffusion; and
4. Fabrication.

The material capture stage adopts the feature classifications identified in Section 2.3.4.1 and the RGB based material capture workflow developed in Probe 1 (see Section 3.2). The second stage develops a workflow that couples material features with perforation and surface deformation, and which draws parallels with products techniques currently available in generic construction materials. The final stage develops a fabrication workflow that employs 3-axis CNC machine simulation and output of a

physical demonstrator panel. Each stage is discussed in more detail in the following sections.

3.4.3.4.1 Material Capture

The demonstration panel was photographed using an Olympus OMD EM-5 mk2 micro 4:3 digital camera, with a fixed 25mm F1.8 lens (50mm equivalent). The panel was positioned vertically on its edge with the camera fixed to a tripod. The camera location was triangulated with the panel to ensure perpendicular alignment, minimising perspective warp of the image. Captured at a resolution of 4400x1770px, one pixel of the image is representative of a 0.5mm square of the overall panel. The image was taken indoors with evenly diffused natural light. Negligible image adjustment was undertaken to correct a minor colour cast across the panel, with the resulting sample image shown in Figure 3.18.

The RGB method of material capture developed in Probe 2 (Section 3.3) was employed to locate the material features within the panel, the results of which are shown in Figure 3.18. It should be noted that, in this experiment, the material capture process was applied to a single side of the panel only. The identification of features using the pre-established resolution and brightness settings required only minor adjustments to be applied to the captured image. This was due to tonal variation across multiple boards within one capture, in addition to a different set of environmental and light conditions employed for the initial image to be taken.

Figure 3.18 Panel feature detection

The feature detection method was sampled at a 1mm resolution and generated a highly complex set of curve geometries; however, the complex calculations that would be required in later stages of Probe 3 would be computationally heavy if this resolution was maintained throughout the workflow. Subsequently, the geometry was rationalised by employing a curve rebuild process that reduced the number of curve control vertices by 95%, the results of which are shown in Figure 3.19. This process maintained

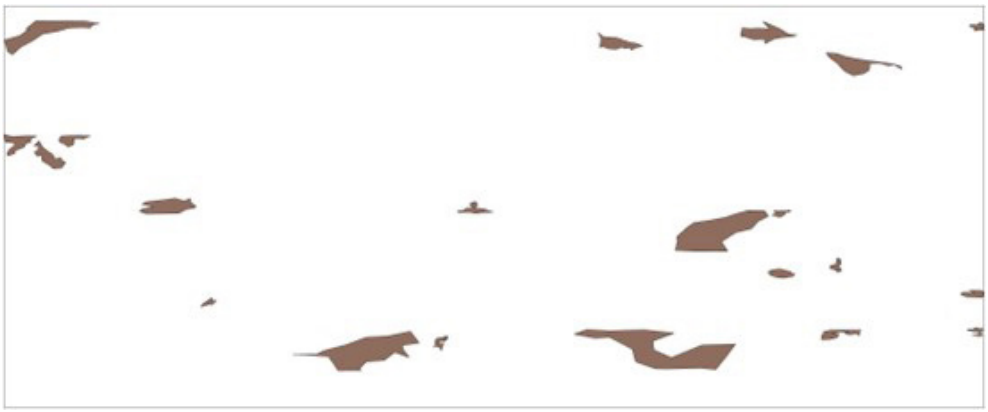

Figure 3.19 Simplification of feature geometry

a relevant level of detail in the discretisation and was critical in simplifying the based geometry, in order to allow more complex computational procedures to be undertaken in later processes of this Probe.

3.4.3.4.2 Acoustic Absorption Design

The performance of the panel incorporates both porous material and resonance absorption methods. Porous material absorption is facilitated by varying perforation diameter, allowing sound waves to travel into the acoustic insulation behind. Conversely, solid areas of the panel are intended to allow sound induced resonance characteristics.

Areas on the timber boards containing material feature exhibited higher irregularity and less consistent internal structure, which impacts machinability during the fabrication process. Initially, removing the knot features from the timber was considered to be a valid method of generating perforations; however, as the level of feature would vary significantly between panels there was no way to ensure the featured areas would correlate with the perforation areas, as required.

Further, engaging the timber directly in relation to the location of natural features decreases the predictability of material failure, due to machining failure. Subsequently, it was determined that featured areas would remain intact, as the material irregularities would not be structurally affected by resonance-based vibrations. Areas that had a clearer material surface were chosen to be perforated, as there was less potential for material failure during fabrication. This strategy matched the design intention that material irregularities would be treated as an integral part of the design outcome.

To provide acoustic absorption over a wider frequency spectrum, perforation diameter was varied across the panel. This was determined by the relationship between the perforation location and global material feature distribution. The area of each detected feature (as determined by

the convex polyline curve) was compared against the total of all detected areas. This established a ratio of significance that each defined area would have on the perforation pattern, with larger material features having a larger impact on the overall pattern.

Each perforation point was compared against all feature locations, and its diameter was adjusted accordingly. The minimum perforation diameter was set at 12mm, a result of the relationship between panel thickness (35mm) and the necessary cutting tool diameter. The upper limit for diameter was governed by the relationship between the performance requirement of the panel (determined by percentage opening), perforation spacing, and the structural capacity of the material left between the perforations.

The experiment aimed for 20% open area and a spacing of 45mm, resulting in a maximum diameter of 32mm and a minimum distance between perforations of 15mm, as shown in Figure 3.20. These variables allow the panel to have a comparable percentage openness comparable with commercially available products, while engaging with a heterogeneous irregular material.

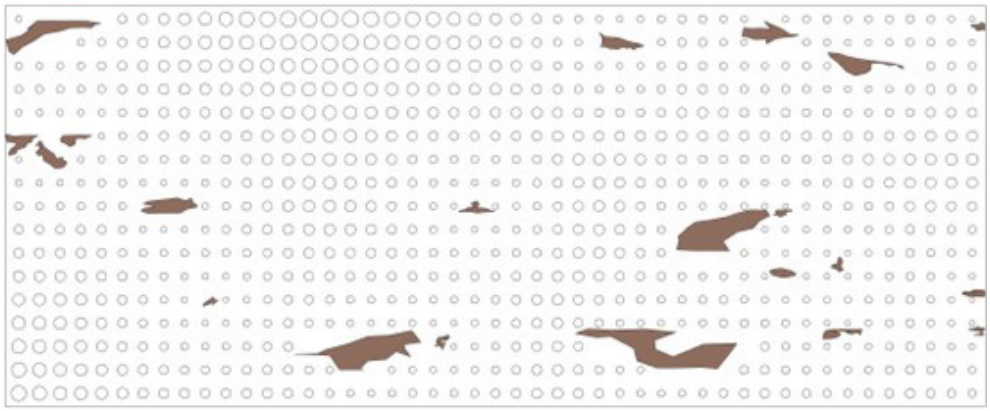

Figure 3.20 Weighted perforations in panel based on half-tone image processing

3.4.3.4.3 Acoustic Diffusion Design

Acoustic diffusion scatters sound waves throughout a space, creating an even distribution of sound to a wide range of locations within a room. As discussed in Section 3.4.2, a common method of achieving this is breaking a surface into smaller, varying faces (often pixelated), thereby allowing sound to be reflected at differing angles. Subsequently, surface deformation was introduced into the experiment to incorporate diffusion performance capacity.

In employing the same strategies as the perforation design, diffusion performance was directly governed by surface deformation and its relationship with detected material features, with areas of higher irregular feature demonstrating less material integrity. Subsequently, these areas had minimal surface deformation applied, while areas of clear timber and less feature were subject to more intrusive strategies.

Each perforation centre point was shifted vertically on the Z-axis. Areas that were determined to have a high level of feature significance within the panel were set to a height of 32mm, creating a maximum of 3mm of deviation from the original panel face. Points farthest away from areas of significance were matched with the minimum panel thickness and set to 12mm. All other points were attributed a height value based on the proximity comparison between these two limits.

The resulting three-dimensional point grid was utilised to generate a triangulated mesh surface, which presented subtle surface deformation was intrinsically connected to material irregularities. The surface (see Figure 3.21) would be used for tool path generation during the fabrication process.

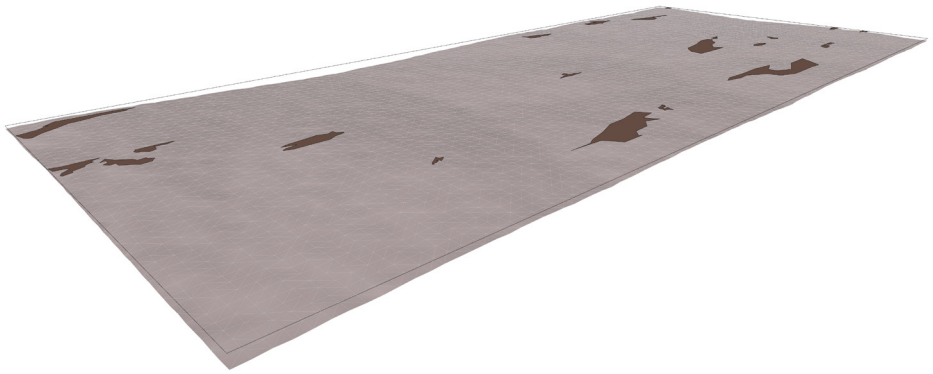

Figure 3.21 Surface deformation for acoustic diffusion

3.4.3.4.4 Fabrication

The capacity of material specific architectural panels for application within the construction industry is proportional to their economic viability within small to medium scale fabrication practices. The major consideration in this regard is the cost of infrastructure required to undertake unique fabrication methods. The workflow in Probe 3 employed digital fabrication equipment widely available within the construction industry currently.

The generation of the panel design in a virtual environment (such as Rhino) allows for an interchange between design intent and potential fabrication methods. The exportation of generated geometry into a Computer Aided Manufacturing (CAM) software package allows for machining to be tested.

The physical fabrication was undertaken using a 3-axis CNC router with a 2400x1200x200mm work envelope and a 4kW spindle. This machine is underpowered in comparison with those commonly found within the construction industry, so the machining strategy was broken into three stages to accommodate working with a solid hardwood panel, and each process had different strategies to work within material and machine constraints:

a) surface deformation,

b) perforation, and

c) finishing.

Surface machining processes were created by applying a 3-axis tooling strategy to an imported surface geometry within VisualCAM® (MechSoft, 2021). As a large amount of material was required to be removed in some areas, the strategy involved undertaking a primary rouging process to remove the bulk of the material. A carbide tipped 12mm triple fluted downward spiral router bit, with an effective cutting length of 32mm, was used for the surfacing machining stages to ensure a clean finish on the surface. The roughing pass was configured to have a step-over of 9mm, with a vertical layer step-down of 6mm. This was dictated by the capacity of the spindle and the 'chip rate' of the cutter.

A secondary parallel machining pass was applied and, unlike a roughing pass (which removes layers of material at the prescribed depth), parallel machining traces the imported geometry to create a smooth finish. The pass was configured with a step-over of 6mm and set to 45 degrees in relation to the predominate face grain direction of the panel. This assisted in machining regions where grain direction varied, minimising material 'tear out' of the final panel surface. Figure 3.22 shows a simulation of the roughing process and Figure 3.23 demonstrates the subsequent parallel machining simulation. The combined machine time for this stage of the fabrication process was 72 minutes, 27 seconds.

The perforation machining stage required a different cutting tool, due to the down-cut spiral tool (used in the roughing pass) ejecting timber chip in a downwards direction, thereby minimising material 'tear out' on the surface. As the panel was sitting on a sliding base during the machining process, the perforations become, in effect, enclosed holes. In this scenario the chip is forced into the hole and the cutting tool continually runs though the waste material, creating friction and heat that subsequently reduces the life span of the cutter.

As a result, an up-cut spiral cutting tool (which ejected timber chip material upwards out of the perforation hole) was used for perforation machining.

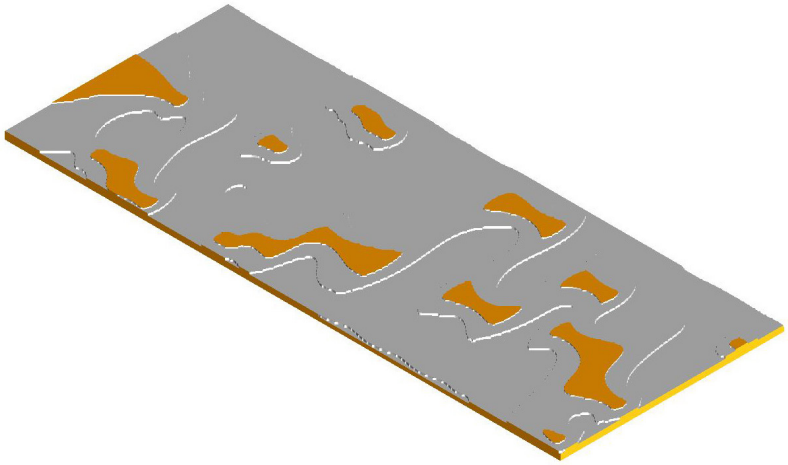

Figure 3.22 Fabrication simulation – roughing process

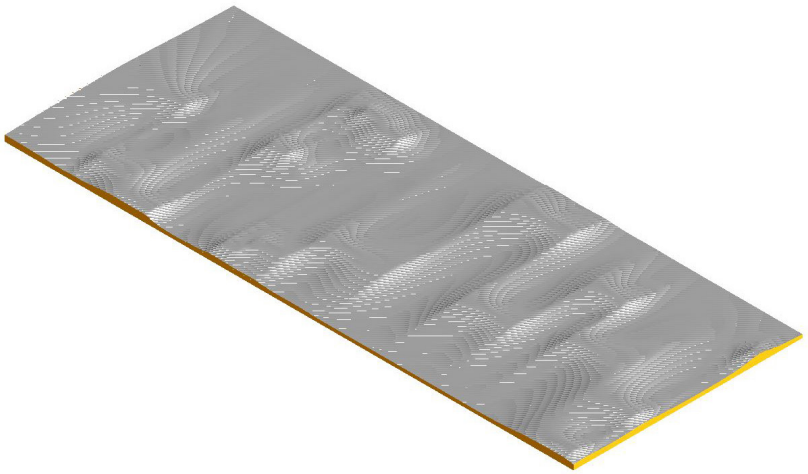

Figure 3.23 Fabrication simulation - parallel finishing process

The machining strategy for the perforations were vertical spirals tool paths, which reduced the volume of material needed to be removed at a given point of engagement. While this was a marginally slower strategy, it was necessary given the maximum depth of perforation and spindle capacity. The 742 holes took a total of 98 minutes 32 seconds to complete, the longest process within the fabrication workflow.

As noted, one disadvantage of an up-cut cutting tool is its tendency to tear material out of the surface as it ejects waste chip. For this reason, an additional finishing process was required using the down-cut cutting tool. The same tool path settings used for the first parallel machining pass were repeated, with two modifications:

a) To set the direction of the finishing to the opposing 45-degree angle to the predominate face grain. This adjustment provided

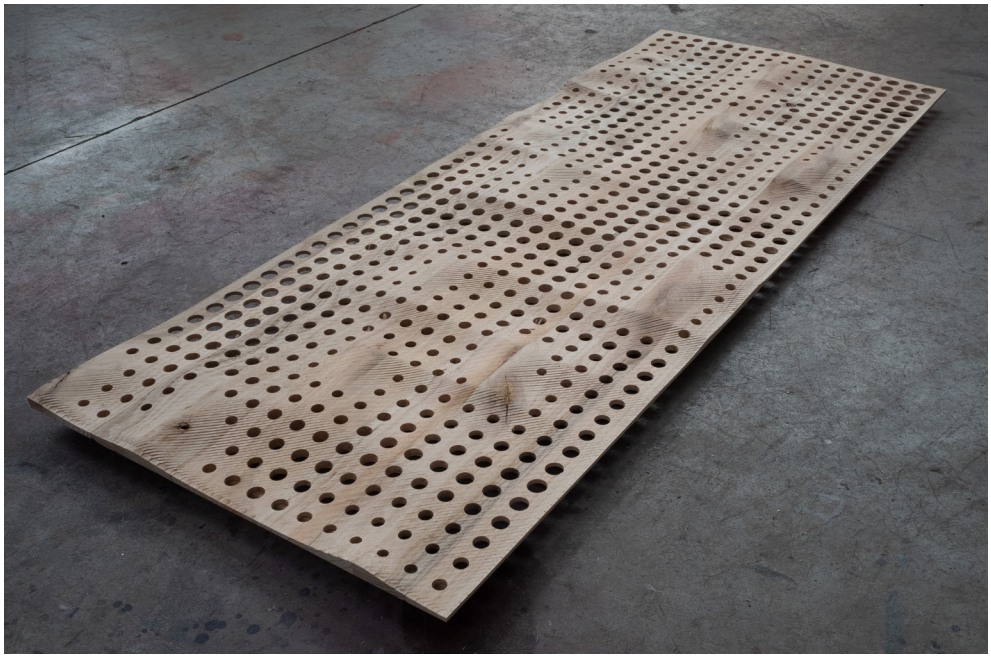

Figure 3.24 Hybrid acoustic panel physical demonstrator

the capacity to clean-up some of the 'stepping' generated by the previous parallel machining process.

b) To increase the depth of cut by an additional 0.5mm, to ensure that any torn surface edges created by previous machining processes were removed. The CNC cutting speed was increased in this final pass, as it was removing a much smaller amount of material.

This process took 31 minutes to complete, 8% faster than the previous parallel finishing process and is illustrated in Figure 3.24.

While the overall increased production time, relative to a standardised panel system, would have a larger carbon footprint, the nature of any tailored design and fabrication solution would demonstrate increased production time (Koren & Muller, 2017), particularly during initial development. This is usually followed by an increase in efficiencies due to process refinement, and a reduction in production time due to wider industry adoption of the new solution. Additionally, as plantation hardwood is highly renewable and currently underutilised within the industry, its use as a material medium within Design Probe 3 contributes to offsetting the higher environmental cost of longer manufacturing processes.

3.4.4 Summary

Probe 3 demonstrated that the identification of naturally occurring knot-based timber features within plantation hardwood boards can be captured and discretised through the adoption of RGB based imaging processes and

computational classification method (as developed in Probes 1 and 2). It employed the feature dataset within a design problem that considered the potential of low-grade timber within a tailored architectural acoustic panel that correlated material irregularities with material augmentation, in line with existing commercially available individual products.

The engagement of material features drove the generation of a performance and aesthetically-based architectural element that engaged fibre-managed plantation hardwood as a potential option for construction. Additionally, the inherent design and fabrication solution generated an opportunity for combining performance characteristics of two acoustic devices within a single product; a capacity that is rarely available in the industry and market.

Yet, this experiment does raise questions in relation to manufacturing viability, aesthetics and extended performance requirements.

The innovative methods developed in Probe 3 have an impact on manufacturing viability, in that the processes of material capture and design configuration introduce extra steps in the workflow, which required additional hardware. To circumvent this, the RGB method of material capture is deliberately configured to use readily available, consumer-grade camera technology, and is integrated within the scalable and adaptable framework offered by Rhino (Robert McNeel & Associates, 2021) and Grasshopper (Robert McNeel & Associates, 2022).

From a fabrication perspective, the workflow developed in Probe 3 resulted in fabrication times considerably slower than those currently seen in standardised architectural panels, of any material. Further, the subtractive machining methods employed in the physical demonstrator removed 42% of the original timber, in the form of residue sawdust. Both of these factors subsequently increased the manufacturing carbon footprint of each panel. However, when considered as a scalable CDF (customisable to individual projects, performance requirements and materials), the additional fabrication time is justifiable as any tailored product will typically require longer time frames for design and fabrication. Critically, the increase in production time affords architects opportunities to engage with material irregularities in ways that open the door to the wider use of irregular materials that are more sustainable (in a range of ways), than those currently available.

The fabrication solutions used in generic processes do not offer the level of variation and adaptability required to achieve the material responsive solutions developed in this experiment. In creating a tailored solution that specifically addresses a particular material condition, it is argued that

production times would increase relative to the level of customisation of augmentation involved.

Further, the use of a low-value material, such as fibre-managed plantation hardwood, can provide cost savings compared with other, more highly valued and performing material options, from both an economic and carbon foot print perspective. Traditionally, most innovative methods that employ a new materials are expensive and slow in their initial developmental stages; yet, as more people engage with new techniques they become increasingly streamlined, resulting in more cost-effective and time efficient implementations.

3.5 Probe 4: Evolutionary Optimisation

3.5.1 Introduction

Design Probes 1, 2 and 3 have thus far allowed the development of methods that consider alternate modes of material capture and cataloguing, and a design and fabrication workflow responsive to material irregularities in a panel-based product. Subsequently, these scenarios have been limited to engaging the irregularities of materials that are pre-determined as either board from a sawmill or an 'off-the-shelf' laminated panel from irregular materials. These Probes have been responsive to the material, but not *material-led*.

Probe 4 inverts this relationship and considers how to strategically engage the unique material characteristics of an inventory of virtual boards as a part of a larger material matrix. It considers the implementation of a MOEA to optimise timber board distribution across a laminated panel, maximising the opportunity for each timber board to be utilised most effectively.

3.5.2 Probe Context

Section 2.3 notes the timber industry currently engages plantation timber in several mass timber products, including CLT, LVL and Glulam. These products are most utilised in structural application in construction; although, non-structural appearance base applications also exist. The dominance of softwood plantation timbers in manufacturing these products is currently being challenged by the adoption of sawlog grade plantation hardwood from sustainably manages forest resources. However, the future capacity of these hardwood plantations is dwarfed by the fibre-managed plantation hardwood reserves across Australia. There are significant market potentials for the adoption of fibre-managed

plantation timber resources to be utilised within the mass timber industry (Derikvan et al. 2016).

CLT technology, for example, provides the opportunity to use low-quality timber materials in a structural panel arrangement, through the process of homogenisation (Cherry et al., 2019). Here, the manufacturing processes remove sections of the raw timber boards that present all but the smallest irregular features and allow a large quantity of short length boards to be re-compiled into a large panel configuration, that is treated as a generic panel to be used in a number of different structural application (Cao et al., 2019).

If this same process was applied to boards sourced from fibre-managed hardwood plantations, a significant proportion of the source material would remain destined for low value by-products at best: or solid fuel and waste material, at worst. A more efficient use of material could see the irregularities remain the final panel; but, in locations where they wouldn't impact the overall performance of the material matrix.

The manufacturing workflow of CLT panels begins with the lamination of large, rectilinear blanks from dressed boards with a nominal 25mm thickness. The panel blank can be treated as a heterogeneous engineered element, with a particular set of performance capacities based on the arrangement of timber boards within it. The thickness of the overall panel is determined by its specification (as either a wall or floor element) and its performance requirements (such as, fire rating, acoustic performance and structural span). The large panel blanks are then CNC fabricated to the required shape and size, as determined by the design.

The building into which that element will be installed will have several known connection points and, in the case of a wall panel, potential for window or door openings to be formed (Svilans, 2020). While it is critical that the location of connection points uses higher quality timber that is free of defects to ensure a solid substrate for structural connection, in reality the entire panel is laminated from typically defect-free boards. The material that is removed to form openings could be utilised for smaller elements within the building; however, this is typically treated as waste.

Due to the panel being laminated from high-grade material, there is significant waste generated from these offcuts. While Robeller & Von Haaren (2020) investigated the potential of these offcuts being used in solid-grid shells, it remains a highly specific building solution, with relatively few alternative applications.

Given that these areas of the panel are treated as waste, they provide an opportunity for correlation with highly irregular section of timber boards to

be located. A challenging aspect of this proposal is the method required to assess a large volume of irregular timber boards and match their location within a panel with the based on the performance requirements. The application of a MOEA in this scenario can optimise material distribution, allowing for a reconciliation of design objectives of placing material features in areas where openings are required, and not placing them where structural connections are required. By engaging a highly localised distribution optimisation the opportunity for utilisation of low-value and highly featured timber boards is significantly increased.

3.5.3 Probe Workflow

3.5.3.1 Virtual Material

While the constrained inventory developed in Section 3.3 contains a highly discretised set of irregular boards and their material features, it is too complex to harness in the development of a proof-of-concept method. The variable length of boards alone would require a sophisticated workflow to calculate the layout solutions that the MOEA would generate, let alone the location of material features. Subsequently, a *virtual* inventory of one thousand boards was generated to accommodate a representative level of irregularity within this experiment.

An inventory of 1,000 boards was generated with specific physical dimensions of 1200mm x 90mm being prescribed. While this is not representative of the diversity within the constrained inventory, or typical lamination processes within CLT manufacturing, it simplifies the layout strategy required within Probe 4. A greater level of irregularity was encoded into the boards through the generation of virtual material features, which was based on the constrained inventory dataset in Probe 2.

Each board was specified to have between 0 and 4 features, randomly located across the board's face. For the purposes of Probe 4, the features were not required to be irregularly shaped themselves and, as such, were represented as circles with a 40mm diameter (Figure 3.25).

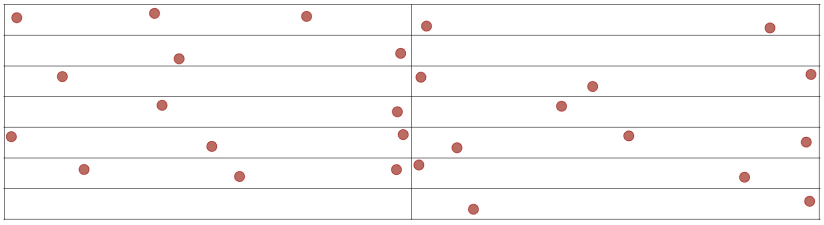

Figure 3.25 Sample of generated virtual boards

3.5.3.2 Panel Specification

While a CLT panel is manufactured with multiple layers of boards with perpendicular grain direction within each layer, the panel specified for the purposes of material distribution comprises a single layer of boards. This simplifies the geometric representation of the panel, in addition to requiring a smaller inventory of virtual boards. Additionally, the butt joints between boards would normally by staggered across the panel in 'real-world' applications; however, this was rationalised for simplification purposes in Probe 4. The single layered panel within this experiment employed a non-staggered board layout that corresponded with consistent length of generated board; yet, this approach is scalable and provides opportunity for future development.

The specified panel (Figure 3.26) had an overall dimension of 7000x1800mm. To provide nominal goals for the feature distribution, three openings were specified (shown in blue) that are representative of door and window openings, and as locations that material features could be located. Conversely, ten structural connection points were specified (shown in green) that were specified as locations where material features were not desirable.

The initial random distribution of boards over the wall panel (Figure 3.27) resulted in seven material features being incorrectly positioned within the ten structural connection zones. While the distribution of features within three openings was successful, only 18 irregularities were present in these areas, representing 8.7% of the 205 features. There was clearly a significant opportunity for a denser distribution of features within these zones, and a capacity for ensuring structural zones were free of irregularities.

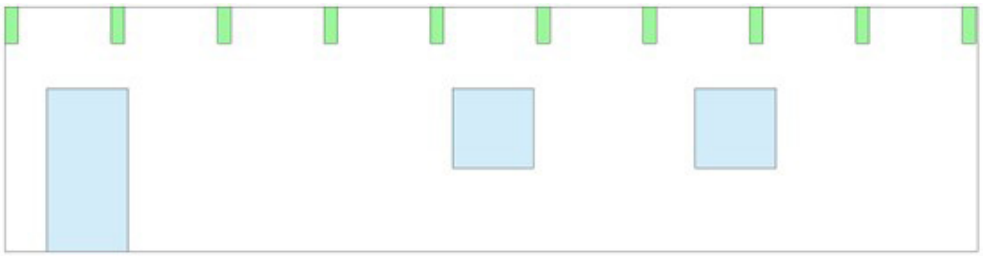

Figure 3.26 Wall panel specification indicating structural zones (green) and openings (blue)

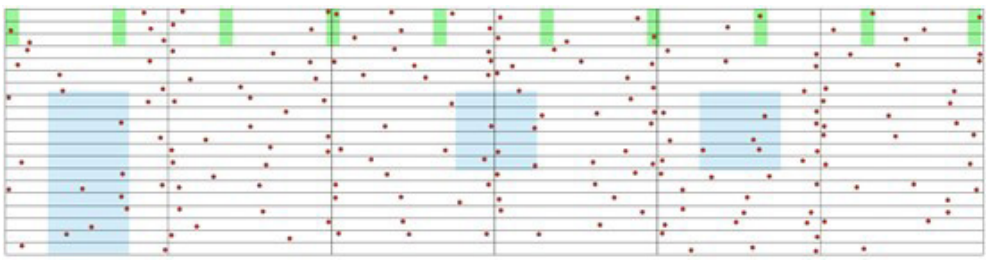

Figure 3.27 Random distribution of virtual boards overlaid across a wall panel

3.5.3.3 Evolutionary Optimisation

The MOEA was run within Grasshopper, using the plugin Wallacei (Makki et al., 2022), with two Fitness Objectives specified:

a) The first determined the number of material features located within structural zones; where each evolutionary iteration aimed to reduce this number by optimising towards a *solution* that contained no instances of incorrect feature placement.

b) The second Fitness Objective assessed the number of features within specified openings and optimised this by searching for solutions that increase the total number of features in these areas.

By establishing this pair of Fitness Objectives, the MOEA aimed to move material features out of structural zones, instead optimising their placement within panel areas where openings were located. While these two Fitness Objectives could optimise together and converge on a single solution, it is important to recognise that they operate within a material inventory and panel design that are both unknown and scalable at the commencement of the workflow. A material inventory with a higher density of material irregularity has potentially less capacity to meet the Fitness Objectives. Similarly, different panel designs could place structural zones in close proximity to openings, resulting the optimisation process unable to reconcile the objects.

The evolutionary workflow (see Figure 3.28) depicts the design problem in terms of the stages and relationships between the phenotype, genotype, and the Fitness Objectives required to iterate material distribution within each solution cycle of the MOEA. Each of the unique timber board contained within the material inventory was allocated a corresponding gene within the gene pool (see Table 3.3), allowing each board to have a sort index applied from a possible 10^9 values. This sort index allow the evolutionary variation of was in which boards from the material inventory were selected, and where they were geometrically distributed, within each evolutionary iteration. Each gene had a numerical domain of 10^9, resulting the allocation of a sort index value that was extremely unlikely to be repeated within the chromosome. Table 3.4 details the evolutionary algorithm's parameters that were applied within Wallacei.

Prior to looping back to first stage for the next iteration, the MOEA evaluates the number of features within specified areas to see if it matches the objectives of decreasing the occurrences within exclusion zones and increasing occurrences within inclusions zones. These values are used for

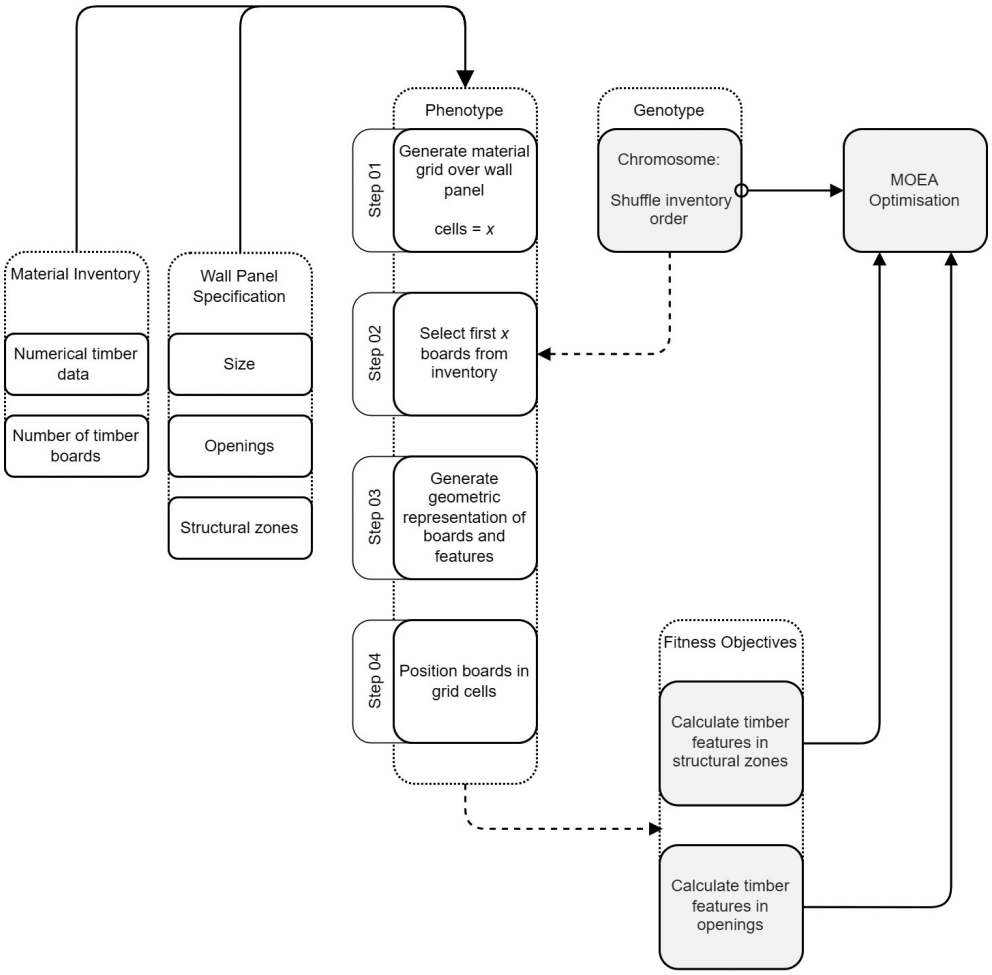

Figure 3.28 Probe 4: Evolutionary workflow pseudocode

Chromosome: Shuffle inventory order		
No. of Genes	**Numerical Domain**	**Function**
1000	0.000000 to 1000.000000 (10^9 values per gene)	To provide a traceable sort index to each discrete timber board dataset from the material inventory, facilitating variation of the boards selected by the phenotype.

Table 3.3 Probe 4: Gene pool specification

Evolutionary algorithm parameters	
Generation size	50
Generation count	100
Population size	5000
Crossover probability	0.9
Mutation probability	$1/n^{\text{n=number of variables}}$
Crossover distribution index	20
Mutation distribution index	20
Random seed	1
Simulation runtime	10m 45s

Table 3.4 Probe 4: Evolution algorithm parameters

evolutionary selection and *mutation* to the next iteration, in addition to representing the fitness of the solution against the design objectives.

The MOEA simulation took 10 minutes, 45 seconds to calculate, with Figure 3.29 detailing the statistical representation of the fitness values. Standard deviation graphs and SD trend line graphs represent the variation in the population for each fitness values. The mean trend line graphs represent the average fitness value per generation. The simulation resulted in 421 solutions within the Pareto front, representing a set of solutions that cannot be optimised further without being detrimental to one of the Fitness Objectives. Further investigation determined that all Pareto solutions had the same fitness values and were, in fact, duplicate solutions with the same board distribution.

Figure 3.29 Statistical representation of the fitness values generated by the simulation.

As such, the MOEA optimised towards a single solution, the first of which being solution {87;0}. In this instance, the design objectives can converge as the process of shifting features out of exclusion areas they are, in turn, able to be concentrated within inclusion areas; however, there is potential for this scenario to not be 100% convergent, especially in cases with limited material inventories or a higher level of material feature.

The material distribution within solution {87;0} (see Figure 3.30) resulted in zero material features being placed within structural connection ones, which was the primary objective of the design problem. Conversely, the solution had 37 features located within opening zones, representing 21.9% of the 169 contained within the 120 distributed boards. As such, the MOEA achieved 21.9% optimisation, representing the best solution available given the characteristics and size of the constrained inventory available.

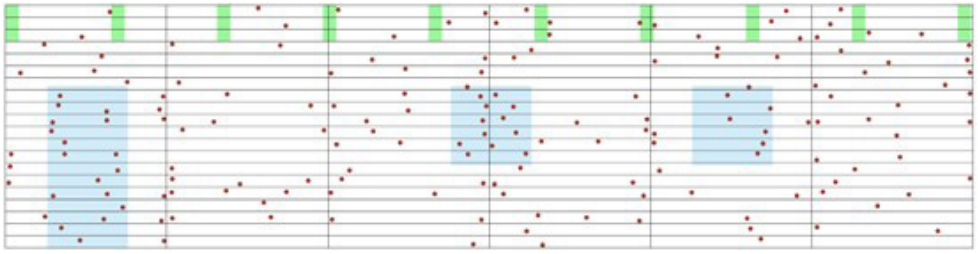

Figure 3.30 Probe 4 pare-to front solution {87;0}

3.5.4 Summary

Design Probe 4 demonstrates that the application of multi-objective optimisation methods can provide a conceptual model that accommodates the utilisation of irregularly featured timber boards in unique material applications. It abstractly coupled the feature classification methods identified in Section 2.3.4 with the RGB based image capture and computational inventory frameworks from Probes 1 and 2. Further, it shows that material irregularity can be engaged on an elemental basis within a panel typology, beyond the generic laminations explored in Probe 3. In doing so, this experiment demonstrates that these workflows are both scalable and adaptable to larger design-centric scenarios.

The specification of a design problem that considers material optimisation within a tailored laminated panel provides a point of comparison with the current practices undertaken in the manufacturing of mass-timber elements for construction. Typically, a mass timber panel (such as CLT, LVL or Glulam) is considered a generic, homogenised element that will perform within a prescribed capacity, regardless of its application within construction.

The workflow developed within this experiment reverses this relationship, establishing a scenario that optimises the distribution of inherent material features in accordance with the specific performance requirements of a customisable design problem. This level of material application is not readily available within an industry context, as a direct link between data-rich material grading and design and fabrication environments is typically decoupled.

While the coupling of material characteristics with specific design performance requirements has been explored in several relevant projects (see Section 2.4) there are relatively few examples of this being undertaken with large, constrained inventories of materials. This is particularly apparent in the consideration of the individualised material irregularity found in fibre-managed plantation hardwood. It is likely this is due to the majority of studies being focused on enhancing existing workflows and materials, rather than considering new instances of each. Further, the complexity of correlating a practically infinitely variable material inventory, with unique design-centric performance requirements, is beyond the typical capacity of the current timber, architecture or construction industries.

The core contribution of Probe 4 in this study is that it addresses this issue directly, by embedding a MOEA within the design workflow, at a point between material discretisation and distribution. In doing so it provides the capacity for a population-based investigation that considers the intricate material variation within the inventory, combined with testing thousands of selection and distribution configurations within a tailored laminated panel. Over the course of evolutionary iteration, the algorithm optimises the placement of material features to areas within the panel that do not require higher performance material.

Given enough computational time, the workflow presented in Probe 4 could potentially find a better solution with more knot features located within panel areas that are to be removed (in window and door locations). However, once the primary objective of avoiding knots in structurally significant connection zones was met, a solution was deemed acceptable. In doing so, this method of solution optimisation reduces the computational requirements, in turn decreasing the overall time required for the design of a tailored panel to be undertaken.

This notion of acceptable optimisation is employed in more complex scenarios in Design Prototypes 1 and 2 (in Chapter 4 and Chapter 5) and is core to negotiating the engagement of material irregularity within performance orientated design contexts.

Finally, Probe 4 develops opportunities for plantation hardwood to be deployed within material configurations that shift beyond the methods

of standardisation currently employed within the construction industry. As such, it demonstrates that the introduction of a material data-chain provides higher levels of material sustainability, when coupled with DIMPs.

3.6 Discussion

The capacity of the architectural and construction industries to engage heterogeneous materials, including fibre-managed plantation hardwood, within the built environment is hampered by five key factors:

a) The entrenched modes of material grading and standardisation that form the predominant material palette available.

b) The data-chain that exists between material supply and design and fabrication is generic;

c) The linearity of existing modes of design, specification, material procurement and construction;

d) The perceived detrimental impact in considering irregularity and unpredictability within material performance and construction tolerance.

e) The complexity of correlating unique material capacities within bespoke architectural design.

The common objective of Probes 1, 2, 3 and 4 was to investigate computational means of engagement that could address the barriers in current industry practices that inhibit the adoption of fibre-managed plantation hardwood as a valuable and effective construction material.

The current grading methods of hardwood timber (see Section 2.3.4) showed there is not currently capacity (under the relevant Australian Standards) for the visual classification of any plantation hardwood timber, including fibre-managed resources, for high value applications within the construction industry. This presents a compelling opportunity for the development of new modes of material classification, specific to plantation hardwood, within the timber and construction industries.

While the image-based feature recognition workflows developed within Probes 1 and 2 employ relatively 'lo-fi' means of identifying material characteristics, similar RGB-based methods are already embedded in the machine grading processes used by the plantation softwood industry. While the latter is of a much larger scale, this suggests that the workflows within Probe 4 have both relevance and capacity for industry implementation, in conjunction within plantation hardwood resources.

Although the softwood industry benefits from image-based feature recognition within its mechanical grading systems, it severs the link between

the datasets and the end user, and caters instead to the standardised classification of grading currently favoured by the construction industry. For plantation hardwood to be considered as a viable construction material, similar datasets must be captured and passed down the supply chain to the end user. This data-chain could enable a higher level of material engagement that can couple inherent elemental characteristics with specific design applications, and diminish the reliance on standardised methods of grading.

The constrained material inventory developed in Probe 2 provides a conceptual framework of the proposed data-chain. When paired with the supply of material, the cataloguing of elementally specific information, within a centralised database, allows a level of material interrogation and specificity currently not available in the architectural and construction industries.

Critically, the data must be available in open-source formats to allow integration with existing workflows and software platforms utilised by architects and fabricators. While the material capture and constrained inventory methods in Probe 2 were integrated within the Rhino/Grasshopper environment, the data was recorded using both numeric and geometric descriptors that accommodate open methods of data export to other platforms.

The mass-manufacturing of standardised architectural elements currently relies on heterogeneous materials through the design and fabrication processes; however, in tailoring material fabrication with performance-based design criteria, innovative modes of mass-customisation facilitate unique material solutions for specific architectural applications.

The architectural panel employed in Probe 3 demonstrated this capacity through the coupling of hybridised acoustic performance requirements with an 'off-the shelf' laminated panel of random timber boards from fibre-managed plantation forests. While the application of this approach resulted in a longer and potentially more expensive fabrication process than using a standardised product, similar time and cost outcomes are to be expected in any bespoke application of digital fabrication and mass-customisation. Additionally, the potential performance gain and aesthetic outcomes acquired through augmenting a panel (based on its material character and capacity) provides an opportunity for irregular materials to be considered in higher value architectural applications.

The most significant challenge in engaging materials of irregular character and performance capacities within design and fabrication is the establishment of the relationship between material potentials and specific applications opportunities within an architectural context. The

complexity of negotiating all configurations of material within a single fabricated component, let alone an entire system of components, is well beyond the capacity of current architectural and construction workflows. The computational optimisation methods investigated in Probe 4 offer a design integrated approach to addressing this issue: coupling elemental level material characteristics with specific performance outcomes.

However, even this approach relies on a data-rich material supply chain to enable an adequate level of material understanding to be embedded within a CDF. Further, the robustness of this approach, as with all of the Design Probes, needs to be validated in applications with more complex design problems and larger material inventories. The Design Prototypes developed within Chapter 4 and Chapter 5 integrate and extend the methods developed within the Design probes within such design scenarios.

4 DESIGN PROTOTYPE 1: ACOUSTI-SIM

4.1 Introduction

The material-driven investigations undertaken in Chapter 3 developed workflows that facilitated the engagement of irregular material characteristics found in timber boards originating from fibre-managed plantation hardwood forests. Through these four Probes, digital techniques of material capture, cataloguing, fabrication, material distribution and optimisation were established. These digital techniques supported a closer relationship between inherent material properties and their performance capacity within design-centric environments.

However, further investigations of the scalability and integration of each Probe, within larger design applications is necessary. As such, *Design Prototype 1: Acousti-Sim* and *Design Prototype 2: Mat-Truss* test the legitimacy of the developed digital workflows as a part of larger DIMPs.

Design Prototype 1: Acousti-Sim develops a multi-scalar approach to material interrogation and performance-orientated design generation. It expands methods of discretisation and performance prediction that provide a finer-grain understanding of indeterminate timber materials. The outcome of this experiment established a micro-scale material discretisation process that was paired with an heuristic evolutionary approach to acoustic simulation and augmentation at the scale of a room.

Further, this experiment engaged generative modes of material utilisation and design generation through the employment of multi-objective evolutionary algorithms. This coupling presented the opportunity for a scalar approach to material engagement, facilitating a discrete design, fabrication and placement strategy that is responsive to the specific performance requirements of an environment.

4.2 Prototype Context

The architectural panel workflow developed within Probe 3 (see Section 3.4) demonstrated that a timber feature could drive the design of material and fabrication engagement to produce a specific technical performance outcome. It developed a method that recognised material features (typically recognised as defects) as having specific characteristics. This subsequently shifted perforation and surface deformation away from these elements, whilst maintaining both its visual and structural presence in the panel. Moving beyond a single panel element, this method can be extended to provide a performative solution that engages material irregularities as active participants in the design of a tailored solution.

Bespoke approaches to acoustic augmentation (beyond ‘off-the-shelf’ products) are becoming increasingly common in complex architectural

projects; particularly, in performance spaces such as theatres, auditoriums and concert halls. Koren & Muller (2017) and Mack (2018) detail, for example, the computational acoustic simulation and fabrication methods undertaken by Herzon & de Meuron for the Elbphilharmonie Hamburg (2017). These methods supported the generation of an integrated architectural surface that embodied a programmatic approach to specific acoustic performance requirements.

Exton (2011) and Giovannini (2011) identify similar processes of design-based computation in the Guangzhou Opera House by Zaha Hadid Architects (2010). In an academic research environment, the series of acoustic surface projects undertaken by Gramazio and Kohler in 2014, 2019 and 2021 employ comparable modes of computational design, with a shift towards emerging modes of robotic fabrication (Gramazio Kohler Research, 2014, 2019, 2021; Rust, Xydis, Frick, et al., 2021; Rust, Xydis, Heutschi, et al., 2021; Vomhof et al., 2014).

While these examples offer a highly complex approach to the design and fabrication processes of acoustic surfaces, they (still) rely on standardised materials and consider acoustic augmentation from a geometric focus, rather than a material-driven one.

In an acoustically-sensitive architectural space, simulation methods can determine areas that require acoustic absorption, diffusion, or a combination of both, to achieve a desired level of performance. This experiment combines a set of performance requirements for a simulated acoustic context with data harvested from a supply of plantation hardwood, to enable the bespoke design and fabrication of an attenuated architectural acoustic surface. The dataset was generated through the employment of RGB scanning techniques to determine the location of material irregularities within each timber board; a catalogue of material drivers could then be established.

The acoustic performance requirements of the room, coupled with the constrained inventory of irregular materials, was processed using evolutionary computational methods to place individual timber elements within a panel (and subsequently in the room) based on the unique irregularities and their inherent potential for impact on an acoustic outcome.

Shifting scales from the architectural panel developed in Probe 3, this experiment coupled the engagement of fibre-managed plantation hardwood with location-specific performance requirements at the scale of an integrated acoustic surface, and moved beyond the consideration of timber as a part of a larger homogeneous prefabricated system. Instead, it considered employing innovative methods of material capture,

computational processing and fabrication to discretely match specific pieces of timber with unique performance requirements. This level of material engagement is rarely considered in architectural applications of this scale, and if applied would allow a specificity of performance that provides a unique and sustainable approach to material utilisation.

4.3 Experiment Setup

The change in scale from an individual panel to room surface, in addition to a higher density of material data within the constrained inventory, resulted in an increasingly complex workflow requirement. To accommodate the volume of data, and the subsequent computational demands, the workflow was split into five stages, as shown in Figure 4.1.

Stage 1 generated an acoustic performance profile of an existing physical space using digital simulation methods accommodated by the Pachyderm™ (van der Harten, 2014) plugin within the Rhino environment. This profile was a baseline for a MOEA to iterate the indicative acoustic material profile of specified wall panels, when searching for the fittest configurations that increased the acoustic performance to the greatest degree. The fittest solutions were then hybridised into a single performance profile, and subsequently checked against the existing room simulation to ensure that the profile was improving the room acoustic environment, as intended.

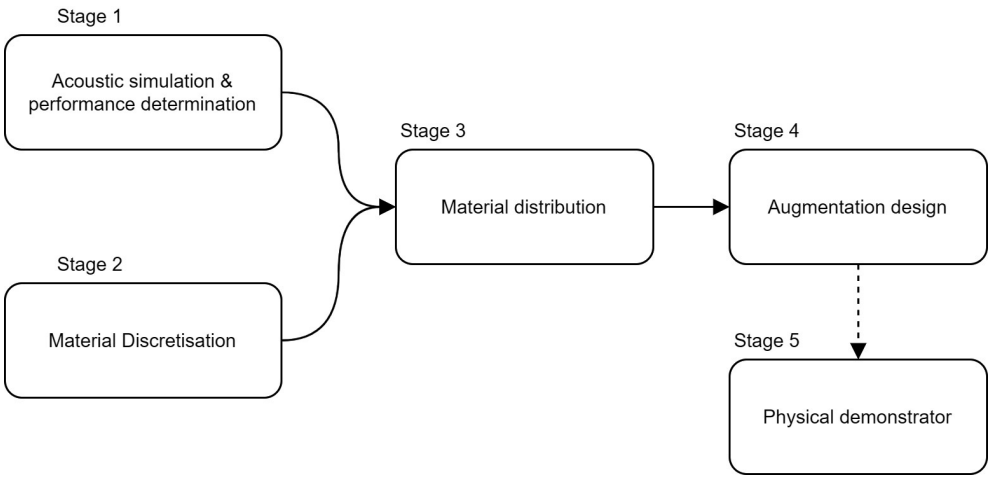

Figure 4.1 Design Prototype 1: Acousti-SIM workflow division of into five stages

Stage 2 employed the material capture and constrained inventory of discretised boards (as established in Section 3.3), to determine a performance suitability rank of individual board segments. Critically, it interrogated multiple faces of the boards, accommodating the consideration of internal feature structures and properties. The multi-surface discretisation process allowed for the conversion of timber board features into both numerical and geometric datasets. This resulted in

assigning each board segment with a capacity coefficient, representing the relationship between clear and featured areas for each board segment.

Stage 3 engaged a MOEA to deploy individual board segments to specific locations within an acoustic surface based on their determined capacity and the hybridised acoustic performance profile. Areas within the profile that indicated little or no acoustic treatment requirements were allocated board segments with high features; while clear timber segments were distributed to surface areas that indicated higher levels of acoustic augmentation.

Stage 4 determined how the acoustic surface should be physically fabricated, by considering the hyper-local material placement within the laminated acoustic surface, and generating a surface pattern that was responsive to the unique material character. It achieved this by correlating the pattern intensity with the hybridised acoustic performance profile of the panel it is contained within.

The computational processes contained in the experiment fostered the specific engagement of irregular materials within an optimised performance-based design framework; however, the very nature of irregular materials rendered it difficult to adequately visualise the outcome in a digital environment. To address this, **Stage 5** realised the translation of the developed digital processes into a physically fabricated demonstration Prototype.

4.3.1 Stage 1: Acoustic Simulation and Performance Determination

The computational simulation and exploration of variable acoustic properties was developed in a sample environment. This experiment used an existing teaching space in the School of Architecture and Design, at the University of Tasmania (Inveresk Campus) as a test room. The room was 15m deep x 12m wide, with a ceiling height of 4.2m (see Figure 4.2). The walls were predominantly painted, off-form concrete with minimal glazing and material variation (there was an area of plaster board lining and

Figure 4.2 Test room used for acoustic simulation.

windows to about 40% of two walls) and the ceiling was metal formwork for the concrete slab above. Acoustically, the room offered a very 'live' environment for face-to-face teaching, with echo and Reverberation presenting significant difficulties for hybrid delivery modes (including video conferencing).

4.3.1.1 Acoustic Simulation of Existing Conditions

Digital modelling of the room was undertaken in Rhino, chosen as it provides access to several plugins employed through this experiment. This ensured that simulation data was directly accessible with the developed design workflow, without leading to file compatibility issues (from the requirements of each independent software). The room was modelled as a shell representation, in that the model did not contain any furniture, soft furnishings or lining interventions. This was done as an acceptable level of acoustic performance was required, regardless of the final function or furniture configuration of the room. As such, the digital model represented wall surfaces as concrete, the floor as carpet tiles, and the ceiling as metal, corresponding to a reasonably accurate translation of the existing physical environment into the digital realm.

4.3.1.2 Acoustic Measurements

Educational spaces, particularly classrooms, have prescribed acoustic performance qualities that should be present to promote healthy indoor environments for learning (Bradley (1986), Hodgson (1999), and Siebien et al. (2000). Rooms with poor acoustic qualities have been demonstrated to lead to difficulties with comprehension and learning (Mealings, 2016). As such, Reverberation Time (T_{60}), Speech Transmission Index (STI), and Early Decay Time (EDT) are considered to be the significant performance criteria for classroom environments (Lombardo et al., 2020; Patel, 2020). Therefore, in the context of the conducted experiment, these three measurements were selected as performance criteria for the digital simulation.

Reverberation Time is identified as the persistence of a sound after it is produced (Patel, 2020). As sound travels through a room, it bounces off the surfaces and objects contained within and gradually loses energy. As the sound waves bounce off many different objects and materials, the reflections interact with each other, creating reverberation. Consequently, Reverberation is a collection of many reflections of the same sound, with varying time delays. Reverberation Time is traditionally measured as the period it takes a test sound to be reduced by 60dB after the source sound

has been interrupted. It is referred to as T_{60} and was first calculated in 1896 by Sabine (Davis et al., 2013).

Sabine's Reverberation Time equation states that RT_{60}=0.161$V/S\alpha$, where RT_{60} is the time in seconds required for a sound to decay by 60 dB, V is the volume of the room in m^3, S is the boundary surface area, and α is the average absorption coefficient of the boundary surfaces. However, it is often impractical in physical testing scenarios (particularly in large spaces) to generate, maintain and measure test sounds powerful enough for a drop of 60dB to be recorded accurately. In these situations, a Reverberation Time of either T_{30} or T_{20} (30dB or 20dB) are measured, and these are multiplied by two or three respectively, to obtain the reference T_{60} value, allowing less powerful test signals to be used. T_{30} was employed in the experiment, ensuring consistency between different measurement and simulation types, with results being converted to T_{60}.

Conversely, Early Decay Time (EDT) describes the rate at which sound energy decreases after the initial sound source. It measures the time taken for the sound level to drop by 10dB in milliseconds and is used to evaluate the sound quality of a space (Ermann, 2015). A lower EDT value indicates that the sound level decreases rapidly after the initial sound, while a higher value indicates that the sound level persists for a longer period of time. A short EDT ensures that the sound level decreases quickly after the initial sound, allowing for distinct speech intelligibility and reducing the chances of sound overlapping or masking.

Further, a short EDT allows for more natural sound decay, giving the space a more 'pleasant and comfortable' acoustical ambiance. On the other hand, a high EDT can lead to poor speech intelligibility, making it difficult for listeners to understand speech and increasing the chances of sound overlapping or masking (Patel, 2020).

Speech Transmission Index (STI) is a method of measuring speech intelligibility within a specified channel (such as a room, telephone line, or public address system). It is an effective indicator of the acoustic performance of classrooms as it considers criteria, including speech level, background noise level, echoes, Reverberation Time, and psychoacoustic masking effects. STI considers six octave bands, covering a range from 125Hz through to 4kHz. Speech intelligibility is measured within a range of 0 to 1, broken into five classifications (see Table 4.1). The International Electrotechnical Commission (2020) specifies a minimum STI of 0.62 for classrooms, while The Association of Australasian Acoustical Consultants Guidelines for Educational Spaces 2.0 (2018) suggests a minimum STI of 0.7 for teaching spaces. In a review of international acoustic standards for classrooms, Mealings (2016) found no definitive STI guidelines; however,

Intelligibility Rating	STI	Intelligibility of words (%)
Excellent	>0.75	100
Good	0.60-0.75	100
Fair	0.45-0.60	100
Poor	0.30-0.45	70-100
Bad	<0.30	<70

Table 4.1 Speech Transmission Index (STI) classifications

she suggests that a range between 0.6-0.75 was most commonly stipulated, which complies with International and Australian guidelines.

As there is no definitive STI value for classrooms available, the recommended Australian guidelines value of 0.7 is adopted within this study. While a higher target value has potential to be met, the use case of the subject room does not require achieving higher performance. However, as the workflows created within this prototype are both scalable and applicable to other room occupation types, they STI performance target can be easily varied to suit alternate circumstances.

4.3.1.3 Acoustic Simulation Parameters

Computational acoustic simulation is often employed during the conceptualisation and design development stages of architectural projects. Specific software platforms, including CATT-Acoustic™ (CATT, 2022), EASE™ (AFMG Technologies GmbH, 2022), and ODEON™ (Odeon A/S, 2022), are employed by acoustic engineers to predict and/or measure the performance of a given room. However, these software platforms are independent from architectural software, provide numerical results, and do not commonly provide an intuitive graphical environment for conveying the complex inter-relations of acoustic performance and architectural intent.

As this experiment required the digital environment to be geometrically iterated (with the simulation needing to be run sequential for each variation) the acoustic simulation framework needed to be established within a design-orientated workflow. The Pachyderm plugin (van der Harten, 2014) provides Rhino with the capacity to run complex acoustic simulations with its native environment, by directly connecting the design environment with simulation. As such, Pachyderm has been employed in many acoustically orientated architectural projects (Hannouch, 2019; Peters et al., 2013; Williams, 2017; Wright et al., 2016) in both early-stage

design and detailed simulation to provide data and feedback on design options and expected acoustic performance.

Developed for the refurbishment of Melbourne's Harmer Hall in 2010, Pachyderm provides a flexible, open-source platform for the investigation of acoustic phenomenon that is similar to many of the more complex engineering specific tools (van der Harten, 2013). It incorporates a number of advanced geometric methods of calculation including ray-tracing, image source and visualisation, finite volume methods, and transfer matrix techniques for acoustic absorption (van der Harten, 2015; 2020).

The ray-tracing method calculates sound waves emitted by an audio source, simulated as rays, that move through a defined space and bounce off geometrically defined surfaces based on their specified acoustic properties. The rays are reflected within the space until they either collide with an audio receiver, or decay over time. Pachyderm visualises these rays geometrically as reflected lines and performs a range of acoustic calculations based on how the rays behave and interact with the specific room.

AS/NZS 2460 Acoustics: Measurement of the Reverberation Time of Rooms (Standards Australia International Limited, 2016) specifies that physical acoustic measurements require the testing of multiple source and receiver locations, with the results averaged, in order to sample the varied performance of different areas of a room. Within this experiment, the hybridisation of acoustic simulation results and performance indicators acted as a guide for augmentation types, in addition to demonstrating there was an improvement in room performance with the inclusion of acoustic augmentation. As such, a simplified approach to simulation setup was employed (see Figure 4.3) in which a single point source (shown as red) and a single receiver location (shown as blue) were specified within the modelled room. These positions represented the average speaker and audience positions within the room.

Pachyderm has two methods of ray simulation:

a) specified ray count ratio, and

b) convergence.

While the calculation method remains constant for both simulation options, computational time is significantly impacted by the number of rays that are being calculated. In their comparison of acoustic simulation software, Parigi et al (2017) determined that consistent simulation results could be obtained by specifying the number of rays at a ratio of 25:1 against the volume of the room being tested. Specifying the number of rays manually ensured the quantity remains constant each time a simulation

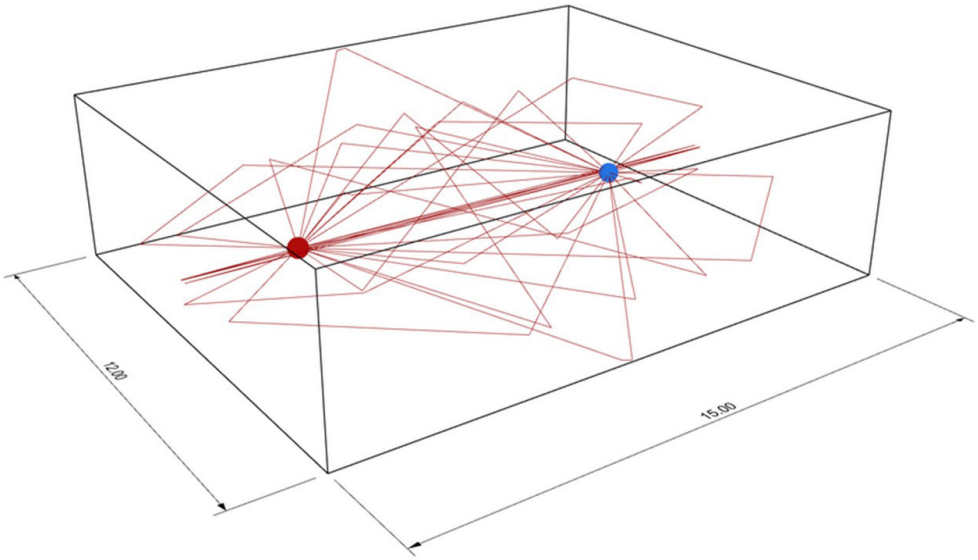

Figure 4.3 Acoustic simulation setup of virtual room. Single point source (shown as red), single receiver location (shown as blue), and primary acoustic reflection rays

was run, regardless of any geometric, material or source/receive location alterations that may have occurred.

Additionally, Parigi et al (2017) established a calculation time that remained relatively efficient and consistent throughout the simulation. Variation in the number of rays, and subsequent length of calculation, is not a significant issue when undertaking a simulation once. However, when embedded within an MOEA optimisation, the acoustic simulation is required to run within each iteration, potentially having a significant impact on the calculation time over tens of thousands of cycles.

Conversely, the convergence method automatically iterated the number of rays while the simulation was running until it determined that an optimal number of rays were collected by the sound receiver. This method is influenced by any changes in the room geometry, materials and source/receiver locations. As a result, the number of rays required for a simulation is unknown prior to execution and fluctuates each time a simulation is run. This variability significantly increases the computational time for running the simulation, particularly when executing within an iterative environment, such as the MOEA employed in this experiment.

It is critical for the simulation and validation of results that the existing room's conditions are established in a consistent manner. For this reason, the 'specified ray count' method was selected. As the physical room has a volume of 756m^3, and a ray count ratio of 25:1 was specified to provide balance between consistent results and calculation time, a ray count resolution of 18,900 was established as a constant for digital simulation validations within the experiment. The ray count density employed within the MOEA stages of the experiment was reduced to accommodate

a balance between computational runtime, simulation accuracy and outcome intention. The digital simulation of the base room yielded a T_{60} of 4.26 seconds, an STI of 0.267, and an EDT of 4.2. These results indicated that the room would perform poorly as an acoustic environment.

The next stage of the experiment engaged an MOEA to iteratively simulate varying panelised configurations to determine the probability of the type and placements of acoustic treatments best suited to have the largest acoustic impact. In this context, the digital simulation results of the existing room could be used as a base line for the evolutionary process.

4.3.1.4 Evolutionary Approach to Acoustic Intervention Typology

The primary objective of the experiment was to correlate the augmentation capacity of irregularly featured timber against the optimum location for the material to be placed within a room, to achieve the greatest increase in acoustic performance. Prior to material placement being calculated, differing acoustic treatment typologies were selected, and their specific location within the room was determined. This process allowed potential material performance capacities to be matched against specific acoustic augmentation types and locations.

The precedents discussed in Section 4.2 demonstrate there is often an objective for acoustic interventions to be integrated into the built fabric holistically, rather than an as a retrofitted or additive surface treatment. In these examples, walls and ceiling twist and blend together, surfaces undulate and deform smoothly, and perforation density varies, as necessary.

This level of ubiquitous treatment is suitable in the design and construction of a new building or space; however, in the context of augmenting an existing space, the opportunity for this level of intervention is often not available or practical, due to the additional cost of replacing significant portions of the exiting built fabric. In light of this, the experiment developed a computational workflow that engaged material and acoustic performance, and visual appearance in a holistic way, while maintaining an approach applicable to the retrofitting of spaces.

Conceptually, the design problem and evolutionary method employed were broken into distinct parts (see Figure 4.4).

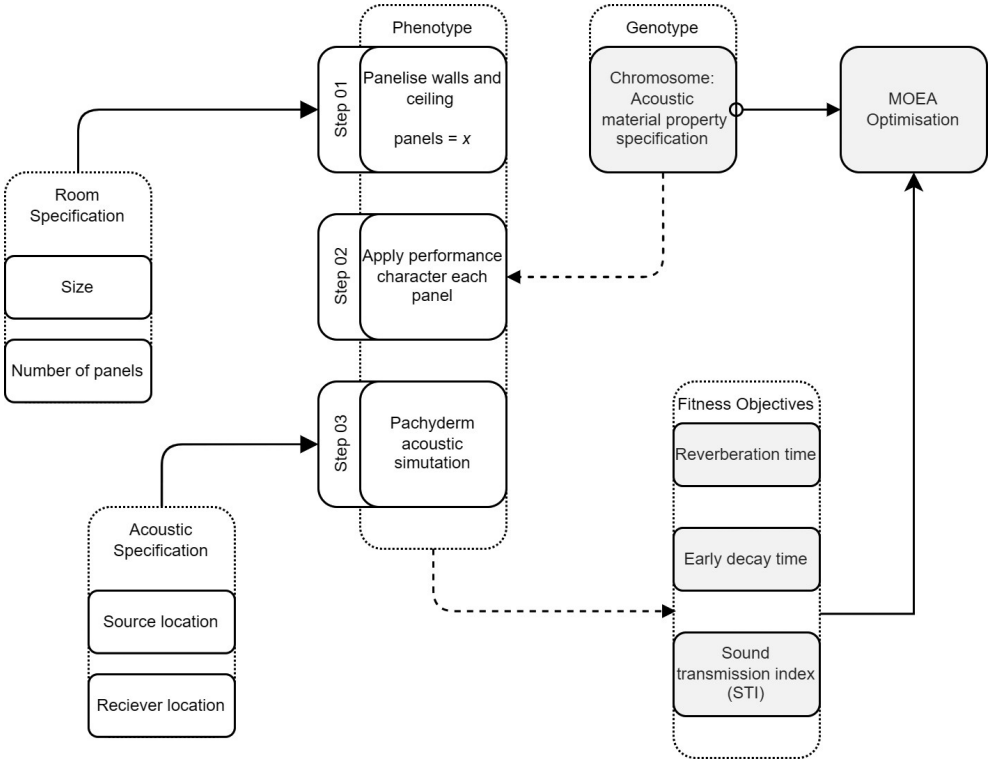

Figure 4.4 Acoustic treatment determination: Evolutionary simulation pseudocode

4.3.1.4.1 Room Panelisation

The sub-division of the rooms' walls and ceiling allowed a higher level of specificity, and variation, of acoustic treatment and positioning throughout the room. With plantation hardwood boards being used as the primary material of intervention, the design and fabrication workflows could be based on either individual boards or panels. Individual board specification offered a greater level of specificity regarding material placement within a room, but created significant complexities in the later material deformation and fabrication stages of the experiment.

Taking a panel-based approach to material placement maintained a suitable level of resolution in terms of material localisation, while avoiding potential fabrication and installation issues by keeping the physical size of elements at a manageable scale. As apparent in the precedents (see Section 4.2), a commonly employed strategy is a panel-based system of either standardised or custom acoustic devices. For this reason, panel-based implementation of unique material placement was pursued. By taking this approach the design and fabrication of the panel could be undertaken using digital fabrication equipment and installation methods common used in current industry practices.

The panel subdivision (see Figure 4.5), was specified at a height of 900mm, with a length of either 2400mm or 3000mm, depending on its location. The vertical subdivision was informed by the physical dimension of the timber

boards, resulting in a lamination of nine boards vertically. Horizontal length was determined by a sheet length compatible with CNC routers commonly available in fabrication workshops (see Figure 4.6). Subsequently, the wall surfaces were subdivided in a matrix of 6x4 panels. This subdivision resulted in panel sizes, as shown in Table 4.2.

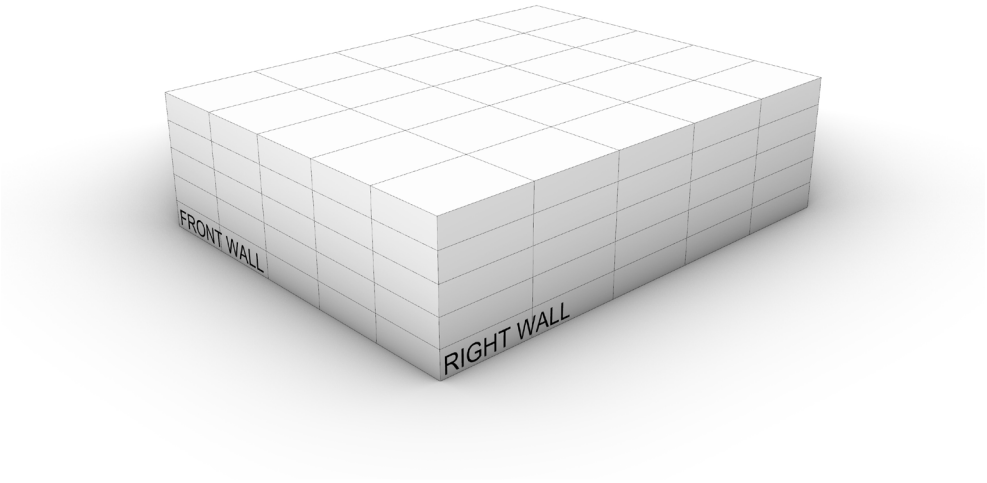

Figure 4.5 Test room wall and ceiling subdivision

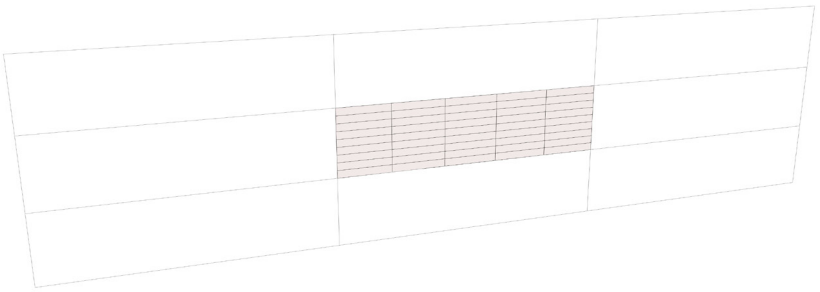

Figure 4.6 Panel subdivision into timber segments

	Subdivision matrix	Panel sizes
Left Wall	5x5	3000x900
Right Wall	5x5	3000x900
Front Wall	5x5	2400x900
Rear Wall	5x5	2400x900
Ceiling	5x5	3000x2400

Table 4.2 Test room panelisation dimensions

4.3.1.4.2 Acoustic Material Properties Specification

The MOEA in this stage was engaged to determine which type of panel augmentation and location made the largest improvement to the room's acoustic performance. Following the architectural panel developed in Section 3.4, three typologies of acoustic interventions were identified for exploration in this experiment:

a) Solid timber panels,

b) perforated timber panels (absorption), and

c) surface deformation (diffusion).

The acoustic properties of each panel type were matched as accurately as possible with real world materials and production data (Cox & D'Antonio, 2017), with absorption and diffusion being specified over six octave bands as specified in *AS/NZS 2460-2002: Acoustics-Measurement of the Reverberation Time in Rooms* (Standards Australia, 2016). Additionally, diffusion had a surface feature depth specified to reflect the likely physical material properties. Table 4.3 shows the absorption properties specified for each material definition, and Table 4.4 shows the diffusion properties.

	Concrete	Solid Timber Panel	Absorption Panel	Diffusion Panel
125 Hz	5	22	80	10
250 Hz	5	18	80	10
500 Hz	5	15	80	10
1 kHz	5	8	80	10
2 kHz	5	9	80	10
4 kHz	5	10	80	10

Table 4.3 Absorption coefficient of material types over frequency range (% energy absorbed)

	Concrete	Solid Timber Panel	Absorption Panel	Diffusion Panel
Variegation	5mm	5mm	5mm	30mm
125 Hz	5	10	10	80
250 Hz	5	10	10	80
500 Hz	5	10	10	80
1 kHz	5	10	10	80
2 kHz	5	10	10	80
4 kHz	5	10	10	80

Table 4.4 Diffusion coefficient of material types over frequency range (% non-specular reflected energy)

4.3.1.4.3 MOEA Fitness Objectives

As discussed in Section 4.3.1.1, the digital version of room was acoustically simulated, using STI, T_{60} and EDT as measures of acoustic performance. As suggested by Bradley (1986), Mealings (2016), and Siebein, et al. (2000), STI of 0.7, T_{60} of 0.6 seconds, and EDT of 0.6 seconds are representative of suitable acoustic characteristics for a classroom environment. Subsequently, these measures were employed as Fitness Objectives within the MOEA.

As outlined in Section 4.3.1.2 the target STI was specified as 0.7. While this value does not reflect the highest possible result for this acoustic measurement, it is considered a good performance result for a room of this size and occupation type. Additionally, the target STI is variable within the workflow, allowing it to be scaled to other subject rooms and different use types. As the MOEA optimisation process aimed to minimise the value of each Fitness Objective, it would inevitably reduce the STI result beyond its goal, achieving worse results. For this reason, the absolute differential between each iteration's STI simulated result and 0.7 was specified as the Fitness Objective, expressed as *0.7-α*. This arrangement ensured that regardless of whatever the Fitness Value is, the lower the value, the closer it is to the intended STI.

In the case of Reverberation (T_{60}), a lower value represents a room that is less reverberant and produces less echo. As noted in Section 4.3.1.2, a T_{60} result of nominally 0.6 seconds and EDT of 0.6 seconds is considered acceptable for classroom environments; however, STI is generally considered a better indicator of the overall room performance. Within the MOEA Fitness Objectives, both the T_{60} and EDT objectives were specified to optimise towards zero, which allowed the STI measurement to be set as the primary Fitness Objective.

Specifying an exact STI goal and allowing T_{60} and EDT to optimise towards zero established a MOEA environment that opened the potential fitness landscape beyond being a purely reductive process. It also created a field of optimised solutions with conflicting results, generating a potential for a larger Pareto front.

4.3.1.4.4 MOEA Iteration Configuration

The configuration of Wallacei (Makki et al., 2022) is critical in generating a successful evolutionary simulation. A balance needed to be sought between iteration population, simulation parameters, algorithm settings, embedded calculations, and computation run time. When a population size is too large, or the embedded calculations are complex, the calculation run time exponentially increases. If the *crossover* and *mutation probabilities*

are too high or low, the solver will not be able to adjust its search breadth accurately enough. As, such, the complexity of the design problem specified within the MOEA was established in a manner that maintained population diversity, while maximising the efficiency of the embedded calculations (see Table 4.5).

Evolutionary algorithm parameters	
Generation size	50
Generation count	100
Population count	5000
Crossover probability	0.9
Mutation probability	$1/n^{\text{n=number of variables}}$
Crossover distribution index	20
Mutation distribution index	20
Random seed	1
Simulation runtime	86h 21m

Table 4.5 Acoustic treatment determination: Evolutionary algorithm parameters

Each iteration of the MOEA varied the acoustic treatment types between the three options, across the 125 panel zones within the room. As each solution presented a different configuration of absorption and diffusion material characteristics, they directly influenced the acoustic simulation performance. As such, each panel in the subject room was allocated an evolutionary gene, with three acoustic treatment options available to each, resulting in 375 possible values to be applied within each evolutionary iteration (see Table 4.6). This translated to a *search space* of 4.4^{e59} possible solutions. The MOEA simulation was specified to have a population of 50 over 100 generations, resulting in 5000 solutions throughout the run.

Each generation of the MOEA required the completion of an acoustic simulation using the Pachyderm acoustic plugin. While variation of the acoustic panel configurations was processed almost instantly within each iteration, the acoustic simulation required a computationally demanding set of calculations to be undertaken. When run in isolation as a single

Chromosome: Acoustic material property specification		
No. of Genes	**Numerical Domain**	**Function**
125 *x* panels	0-2 (3 values per gene)	To allow the MOEA to alter the acoustic performance characteristics of each panel within each iteration.

Table 4.6 Acoustic treatment determination: Gene pool specification

process, the computational runtime was 90 seconds, with the acoustic simulation component consuming 85 seconds of that time.

Five manual iterations were run, and the resulting variation in calculation time was ±4 seconds. This minor discrepancy is a result of the different configurations of acoustic panel types requiring varying levels of acoustic computation. When scaled up to the MOEA solver, each iteration required an average of 62 seconds per cycle, resulting in an overall calculation time of 86 hours and 21 minutes. The significant decrease in per-iteration calculation time was a result of the MOEA not being required to recalculate the entire workflow at each iteration, only the panel configuration. As discussed in Section 3.5, a simulation process that takes 86 hours to calculate is a relatively large amount of time to be consumed by a design simulation process; however, this was to be expected in a MOEA that had conflicting Fitness Objectives and included a complex acoustic simulation within each iteration.

The conflicting nature of the Fitness Objectives is shown in the parallel coordinate plot of Fitness Objectives, depicted in Figure 4.7. Fitness Objectives 1 and 2 represented Reverberation and Early Decay Time, and it was evident they were convergent and demonstrated a correlated improvement as the algorithm progressed; however, the performance of Fitness Objective 3 (STI) demonstrated an inverse relationship, with higher performing solutions having poorer results in relation to Fitness Objectives 1 and 2. It was evident that the MOEA would not generate a solution in which all Fitness Objectives converged. (The statistical analysis of each Fitness Objective is detailed in Figure 4.8).

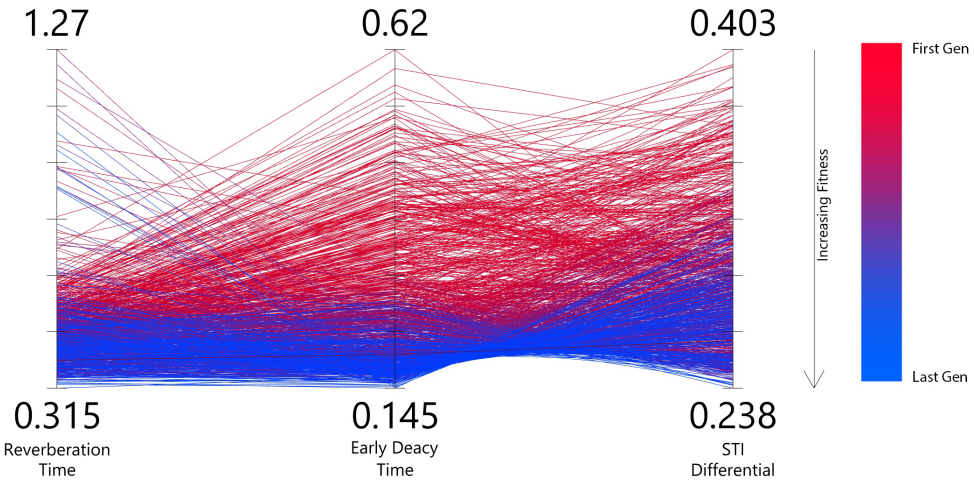

Figure 4.7 Parallel coordinate plot of fitness values of each solution

4.3.1.5 Hybridisation of Fittest Solutions

Through evolving a population size of 5000 solutions, the MOEA generated 45 Pareto front solutions, in which no single Fitness Objective could be improved without having a negative impact on the other objectives. This presented a problem as to how a single optimal solution could be selected when there were no converging results. A range of techniques were available within the MOEA for reducing the solution set to either a single or smaller pool of solutions (Showkatbakhsh & Makki, 2022), including:

- selecting the solutions with the highest performing result for each of the Fitness Objectives (solutions 71;28, 85;37, 80;39);
- finding the solution that had the most 'average' result across the solution set (solution 83;37); or
- selecting the solution that demonstrated the closest relative distance between Fitness Objectives (solution 42;48).

Further, a innovative method of analytical reduction is provided by Wallacei: K-means clustering of the Pareto solutions. This unsupervised machine learning method clusters solutions together based on their fitness 'proximity', allowing a more localised representation of the Pareto front, while maintaining a fair representation of the solution set's diversity (Makki, 2019; Malki et al., 2016).

This technique was applied to the Pareto solutions set with a K-value of nine, with between 2 and 20 calculated within each, as shown in Table 4.7. The geometric representation of the acoustic panel variation within the clusters is shown in Figure 4.9. Regardless of which analysis method was employed, each presented a dataset that specified the acoustic treatment profile of each individual panel within the room as being of a single type. This was contrary to the ambitions of the experiment, which was aimed

Cluster	Central solution	Solutions in cluster
1	73:30	9
2	96:38	5
3	81:42	6
4	87:37	4
5	98:40	7
6	85:35	6
7	54:29	2
8	84:40	4
9	72:31	1

Table 4.7 K-means clustering of 45 Pareto solutions – geometric acoustic panel variations

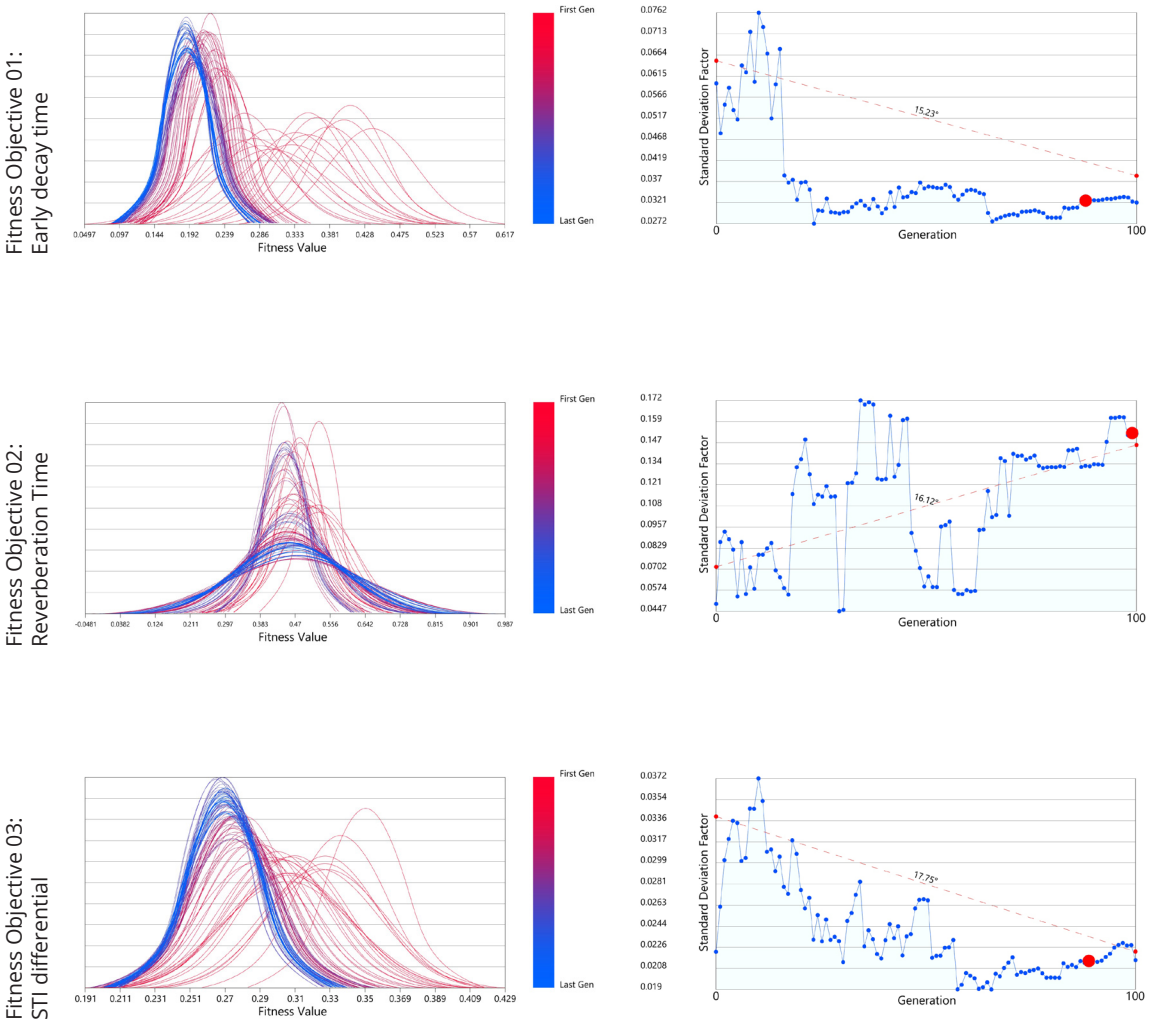

Figure 4.8 Statistical analysis of each Fitness Objective

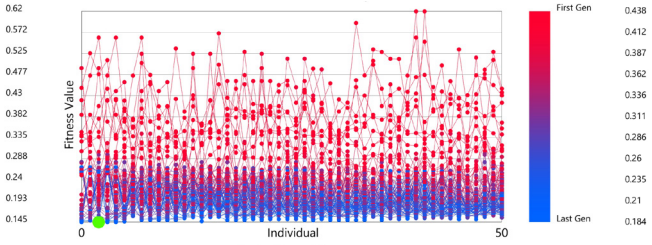

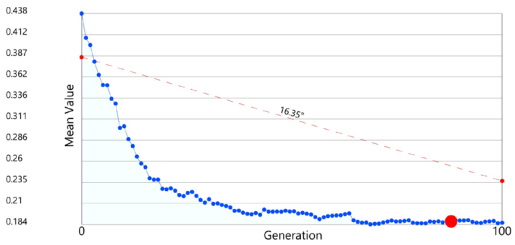

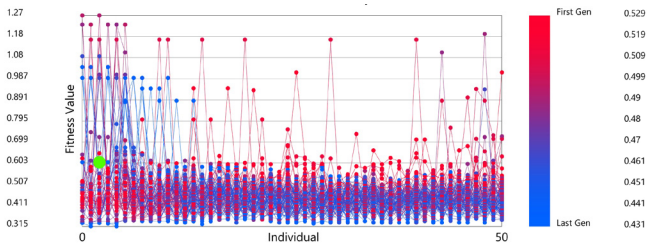

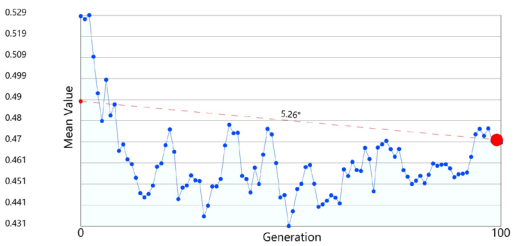

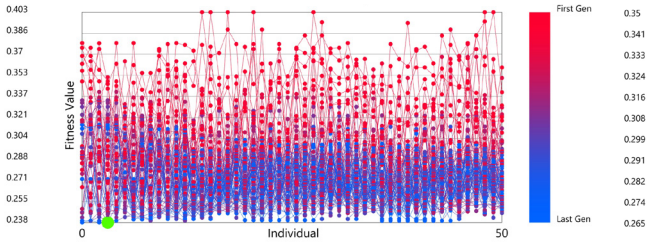

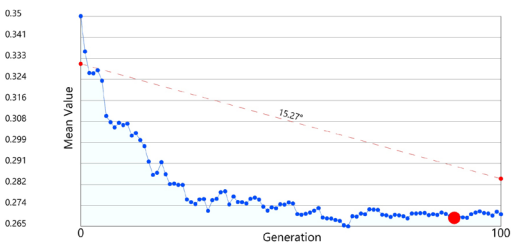

Fitness Values Graph

Mean Values Trendline

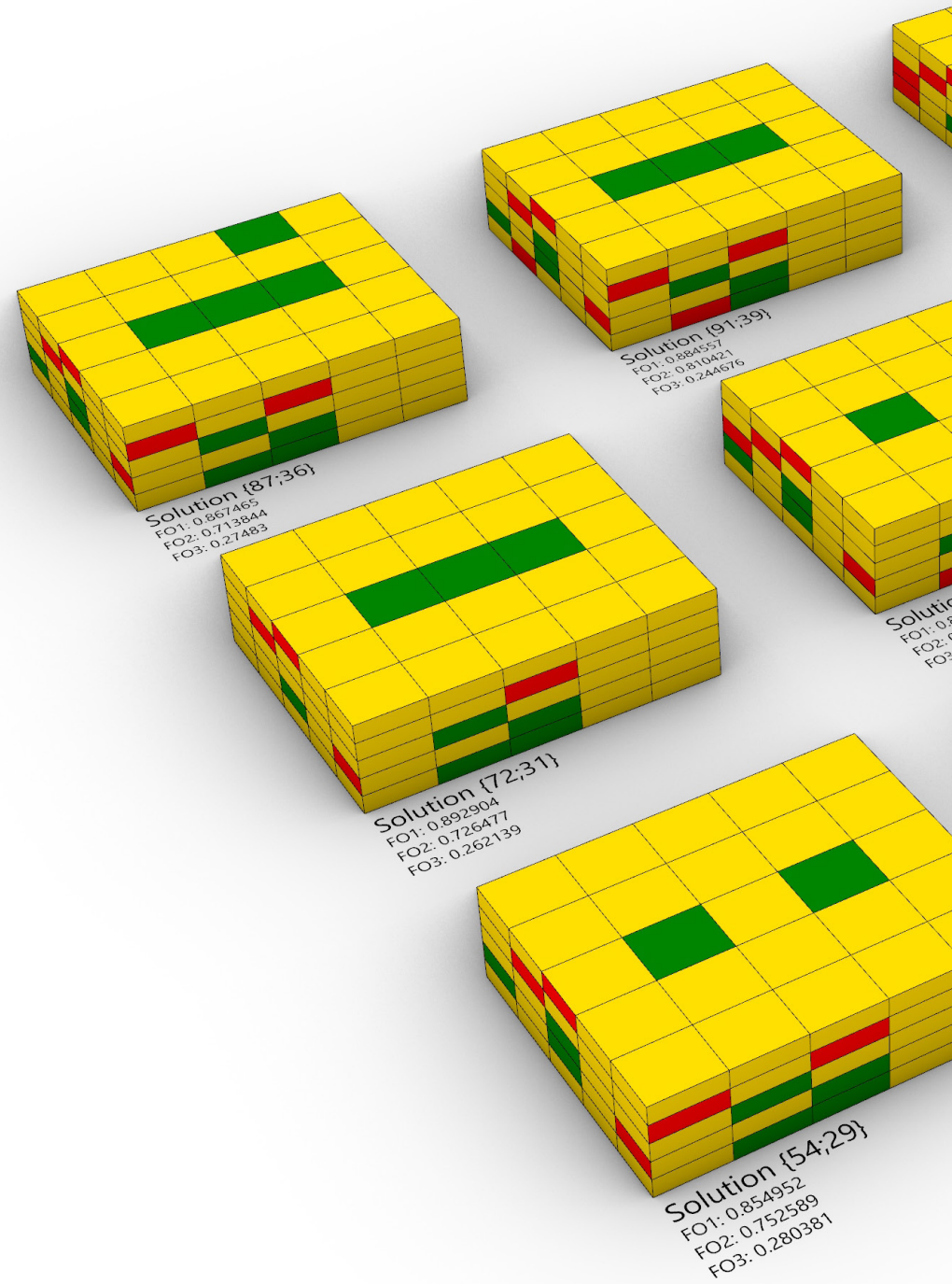

Figure 4.9 K-means clustering of 45 Pareto solutions – geometric acoustic panel variations

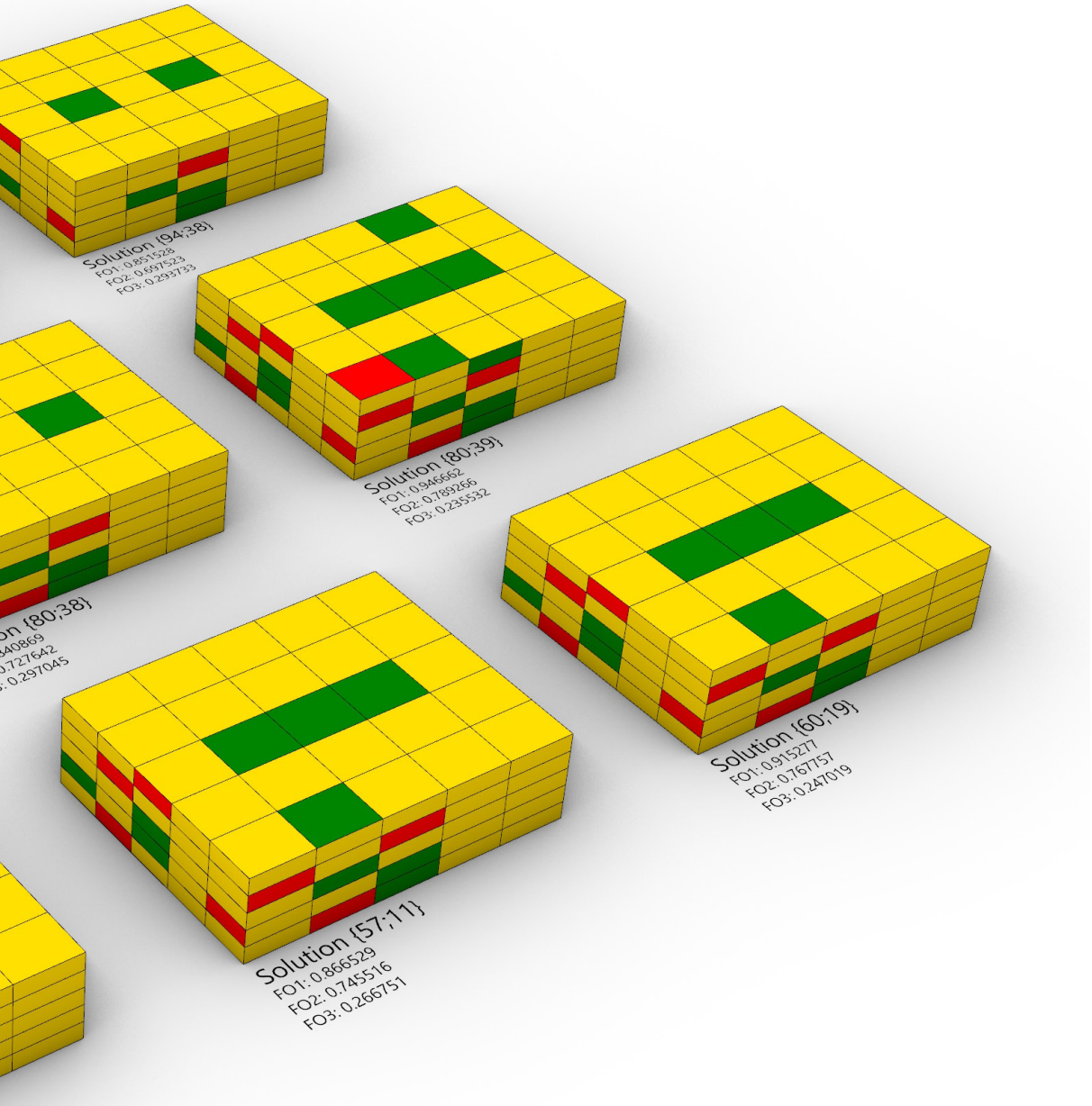
Solution {94;38}
FO1: 0.851528
FO2: 0.697523
FO3: 0.293733
Solution {80;39}
FO1: 0.946662
FO2: 0.789266
FO3: 0.235552
Solution {80;38}
Solution {60;19}
FO1: 0.915277
FO2: 0.767757
FO3: 0.247019
Solution {57;11}
FO1: 0.866529
FO2: 0.745516
FO3: 0.266751

at creating an integrated acoustic panel system that seamlessly merged between treatment types, regardless of location.

As established in Section 3.4, the hybridisation of acoustic performance characteristics within a single panel could to be generated concurrently with the utilisation of irregular materials. Subsequently, the focus of the solution analysis and selection process shifted away from an objective set of conflicting Fitness Objectives, morphing into a hybrid approach that sought to merge the Pareto solutions into a single solution, which established a ratio of acoustic performance for each panel.

By employing a hybridisation method of Pareto selection, the relationship between acoustic augmentation type and frequency of occurrence could be determined. For example, of the 45 Pareto solutions, a single panel may have been found to have one instance of nil augmentation properties, absorptive properties 30 times, and diffusion properties 14 times. This establishes a relationship whereby the panel required a range of different performance characteristics simultaneously at a percentage-based ratio of 2:67:31 (see Figure 4.10). Each panel within the room matrix had a specific ratio (employed in Stages 3 and 4 of the experiment) in relation to material distribution and augmentation design.

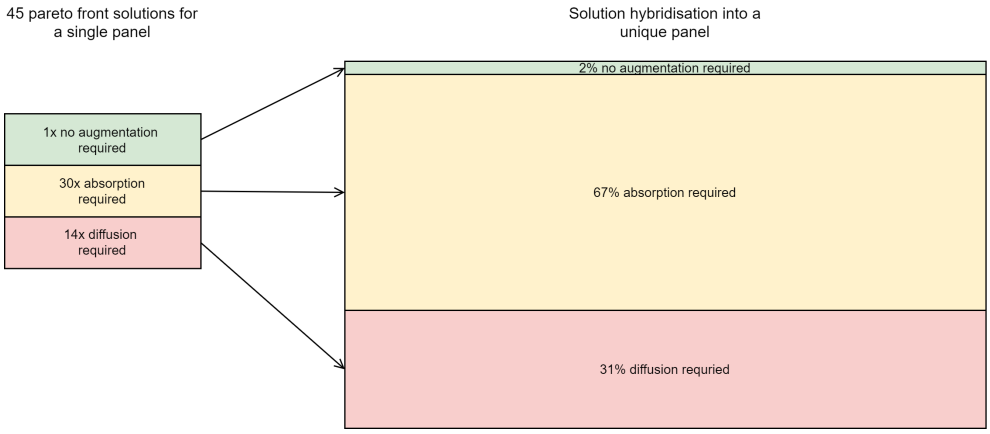

Figure 4.10 Hybridisation of Pareto front solutions into a single panel

The hybridisation of the Pareto fronts generated a single solution that did not represent the highest performing calculated outcome; rather, it accommodated a finer-grain understanding of the range of outcomes that foster an acoustic improvement at a macro scale. As it was no longer a 'fittest' solution, the hybridisation method needed to be validated to ensure it was creating a solution that increased acoustic performance. This process required the hybrid ratio of each panel to be developed

geometrically, with the acoustic simulation being run on the resulting digital model.

The translation of the Pareto ratio to geometric representation is undertaken through a panel subdivision process. Each individual panel was divided horizontally into areas that correspond to the specific ratio. Figure 4.10 illustrates this process, in the context of the room, with green, yellow, and red representing solid timber, absorption, and diffusion panel types, respectively.

Following this subdivision, the room was found to have an acoustic intervention ratio of 15:69:16. While there is potential for 375 acoustic augmentation instances across 125 panels, the hybridised solution allocated 320 individual instances of varying sizes across the room. This is due to the results of the simulation establishing that any individual panel could contain 1, 2 or 3 types of acoustic augmentation specification.

4.3.1.6 Results

The validation of results required the acoustic performance of the hybrid solution to be simulated using the same test environment as the base line and evolutionary simulations. The validation simulation took 12 minutes 46 seconds to calculate. This increase in calculation time was due to the high number and variation of acoustic material locations within each panel. The simulation had a Reverberation result (T_{60}) of 0.75 seconds and an STI result of 0.43 (Table 4.8).

	STI	**Reverberation (T_{60} in seconds)**
Suitable results	0.7	0.6
Baseline simulation	0.169	1.77
K-means Pareto solution average	0.58	0.46
Hybrid solution	0.53	0.75

Table 4.8 Comparison of STI and T60 results from acoustic simulation

The validation process found the hybrid solution had an increased acoustic performance over the initial existing room simulation. While these results demonstrate that the hybrid solution did not perform as well as the Pareto solution average, it did obtain results that were greatly improved over the baseline simulation. While this discrepancy was unexpected, it is reflective of the Pareto hybridisation processes enabling each of the 125 panels to contain a mix of augmentation characteristics.

This was a desired outcome of this experiment, and extended the capacities developed in Section 3.4. In contrast, if the average of the Pareto solutions

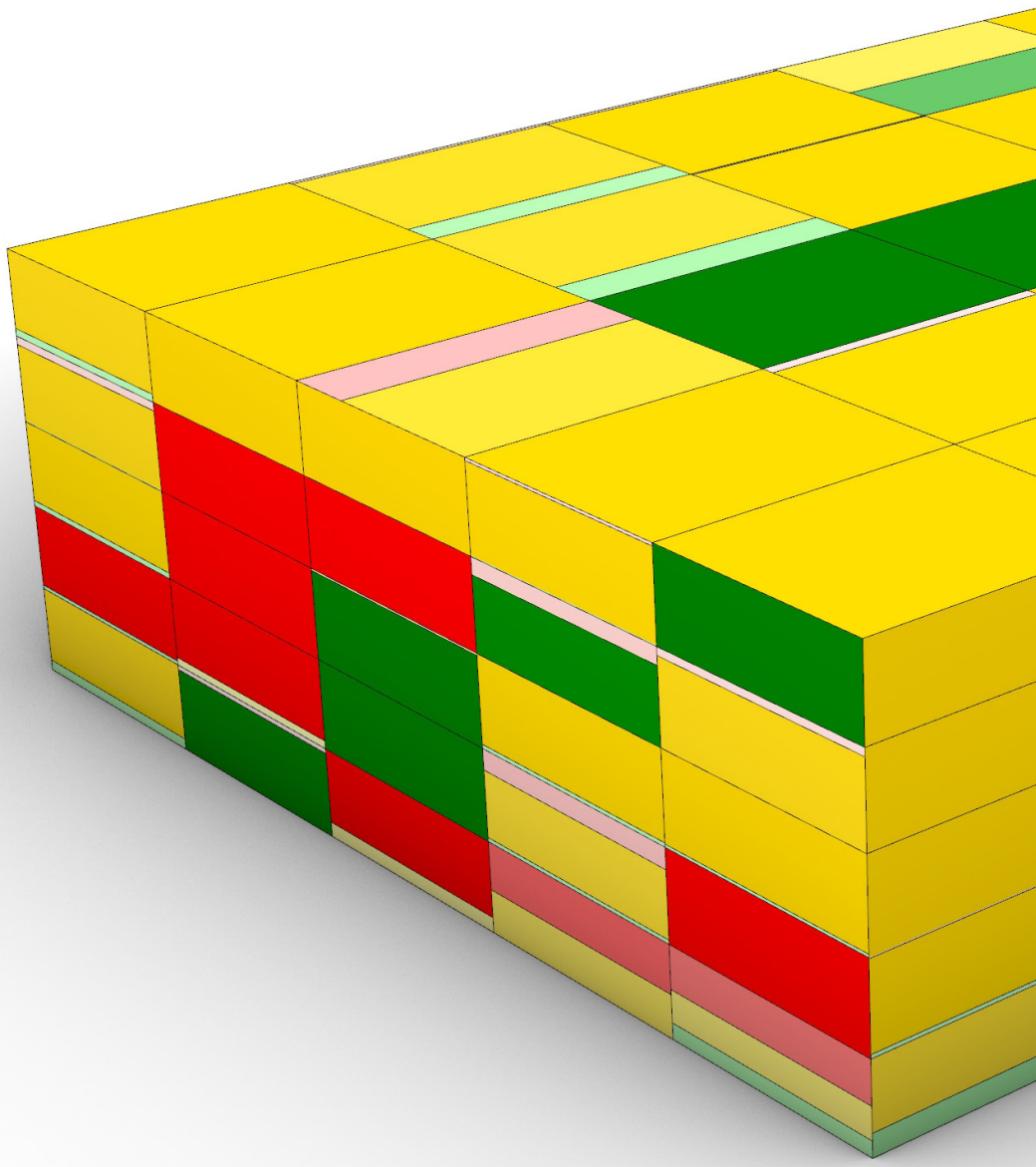

Figure 4.11 Hybridisation of 91 Pareto solutions represented as geometric room panels

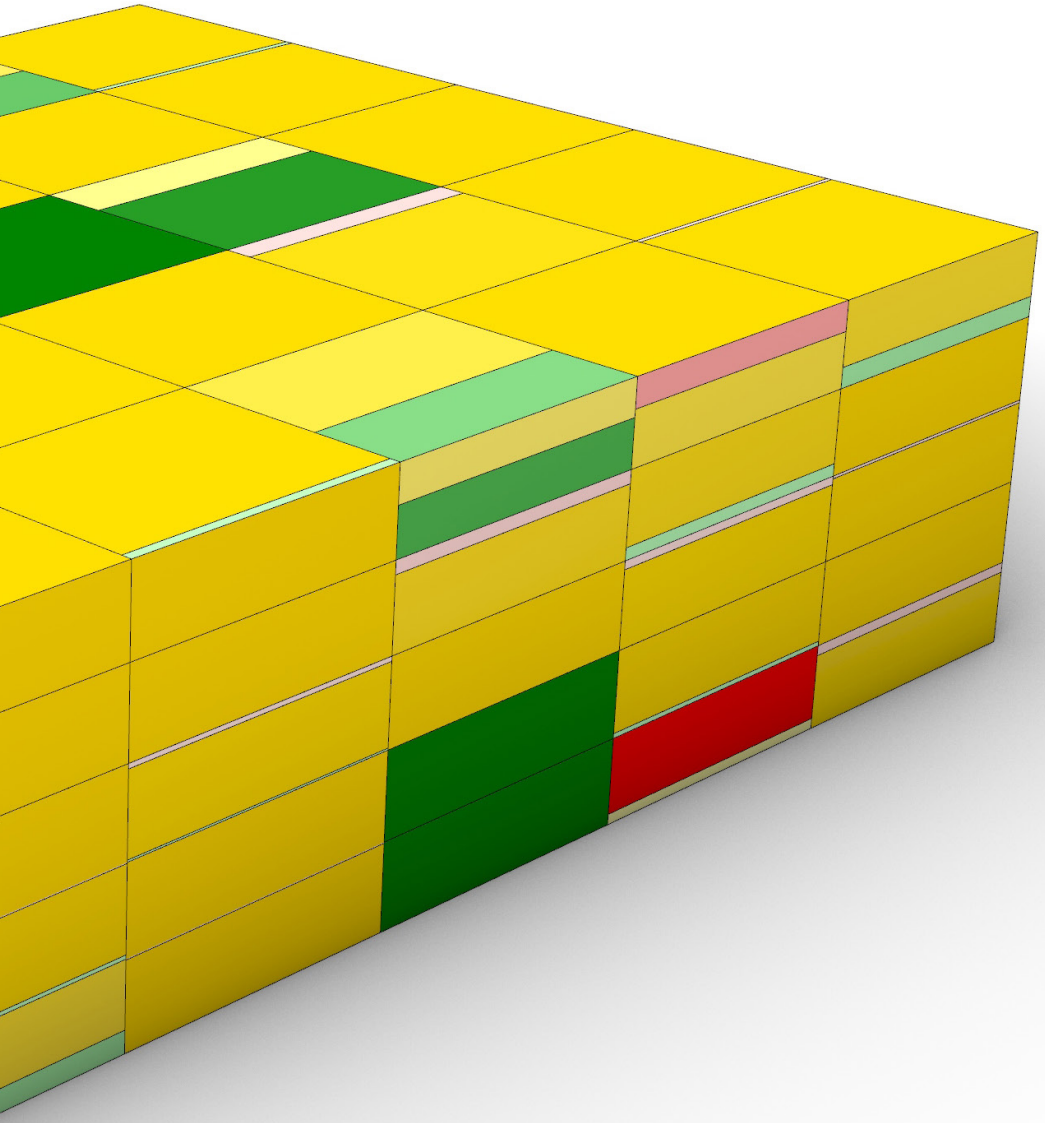

was used, each panel would have received a single acoustic performance requirement, removing the opportunity for different configurations of acoustic augmentation within each single panel.

It is important to note that the hybridised acoustic characteristics objectives in this stage build on the 'acceptable optimisation' strategy, outlined in Section 3.5. Significantly, as the performance profiles for each panel were presented as ratios of augmentation type, rather than specific acoustic results, the distribution of material could be correlated with less complexity. This shifts the experiment's focus on investigating the capacity for material utilisation and augmentation/fabrication type, instead of attempting to reach ultimate acoustic objectives.

In the experiment's context, not reducing the simulation to a single optimal solution did not pose a significant issue as this stage was being employed to determine material placement and fabrication strategy, rather than a definitive acoustic solution.

Both of the following stages afforded a level of optimisation that sought to match potential acoustic improvement with specific material features of each unique timber boards within the constrained inventory (Section 4.3.2). While the hybrid acoustic characteristics were determined for the entire subject room, it was considered valuable to move beyond the virtualised material representation (see Section 3.5) and test the capacity of the discretised data within a design scenario. As the constrained inventory had a finite volume of timber boards, Stage 2 and 3 of this experiment considered the material distribution and fabrication strategies for nine of the calculated panels. Significantly, the unique timber boards are distributed across the nine panels by correlating discretised material features with specific hybrid acoustic objectives.

4.3.2 Stage 2: Material Discretisation

4.3.2.1 Material Discretisation

The experiment required the existing constrained inventory (established in Section 3.3) to be discretised based on their capacity to be physically augmented through fabrication processes. This capacity was later used for both customised material distribution and acoustic intervention; however, geometric representation did not provide a level of resolution adequate for these processes to be undertaken successfully. Subsequently, the geometric representation was required to be expressed within a numerical context.

Notably, although a feature may have significance within a single board, it does not necessarily translate to the same significance within the

acoustic surface, requiring a higher resolution of discretisation for both board segment size and feature representation. If the boards were to be considered at their original length, there would be regular instances where boards would need to be docked to fit within a single panel, creating significant material waste. By dividing the boards into smaller segments, the volume of material discarded (as offcuts) is significantly reduced. In responding to this, a relationship was established with the final acoustic panel dimensions, which is in turn influenced by the subject room size.

The room had been subdivided into panels (Section 4.3.1.4.1) consistent with industry standard sized panels that could be fabricated with the available equipment. This allowed a board segment length of 600mm to be used as it divided equally into both panel widths. The board segment length was defined parametrically within the presented workflow to allow flexibility in other scenarios where rooms were different sizes. The segmentation process provided a greater level of material utilisation. In any given board the offcut could be between 1 and 599mm, with the average across the available inventory found to be 210mm. This level of segmentation resulted in 489 segments being created, with each being paired with the corresponding identified features.

The feature classification process employed a multi-scalar approach to discretisation, allowing a sample resolution of between 3mm and 30mm to be specified. It encapsulated both numeric and geometric representations of each board segment and its contained features. The translation of detected features to a finer subdivision was undertaken by a geometric process that intersected the outlines of detected features with the subdivided cells and generated points were matched with the corresponding subdivided cells. If a cell had matched curved intersection points, then it was determined to contain a detected feature. Conversely, a cell with no intersection points was classified as an area of clear timber (see Figure 4.12).

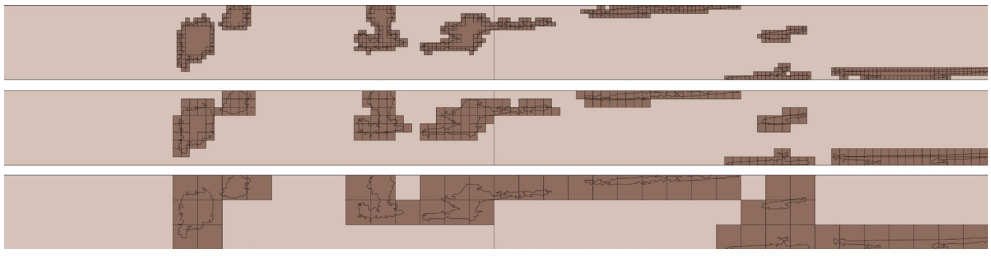

Figure 4.12 Board subdivision with discretised features shown in brown.

Once all cells were processed, adjoining cells of the same classification were merged. The accuracy of this process has an immediate relationship

with the resolution of subdivision and the subsequent calculation time (an example of which is shown in Table 4.9). The impact of the discretisation resolution is illustrated by using a single board (board_ID_20), which had a total area of 2800 cm^2 and a detected featured area of 85.59cm^2, representing 3.05% of total featured area.

Table 4.9 Subdivision resolution and feature classifications (board_ID_20)

Discretisation Resolution	Detected area (cm^2)	Featured cells' area (cm^2)	Cell accuracy	% of board featured	Calc. time (sec)
3mm	85.59	116.28	73.6%	4.15%	521.9
5mm	85.59	130.75	65.4%	4.67%	77.3
10mm	85.59	163.00	52.5%	5.82%	16.0
30mm	85.59	279.00	30.7%	9.96%	9.6

It is evident that a coarse level of resolution created established a greater area of feature representation due to the generated intersection points being spaced further apart. At a sample resolution of 30mm, 9.96% of the board area was classified as being featured, while a resolution of 3mm classified the same board as having 4.15% feature. However, there was a significant difference in computation time between the two resolutions: 30mm resolution taking 9.6 seconds per board compared with 521.9 when using a 3mm resolution. This increase in computation time represented a significant 'bottle neck' in the detection process. Subsequently, a sample resolution was required that balanced accuracy and computation time.

Svilans (2020) discusses the impact of discretisation resolution and computational processing time, and determined that the scale of resolution should be matched to the relative scale of the intended outcome. In a production environment, a lower resolution would most likely be employed, as time efficiencies would be prioritised over material waste. However, as this experiment seeks to engage material at a finer level, computational time is of less concern, thus allowing a closer pairing of resolution and material engagement.

The fabrication parameters employed in the augmentation design phase of the experiment utilise a 20mm cutter head. A discretisation resolution

of 5mm (see Figure 4.13) was determined to be a good match for the fabrication process, allowing a greater discretisation efficiency.

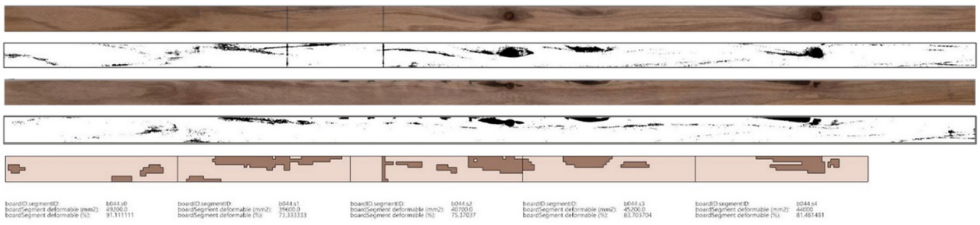

Figure 4.13 Discretisation of timber boards at 5mm resolution

4.3.2.2 Results

The discretisation process resulted in a constrained material inventory of 428 segments that originated from 84 timber boards. The inventory comprised both numerical and geometric information about each board segment and the corresponding detected clear and featured areas. The numeric representation comprised a board segment identification tag, in addition to the percentage of the board that is clear, with the featured areas being the remaining percentage.

The geometric representation was reduced in complexity from the original surfaces to boundary curves of each of the clear and featured areas within each segment. This shift in representation was required to minimise the volume of data being stored and transferred to the following stages of this framework, as curve-based geometry carries less complexity and results in smaller file sizes. Further, curve-based geometry is less computationally demanding to both calculate and visualise on screen.

4.3.3 Stage 3: Material Distribution

Two datasets had been established within Stage 1 and 2 of this experiment:

a) The first contains the hybridised acoustic performance profiles for each of the 125 panels within the test room. The performance profile of each panel is the result of the hybridised Pareto solutions that depict the number of times each acoustic intervention type (solid panel, absorptive panel or diffusion panel) occurred in each solution.

b) The second is the constrained inventory of timber board segments. The numerical and geometric information within this inventory details the percentage of each 600mm segment that contains a naturally occurring timber feature. This is representative of the potential augmentation capacity of each

segment that can be coupled with the hybridised performance profile.

Stage 3 of the experiment engaged a second evolutionary algorithm that aimed to distribute the material within the constrained inventory across a selection of panels from the room, pairing potential acoustic capacities with specific panel design objectives. Critically, this process sought to generate a balance between material distribution and panel performance character by considering the location of each segment relative to the entire room, rather than any single panel.

4.3.3.1 Selection of Subject Panels

This experiment had been designed in a manner that is scalable. Ultimately, the material distribution would consider all the panels within a room and have access to a large material inventory, allowing the whole room to be considered within the evolutionary calculations. In this case, the material stock available was limited to 80 boards, resulting in an inventory of 428 board segments with a length of 600mm. Considering this limitation, the material distribution process was scaled to consider nine panels, each comprising 45 positions for material to be placed, arranged in a 9x5 matrix. In total, the selected nine panels required 405 pieces of material to achieve full coverage.

The number of pieces required within the Design Problem was an important factor with the evolutionary solver, as it meant that there was no duplication of material inventory, and that there was an excess of 23 segments to consider in each iteration of the solver calculations. In a full room implementation, excess material would be available for distribution. Each material segment was paired with its featured area percentage to allow the solver to search for a fittest solution matching material potentiality with panel acoustic augmentation.

The constrained inventory of material allowed for a total of nine room panels to be selected for further engagement in this experiment. Several criteria were employed to select which panels were utilised.

a) The first required the panels to be grouped together, rather than being spread across the room. This is important, as the subsequent acoustic augmentation design processes required the panels to form a continuous surface within the room, rather than as a series of individual entities.

b) The second determined that the group of panels should be in an area within the room that would have significant potential impact to acoustic augmentation. As the acoustic

simulations were undertaken with single sound source and receiver locations, the areas of larger impact would be halfway between the two locations on the side walls and floor and ceiling. Secondary locations for consideration were deemed to be centralised on the front and back walls of the room.

c) The third sought to select a group of panels that demonstrates a variety of acoustic augmentation types. Groups that contained a range of different individual and mixed performance goals would demonstrate the capacity of the evolutionary approach to material distribution with greater clarity.

Taking these criteria into consideration meant that the central nine panels (81-83, 86-88, and 91-93), arranged in a 3x3 grid, on the left-hand wall, were the most appropriate for material distribution experimentations. Figure 4.14 shows these panels and the geometric representation of their determined acoustic intervention profiles. Within this group:

- green represented areas indicated no required acoustic augmentation and subsequently specified as solid timber;
- yellow indicates areas that indicated preference for absorption characteristics; and
- red conveys diffusion characteristics.

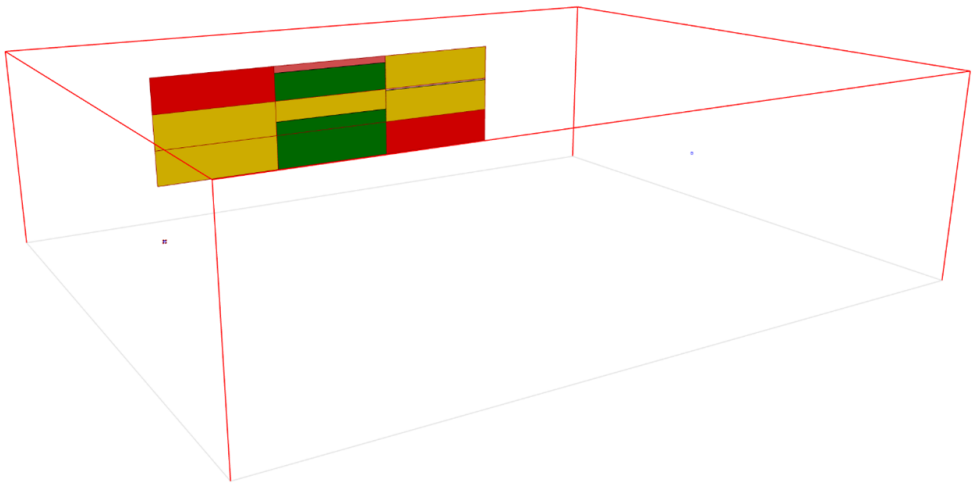

Figure 4.14 Nine panels selected for experimentation

Table 4.10 details the numerical correlation of the panels and their subsequent acoustic performance profile. The specificity of a panel's performance profile played an important role in the design of the acoustic augmentation and fabrication frameworks that are developed within Section 4.3.4. However, for the purposes of custom material distribution,

the detailed acoustic character could be further rationalised, as shown in Table 4.11.

As established in Section 3.4, timber that contains areas of knot-based features is less suited for significant augmentation within the fabrication process. This is due to the integrity of the timber features becoming structurally unstable as material is removed. Both absorption and diffusions acoustic augmentation require material to be physically augmented or removed from the panels through subtractive processes. For this reason, absorption and diffusion Fitness Objectives can be merged.

As shown in Table 4.11, this results in the central column of three panels (panels 86-88) required a minimal amount of acoustic augmentation, in contrast with the outer two columns (six panels in total) that required full augmentation. When these Fitness Objectives are compared with the constrained material inventory (specifically the augmentation capacity) it was expected that the material distribution algorithms would place boards

Table 4.10 Acoustic Fitness Objectives

Panel	Solid Timber %	Absorption %	Diffusion %
81	0	0	100
82	0	95.6	4.4
83	0	100	0
86	100	0	0
87	39.56	50.44	10
88	80.21	0	19.79
91	0	100	0
92	0	100	0
93	0	0	100

Table 4.11 Hybrid performance targets

Panel	Non-augmented %	Augmented %
81	0	100
82	0	100
83	0	100
86	100	0
87	39.56	60.44
88	80.21	19.79
91	0	100
92	0	100
93	0	100

with greater featured areas on panels 86-88 and boards with less material feature on panels 81-83 and 91-93.

4.3.3.2 MOEA Approach to Material Distribution

The material distribution component of the experiment was undertaken by an evolutionary algorithm that sought to match featured material with areas within the room that require minimal acoustic performance augmentation. Wallacei (Makki et al., 2022) was employed as the evolutionary solver; however, it was utilised to run a single objective problem, as opposed to the multi-objective application in the acoustic simulation stage. Figure 4.15 outlines the evolutionary workflow established for material distribution.

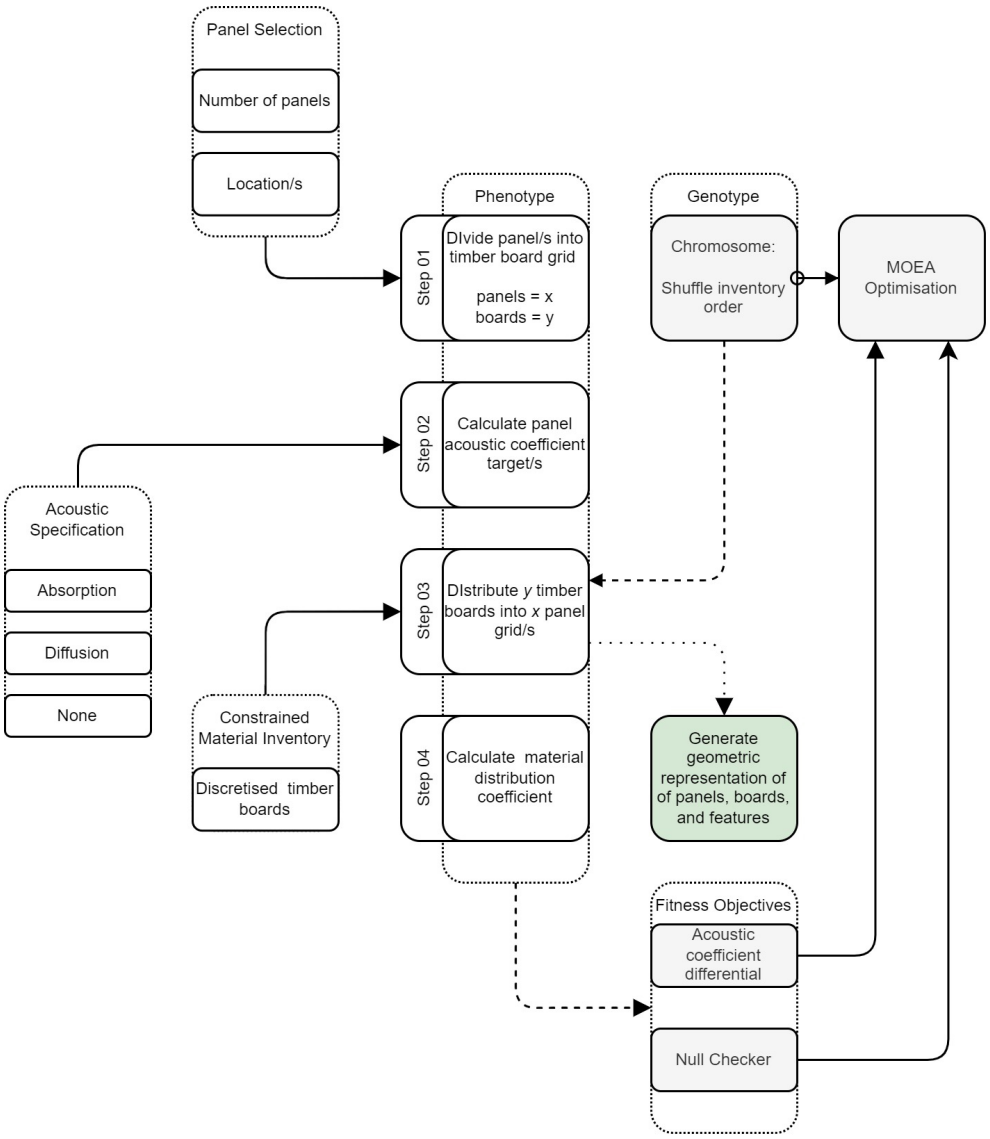

Figure 4.15 Acoustic material distribution: Evolutionary simulation pseudocode

4.3.3.3 MOEA Fitness Objectives and Genes

The evolutionary objective established in the material distribution process sought to match a panels' acoustic profile with the augmentation capacity of board segments within the constrained inventory of material. The genes that are varied within each iteration of the evolutionary solver corresponded to a unique configuration of material segments across the nine panels.

Two sets of data were required for this process to be calculated and iterated:

a) the ratio of augmentation character requirement of each panel; and

b) the percentage of each board segment that is featured.

Each selected panel had a specific hybridised acoustic performance profile (see Table 4.11) to be representative of the material augmentation objectives required to generate the desired performance profile. This translation allowed a direct calculation with the board segment data and simplified the material distribution algorithm significantly. The second dataset entailed the unique augmentation capacity of each board segment within the material inventory, as captured within the discretisation process.

At the commencement of each evolutionary iteration, each of the 428 board segments was allocated an ordering value (as specified in Table 4.12). Ideally, this value was between 0 and 427; however the method applied within Grashopper3D allocates *gene* values at random and the likelihood of repeated values within the population is very high. If a segment was allocated the same value as another it would mean that those pieces would be placed within the distribution matrix in the same position. Two methods were employed to eliminate the potential of repetition within the evolutionary cycle.

Chromosome: Shuffle inventory order		
No. of Genes	**Numerical Domain**	**Function**
428	0.000000 to 1.000000 (10^6 values per gene)	To provide a traceable sort index to each discreet timber board dataset from the material inventory, facilitating variation of the boards selected by the phenotype.

Table 4.12 Acoustic Material distribution: Chromosome specification

The first duplication prevention measure considered the vast search space established, as developed within Design Probe 4 (see Section 3.5.3.3). The unique sorting index that influenced the position allocation of each timber

segment within the material inventory was expressed with six decimal places within the genotype. Applying this level accuracy across the 405 board segments was required to populate the nine selected panels and established a practically infinite search space. This scale yielded a potential for repetition of almost zero; however, as the evolutionary solver selected the fittest gene values from each generation to take to the next, the probability of repetition occurring increased as the solver progressed into each subsequent generation, as it was, in effect, locking gene values. During testing with smaller iteration cycles, repetition was detected in isolated instances. For this reason, a second method of filtration was required to ensure repetition did not negatively influence the solvers capacity.

The second method leveraged the evolutionary solver's capacity to disregard 'Null' values. This process established the number of board segments available for distribution (in this case 428), then determined the number of unique position values generated within the list. If there was no repetition in the position list, the filter returned a value equal to the number of segments and allowed the remainder of the distribution routine to calculate.

As there were approximately one million potential value positions available to each segment, the likely hood of repetition was very small; however, if repetition was detected, the number of unique values would be less than number of board segments. In this scenario a 'Null' value was generated, subsequently triggering the evolutionary solver to disregard this iteration within its calculation. This method provided a backup process to ensure that (however unlikely), positional repetition within the *gene pool* was culled to ensure the evolutionary solver was not influenced by erroneous data.

In most cases, there was no repetition detected and the remainder of the calculations within the iteration were undertaken. Each of the selected panels required a fixed number of board segments, which then required the inventory to be split into nine sub-groups, with the remaining 23 segments discarded within each iteration. The main calculation within the solver determined the suitability of the material allocation within each iteration, against the panels' hybrid performance-based augmentation goal (see Table 4.11).

In determining the material positioning suitability of each iteration, a coefficient was established between the combined augmentable factor of each board segment (see material discretisation in Section 4.3.2.1) and the panel in which they sat. The difference between the target and coefficient of each panel was expressed as a panel's *differential*. By combining the

differential of each subject panel, a single Fitness Objective was established, allowing for an efficient computational workflow.

Unlike the evolutionary process within the acoustic determination simulation in Section 4.3.1, the material distribution stage used a single Fitness Objective (discounting the 'Null' value filter). Additionally, the evolutionary process was restricted to simple mathematical operations, with geometric representations being referenced to numerical data. The evolutionary algorithm parameters employed are shown in Table 4.13.

Evolutionary algorithm parameters	
Generation size	50
Generation count	100
Population size	5000
Crossover probability	0.9
Mutation probability	$1/n^{\text{n=number of variables}}$
Crossover distribution index	20
Mutation distribution index	20
Random seed	1
Simulation runtime	2m 32s

Table 4.13 Acoustic Material distribution: Evolutionary algorithm parameters

For these reasons, the computation time was expected to be relatively fast. In this scenario, an increased evolutionary population could potentially be explored, allowing consideration of a wider field within the evolutionary search space; however, in testing varying generation relationships (see Table 4.14), negligible improvements in the fitness results were achieved, with the negative effect of a significant rise in computation time.

Expanding the *generation size* from a baseline of 50:100 to 75:150 resulted in a 325% increase in calculation time and a 3.1% improvement on

Generation size: count	Population Size	Calculation time (m:s)	Fitness result
50:100	5,000	2:32	199.948944
75:150	11,250	8:15	193.381043
125:250	31,250	56:40	186.673224

Table 4.14 Impact of generation relationship size on optimisation fitness and calculation time

fitness result. The expansion from the baseline to 125:250 increased the calculation time by 2,236% while yielding an increase of only 6.7%.

Subsequently, an evolutionary population of 100 generations of 50 iterations was employed. The 5,000 iterations took 2 minutes 32 seconds to complete, representing an efficient workflow that distributed a constrained inventory of irregular materials across a series of optimised performance profiles in a tailored fashion. The material distribution processes resulted in a single optimal solution within the Pareto front that represented the fittest iteration within the evolutionary population. Table 4.15 and Figure 4.16 show the results of this solution in geometric and numerical forms, while Figure 4.17 details the statistical analysis of the evolutionary solutions.

Panel	Coefficient target	Coefficient result	Coefficient differential	# of segments containing feature
81 (0)	100	98.592	1.408	10
82 (1)	100	98.407	1.593	14
83 (2)	100	98.967	1.033	11
86 (3)	0	91.757	91.757	30
87 (4)	60.44	90.000	29.260	28
88 (5)	19.79	90.386	70.606	36
91 (6)	100	99.423	0.577	7
92 (7)	100	97.946	2.054	12
93 (8)	100	98.382	1.618	12

Table 4.15 Material distribution results

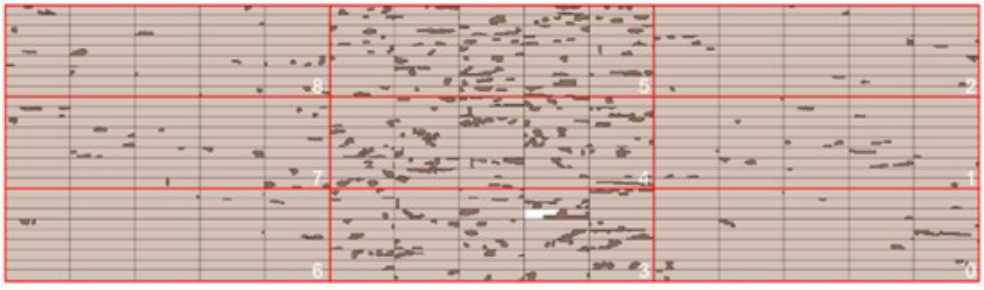

Figure 4.16 Material distribution of timber segments across 9 panels

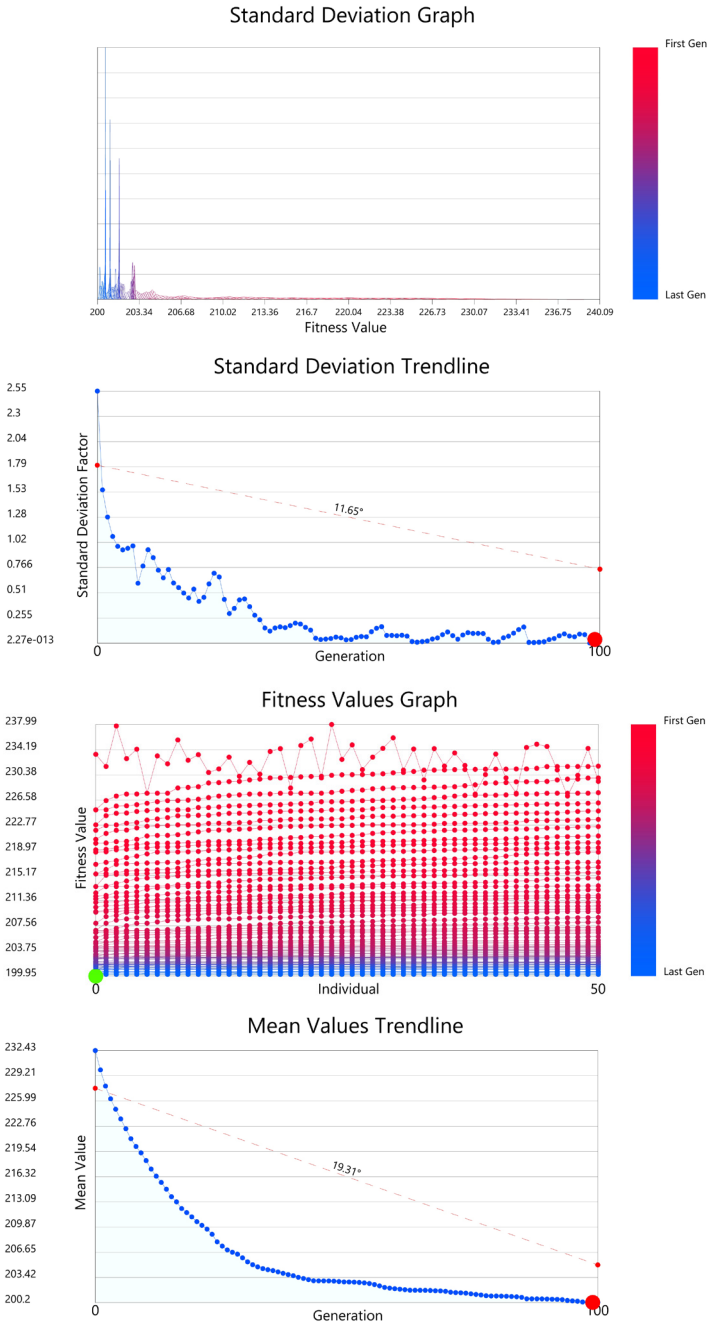

Figure 4.17 Statistical analysis of evolutionary solutions

4.3.3.4 Results

The optimisation workflow within this experiment sought to optimise the distribution of timber boards so that those with fewer natural features would be positioned within panels that require a higher level of augmentation, to meet the hybridised acoustic performance profile. Conversely, board segments with a higher percentage of natural features would be located within panels that had a lower acoustic requirement. Figure 4.16 shows panels 86, 87 and 88 were allocated the greatest

volume of featured material, which correlated with these panels having the least amount of acoustic performance requirement (see Table 4.15). Conversely, panels 81-83 and 91-93 had very small coefficient differentials, and were allocated material with very few natural features, relative to their performance requirement.

There was a clear anomaly in results relating to coefficient differential in panels 86, 87 and 89; however, this anomaly was the result of a disparity between ideal and actual conditions, rather than a failing of the algorithm. In this situation, the numerical results did not adequately represent the actual case. There was significantly higher differential value for those panels that had less acoustic augmentation requirements.

This outcome could be explained by considering a panel that had no performance requirement for acoustic augmentation. In this case the panel had a coefficient target of 0. In a scenario where the inventory of board segments was infinite, the evolutionary solver would be able to place 45 segments that were highly featured and contained no clear area able to be augmented. This would generate a coefficient of 0, resulting in a differential of 0, representing a completely optimised solution; however, within the constraints of this experiment (and those of reality) the material inventory was based on physical timber samples. It is improbable that any segment of board would be 100% featured, meaning that it was practically impossible for a panel that had a coefficient target of 0 to have a low differential value. Conversely, it was much more likely for a panel that had a coefficient target of 100 to have a very low differential.

A more accurate numerical representation of this phenomena was achieved by considering the number of allocated featured segments within a panel with a low coefficient target. Panels 86-88 had an averaged featured segment count of 31 of a possible 45, while the remaining six panels had an average of 11. This indicated that featured board segments are being placed in panels that require less acoustic augmentation, at an occurrence rate nearly three times more frequently than panels with a higher acoustic augmentation requirement. Further reinforcing this is that these 31 board segments are representative of the most highly featured of the available inventory. This means that while there is capacity for an average of 14 additional featured segments per panel, this may not yield the highest area of feature overall or generate an optimised solution across all subject panels.

The evolutionary solver is employed to optimise the distribution of a unique inventory of material, across a series of panels that have individual hybridised performance profiles. In an ideal scenario it would discover the perfect solution; however, given that it is interrogating a constrained

inventory of known material, it will seek to distribute the segments in a manner that results in the 'fittest' solution balanced across the subject panels.

4.3.4 Stage 4: Augmentation Design

The augmentation and fabrication methods employed in this experiment shifted beyond those developed in Section 3.4. The previous processes used material character of a pre-laminated panel, with perforation size, and surface augmentation generated by proximity to timber knot-based features. This more sophisticated experiment generated a hybrid of absorption and diffusion acoustic characteristics, within a framework that saw the capacity of a panel maximised internally on a set of predefined parameters. It also considered each panel as an individual, without the capacity to be influenced by wider acoustic criteria.

The material distribution methods employed in this experiment required augmentation and fabrication methods that moved beyond an individual panel and considered the context of the global acoustic requirements of its environment. Further, the methods developed required a greater integration with surrounding panels to generate a seamless connection between neighbouring panels that could create a coherent visual application.

Material features identified in this experiment are captured and discretised by their appearance on the front and rear surfaces of the board. While a knot-based feature is commonly considered a defect, in this case it is integral to the localised condition of the individual board segment, and subsequently the panel within which it sits.

The tailored material distribution method employed positioned board segments based on their capacities for augmentation, relative to the acoustic performance character required at a specific location within a room. The outcome of this distribution process was material that was higher in features, located in areas where less acoustic intervention was required; clearer pieces of timber were positioned where larger amounts of acoustic intervention was needed. This established an immediate

relationship between material feature and augmentation intensity within a whole spatial environment.

As with the material augmentation design (in Section 3.4), the developed workflow is divisible into smaller stages. Five interlinked stages are required within the workflow, which can be grouped into two discrete categories:

a) generation of augmentation geometry; and

b) the correlation of geometry with acoustic performance requirements.

Figure 4.18 illustrates how the five individual stages are spread across

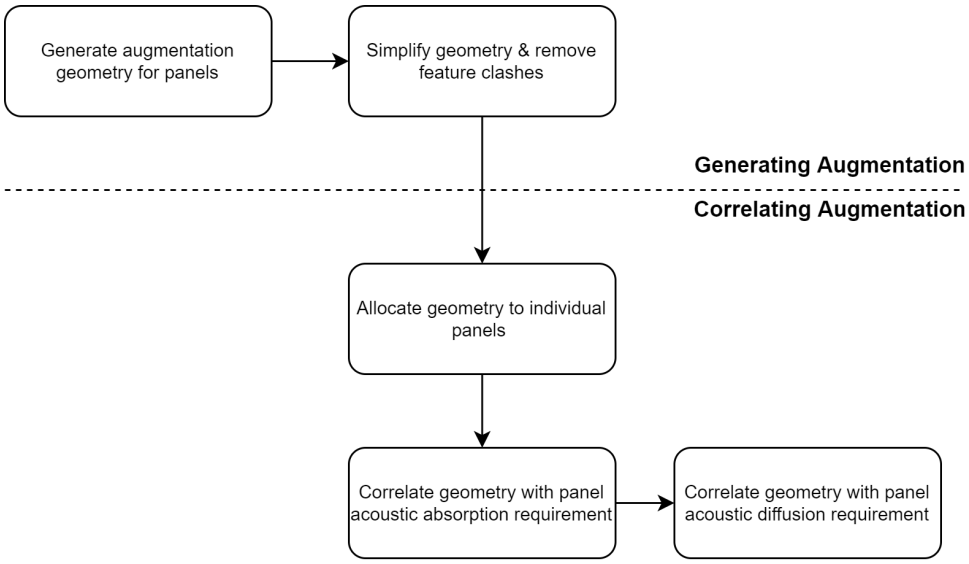

Figure 4.18 Augmentation design workflow

these groupings.

4.3.4.1 Multi-Performance Augmentation Generation

The added complexity within this experiment was three-fold:

- the augmentation design needed to be locally unique to multiple regions within the room, while maintaining a consistent visual language across the global condition;
- it needed to be responsive to the acoustic performance profiles of each individual panel (see Table 4.11); and
- it needed to hybridise the strategies employed for absorption and diffusion acoustic augmentations, thereby establishing

a closer linkage between fabrication method and design outcome.

With these complexities in mind, the first consideration was to establish a linkage between material feature locations and the generation of augmentation geometry. This linkage had to consider the significance of the feature at a global scale, in addition to the relative proximity to a feature location. This method of linkage and generation is commonly approached in parametric design workflows, by using an 'attractor-based system'. Variations of this typology of workflow establishes geometrically significant locations that act as points of origin, and subsequently employ proximity-based relationships with these points to generate and augment a design outcome. There are varying methods within Grasshopper to execute these workflows (such as distance, image mapping and vector fields); however it is challenging to employ these systems in combination, whilst maintaining an acceptable level of control over the outcome. Subsequently, this experiment employs the Grasshopper plugin FlowL™ (uto, 2020).

FlowL allows for the visualisation of vector fields within Grasshopper, generated through the specification of positive and negative point charge locations. It allows for variation in charge strength for each unique point and generates path geometry by employing the Runge-Kutta 4th Order Method (Weisstein, 2022) to solve time-based vector movement in particles. The use of this plugin allows for a greater accuracy in the mapping of vector fields, with a highly accelerated computation time, in comparison with the native vector methods within Grasshopper. FlowL offers three 2D methods of vector path generation:

- 2D vector field equipotentiality,
- 2D streamline, and
- 2D vortex generated streamline.

The differing output of these methods is shown in Figure 4.19. Of these three options, the first, equipotentiality, was selected as the preferred method as it demonstrates a greater capacity to be interlinked with the clustering of material feature in the generated wall panels. Additionally, the methods it uses to navigate vector paths through the feature field allows for a high level of contiguous augmentation between individual panels.

The implementation of FlowL in the experiment was applied to the nine selected panels (as identified in Section 4.3.3.1). This implementation is a linear process situated external to the evolutionary simulation processes due to the significant computational time required for application over

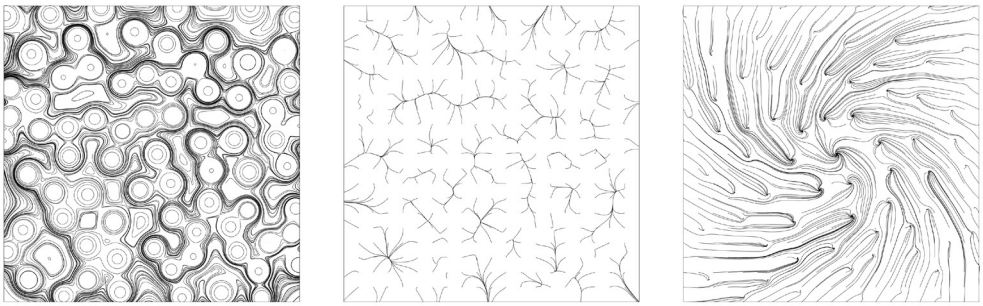

Figure 4.19 FlowL vector field methods. (L to R) Equipotentiality, streamline, and vortex

this area. Each variation and adjustment of the augmenting design requires 22 minutes 15 seconds to complete. Including this step within the evolutionary process of 500 iterations would have increased the computation time by approximately 1,854 hours, making the evolutionary simulation impractical.

Two methods were explored to determine the significance of relationship between feature significance and vector charge value. The first was to determine the range feature areas present across the entire design area. These values were then remapped against an acceptable charge range between 0.5 and 1.5, with 1.5 representing the largest features. While this established a unique value of influence for each material feature, the geometric output contained significant overlaps and 'Null' solutions, due to the method employed by FlowL that merged all vector charges together, resulting in areas of high features having disproportionately large charge values.

The second method extracted the outlines of all features and inserted evenly spaced points along each curve at 50mm intervals, with an equal charge value being specified ubiquitously. This allowed the charge points to be grouped relative to each feature, rather than the whole design area resulting in larger features being represented by more perimeter points (subsequently having a larger combined charge value). This second method was selected to proceed with in the experiment, as it better reflected the nature of the timber.

The equipotential method within FlowL required six inputs for successful operation (Figure 4.20): points charges, charge values, start points, damping, iteration and step size. The point charges and charge values were specified as the 50mm interval points (as above), with a charge value of 1. The start points are the initial location from which field curves will originate, prior to any vector forces acting on them. It is common for these to be specified at random; however, due to the design requirements of this experiment an evenly spaced orthogonal grid was adopted.

A 75x200 matrix of points as overlaid on the area covered by the nine subject panels, representing a spacing of 50mm in the x and y axes. Prior

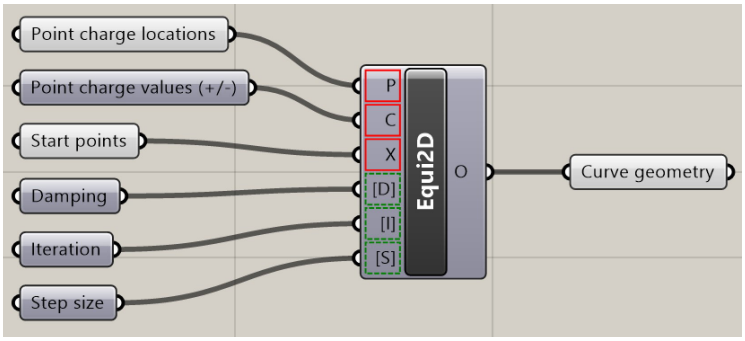

Figure 4.20 Parameter input requirements of the FlowL plugin within Grasshopper

to the generation of vector lines, all grid points that were positioned within a feature boundary were removed from the matrix, reducing the number of points by 9.5% to 14,421. These points were specified as the start point of vector field paths. The dampening value correlates to the degree that the generated field curves confirm to each step location, with a value of 4 being specified.

The final two parameters - iteration and step size - describe the number of instances in which the origin point will be influenced by the vector field and the corresponding distance between each instance. An iteration value of 300 was specified, with a step size of 10. Figure 4.21 illustrates the progressive steps required to generate the vector field lines, based on the selected nine-panel array.

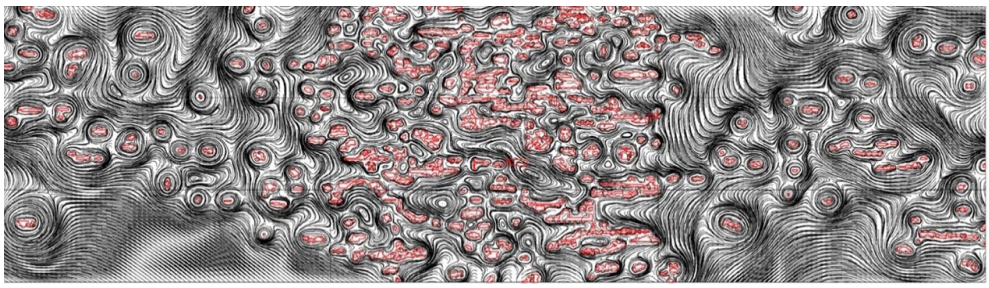

Figure 4.21 3D Curve generation from vector field influence

The curve generation process is computationally heavy, taking 22 minutes 15 seconds to calculate the nine selected panels. An additional process of simplification and evaluation was applied, allowing curves to be grouped based on the specific panel. The raw curve geometry generated by FlowL contains inconsistencies in relation to point count and extent. These were corrected with an intermediate step that rebuilt the curves with 20 control points and a degree of 3, allowing all geometry across the nine panels to contain a consistent geometric description.

This process resulted in 13.5% of all curve geometry extended beyond the combined boundaries of the nine panels (an area not covered by

the scope of the design area). All curves were trimmed to the boundary, reducing the amount of geometry and calculation time significantly. In some cases, curves crossed the boundary twice, resulting in a single line being split into two pieces, with a gap in between. In these circumstances, the directionality of the curves would unpredictably flip. This was remedied by testing the directionality of all curves and flipping those that did not match the original counter-clockwise direction.

Continuing curve rationalisation, instances occurred in which field lines crossed over material feature areas. Figure 4.22 illustrates seven instances are shown where field geometry intersects with material features (in red). This is a result of the vector field directing the path of curves between closely spaced featured areas, ultimately forcing the curves to cross over. It was found that in 416 instances, curves crossed feature boundaries across the nine panels. Removing these curves for the dataset reduce the total number of curves to 6,726, from an original 7,146. An additional 197 curves were culled by removing lines that were shorter than 100mm in length, resulting in a total of 6,529 curves being classified as valid for augmentation purposes, equating to an 8.7% reduction in geometry.

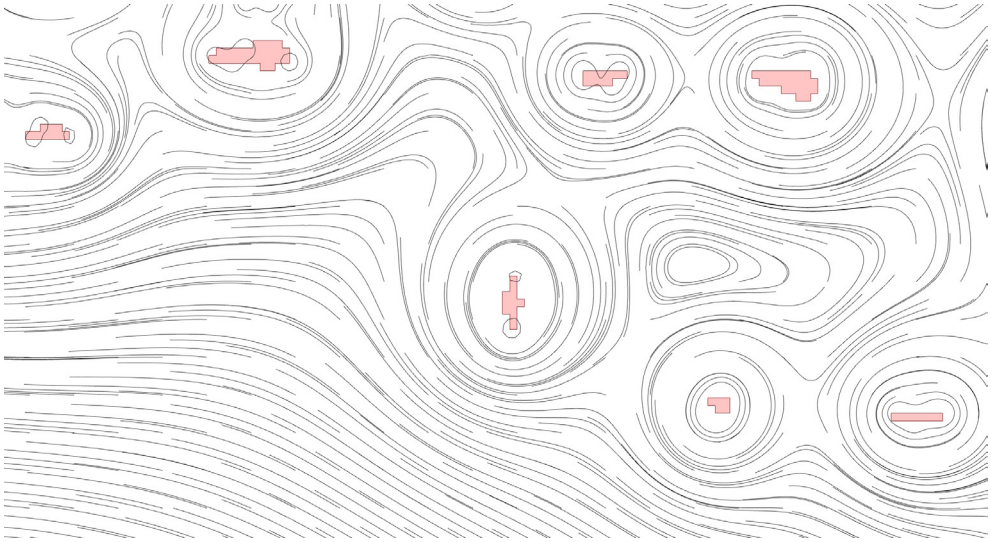

Figure 4.22 Intersection detail between detected material feature (red) and generated field geometry

The final stage of the curve rationalisation process matched curves to an individual panel. This facilitated the augmentation of a group of curves to be matched with the acoustic performance requirements of each panel; however, the need for continuity between panels to create a seamless surface remained. To address this duality, curves were matched with panels based on the location of their mid-point. Other point-based methods of grouping were explored; yet, the specification of start or end points resulted in the workflow being unable to determine which panel the

curve should be allocated, due to the start point location being co-located with a panel boundary. Further, the specification of the curve midpoint (as the determining feature) allowed a larger number of curves to cross between panels, which then accommodated greater continuity between panel and performance augmentation.

4.3.4.2 Acoustic Performance and Augmentation Correlation.

Of the three panel types specified in the acoustic simulations, absorption and diffusion-based performance profiles required a varying level of material augmentation. These acoustic properties were matched with timber segments that contained a great volume of clear, featureless material. The third acoustic type was specified as having no acoustic requirements, and was matched with segments that were high in features. The acoustic performance hybridisation process allowed any combination of these characteristics within a single panel and the material augmentation methodology demanded a variable strategy that was responsive to both material feature and acoustic performance profiles.

As discussed in Section 3.4, absorption-based performance is characterised by panel perforation of varying placement and density, in addition to the resonance of the panel against insulative backing material. Meanwhile, diffusion is characterised by surface deformation of varying depths and widths which allows the scattering of reflecting sound waves within a room. As areas of augmentation are geometrically linked with a series of curves, a hybrid strategy that allowed them to respond to both absorption and diffusion requirements was sought. In considering these parameters, a fabrication method had to be investigated and integrated into the augmentation process.

CNC machining was selected as the fabrication method due to its rapid and efficient augmentation of solid timber materials and its wide availability in industry today. While there are more capable multi-axis machines used, the most prevalent machines in industry have a 3-axis capacity with a 1200x2400mm table size and 100mm clearance. The machine used in this experiment is a SMC Accord 400 5-axis CNC with a 1500x6000 table and 300mm of gantry clearance. This presented the opportunity to undertake more complex machining operations; however, the methods explored in this experiment limit the machine's ability to 3-axis, which actually is a closer representation of industry capacity.

In utilising three axes of fabrication, the X and Y planes are associated with the flat panels' dimensionality, while the Z-axis allows the cutting tool to plunge vertically into the material at varying depths. The augmentation curves are intended as paths that the CNC machine will follow on the XY

plane of the material. This leaves the depth of cut along the curves in the Z-axis as the remaining geometric fabrication parameter available to achieve variable acoustic augmentation.

However, the choice of cutting tools also has capacity to introduce a fabrication-based parameter, in addition to the prescribed geometric tool paths. The selection of CNC cutter profile has a significant impact on the level of detail and surface finish on the resulting fabricated artefact. The range of cutter heads (Figure 4.23) are manufactured to undertake a range of tasks, including roughing, finishing, profiling and morticing. Customised cutting heads are also available for specific applications and materials. Of those available, it is common for straight and ball-end cutting tools to be favoured in industry, as they are widely available and relatively cost-effective. These cutter types have different applications, but both can be used to cut at varying depths in the Z-axis.

Figure 4.23 A range of CNC cutter head profiles

A straight cutter will always produce a vertical cut into the material, typically with a flat bottom, regardless of the depth of cut on the Z-axis. A ball-end cutter, however, will produce a varying width cut into the material, as shown in Figure 4.24. This capacity to vary the width of cut at varying depths engenders a new design variable that introduces scalable surface augmentation and perforation size, and which can be correlated to acoustic performance requirements.

The timber boards used in the experiment are 32mm thick. Using a 19mm ball-end cutter with an effective cut depth of 32.5mm (see Figure 4.25), a wider range of augmentation variability exists. When engaging with areas of material that require acoustic diffusions the cutter can create surface augmentation at a width of between 0.1 and 19mm based on a depth range of -0.1 and -9.5mm. Additionally, it can increase its depth to -31mm at a

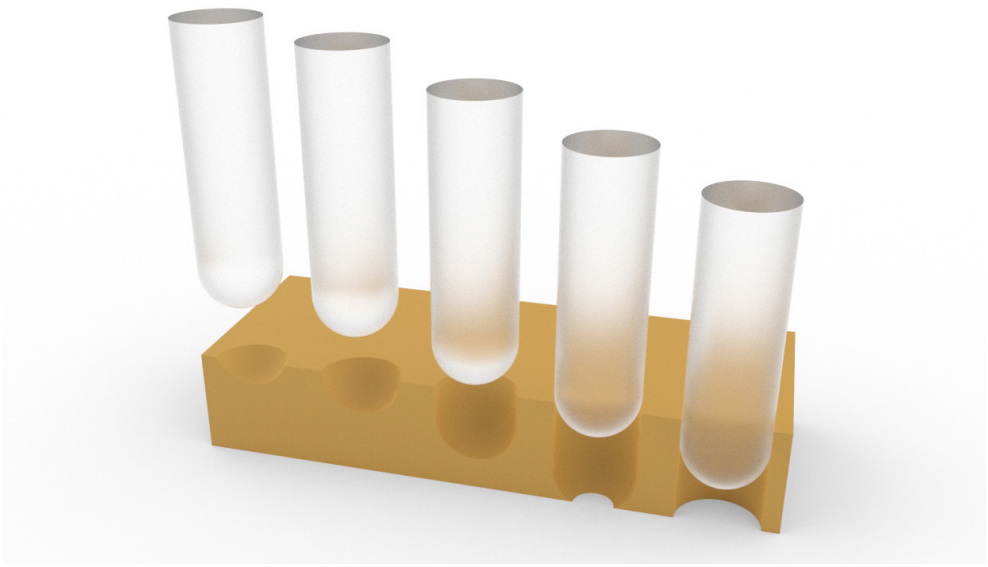

Figure 4.24 Impact of ball-end cutting tool at varying depths

Figure 4.25 19mm round nose, double flute cuter head with a 32.5mm cut depth

fixed with of 19mm. In both scenarios, the bottom of the cut will have a curved finish, matching the profile of the cutter.

When machining areas that require acoustic absorption, varying diameter and length perforations can be realised. If the cutter engages the material, a circular perforation with a variable width of between 0.1 and 19mm can be created. This varying diameter can be utilised in the *XY* plane as well. As the cutter head follows the prescribed geometry it can vary its depth of cut as it travels along each curve. Once the Z-axis depth surpasses that of the material it breaks through the bottom face, creating a small perforation. Along the remainder of the curve the Z-axis depth can either maintain this

depth and width relationship, or continue to cut deeper and generate an elongated perforation of varying with. Within the material constraints, a total cut depth of -32.1mm creates a 0.1mm perforation, while a depth of -41.5mm allows a perforation of 19mm wide. However, a cutting depth greater than the tool's effective length of 32.5mm requires the fabrication to be undertaken in two passes.

The variable depth ranges allowed the augmentation curves to be matched to acoustic performance requirements, accommodating the custom tuning of the panel to its requirements. The depth and type of fabrication intervention for each curve was controlled by three correlations:

a) proximity to material feature;

b) length of curve; and

c) panel acoustic performance requirements.

The feature of proximity influenced the initial depth of the curve. A range of +0.01mm and +10mm above the panel surface was specified at the commencement of each curve. This ensured that, regardless of feature proximity, the augmentation would always have a smooth transition into the material. The further away a curve was from a material feature, the smaller the distance between the material surface and initial tool path depth. This embodied a delayed material engagement within curves that were located closer to material features, creating clearer areas around feature locations.

The curve length dictated the location of the end point of each augmentation path. The depth of each end point was correlated to the panel's total augmentation requirement. For example, Panel 87 (see Figure 4.26) has 621 augmentation curves and a total augmentation requirement of 60.44%. As all augmentation curves initially create both diffusion and absorption characteristics, 375 of these curves were set with an end point depth of -41.5mm below the top surface creating a maximum width (19mm) perforation. The remaining 246 curves (39.56%) were specified at -31.5mm, creating a deep diffusion profile without any absorption-

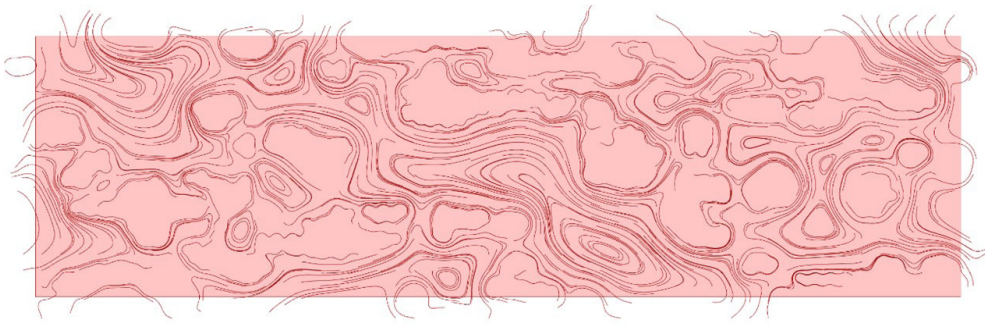

Figure 4.26 Curve distribution generated for augmentation of Panel 87

based perforation. The remaining 60.44% of end points have a full depth augmentation specified.

The fine tuning of augmentation properties correlates to the hybridised performance requirements of each panel. The performance requirements of Panel 87 were found to need an absorption capacity of 50.44%, a diffusion capacity of 10% and an un-augmented area of 39.56%. Areas that were determined to have no acoustic requirements were still subjected to minimal surface augmentation to ensure a relative visual continuity across the room's surface. This was accommodated in the specification of the curve start point depth (as noted in Section 4.3.4.1) in addition to prescribing a maximum depth of -7.00mm to these curves. However, the relationship between absorption and diffusion requirements needed further adjustment. This relationship is converted to the falloff point, or curve steepness. In the case of diffusion, the curve slowly increases in depth, until it reaches a point where it achieves full depth, maximising the diffusion surface area. In contrast, a panel that has a higher requirement for absorption has significantly steeper fall off to full depth, which increases the amount of perforation in the panel. The adaptability of this relationship allowed for the augmentation and fabrication processes to be aligned with the acoustic Fitness Objectives generated by the evolutionary simulation stage of the experiment.

4.3.4.3 Results

In this stage of the experiment, two key objectives were sought:

a) the generation of a hybrid acoustic augmentation design linked to material feature and hybridised simulation performance; and

b) a fabrication strategy that provided variables for consideration in developing the augmentation strategy.

It is evident these two objectives have been met. The vector field driven method employed to generate augmentation geometry was primarily established through the previous material discretisation and custom material distribution stages of the experiment. This used inherent material feature as a design generator, integrated it into the design and maximised its material utilisation. Further, the engaged method allowed for panel augmentation that was aware of, and responsive to, the surrounding performance and material conditions, facilitating a holistic approach to the surface of a set of panels, rather than to each panel individually.

The developed fabrication and tooling method accommodated additional design parameters to be integrated within the design workflow. The

specification of a ball-end cutter, coupled with adjustable depth, generated the opportunity for a wider range of surface augmentation. This then expanded the design language available to the workflow by tuning augmentation specifically to the performance criteria of the panel.

However, the results of the design workflow were unable to be fully realised in a 3-dimensional digital environment. While the tool paths could be previewed digitally as both curves and solid geometry, the nature of its impact on the actual material is only fully realisable in a physical environment. It is virtually impossible to predict the true nature of visual impact of the workflow at this stage, as the internal quality of the material is unknown prior to being acted on in the fabrication processes. Subsequently a physical demonstrator is required to convey the inherent complexity of material integration, acoustic augmentation, and fabrication processes evident in a final artefact.

Further, the demonstrator would be fabricated using industry standard CNC equipment, to determine the capacity of current industry processes in relation to innovative modes of material engagement and fabrication.

4.3.5 Stage 5: Physical Demonstrator

The creation of an accurate digital representation of irregular and naturally occurring materials is a complex task that is difficult to execute with a high level of accuracy. This is clear in the embedded material discretisation process of this experiment that pixelates material feature. While this process provides a workable dataset for computational processes, it disengages the materials' visual subtleties from the process. The material intervention required within the acoustic augmentation and fabrication stages further abstracts the relationship between digital and physical mediums.

It is increasingly difficult to gain an accurate representation of the manner in which irregular material structures will inter-mesh with fabrication-based deformation and perforation interventions. Subsequently, a physical demonstration of the process was required to truly understand the embedded processes and their impact on material intricacies, in addition to the capacity of the digital processes generated from the material feature set.

The physical demonstrator served to test the developed workflow by creating of a full-scale mock-up of a single acoustic panel. It focused on testing the capacity of the acoustic augmentation and fabrication process, enabling a greater consideration of the visual aesthetic of the workflows'

output. Board discretisation, segmentation and material distribution processes have been adjusted accordingly to suit the scale of this study.

4.3.5.1 Material Discretisation, Distribution, and Panel Lamination

The developed workflow of material discretisation and board segmentation was intended for large scale applications that have the benefit of substantial material inventories. In the context of this research, a limited inventory was available for all material-based design experiments. Subsequently, the physical material available had to be maintained for multiple experiments. This had an impact on the capacity to execute the workflow in its entirety and, as such, modifications to the process were required.

The design workflow called for the material to be discretised in board form, followed by splitting each board into segments. 84 boards were deemed suitable by the initial classification (Section 4.3.2), which resulted in an inventory of 489 segments of 600mm in length. The material distribution stage evaluated the potential of the segments and optimised their position across the panel set by correlating them against the specific acoustic requirements.

Each panel required 45 segments that could potentially originate 45 individual boards. For this workflow to be strictly adhered to, all the material stock would need to be cut into segments, making it inappropriate for other design experiments within this research. As a result, the design workflow was adjusted to accommodate larger board segments laminated into a panel.

As the workflow adjustments created a disjoint between the evolutionary simulation results and the capacity of the physical demonstrator, the correlation between material distribution and acoustic performance is considered an abstract representation of the process. This allowed the demonstrator panel to employ specified acoustic performance criteria and material distribution that highlighted the fabrication capacity and resulting visual appearance. It is desirable for the panel to demonstrate a range of material and fabrication potentials, rather than being representative of a single panel augmentation or material distribution.

From an acoustic perspective, the panel needed to establish that a hybrid acoustic augmentation could be embodied within a single panel. The performance simulation determined that areas that required no acoustic intervention were deemed to be solid timber. These areas would have minimal surface augmentation for visual coherence, and located in areas away from material feature. This established that testing this type of panel augmentation was not required, as it was inherently embodied in the feature avoidance component of the augmentation design. This further

implied that a mix of absorption and diffusion characteristics was required in the demonstrator and impacted the selected acoustic specification and material distribution. Subsequently, a performance goal of 80% diffusion, 10% absorption, and 10% solid was selected as the ratio for the panel to hybridise.

In considering material distribution, the acoustic performance ratio of 80:10:10 correlated to panels that presented 90% of material that clear to small-featured board segments, with the remaining 80% containing medium to large feature segments. A total of ten boards that exhibited a range of features were selected from the inventory for use in the demonstrator panel. Each board was cut into segments to accommodate dispersion of similar origin material across the panel. Several staggered layout configurations were trialled, with the objective to establish a relatively even distribution of material feature across the panel. This is consistent with the evolutionary simulation of material distribution (outlined in Section 4.3.3). The segments were laminated together employing the technique detailed in Section 3.4, with the demonstration panel measuring 2300x1080mm (Figure 4.27).

Figure 4.27 Demonstrator Panel (2300x1080mm)

As the acoustic performance and material distribution processes were completed manually, the material discretisation process was required to be employed after the panel was laminated. While this differs from the order of processes developed in the primary workflow, it maintains the same interrogation of material feature. Identical variables to those in the primary workflow were employed in the demonstrator, ensuring consistency in feature detection and material processing. The panel was subdivided into a 5mm overlay, with a threshold detection process being undertaken utilising the Aviary plugin. Figure 4.28 illustrates the results of the discretisation process after sample filtering is undertaken. It is evident

Figure 4.28 Feature detection of demonstrator panel

that the detected feature areas have been merged (based on proximity) and small and invalid features have been culled.

4.3.5.2 Augmentation Adaptation

As established in the primary workflow (see Section 4.3.4), the demonstrator panel has a secondary subdivision that established the start points of the augmentation design. A 40mm grid was applied to the panel, resulting in 1,800 start points. A total of 98 points were located within the boundary of detected features and were subsequently culled (Figure 4.29). The generation of vector fields adhered to the parameters established in the primary workflow using FlowL.

Figure 4.30 illustrates the generated flow curves generated from the feature driven vector fields. All generated curves that intersected with feature areas were culled from the geometry set, establishing areas clear of augmentation. This filtering process also removed all curves that were

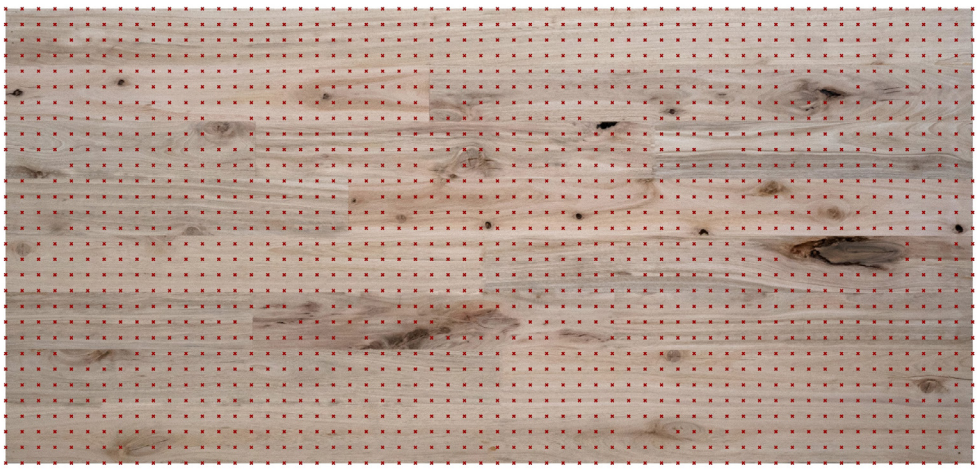

Figure 4.29 Augmentation field origin points

Figure 4.30 Vector field augmentation curve generation

less than 100mm in length. The final augmentation pattern totalled 2130 individual lines, with a length range of between 100mm and 260mm.

The final component of the augmentation design associated the typology of augmentation to the acoustic performance requirement of the panel, resulting in an 80:10:10 split between diffusion, absorption and solid properties. Of the 2130 augmentation curves, 213 were required to generate an absorption characteristic. As discussed in the primary experiment workflow (see Section 4.3.3), these 213 curves were specified to have an end depth of -41.5mm below the top surface creating a maximum width (19mm) perforation. The remaining 1,917 curves (80%) were programmed to a height of -31.5mm, creating a deep diffusion profile without any absorption-based characteristics.

The augmentation curves were filtered to remove geometry that intersected with featured areas, establishing areas of solid un-augmented timber within the panel. The panel had an area of 2.486m^2, requiring 0.2486m^2 of un-augmented surface area to meet its 10% solid panel objective. Figure 4.30 shows that a significant amount of the panel remained clear of augmentation around each of the timber features. The nominal area of these areas was combined, with a total of 0.2958m^2 free of augmentation. This equated to 11.89% of the overall panel, demonstrating a high correlation between the material/augmentation design and the inherent acoustic goals. The differential of 1.89% was minimised further by the augmentation curve commencement depth assigned within the primary workflow (+0.1 to 10mm). This resulted in a panel surface clear of augmentation of nominally 10% match in the acoustic performance goals specified.

The final stage of augmentation design required the preparation of curve geometry for fabrication export. The CNC cutting tool specified for the experiment was a 19mm ball-end cutter with two cutting flutes and an

effective cutting depth of 32.5mm; however, the cutting depth required for the designed 19mm wide perforation was 42mm, more than the specified cutting tool accommodated. Subsequently, the augmentation geometry had to be split in the Z-axis to allow the fabrication to be undertaken in multiple passes.

The machining capacity of the tool was dependent on the CNC machine being used for the demonstrator and the material being cut. Kotlarewski et al's. (2019) machinability studies in plantation hardwood employed a cut depth of nominally 1.5x the diameter of the tool when using an entry level CNC machine, in a two-pass configuration. While the CNC machine used in this experiment is of a significantly higher capacity, the cutting tool had less capacity, regardless of its greater diameter. It was a 19mm finishing style cutter with a double-fluted straight blade profile, as opposed to the more capable 9.5mm triple-fluted spiral rough cutter used in Kotlarewski et al's (2019) machinability test.

Considering these parameters, a two-pass fabrication system was required to be established. The maximum depth of material engagement in the experiment was specified to 19mm, matching the diameter of the cutting tool. This resulted in augmentation geometry being split into two sets of passes (Table 4.16).

Table 4.16 Augmentation geometry depth classification

	Depth range	Number of curves	Total curve length (m)
Pass 1	0mm to -19mm	2130	467.886
Pass 2	-19mm to 42mm	628	5.107 (1.1%)
Total		2,758	472.993

While the second pass covered a range of 23mm, the load on the tool was less, as the additional depth had a smaller volume of removal due to the curvature profile of the cutter. The significant difference in length was due the panel requiring significant diffusion characteristics, resulting in the curve threshold generating a steeper falloff to absorption-based perforations.

4.3.5.3 Fabrication Process

The CNC router used in the experiment accommodated multiple work areas due to length, allowing two full sheets of standard sized material to be placed on the table concurrently. The laminated panel was placed on the CNC table and secured in the primary work area using the integrated vacuum hold-down. Figure 4.31 shows this positioning, in addition to the

Figure 4.31 Panel positioned in the CD zone of the CNC router

'sacrificial' layer of MDF, between the table and the panel. An unusually thick (21mm) 'sacrificial' layer of material was required to accommodate the additional depth of cut required to generate full width perforations through the panel. While this had an impact on the strength of the vacuum hold down, it was still capable of securing the panel during fabrication.

The CAM software selected for fabrication simulation and CNC g-code generation was VisualCAD/CAM (MechSoft, 2021) for three reasons:

a) it supports Rhino files natively, thereby eliminating potential of geometry degradation during file transfer;

b) it is compatible with the CNC machine available for fabrication; and

c) it can predict potential machining conflicts and simulate the fabrication process.

These factors are significant in for the application of this method within an industry context.

The CNC machine used in this experiment was a SMC Accord 400 5-axis CNC with a 1500x6000 table and 300mm of gantry clearance. VisualCAD/CAM was configured in accordance with the specific machine settings, and the post-processor was locked to 3-axis machining. The 19mm ball end CNC cutter was assigned to Tool Position 19 on the rotating carousel and specified to have a spindle rotation speed of 18,000rpm and maximum feed rate of 6,500 mm/min. This feed rate is considered nominal, as it doesn't accurately accommodate several machine specific variables, such as acceleration, tool path prediction, tools changes and traverse speeds.

Table 4.17 documents the machining time that the VisualCAD/CAM predicted for each of the passes, compared with the actual time taken. The augmentation curves were exported in the SCM/Morbidell g-code format into two separate pass files, totalling 159,365 lines of operational code. The simulation of fabrication process is illustrated in Figure 4.32 and the fabricated panel is shown in Figure 4.33 and Figure 4.34, for comparison.

Table 4.17 Fabrication times of the physical demonstrator

	Total curve length (m)	Predicted time (h:m:s)	Actual time (h:m:s)
Pass 1	467.886	12:05:12	07:08:00
Pass 2	5.107	00:14:48	00:37:10
TOTAL		12:20:00	7:45:10

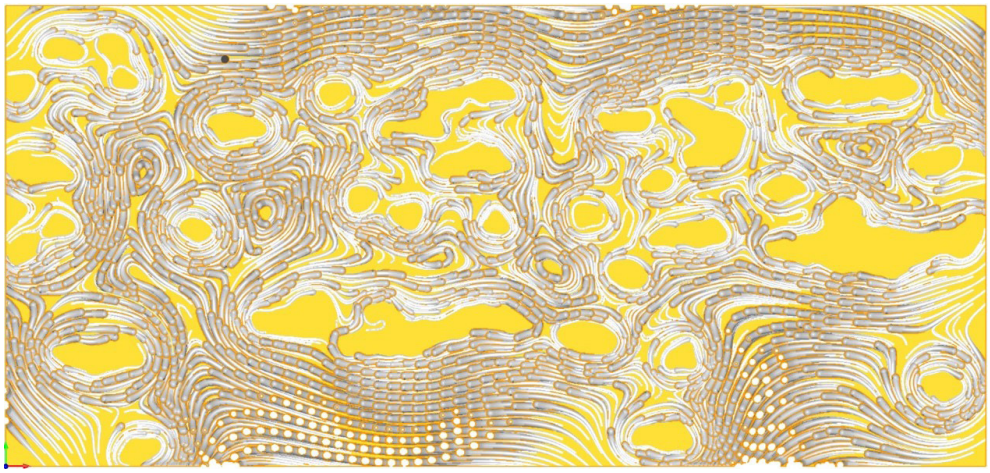

Figure 4.32 Machining process simulation generated by VisualCAD/CAM

As noted, there was a significant discrepancy between predicated and actual machining times. This discrepancy between the total times taken is a result of VisualCAD/CAM being unable to fully accommodate the automatic processes hard coded into the CNC machine. The result was that the actual time taken is significantly less than the prediction.

There was also a discrepancy in the relative times taken to machine each of the passes. Pass 2 had 628 curves, a total length of 5.107m, and a machining time equivalent to 2% of the total of the total predicted machine time; however, the machine time was equivalent to 8% of the total machine time. This difference is representative of the geometric nature of Pass 2. The curves it contained were relatively short in length compared with

those in Pass 1, which impacts the CNC machines capacity to accelerate to full feed rate due to each line being too short to reach maximum velocity.

4.3.5.4 Results

It is clearly demonstrated in Figure 4.33, Figure 4.34, and Figure 4.35 that the established design and fabrication processes created a wide variation of diffusion and absorption surface augmentation across the panel. The correlation between timber features and areas of no fabrication is high, with minimal occurrences of encroachment. This also demonstrates that the feature detection, augmentation design and fabrication alignment operated at a high level of consistency and precision.

The full fabrication process required a total of 7 hours and 45 minutes to complete the machining processes, undertaken as a single continuous process. As a single demonstrator panel was created, there was little opportunity for optimisation of machining strategies. Performance increases could be obtained using a custom cutting tool. A triple or quad fluted ball-end cutter, with a longer effective cutting length, could accommodate full depth material removal in a single pass. While custom tools generate additional expense to the process, they would allow a considerable feed rate increase, significantly reducing machining time. Additional performance increases might be achieved through curve rebuild optimisation and ordering.

A single cutting tool was utilised for the fabrication process. While the tool maintained its capacity to remove material effectively for the duration, tool wear was beginning to create a dull cutting edge (apparent in Figure 4.36). In some areas, minor tear-out is evident in the timber due to dull cutting edges. This could also be linked to the direction of cutting and the relationship with the grain of the timber.

Activating cutting tool monitoring in the CNC machine could have allowed interruption of the machining process for tool changing; however, tear-out caused by the incorrect direction of cut is a common issue when working with timber. This occurrence could have been reduced by a more advanced material discretisation process that captured internal grain direction, or closer inspection of board segment placement in the panel lamination process.

Figure 4.33 Top view of fabricated demonstration panel

Figure 4.34 Perspective view of fabricated demonstration panel

Figure 4.35 Detail of demonstration panel, showing augmentation and perforation of surface

Figure 4.36 Detail of demonstration panel, showing surface augmentation and material tear-out

4.4 Discussion

The objective of this experiment was to establish a multi-scalar approach to material interrogation and employ evolutionary modes of computational simulation to optimise material utilisation and acoustic augmentation profiles within a design framework. It sought to shift approaches to architectural scale by considering the acoustic potential of material as a room surface, as opposed to an individual panel. The computational workflows established address these goals, and also employed innovative methods of acoustic simulation and augmentation that utilised a constrained inventory of heterogeneous material.

The acoustic simulation and performance determination stage employed computational acoustic simulation to determine the acoustic qualities of an existing room used for educational purposes. Typically, this process is undertaken within independent software, severing the immediacy between acoustic performance and digital design environments. However, this workflow Prototype integrated acoustic simulation directly within Grasshopper, providing an intuitive graphical environment for conveying the complex inter-relations of acoustic performance and architectural intent. It also provided the capacity for interconnection with MOEA that determined the placement of differing acoustic augmentation types within the room.

An innovative hybridisation method was employed to optimise the 45 Pareto front solutions, which facilitated the specification of multi-objective performance profiles for each panel within the room. These profiles were employed in the material distribution and augmentation stages of the experiment, thereby supporting the engagement of a latent material within the construction industry to be utilised in a higher-value architectural application.

The material discretisation stage extended previously developed RGB-based capture workflows, by integrating a machine learning enabled feature detection process and multi-face capture to predict the internal structure of the timber using consumer grade hardware. The introduction of these features established a multi-scalar approach to material discretisation that could be matched to specific design and workflow requirements.

A multi-scalar approach to material discretisation engendered the capacity for custom methods of material utilisation to accommodate specific performance goals. In combination with the division of boards into shorter segments, this supported a higher utilisation of available material within

the design workflow. This, in turn would reduce the volume of material normally designated as waste.

As the length of board segmentation is parametrically defined, a higher level of scalability in material discretisation is promoted that is not bound by defined physical board lengths. Ultimately, the material distribution would consider all the panels within a room and have access to a large material inventory, which would allow the whole room to be considered within the evolutionary calculations. As such, this expands the realm of potential application in other design workflows that engage irregular materials.

The intrinsic linking of material distribution and hybridised acoustic performance profiles supported the integration of multi-purpose acoustic augmentation. The project demonstrator exhibited strong correlations between material feature, acoustic typology and fabrication methods. Further, it demonstrated that opportunities exist for constrained inventories of heterogeneous material within performance orientated architectural products.

Three limitations of the experiment were identified. The first is that the final performance of the workflow is subject to material available within the constrained inventory. The capacity of the material distribution and augmentation stages to conform to the acoustic performance profiles are subject to material that has already been discretised. Due to the varied nature of plantation hardwood, the constrained inventory could easily lean towards specific material profiles. To circumvent this, a significantly larger population of inventory would need to be discretised and ready for distribution; however, this potentially impacts factors, such as stock levels, storage space, inventory recall and the supply chain (only some of which the designer and fabricator can control).

To circumvent this limitation, an optimisation strategy was employed that hybridised the discovered optimal solutions for acoustic material type, shifting away from an objective in which ultimate acoustic performance is the primary design objective. The limitation of material inventory reduced the capacity for the MOEA's to settle on a single solution; that is, never being able to achieve perfect optimisation. For this reason, material distribution and augmentation within any panel was based around material utilisation and suggestive acoustic profiles. It is evident that a level of mediation between Fitness Objectives and material heterogeneity is required within digital workflows in order to reconcile the overall objectives of a design problem.

A second limitation is related to the computation and fabrication time required for the workflow to be completed. This is a significant

consideration within the architectural and construction industries as increases in processing time have a direct correlation with cost. While there are certainly areas of the workflow that could be re-written to reduce computational time, the linear nature of the computational workflow inhibits significant gains. One solution is that fabrication geometry and data could be incorporated as a Fitness Objective within the MOEA and aim to optimise the generation of augmentation curves and reduce fabrication times; however, the increase in calculation time generated by an iterative approach to complex vector field calculations would significantly outweigh any fabrication time gains achieved. Ultimately, an increase in computational power, or capacity to undertake the calculations in parallel, would accommodate a significant reduction in calculation time. This could be achieved by shifting to a software platform that supports higher levels of multi-core processing, or a hardware platform that allows faster core calculations.

A third limitation of the experiment is that it explores a method of material utilisation in non-structural scenarios. While the development of a tailored acoustic surface provides the opportunity to utilise out-of-grade plantation hardwood in architecture, structural application in construction offers a greater opportunity for adoption of non-standardised materials by industry. As such, the development of sustainable, material-driven computational workflows (which are more aligned with industry needs) is the basis of the explorative experiment discussed in Chapter 5.

5 DESIGN PROTOTYPE TWO: MAT-TRUSS

5.1 Introduction

The material driven acoustic augmentation experiment discussed in *Design Prototype 1: Acousti-SIM* (in Chapter 4) developed a design orientated evolutionary workflow that employed tailored performance criteria, material distribution and fabrication methods to generate architectural panels capable of providing hybrid acoustic absorption and diffusion characteristics. It employed an innovative evolutionary method to generate hybrid performance criteria for material distribution against which to correlate material availability and suitability.

The material discretisation method (developed in Section 4.3.2) allowed the capture of timber features on multiple faces of single boards, which could be employed within the design workflow. This extended the consideration of irregular materials in performance-based environments. Finally, it considered material utilisation and waste minimisation using the segmentation of boards into shorter sections. This allowed a closer pairing with unique panel performance criteria.

Design Prototype 2: Mat-Truss builds on *Design Probes 1-4* and *Design Prototype 1* to generate new workflows at a different scale that increase the applicability and adoption of the developed methods at a higher rate by industry. *Prototype 2* examines the capacity of a design-centric MOEA workflow that seeks to engage a constrained inventory of irregular materials in the generation of a structural truss. In doing so, it employs a material discretisation method similar to that in Section 4.3.2 to establish a constrained material inventory. However, *Prototype 2* increases the focus with which the dataset is engaged, allowing specific material character to inform material distribution within an integrated MOEA workflow. This process gives rise to a conflicting MOEA solution set requiring the development of an innovative method for optimal solution filtration and selection.

Finally, *Prototype 2* considers the inventory distribution as whole boards, allowing the creation of a workflow capable of recovering generated material waste and re-introducing it into the material inventory.

The experiment in Chapter 5 employs the material discretisation methods explored in Section 4.3.2, but shifts its application from an architectural acoustic panel to a materially specific performance-based timber truss. Through the employment of the NSGA-2 MOEA algorithm, (see Section 3.5 and Section 4.3), the experiment interrogates the constrained material inventory to establish the connection and performance potential of each element within a single truss. It aims to optimise both material placement and the structural performance and suitability of the generated solution. Further, *Prototype 2* aims to minimise material waste within the workflow

by returning generated offcuts to the constrained inventory for use within subsequent trusses. This coupling facilitates the integration of a multi-scalar approach to material engagement, offering a discrete design, material placement, optimisation and fabrication workflow responsive to irregular geometric structural arrangements.

5.2 Prototype Context

The use of indeterminate materials of unknown character in design and construction as structural elements is significantly underutilised (as outlined in Section 2.2). In the case of timber, the nature of the way in which it grows creates a level of material complexity that makes it unpredictable – leading to considerable volumes of material deemed unsuitable for structural or construction applications.

Prior to its use in construction, hardwood in Australia is gradated against a set of standards prescribed in *AS-2082-2007: Timber-Hardwood-Visually stress-graded for structural purposes* (Standards Australia, 2007), in which the structural quality of timber boards is ascertained through a visual assessment. This subsequently eliminates opportunities for a significant proportion of the material to be considered for use as high value construction elements. The grading processes of a timber board can deem it as 'out-of-grade' due to a single defect (see Section 2.3.4). This processes alone generates significant volumes of low-grade or waste material that could otherwise be used for higher value applications in design and construction.

The material capture methods developed in Section 4.3.2 established a workflow that discretises material to a degree that allowed highly featured timber elements to be engaged in a non-structural application. While this material interrogation, and the subsequent distribution processes, allowed for a multi-scalar approach to the coupling of material capacity with design optimised performance requirements, it still used the material in a lower-grade application. As such, it does not yet address the waste produced through the grading process.

The application of similar methods of material discretisation and optimising distribution for usage in a structural element the mass timber industry globally is well documented. Svilan's research into computationally enhanced mass timber elements considers these as "functionally-graded glulam assemblies" (Svilans, 2020, p. 224), in which scalar methods of material understanding facilitate the placement of discrete timber boards in architecturally complex glue-laminated elements.

In this context, material features (including fibre direction, feature locations and orientation) are discretised informing the characteristics of

each element (Svilans, 2021a; Svilans et al., 2017). This work is extended further by the RawLam project (Royal Danish Academy, 2022) that employs advanced optical and CT scanning techniques to optimise the primary processing of timber logs, facilitating discrete material placement and optimisation of hyper-local structural requirements within a LVL style structural element.

While these investigations consider advanced methods of material discretisation, they result in engineered material configurations, rather than considering the timber in common board form. Further, the discretisation methods employed in these experiments utilise complex, industry placed equipment currently not used in hardwood production lines in Australia.

Several relevant precedents also explore the structural configuration of natural, irregular timber components. Monier et al (2013) use laser scanning to discretise a single irregular timber branch, with additional inventory being created through digital extrapolation. The computational method employed for material engagement distributes material across a pre-determined architectural surface. Remaining as a digital exploration, Monier et al's study is primarily concerned with the conforming of irregular materials onto a pre-determined surface. In contrast, *Prototype 2* facilitated material driven, structurally specific form generation that is not pre-determined.

In their comprehensive review of whole timber construction, Bukauskas et al (2019) outline a diverse range of methods that encompass the discretisation, characterisation, preparation, connection detailing and structural application irregular timber materials.

The Woodchip Barn project (2016) (see Chapter 2.4.2.2.1), employs a hybrid of photography and photogrammetry material capture methods to generate a constrained inventory of trees available for harvesting and construction (Self, 2017; Self & Vercruysse, 2017). It engages this inventory computationally by employing an evolutionary solver to test material distribution, structural performance, and fabrication capacity in the generation of a Vierendeel-style arching truss (one that comprises rectangular rather than triangular frames, end employs moment joints to resist substantial bending forces), exploiting the natural structural capacity of fork junctions (Mollica & Self, 2016). While these methods use the irregularities of whole timber logs as a viable material for construction, they do not address the most common form of timber within the construction industry; namely, sawn board. *Prototype 2* seeks to employ similar methods

in conjunction with sawn boards, from Australian plantation hardwood timber resources.

Bukauskas et al. (2017b) identify two applications of optimising a constrained set of irregular elements within a structural form:

a) the reuse of structural steel elements from dismantled buildings; and

b) the utilisation of unsawn timber elements in structural configurations.

These methods are further explored in Bukauskas' doctoral study (2020), which investigates his application of constrained inventories of material in the development of truss-based structures. These methods were employed concurrently by Baber et al. (2019, 2020) in the development of a funicular structure, which allocated short length offcut elements to curved segments within a small prototype pavilion.

These projects seek to engage a primarily dimensional based variation within a constrained material inventory, considering them to be pre-graded elements of known structural capacity. The methods developed in this experiment and Chapter engage material at a feature-based level, thereby expanding opportunity for design outcomes to be driven by unique material irregularities.

It is evident from the studies undertaken by Bukauskas et al. (2017b) and Baber et al. (2019, 2020) that computational methods of using constrained material inventories in structural applications (with a particular emphasis on truss-based scenarios) are already available in custom, engineering focused workflows. However, they predominantly utilise either unsawn whole timber elements, or materials of a predetermined capacity that have irregular features and defects removed prior to processing. The projects of Bukauskas et al. (2017b) and Baber et al. (2019, 2020) show a limited capacity for the consideration of materials of varying irregularity, as is evident in sawn timber from pulplog grade hardwood plantations.

Further, there is still limited investigation regarding the opportunities MOEAs could afford the CDFs employed. Most of the developed workflows (discussed in Chapter 2.4) engage material as geometrically defined elements that have a consistent performance profile throughout each element. This supports an approach that simplifies material potentially, allowing the design problems to be interrogated as linear processes, which seek to match inventory items to corresponding applications within a structural configuration. While this reduces the computational complexity of the process, it eliminates the capacity to understand material potential beyond standardised performance classifications.

Subsequently, *Prototype 2* seeks to address these limitations through the implementation of a MOEA-based workflow, which provides the opportunity for interaction between structural performance and geometric configuration with highly specific material distribution and connection arrangements. This could allow the generation of a greater range of potential solutions that would otherwise be unavailable using more traditional approaches to the specification of the design problem. In doing so, *Prototype 2* discretises a constrained inventory of highly irregular sawn timber boards to generate truss-based structural solutions without a pre-determined geometric configuration.

5.3 Experiment Setup

The sequential evolutionary algorithms employed in Chapter 4 exhibited a computationally demanding workflow that was disproportionately split between the two implementations. Nominally, 98% of the computational load was allocated to the generation of the design problem performance criteria, while the material distribution and optimisation required only 2%. This is mostly due to the complex acoustic calculations required within the MOEA to define the design problem; however, the material distribution and optimisation could be calculated using a less computationally-demanding optimisation process.

In contrast, the truss generation and structural simulations implemented within *Prototype 2* can be encoded within a single MOEA. In principle, this experiment has two overarching design goals:

a) to generate a truss that uses irregular sawn hardwood boards to determine its geometric configuration and performance optimisation; and

b) to span 10m while demonstrating a displacement within a set threshold range.

Rather than dedicating an entire MOEA to generate the material distribution performance requirements, this experiment directs its computational complexity towards structural fitness optimisation and material efficiency.

In encoding the generation of a truss within the computational workflow, a Warren truss (uses equilateral triangles to spread out the loads) with a flat top deck (Mork et al., 2016) was selected as the base geometric framework. Warren trusses are a commonly employed truss design and offer excellent material utilisation-to-span ratios (Satheesh Kumar Reddy & Nagaraju, 2019); however, within this experiment the traditional approach of creating trusses with parallel top and bottom chords is omitted, favouring a Warren truss configuration that demonstrates irregular triangulation within the web and bottom chord segments (see Figure 5.1). This uses the material irregularities while maintaining structural integrity within the truss.

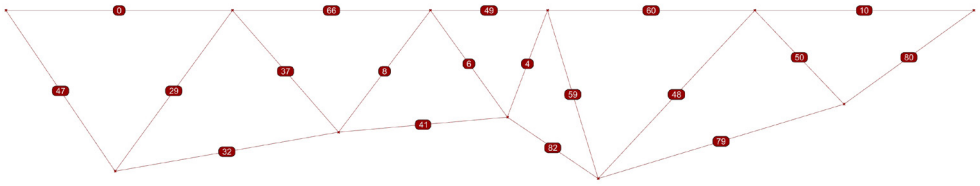

Figure 5.1 Design constraints for floor truss generation

This truss configuration establishes the opportunity for a wider variety of material from the constrained inventory to be considered anywhere within the truss, with the embedded structural analysis ensuring that optimal material utilisation results in trusses that perform within the prescribed specification. Considering this, the maximum depth of any generated truss is not constrained, as it is limited by the material selected from the constrained inventory. This affords the computational workflow

to optimise structural performance and material efficiency as its primary objectives.

Each iteration of the developed workflow generates a single optimised truss, with the affordance of updating the material inventory between iterations. The computational workflow is divided into five discrete stages (Figure 5.2).

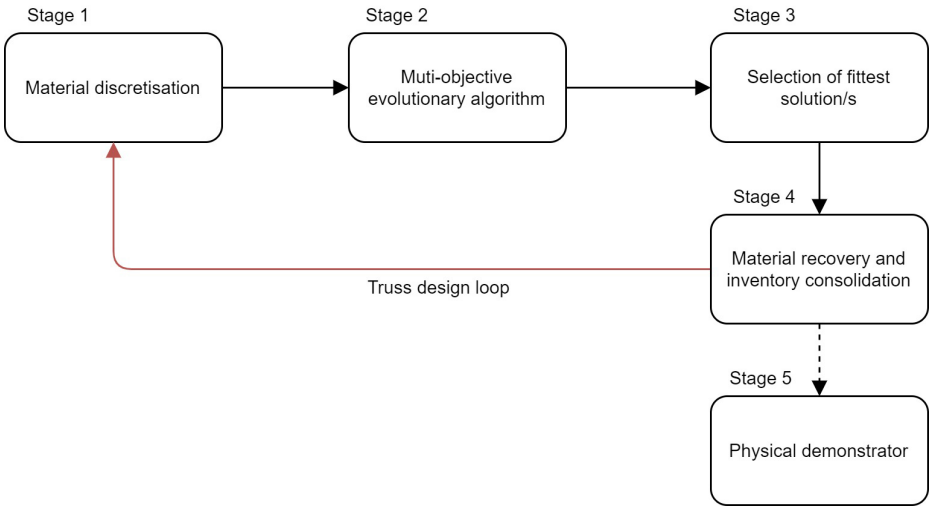

Figure 5.2 Division of experiment workflow into five stages

Stage 1 adapts the material capture and discretisation process established in Chapter 4 to match the data resolution required for a larger scale material distribution optimisation. Further, this Stage interrogates the material inventory to determine significant zones of clear timber within each board. These zones are subsequently classified as areas of potential physical connection within the truss configuration. This process is discussed further in Section 5.3.1.

Stage 2 employs a MOEA and contains three hierarchical processes, as follows:

a) The first process finds pairs of potential connection points within each individual board.

b) The second process optimises the distribution of timber material to generate a valid truss configuration.

c) The third sub-process is responsible for optimising the structural performance of each truss iteration. It employs finite element analysis and optimisation processes that determine the structural capacity under a prescribed load condition.

The output of this sub-process marks the end of the MOEA process, with pool of evolutionary solutions now available for validation and selection. These processes are discussed further in Section 5.3.2.

Stage 3 interrogates the evolved population from Stage 2 through a series of objective filters. These filters significantly narrow the field of valid options, allowing a final subjective filter to be undertaken. The output from this stage is a single materially optimised truss solution. This process is discussed further in Section 5.3.3.

Stage 4 processes the selected truss solution and generates board offcuts from each segment that are outside of the truss requirements. These offcuts are assessed for reuse viability within the next iteration of the workflow. Stage 4 is the end of the design loop, with additional trusses repeating this workflow from Stage 2. Stage 4 is discussed further in Section 5.3.4.

Stage 5 realises the translation of the developed digital processes into a physically fabricated demonstration Prototype, and is discussed further in Section 5.3.5.

5.3.1 Stage 1: Material Discretisation

The RGB-based capture techniques developed Section 3.3 provided a reliable level of imagery that allowed the multi-face discretisation method to extract and leverage material datasets (see Section 4.3.2). Additionally, the developed discretisation method sampled material information from the image dataset at a 5mm resolution. The highly detailed relationship between clear and featured areas of material was critical to the successful application of material distribution and acoustic augmentation.

The truss experiment discussed in *Prototype 2* interrogated the same constrained inventory of material and image dataset as the acoustic panel experiment (detailed in Chapter 4; but with fewer boards than those used in the physical demonstrator discussed in Section 4.3.5). However, the design problem presented in the truss experiment did not require the same level of detail within the discretisation process, due to established relationships between connection points and featured timber areas. This provided an opportunity to demonstrate the scalability of the discretisation method. The existing method can be adapted to suit the design problem as required. The three alterations required to the established method are in relation to scale of *subdivision*, *segmentation* and *dataset extrapolation*, discussed following.

Further, the feature recognition method developed in Section 4.3.2 captured material features on the front and rear faces of a board,

subsequently hybridising this data into a single plane of geometric data prior to discretisation. Due to this hybridisation, the methods employed within this experiment do not require the consideration of mirroring or rotation of timber boards within material distribution, connection point generation or fabrication processes. This is due to the methods employed being aware of the material features from both board faces, thereby allowing simultaneous consideration of feature impact within its calculations.

5.3.1.1 Subdivision Scale

The *subdivision scale* of a timber board refers to the resolution of data transfer between the raw detected features and the discretised representation of those features. Resolutions of between 3mm and 30mm were explored in Section 4.3.2, to determine the discretisation accuracy and its effect on computational runtime (as shown in Table 4.3.8).

The four resolutions tested (3mm, 5mm, 10mm, and 30mm) offer a range of options to be selected from within the architectural context of a timber truss. The process used to generate the acoustic panel in Section 4.3.2 used a 5mm gridded matrix, offering a granular level of detail specific for that application. It was found that this resolution was most suitable for the subsequent processes, and offered a comparable scale, *after* the boards had been cut into 600mm segments.

However, the truss configuration and connection detailing within this experiment required a less granular level of material information. A primary concern within the design problem was that timber boards were positioned within each truss segments, such that physical connection locations occurred in areas of timber that did not contain a material feature.

Consequently, the employed methods translated detected timber features to the full width of the board, resulting in a standardised 90mm feature zone across the board in the Y-axis. This would allow for a discretisation scale of 90mm to be considered; however, it was found that this resolution was too coarse in the X-axis of the board. Subsequently a sub-division based on a 30mm grid was selected, which provided sufficient detail to determine feature significance (Figure 5.3), whilst not unnecessarily precluding clear sections of the board from being considered as connection points.

Figure 5.3 Detected features (black outline) with subsequent discretisation (dark brown) employing a 30mm resolution

Adjacent discretised cells were grouped together to represent the extent of the whole feature. Additionally, the prominence of each registered feature informed the size of a buffer zone around it in which no truss connections can occur. The inclusion of this buffer zone (outlined in Section 5.3.1.3.2) makes the impact of each feature larger in the boards' X-axis. The presence of these processes removes the need for the high resolution of subdivision (as employed in Chapter 4).

5.3.1.2 Segmentation

A primary objective of this experiment was to interrogate the use of whole timber boards in structural applications. Subsequently, the splitting of boards into smaller sections (also as applied in Chapter 4) was not required; however, it was probable that the MOEA would generate optimal truss solutions inglements that were shorter that the existing material inventory. To address the waste this created, Stage 4 (see Section 5.3.4) details a method that considers the reclamation of timber offcuts into the constrained inventory for use in subsequent truss generations.

5.3.1.3 Inventory Dataset Extrapolation

The data extrapolated from the constrained inventory included board character classification, correlation of feature significance and buffer zone, and identification of physical connection zones. This additional data was subsequently used in the MOEA in Stage 2 (Section 5.3.2), and for the filtering of fittest solutions in Stage 3 (Section 5.3.3).

5.3.1.3.1 Board Character Classification

The classification of board character represents its suitability as a structural element in compression, tension or mixed load scenarios. Naturally occurring features in timber have an impact on its physical and mechanical properties, affecting its structural performance widely. Foley (2003), As et al. (2006) and Lukacevic et al. (2015) found that both the size of a knot-based feature, and the localised grain condition surrounding it, directly impacts the structural capacity in both compression and tension load scenarios; particularly, in cases where centrally located, or structurally loaded perpendicular to the grain direction.

The results of these studies indicate that boards with a higher level of knot-based features demonstrate an increased failure rate when loaded in compression, while the tensile strength was significantly less impacted. While these studies predominantly investigate the capacity of softwood

timber, similar characteristics are observed in plantation hardwood *E. nitens* (Derikvand et al., 2019; Piter et al., 2004).

These observations were also inherently reinforced within the grading standards (discussed in Section 2.3) in which higher levels of material feature correlate to lower structural performance (Standards Australia, 2007; Wood Solutions, 2017).

The context of the design problem required the classification of inventory elements in accordance with potential structural performance characteristics. This process was established by calculating the relationship between individual board area and detected features. In applying this method to the constrained material inventory, a featured area relationship was found to have a range between 0% and 33.89%, representing an average of 14.46%. Boards 53 and 68 exhibited the lowest and highest featured area (these boards are shown in Figure 5.4).

Figure 5.4 Discretisation of boards 53 (top) and 68 (bottom), representing the lowest and highest featured areas

The boards were grouped by featured area percentage and split into three classifications of loading performance:

- compression;
- tension; and
- equilibrium.

These groupings are treated as potential material performance indicators within the experiment, and are intended to match the performance characteristics demonstrated in the precedent studies in Section 5.3.1.3.1.

23 boards with a featured area of less than 10% were classified as suitable for compression. Boards that exhibited greater than 20% featured areas (of which 17 were found) were classified as being suitable for tension. The remaining 35 boards exhibited a featured area of between 10% and 20% were found, subsequently classified as boards that would potentially perform well in both tension and compression.

The structural simulation undertaken in Section 5.3.2.3 quantified the load condition of each segment within a generated truss, and identified a segment as acting in compression, tension or a state of equilibrium. The fitness of material distribution within a solution could then be validated against the material character dataset. This provided the basis for using the discretised material inventory to extract a board character classification.

The classifications were subsequently used as the basis of a validation method for the structural fitness of a generated truss solution, as detailed in Section 5.3.3.

5.3.1.3.2 Correlation of Feature Significance and Buffer

The significance of a timber feature within a single board is the relationship between the area of the board and the dimensional properties each. The first step in establishing a buffer zone is the expansion of each feature to the full width of the board (90mm on the Z-axis). A connection point can therefore not occur adjacent to a feature on the X-axis, where its structural integrity would be compromised.

As noted in Section 3.2, the size of a detected feature within a sawn timber board can typically be correlated with the impact it has on the areas immediately adjacent to the feature location. This is especially evident in relation to timber knots. It was found that larger knot-based features had a greater area of influence on timber grain, fibre regularity, and colouration along the length of a timber board (the X-axis). Analysis of the collected data from Section 3.3 found that the areas of influence were typically between 25 and 125mm in each direction along the X-axis. While this phenomenon was observed within a random sample of ten boards from the available material inventory, and was present in similar studies (Guindos & Ortiz, 2013), this approximation was accommodated within the workflow as a proof of concept that requires further investigation beyond the scope of this thesis.

The range of 25 to 125mm was then correlated against the detected features within the constrained inventory. The size of a feature, determined by its dimension in the X-axis, scales the buffer zone proportionally to the relative size of the feature; however, a potential issue arose when this was applied on an individual board basis. If a feature is determined to be outside of the specified range found, then the buffer zone would not be able to adjust adequately in response.

To rectify this issue, the buffer zone is required to be applied proportionally to all discretised features found within the constrained inventory. The inventory of 81 boards contains a total of 521 discretised features ranging in length (X-axis) from 29mm through to 1257mm. Subsequently, each feature would have a buffer zone applied to each side of the feature proportionally scaled between 50 and 150mm. As a result, the detected features are translated into zones in which no physical connections can occur, ranging in size between 129mm on the smallest features, through

to 1557mm for the largest features. Figure 5.5 illustrates the relative *non-connection* zone for varying size discretised features.

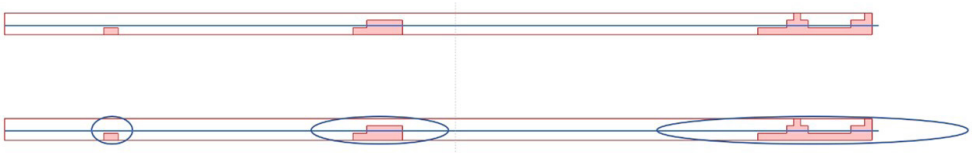

Figure 5.5 Extent of non-connection buffer zone around features of different dimension in the X-axis of a sample board

5.3.1.3.3 Identification of Physical Connection Zones

With zones of *non-connection* for each board determined, a merging process is undertaken to eliminate geometric anomalies. In cases where two buffer zones overlap, there is potential for errors within the workflow when identifying the parts of the boards that can contain connection zones. This issue is addressed by combining adjacent buffer zones using a similar method to that used to combine adjacent features. The geometric process of determining board areas that can contain connection points is shown in Figure 5.6.

The centreline of each timber board is split by the non-connection buffer zone geometry. Each resulting line segment is tested in relationship to non-connection zones, and segments that are found to be within the non-connection zones are culled. The remaining segments that correlate to board areas containing feature-free timber are classified as zones of potential connection.

In some instances, boards that contained only clear timber generated a non-valid solution. As clear boards do not contain areas of non-connection, the intersection process would not be successfully completed. A non-valid solution occurred in situations where a *non-connection* zone is not present on the board, indicating that the board is clear of feature. This implies that the full length of the board is a possible connection zone. To resolve this issue a fail-safe was built into the workflow: in instances where intersections were not generated, the potential connection zones

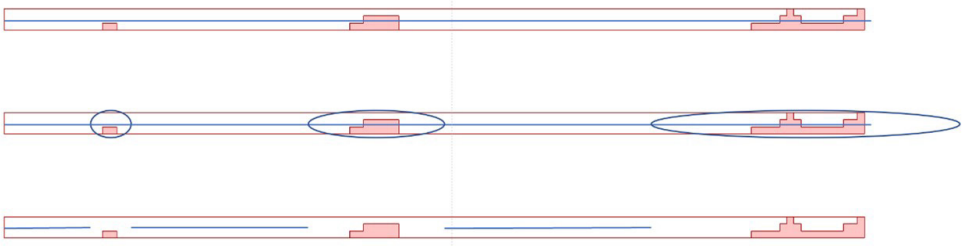

Figure 5.6 Geometrically establishing zones of potential connection

were automatically replaced with a single curve, equal in length to that of the board.

5.3.1.4 Results

This stage resulted in 81 boards being analysed for inclusion in the subsequent MOEA workflow, outlined in Stage 2. The process established zones within each board of the constrained inventory that are suitable for physical connection points. It determined that 236 potential connection zones were available across the inventory, with between one and six distinct zones being present per board at an average of 2.9 zones. The physical dimensions of these potential connection zones ranged in length between 56mm and 3,456mm, with an average of 493mm.

Each iteration of the evolutionary workflow in Stage 2 varies which boards were used, and the precise location within the established potential connection zones at which the truss segments physically intersect. This provided an extremely large search space for the workflow within which to operate, allowing solutions to consider material efficiencies that are not bound to traditional methods found in existing industry practices.

5.3.2 Stage 2: Multi-Objective Evolutionary Algorithm

Stage 2 employs a MOEA workflow to distribute boards from the constrained inventory across a Warren truss. The span requirement of the truss was specified as 10m, as it represents the opportunity to generate solutions that employ configurations beyond the maximum length of the boards within the material inventory. Additionally, a 10m span represents a design objective that is larger than pre-fabricated hardwood trusses commonly available in the Australian construction industry, as standardised elements (Pryda, 2022). The workflow is illustrated in Figure 5.7 and is divided into three distinct parts:

- Part A: Locating connection points;
- Part B: Generating truss geometry; and
- Part C: Structural simulation analysis.

The workflow established five Fitness Objectives and three chromosomes within the optimisation process. The generation of connection points on each board within the inventory was processed in Section 5.3.2.1, driven by two chromosomes.

The inventory distribution chromosome is employed within Section 5.3.2.2, shifting the configuration of each truss iteration.

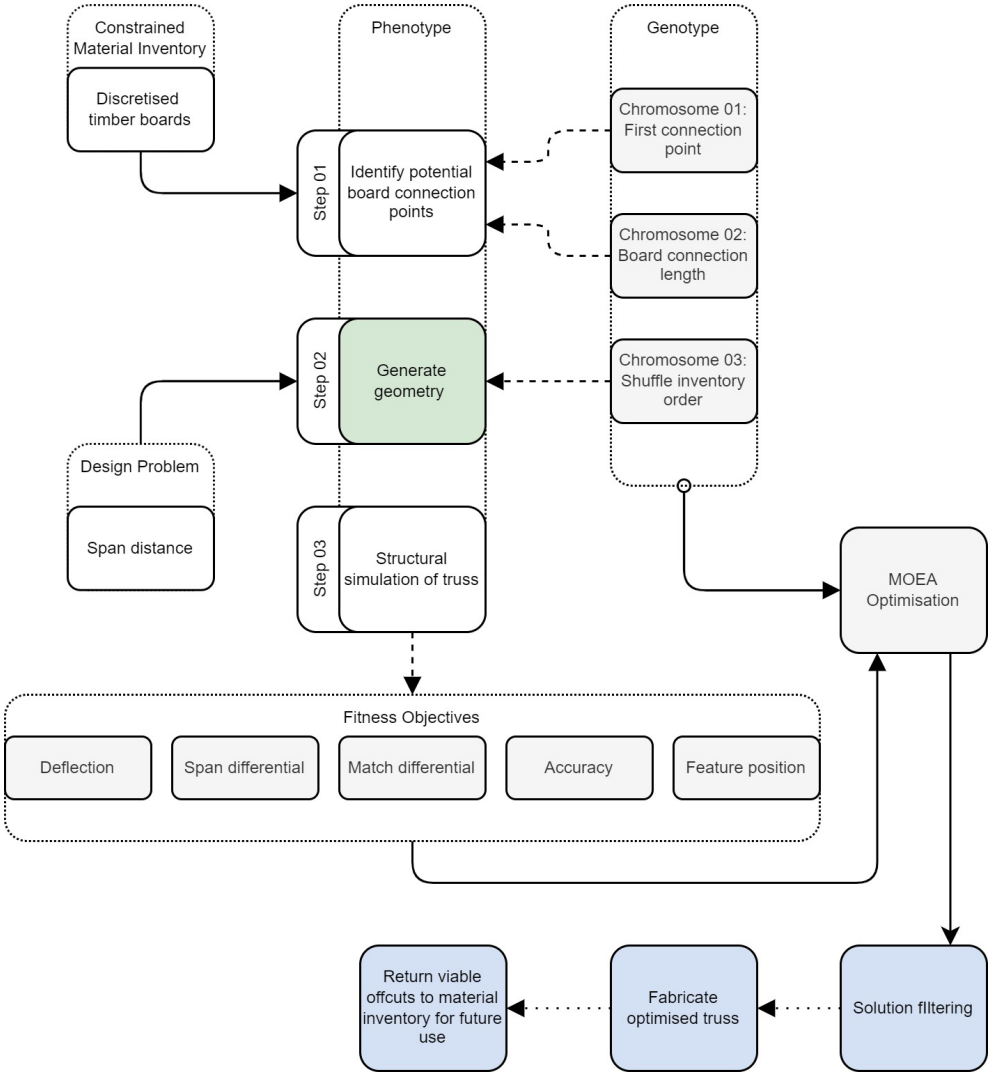

Figure 5.7 Truss generation: Evolutionary simulation pseudo code

Section 5.3.2.3 contains the structural simulation and analysis processes, calculating the performance and fitness of the generated solutions.

Table 5.1 details the optimisation genotype, comprising three chromosomes. Table 5.2 details the parameters specified within the evolutionary algorithm.

5.3.2.1 Iteration of Potential Board Connection Points

The material discretisation workflow (discussed in Stage 1, Section 5.3.1) identified zones within each board that could potentially contain a physical connection point. Each geometric segment within the Warren truss required two connection points to form a valid geometric arrangement. An almost infinite number of potential geometric configurations could be generated due to two factors:

a) the ability of two connection points to be located anywhere with the connection zones, resulting in a practically limitless number of possible connection point pairs on every board (see Figure 5.8), and

b) the number of genes specifying how material is distributed and where connection points are located.

Subsequently, connection points were iterated in each cycle of the MOEA workflow, allowing for the testing of a greater number of design potentialities.

Truss Generation: Genotype Specification		
No. of Genes	**Numerical Domain**	**Function**
Chromosome 01: First connection point		
150	0.000 to 0.200 (200 values per gene)	To provide a variable connection point within the first 200mm of each board within the constrained material inventory
Chromosome 02: Board connection length		
150	0.090 to 2.400 (1,500 values per gene)	To find a variable and valid test length between 900mm-2400mm for each board within the constrained material inventory
Chromosome 03: Shuffle inventory order		
150	0.000000 to 1.000000 (10^6 values per gene)	To provide a traceable sort index to each discreet timber board dataset from the material inventory, facilitating variation of the boards selected by the phenotype.

Table 5.1 Truss generation: Genotype specification

Evolutionary algorithm parameters	
Generation size	75
Generation count	150
Population size	111250
Crossover probability	0.9
Mutation probability	$1/n^{\text{n=number of variables}}$
Crossover distribution index	20
Mutation distribution index	20
Random seed	1
Simulation runtime	3hr 14m 09s

Table 5.2 Truss generation: Evolutionary algorithm parameters

Figure 5.8 Iterations of connection point location and impact on geometry

5.3.2.1.1 Point A Determination

Connection Point A was specified as being the closest of the two points to the origin (0, 0, 0) of each board. It was consistently positioned within the first potential connection zone, as ordered from the same board end. As the length dimension of each zone varied significantly across the inventory, a simple distance range was unable to be specified as a gene within the workflow. As such, it needed to be expressed as a percentage along each of the connection zones. The location of Connection Point A on each board was iterated within the MOEA and was specified to be located within the first 20% of the first valid connection zone (Figure 5.9). This ensured that the first connection point on any given board would maximise the material utilisation when distributed within a truss geometry.

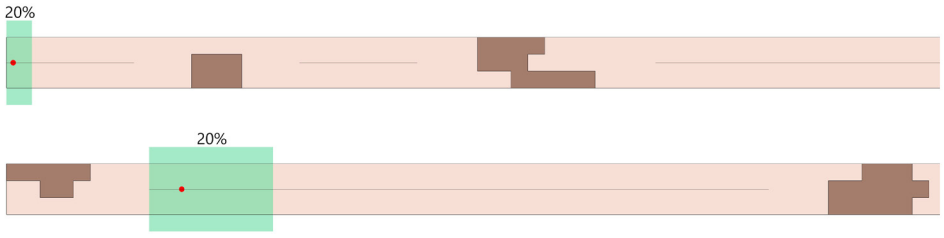

Figure 5.9 Iterative location of connection Point A as demonstrated on Board 60

As Point A could shift anywhere within the first 20% of each zone of connection, there was potential for it to be in proximity the end of the board. This affects the connection point's capacity to have adequate material overlap for a successful physical connection to other truss segments (as noted by *AS-1720: Design Methods for Timber Structures* [Standards Australia, 2015]). However, the percentage range was required to be specified as this range to accommodate scenarios, where the first connection zone is located further along the board.

To counter this issue, an internal check was created that determined Point A's location relative to the end of the board. If the iterated point was found to be within a threshold zone (90mm) of the board its X-value was substituted with a value of 90mm (Figure 5.10). This ensured that Point A was always positioned at a suitable distance from the origin of the board for a physical connection. Point A was then used as the basis for determining Point B.

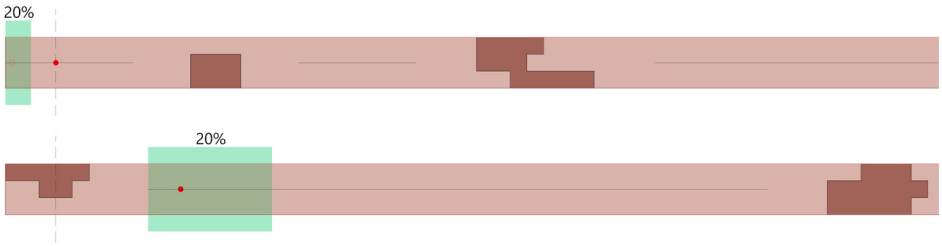

Figure 5.10 Relocation of connection point A when initially within board end threshold zone

5.3.2.1.2 Point B Determination

Each element within the material inventory varied in length and had between one and six valid zones of connection, a selection of which is shown in Figure 5.11, in green. The length of each of these connection zones ranged in length from 56mm to 3,456mm. A valid location for Point B could be located within any of these regions, have an intrinsic relationship with Point A and have a direct impact on the board's location within each truss solution. For this reason, the location of Point B on each board was required to be specified by its own chromosome within the MOEA; however, a more robust method of implementation was required in comparison to Point A.

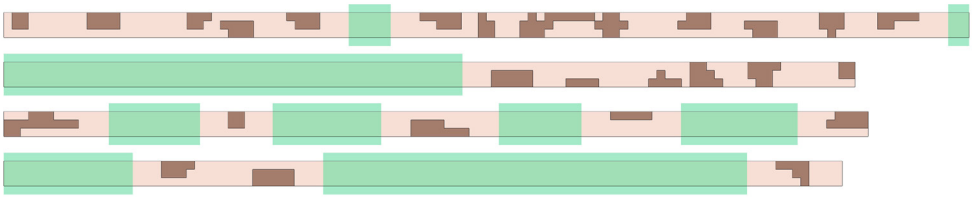

Figure 5.11 Selection of boards from the constrained inventory demonstrating a range of varying connection zone scenarios

Point B was specified as a distance value of between 900mm and 2,600mm, relative to Point A. This restriction acted as an origin point for Point B generation: that is, the nominal distance that the MOEA should attempt to position the point relative to Point A. While this value was most likely unique for every inventory element in each iteration, there was potential for repetition with 81 boards being allocated one of 1,500 values. However, the possibility of repetition was small enough as to be considered irrelevant, as each board has a unique set of connection zones and Point A locations. The distance range had three significant impacts on the MOEA:

1. Each iteration was more likely to generate a valid Point B for each inventory item.
2. More critically, aspect was the effect on the physical depth of each truss solution. As the MOEA was primarily concerned with minimising the structural displacement of the solution, it subsequently favoured trusses with a deeper cross section - typically generating stronger trusses with less displacement. Specifying a truss segment length range (measured as Point A to Point B) provided a safeguard against generating solutions that were impractically deep.
3. The distance range offered related to material wastage. By limiting the range to a maximum of 2,600mm the unused portion of each element was more likely to yield a salvageable length of timber that had potential for re-introduction into the material inventory. This contributes to the system being scalable and adaptable, as this variable can be adjusted by the end user to suit material inventories with shorter or longer boards.

The Point B value was then varied within each iteration of the MOEA. In most situations the distance correlated with a zone of connection, with a Point B being generated successfully (as shown in Figure 5.12); however, it was found that 17% of the generated solutions fell outside valid connection zones. These invalid solutions either occurred within a featured non-connection zone or were positioned beyond the total length of the board. The correction process eliminated the Point B location errors, as they significantly increased the likelihood of an invalid truss solution being generated.

Point C (as shown in Figure 5.12) is representative of a positional error in the generation of the second connection point. In this instance, the iterated distance generated Point C within the buffer zone of a material feature. To resolve this issue, a proximity-based solution was implemented that repositioned an invalid point to the edge of the closest connection

zone. By employing proximity-based repositioning, the connection length had the potential to become either longer or shorter than the initial value. However, this had a negligible impact on the outcome of the generated truss, as the connection point would always be positioned within a clear zone of timber. This produced a valid second connection point, regardless of its original location being within or beyond the boundary of the board.

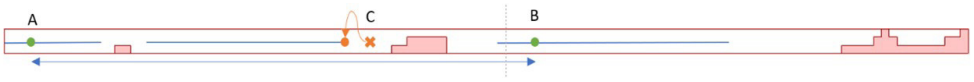

Figure 5.12 Positioning of connection Point B as demonstrated on Board 60

A final connection point positional-error check was integrated within Stage B. As the proximity-based solution moved a point to the closest connection zone, there was potential for the distance between Point A, and the re-positioned Point B, to be outside of the prescribed distance range. For example, a random iteration of the Point A and B chromosome (on 81 boards) generated five instances where Point B was repositioned, two of which resulted in a connection length (distance between Points A and B) being less than the prescribed 900mm.

A similar scenario could potentially be encountered if the repositioned Point B resulted in a connection length greater than 2,600mm; however, in five randomised iterations there were no instances of this occurring. The employed method of resolving this issue assessed each iteration of the MOEA, and boards found to have a connection length beyond the prescribed 900-2600mm range were removed from consideration in subsequent stages.

While the number of boards with valid connection distances varied within each MOEA cycle, there was never opportunity for the iteration to continue being processed with invalid board and connection relationships. Using the same randomised genes above, six boards were deemed unsuitable for MOEA consideration. The remaining 75 boards presented a connection length ranging between 905mm and 2380mm, with an average of 1638mm. These boards provided the basis for distribution within the truss generation portion of the MOEA, as described in the following sections.

5.3.2.2 Generating a Truss

Chapter 5 combines timber elements that were captured and catalogued within a constrained inventory (see Section 3.3) to create a truss. The MOEA generates a population of valid truss geometries comprised from various

configurations of timber elements. Accordingly, the remaining Chapter discussion is split into five Parts:

a) Inventory selection;

b) truss top chord;

c) truss web segments;

d) truss bottom chord; and

e) and geometry transfer.

5.3.2.2.1 Inventory Selection

Timber boards were initially distributed randomly, facilitating element placement in each evolutionary iteration; however, the selection of boards to allocate within a truss geometry was limited by several factors, including:

- the number of boards within the material inventory could vary between each truss iteration;
- the board indexation within the material inventory had the potential to be non-sequential; and
- the quantity of boards to distribute was unknown until later in the overall MOEA workflow.

To resolve these complexities, a innovative material selection and distribution workflow was required.

At the outset, the number of genes within the sorting chromosome of the MOEA was specified to be larger than the number of boards within the material inventory. With 80 boards being discretised within the inventory, the chromosome was specified to have 150 genes. This value would need to be increased accordingly in scenarios where the material inventory is scaled to a commercially viable size.

The mechanism applied to sort the genes was adopted from the method developed in *Design Probe 4: Evolutionary optimisation* (Section 3.5) and applied within *Prototype 1: Acousti-Sim* (Section 4.3.3). Each gene was assigned a sorting index value of between 0 and 1, with a six decimal place precision, that was varied and optimised within each MOEA iteration. The truss generation workflow was configured to consider the required number of boards from the material inventory from the start of the dataset within each iteration. As such, the application of a sorting index to each gene (board) within the evolutionary simulation allowed the optimisation

of board order within the material inventory, thereby placing boards that were within higher performing solutions at the beginning of the dataset.

While it was unlikely that repetition would occur in assigning nominally 150 random values from a pool of 1,000,000 potentials, it was possible, however, it should be noted that the likelihood of repetition using six decimal places is directly proportional to the number of boards in the material inventory being sampled. If the material inventory contained 20,000 elements, for example, then the number of decimal places in the sorting values would need to increase accordingly. Within the context of this experiment, a precision of six decimal places ensured that the likelihood of two boards being assigned the same sorting gene value was practically eliminated.

After the sorting chromosome was varied within each MOEA cycle, it needed to be reduced to match the number of available boards within the corresponding iteration of the material inventory. The quantity of boards with valid connection points was determined, and the number of genes within the chromosome was accordingly culled to match. This resulted in a unique gene value being allocated to each available board, coupled with a sorting index.

Each iteration of the MOEA assigned a different value to each gene, with the chromosome subsequently being sorted numerically. This numerical ordering disassociated the genes from its original index value. However, it facilitated the unique reordering to be correlated with the discretised material inventory data (as established in in Section 3.5, Section 4.3.3), inclusive of the inventory ID. As a result, the could sequentially select different sets of boards, and test varying material distribution and truss configurations within each MOEA cycle. Extending this further, it provided capacity for subsequent applications of the overall workflow to generate new trusses, while being responsive to material inventory changes.

The governing logic for distributing the selected inventory elements within each truss iteration is undertaking within the following Parts B, C, and D, and is shown in Figure 5.13.

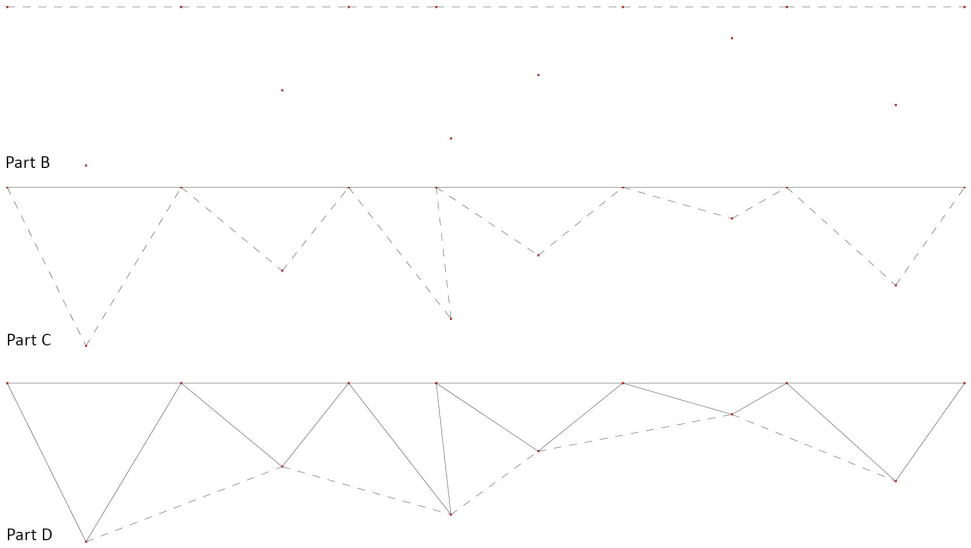

Figure 5.13 Truss generation logic

Part B deploys inventory elements to the top chord, attempting to match the total elemental distance with the span objective.

Part C generates the truss web segments, creating triangulation from each of the top chord intersection nodes.

Finally, Part D searches the remaining material inventory for elements that are the closest match to the generated distances between bottom chord triangulation points.

5.3.2.2.2 Truss Top Chord

As discussed in Section 5.3, the span distance of the truss was a design goal for the overall configuration. The arrangement of elements within the top chord was required to be nominally equal to the specified span of 10m. Additionally, this arrangement influenced the configuration and specification of all elements within the web and bottom chord segments. The differential between the calculated span and the design goal was encoded as a Fitness Objective within the MOEA.

In determining the number of boards required for the top chord, the algorithm extracted the connection lengths from each board within the current iteration. It selected boards progressively in their iterated order, adding the length of each together until it encountered a combination that was larger than the specified span goal.

Table 5.3 shows a selected portion of the re-ordered material inventory from iteration 122;68. In this iteration, the cumulative length exceeded the span design goal at an index of 4, equating to five boards.

Table 5.3 Top chord board selection (solution 122;68)

Index	Board ID	Connection length (m)	Culminative length (m)
0	37	1.671	1.671
1	66	2.161	3.832
2	60	2.147	5.979
3	0	1.852	7.831
4	4	2.170	10.002
5	52	1.850	11.852
...	....	...	...
75	38	1.347	126.204

Figure 5.14 illustrates the geometric representation of this process, with the board ID and corresponding connection length of each utilised element being annotated. The cumulative length was tested against the design goal length, the result of which is a negative number, in this case -0.002m (2mm). Establishing this calculation as a Fitness Objective required the number to be converted to its absolute, resulting in the value of this solution being 0.002m.

Figure 5.14 Top chord of truss (solution 122;68)

As the material inventory had a prescribed a dataset based on physical timber boards, boards utilised in the top chord were removed from the available inventory for the calculation of other segments within the truss. The board ID's and associated data are stored in a sub-list to allow offcut and material recovery calculation to be undertaken in Stage 4 of the workflow (see Section 5.3.4).

5.3.2.2.3 Truss Web Segments

The inherent geometric configuration of a Warren truss arrangement required the number of diagonal web segments to equate to twice the number of top chord elements. Therefore, the next ten boards from the re-ordered inventory list were selected for distribution within the truss web segments. These boards are detailed in Table 5.4 for Solution 122;68. The boards were grouped in pairs by partitioning the sorted list, representative of the position that would create a triangular web section in conjunction with a top chord element.

Index	Board ID	Connection length (m)
...	...	...
5	52	1.850
6	29	2.060
7	47	2.191
8	10	2.272
9	8	1.569
10	6	1.418
11	59	1.816
12	49	1.213
13	58	1.750
14	24	1.606
...	...	...

Table 5.4 Truss diagonal web segments board selection (solution 122;68)

Each pair of boards was required to form an intersection point that served the dual purpose of creating a triangular vertex and establishing the intersection points on the bottom chord. This was undertaken by inscribing an arc from each correlated top chord vertex (as shown in Figure 5.15).

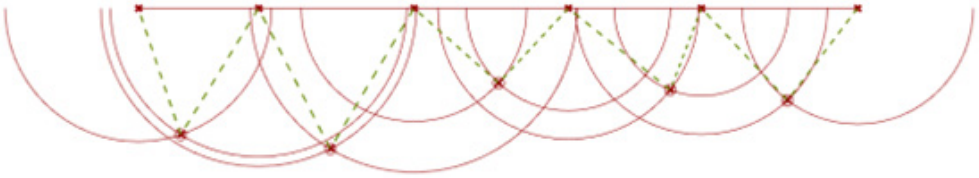

Figure 5.15 Web segment intersection arcs & point/element generation (solution 122;68)

Five intersection points were generated in this iteration, with the resulting web segments shown using a 'dashed' line. The irregular alignment of points indicates that structural performance is being optimised against material distribution instead of geometric regularity. Additionally, these intersection vertices formed the base geometry for allocation of material within the bottom chord of the truss.

However, this method may potentially lead to the generation of an invalid truss in two circumstances:

- if a pair of relatively short web segment do not generate an intersection vertex; or
- if the web segments self-intersect.

In the case of the first circumstance, the number of vertices in a valid solution should equate to the number of top chord elements. This provided the opportunity for comparative numerical validation to be employed.

Should the number of vertices and top chord elements not correlate, then a 'Null' result is returned, which is automatically disregarded by the algorithm and culled from the population.

The second circumstance occurs when the iteration order is such that the configuration of web triangulations caused neighbouring segments to cross over each other. As such, curve intersections were tested for, and solutions with self-intersecting segments also culled from the population through 'Null' attribution.

By embedding these two geometry-based validity triggers, the potential for invalid solutions to influence the population generated by the MOEA was eliminated. Although this increases the number of generations the MOEA was required to calculate (thus increasing the computation cost) it simultaneously strengthened the evolved population by ensuring all solutions are valid ones. As per the top chord, the boards distributed within the web segments are removed from the available inventory of the current iteration.

5.3.2.2.4 Truss Bottom Cord

In contrast with the iterative order method employed by both the top chord and web segments, the bottom chord method required a wider interrogation of the remaining material inventory. As the bottom chord vertices were derived from the web segment intersection vertices, their location relative to the top chord is unique in each instance. Therefore, their locality to each other is also unique to each instance (Figure 5.16). As a result, the material distribution was unable to simply select the next successive boards from the ordered inventory list.

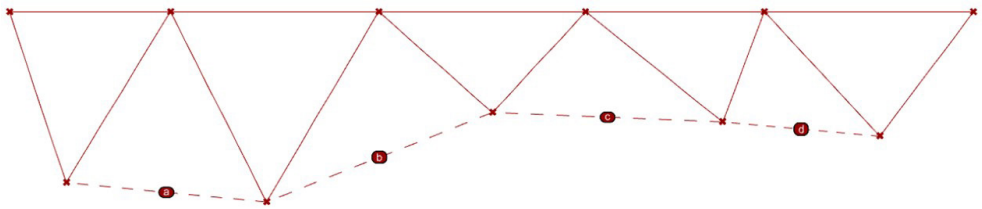

Figure 5.16 Bottom chord segmentation (solution 122;68)

The correlation of the iterated bottom chord segment length and the successive inventory elements is shown in Table 5.5. It is evident that a *divergence* existed between the two and represented a mismatch between the truss requirements and material distribution. The extent of the mismatch was calculated for each item by subtracting the inventory item length from the measure length. The differential of all segments was

Index	Measured length (m)	Inventory index	Board ID	Length of inventory item (m)	Differential (m)
a	2.088	15	61	1.756	0.332
b	2.515	16	68	1.087	1.428
c	2.389	17	28	0.806	1.583
d	1.636	18	3	1.421	0.215
				Differential Total	3.558

Table 5.5 Correlation of iterated bottom chord segments and ordered inventory (solution 122;68)

totalled, with the result being established as a Fitness Objective within the MOEA.

Ideally, the differential of each segment would be calculated and optimised individually, however, the applied MOEA required that a Fitness Objective be represented by a single numerical value. Additionally, the MOEA employed in this experiment requires Fitness Objectives to be pre-determined, meaning there is no capacity to adjust the number of objectives to match the variable number of web segments, while the algorithm is running. Subsequently, within this scenario, the MOEA searches for combinations of boards and seeks to reduce the total differential to 0m in search for the closest matching available set of boards to the measured length. If the total differential does not optimise 0, the solution still has potential to be viable, as there are alternate boards remaining in the inventory that could provide a closer match.

An integrated validation check was performed to ensure that the closest match within the remaining inventory did not result in duplicate allocation of the same board. This scenario is avoided by the introduction of a Board ID Check, to ensure that all distributed boards are unique. Occurrences where duplication was evident, were deemed to be 'Null' solutions and excluded from the MOEA population. The equalisation of the differential was undertaken within each evolutionary iteration by searching for boards within the remaining inventory that had the closest iterated connection length to each of the bottom chord segments. Within solution 122;68, a differential of 13mm is obtained (see Table 5.6).

Table 5.6 Results of search matching segment length with remaining inventory elements (solution 122;68)

Index	Measured length (m)	Inventory index	Board ID	Connection length (m)	Differential (m)
a	2.088	58	13	2.077	0.011
b	2.515	40	2	2.521	-0.006
c	2.389	65	65	2.357	0.032
d	1.636	59	80	1.660	-0.024
				Differential Total	0.013

While this does not represent an exact match, tolerance exists within the material discretisation and connection length processes in two instances.

a) The first tolerance was the specification of the minimum buffer zone around a detected feature, equating to potentially 8mm on either side of a knot features area of influence. In Section 3.2, the knot influence area was found to be a minimum of 42mm; however, this was increased to 50mm to accommodate instances at the lower end of the dataset.

b) The second tolerance existed in the material connection length. While possible, it is unlikely that a Point A or B of the connection length would be positioned at the very extremity of an allowable connection zone between feature buffers. Subsequently, the proximity of a connection point to a buffer zone translates into additional clear area being available around the point.

One method to address the differential not converging to zero was to expand the population size of the MOEA. In this scenario, the population was configured to have 150 generations, each with a population size of 75 individuals, resulting in 11,250 solutions throughout the run. Within the set of generated solutions, the most optimised bottom chord differential was 4mm in solution 106;6 (see Figure 5.17); however, this did not result in favourable results across other objectives. Increasing the search space for the solver to operate within allowed for a greater number of solutions to be generated, which increased the potential for finding a more optimised bottom chord differential solution, in addition to a stronger convergence between the Fitness Objectives overall.

5.3.2.2.5 Geometry Transfer

The final part of Stage 2 transferred the key geometric data from the truss iteration into the structural simulation (as outlined in Section 5.3.2.3).

All calculations undertaken in constructing a valid truss relied on simple geometric and numerical data. The geometric component pertained to the

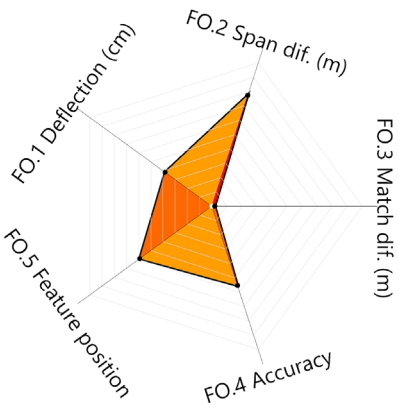

FO.3 Match dif. (m)
Rank 0

Generation 106 // Ind. 6

FO.1 Deflection (cm)
Rank: 4159 / 11250
Fitness Value: 2.151693

FO.2 Span dif. (m)
Rank: 8650 / 11250
Fitness Value: 0.689106

FO.3 Match dif. (m)
Rank: 0 / 11250
Fitness Value: 0.004916

FO.4 Accuracy
Rank: 6117 / 11250
Fitness Value: 4

FO.5 Feature position
Rank: 6545 / 11250
Fitness Value: 5

Figure 5.17 Highest rank bottom chord differential (FO.3) in comparison with other objectives.

vertices representing connection nodes and straight curves represented the segments of each element within the truss. This geometric data was matched with the numerical data (the board index and ID information that correlate to the material inventory) allowing more complex geometric data to be extracted as required.

The contrast in complexity is demonstrated in Figure 5.18, with the simple representation being shown as curves, vertices and ID tags, while the more complex representation demonstrates the truss as populated with the dataset from the discretised board geometry.

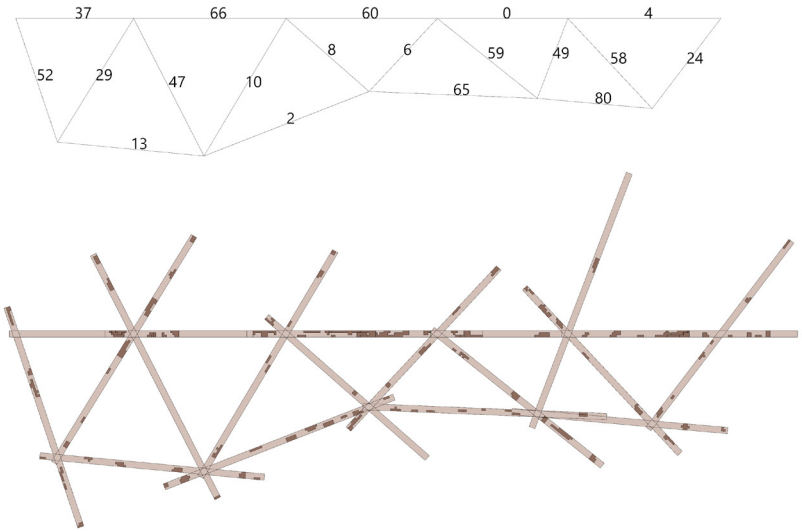

Figure 5.18 Geometric representation of truss solution 122;68 transferred to MOEA structural simulation, simple (above), and complex (below)

It should be noted that the complex representation is shown prior to additional trimming, waste recovery and fabrication processes (as outlined in Section 5.3.4 and Section 5.3.5.1). A consolidated list of distributed boards within truss solution 122;68 is compiled in Table 5.7.

	Index	Board ID	Connection length (m)
Top chord segments	0	37	1.671
	1	66	2.161
	2	60	2.147
	3	0	1.852
	4	4	2.170
Web segments	5	52	1.850
	6	29	2.060
	7	47	2.191
	8	10	2.272
	9	8	1.569
	10	6	1.418
	11	59	1.816
	12	49	1.213
	13	58	1.750
	14	24	1.606
	15	61	1.756
	16	68	1.087
	17	28	0.806
	18	3	1.421
Bottom chord segments	58	13	2.077
	40	2	2.521
	65	65	2.357
	59	80	1.660

Table 5.7 Inventory items for truss solution 122;68

5.3.2.3 Structural Simulation: Finite Element Analysis

Thus far, the evolutionary process had established iteration-based variation in the connection points within each board (Part A) and the material distribution and configuration within the truss geometry (Part B). These components of the evolutionary algorithm ensured that each generated solution met the required span and generated a valid truss

configuration. Part C of the MOEA workflow addresses the primary Fitness Objective of structural capacity.

The software tool employed for structural simulation, analysis and visualisation is Karamba3D™ (Preisinger, 2013; Preisinger & Heimrath, 2014), a parametric structural engineering tool, which provides accurate analysis of architectural arrangements (including spatial trusses). It operates as a plugin within the Grasshopper environment, offering a fully embedded solution that allows for the integration of parametric geometric models, finite element calculations and evolutionary optimisation algorithms, such as Wallacei.

In its most basic application, Karamba3D provides the capacity to simulate single instances of structural arrangements, doing calculations (including displacement, elemental internal forces and utilisation) in addition to a range of visualisation options. However, when deployed within an evolutionary algorithm, this data can be used as optimisation objectives, shifting the plug-in's application beyond simulation to become an embedded generation tool (Preisinger, 2013).

This optimisation process commonly generates solutions that are found to have non-regular elemental configurations (Garcia et al., 2021; Johan et al., 2019; Tam et al., 2017), which can subsequently be matched to inventories of irregular materials (Amtsberg et al., 2022; Brütting, Senatore, et al., 2019).

For Karamaba3D to generate reliable analysis of each iteration within the MOEA, particular attention was required in establishing the simulation environment. The first set of parameters related to the specification of material properties, which was particularly challenging when utilising ungraded, variable material, such as plantation hardwood.

The second set of parameters was concerned with the support and load condition of the simulation, which was assigned to points from within the geometric model. The scope of the simulation environment allowed the results to quantify truss displacement, elemental internal forces and material feature location, within compression elements.

5.3.2.3.1 Simulation Parameters

Structural simulation environments require external and internal conditions to be specified to establish a loading scenario. In this case, the first of these conditions was the placement of support points, both external to and within the truss geometry. As the truss is intended to span 10m, the external support points were spaced accordingly along the X-axis. These support points were configured to have their location specified as

fixed on each axis, with rotational movement permitted in the Y-axis only. These constraints ensured that the simulation was free of buckling under loads that would otherwise generate onerous results.

The internal support points of the truss were specified to control the relationship between each of the segments. These supports were configured to restrict positional movement, while allowing rotational movement only on the Y-axis. This ensured that when the truss was loaded, the relationship between segments was maintained, spreading the load across the whole truss, rather than individual components.

The loading conditions of the truss considered two external forces acting on it.

a) The effect of gravity on the structure: Karamba3D integrates gravity as a force on mass, determined by the total volume of the material in relation to its nominal density, and acceleration due to gravity is taken as 10m/s^2.

b) The live load that a truss of this span was likely to be required to support.

A uniform point load of 10kn/m^2 was applied along the connection vertices of along the top chord of the truss (Figure 5.19). Equating to 1,000Kg/m^2, this load case was significantly higher than would be expected in a typical residential (2kN/m^2) or medium scale commercial application (3-7kN/m^2). However, it was more likely to be consistent with the load expectations of a pedestrian bridge which, given the longer 10m span, had the potential to be a practical application of the designed truss. Increasing the load requirements correlated to an increase in truss depth, but within the context of this experiment, the solution depth was not a design constraint.

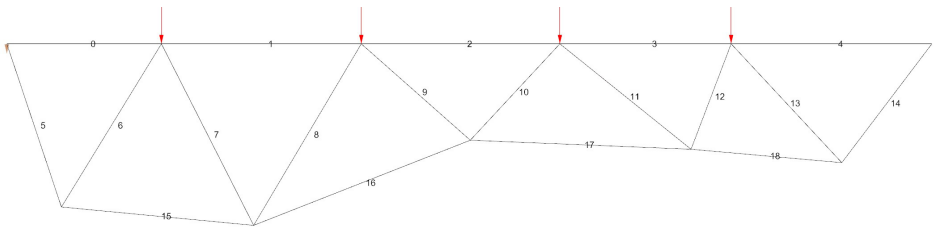

Figure 5.19 Structural simulation loading conditions

5.3.2.3.2 Material Specification

Karamba3D requires a set of specific material properties to be specified to represent the performance capacity of a structural element, as outlined in Table 5.8.

Karamba3D parameter	**Measurement**
E	Young's modulus (kN/cm^2)
G12	In-plane shear modulus (kN/cm^2)
G3	Transversal shear modulus (kN/cm^2)
gamma	Specific weight (kN/m^3)
alphaT	Coefficient of thermal expansion (1/C°)
ft	Tensile strength (kN/cm^2)
fc	Compressive strength (kN/cm^2)

Table 5.8 Material parameters required by Karamba3D

This introduces a problem when using non-standard materials. As the material inventory depicted a high level of variation, a precise simulation would require each board to be specified individually within Karamba3D. As several of the test methods required to obtain this data were destructive, it was not feasible to undertake these tests (as a limited inventory was available for this study). This scenario would also be present in industry, as destroying the boards to extract a dataset is counterintuitive to retaining them for use.

As such, alternate material specification methods were utilised within this workflow. Two methods of material property specification were explored to generate necessary material information.

The first approach sought to establish a generalised set of material properties for the constrained inventory. Significant studies into the physical and mechanical properties of plantation *E. nitens* have been undertaken since the early 2000s, coinciding with many plantations reaching maturity. Washusen et al. (2009) undertook a detailed investigation into sawn board recovery and grading capacity of thinned and pruned (sawlog) forests. Later studies undertaken by Derikvand et al. (2018, 2019) utilised visual and manual grading methods to determine the impact of material irregularities on performance of un-thinned and un-pruned (pulplog) plantations. The findings from the latter's studies were employed as base

material performance properties for the structural analysis in Chapter 5 for two reasons:

a) They were generated from standardised and statistically significant material testing; and

b) They considered pulp-log grade plantation hardwood sourced from Tasmania, Australia.

The dataset required conversion into the correct units, typically from MPA and kg/m^3 into kN/cm^2 and kNm^3, and these values were entered into Karamba3D (as shown in Figure 5.20.) It should be noted that Karamaba3D's strength hypothesis (S-Hypo) and coefficient of thermal expansion (alphaT) parameters have negligible impact on the simulation in the context of this experiment and were subsequently specified as their defaults being Rankin and 0.000005, respectively.

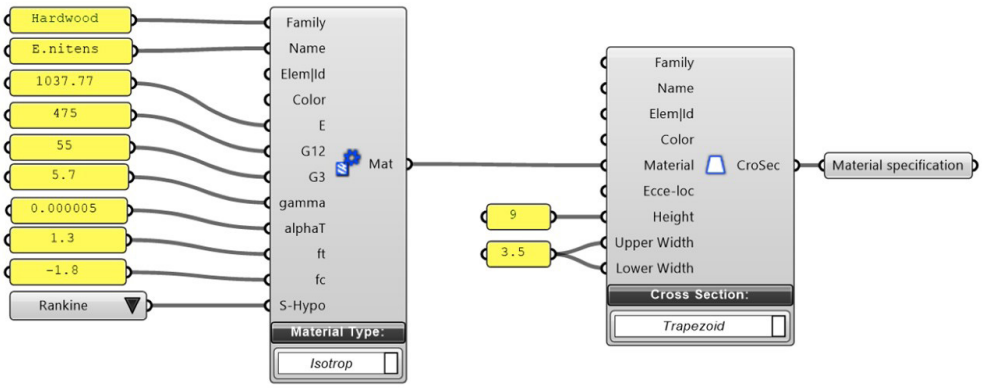

Figure 5.20 Material parameter specification within the Karamba3D simulation environment

Further, although timber is an *orthotropic* material, Karamba3D's calculation engine only consider this characteristic when simulating shell structures. Consequently, the material type was specified as *isotropic*, as recommended by Karamba3D's technical documentation (Preisinger, 2022).

The second method of material specification was undertaken by two evolutionary Fitness Objectives, generated from a successful structural analysis. The first objective employed Karamaba3D's capacity to determine axial stresses within a structure on an elemental basis, allowing the comparison of each segment of the truss against the material character classification (as determined in Section 5.3.1.3.1).

The second objective sought to minimise discretised material features from the central zones of truss segments, where compressive internal forces are present. Both Fitness Objectives are detailed as follows.

5.3.2.3.3 Truss Displacement

The displacement of the truss is considered a primary evolutionary Fitness Objective within the workflow. The finite element analysis Karamaba3D undertakes considers the load and support conditions against the specified material characterises to determine the displacement of the structural arrangement. Figure 5.21 illustrates the distribution of displacement of solution 122;68. It should be noted that the illustrated deformation in the Z-axis is scaled by a factor of five for clarity. It was evident that the greatest displacement of the truss (in this case 2.81cm), occurs centrally resulting in a linear deformation of the truss on the Z-axis.

A completely optimised solution would demonstrate no displacement under load. Consequently, the displacement target within this object was specified as 0cm; however, a method of limiting solutions within an acceptable displacement range is discussed in Section 5.3.3, as a means of accommodating potential solutions that demonstrate higher optimisation across all Fitness Objectives.

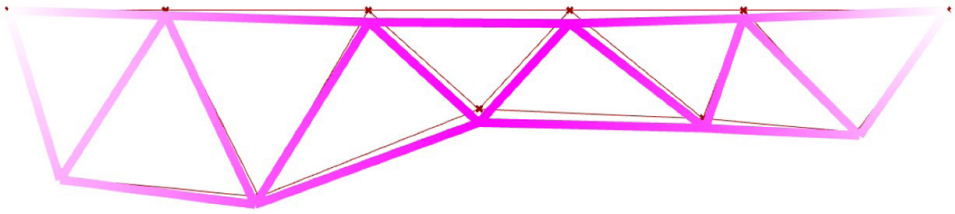

Figure 5.21 Displacement of truss solution 122;68. Colour intensity represents amount of displacement on the Z-axis

5.3.2.3.4 Elemental Analysis of Axial Stress

As a result of calculating the overall truss displacement, Karmaba3D has the capacity to individualise the internal axial stresses of each element within a structural arrangement. Figure 5.22 illustrates these forces within Solution 122;68, where compression and tension are represented as a gradient between red and blue respectively.

The constrained material inventory generated a material character classification of each board. This classification identified timber boards that would perform well in compression, tension or hybrid stress scenarios, based on the discretised volume of material feature. This allowed a Fitness Objective to be established that compared the calculated axial stress of each truss segment against the predicted load suitability of each distributed timber board used. In a completely optimised scenario, the number of

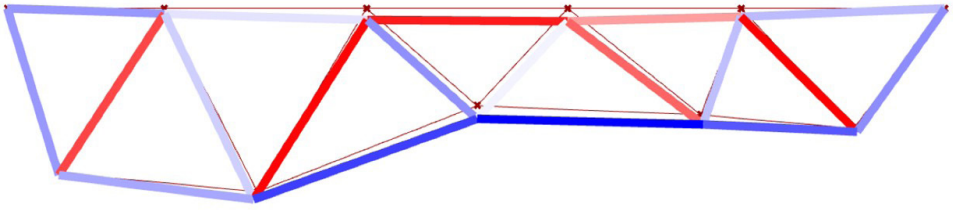

Figure 5.22 Internal axial stress of each segment within truss solution 122;68

incorrectly placed boards, based on their material character classification should be zero. As such, the Fitness Objective was configured to minimise the number of mismatched boards.

5.3.2.3.5 Features Distribution in Compression Elements

The final Fitness Objective generated from Karamba3D calculations considered the location of material feature within each truss segment relative to the axial stresses present. As determined in Section 5.3.1, knot-based features are prone to failure in truss segments with compression axial stress; particularly, when located centrally within the segment span.

Subsequently, this objective interrogated the material distribution within compression segments and determined the number of features present in the central third of each segment. Again, an optimised solution would contain zero features within these central zones, allowing an optimisation objective to be configured accordingly. Figure 5.23 illustrates the overlay of the distributed material features relative to the centralised zones of truss segments exhibiting compression axial forces.

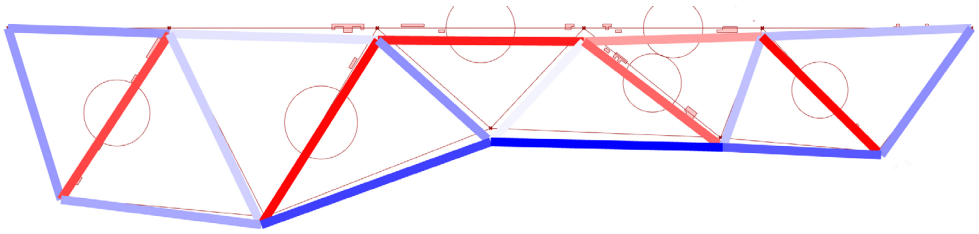

Figure 5.23 Location of material features within truss segments demonstrating compression-based axial loading within truss solution 122;68. Circles indicate areas within compression segments that should be free of material feature.

5.3.2.4 Results

The MOEA was configured with 150 generations, each containing 75 solutions. This represented an evolutionary population of 11,250 valid solutions. Numerical and basic geometric descriptors allowed each potential solution to be validated almost instantaneously prior to any structural calculations being undertaken. On average, a valid solution took 0.65 seconds to be analysed by Karamaba3D's structural performance. The discarding of invalid ('Null') solutions early within the workflow greatly increased Wallacei's capacity to optimise towards global convergence of

Fitness Objectives. However, the gain in workflow efficiency was potentially limited by the conflicting nature of the five Fitness Objective, and the generation of 'Null' solutions.

The MOEA simulation took 3 hours 4 minutes 9 second to complete, representing an average of 0.98 seconds per solution; however, the five 'Null' solution checks integrated within the MOEA generated a total of 22,200 'Null' solutions. The number of invalid solutions is almost double that of the number of valid solutions, representing 33% of the total calculation time. While this volume of invalid solutions appeared to be disproportionally large, the relatively cheap computational cost of the formulated design problem allowed for the integration and generation of 'Null' solutions as a mechanism to discard undesirable solutions without influencing the outcome of the valid solutions.

From the 11,250 valid solutions, the fittest solution for each evolutionary Fitness Objectives was spread across the generation pool, as shown in Table 5.9, Figure 5.24 Figure 5.25, and Figure 5.27. It is evident that the highest-ranking solution for each Fitness Objective yields significantly compromised results in most other objectives, indicating that the Fitness Objectives do not converge to a perfectly optimised solution, which is to be expected from a multi-objective conflicting design problem.

Fitness objectives 4 and 5 were expressed as an integer and had a relatively small search domain (as illustrated in Table 5.9). It was highly likely that both would completely optimise, and that there would be multiple solutions in which this occurred. Inspection of the solution set showed that FO4 first optimised in solution 10;5, while FO5 achieved optimisation in solution 4;0. A closer inspection of the dataset was revealed that there were 858 occurrences of FO4 and 1,396 instances of FO5 achieving an optimum result (a value of 0). In both cases, these duplicate results were spread across the simulation.

Fitness Objective	Fittest solution	Value	Domain
1: Displacement	149;5	0.96cm	0.96 – 8.9031^{e+11}cm
2: Span differential	119;6	0.1mm	0.1 – 2147.1mm
3: Bottom chord differential	106;6	4.9mm	4.9 - 2370mm
4: Incorrect character matches	39;0	0	0 - 13
5: Features in compression zones	133;26	0	0 - 18

Table 5.9 MOEA Fitness Objective results

Figure 5.24 reinforces this observation, plotting each Fittest Objective relative to the corresponding results for the other objectives within that specific solution. Additionally, the solutions generated a small pool of erroneous results, particularly in relation to the structural displacement detailed in Fitness Objective 1. In 1.3% of solutions the displacement was calculated to be more than 15m, with some instances being above 1,000m. In these scenarios the MOEA generated a valid truss; however, the structural simulation performed by Karamba3D resulted in complete structural failure. The MOEA generated a total of 638 Pareto solutions, representing a large pool of potential truss configuration to analyse. K-means clustering was initially employed as a method of grouping Pareto solutions into nine sets (see Figure 5.25); however, the centralised average solution of each cluster represented a compromised outcome and so was not suitable to proceed with.

In considering the lack of convergence in the solution set and the quantity of Pareto solutions, it was deemed ineffective to employ the typical toolsets within Wallacei to select an optimised truss solution in order to move forward with into the later Stages of this experiment. Therefore, an alternate method of qualification was required to be implemented, which allowed a finer interrogation of the 11,250 solutions generated by the MOEA. This hybrid multi-stage selection method is discussed in Stage 3 (see Section 5.3.3).

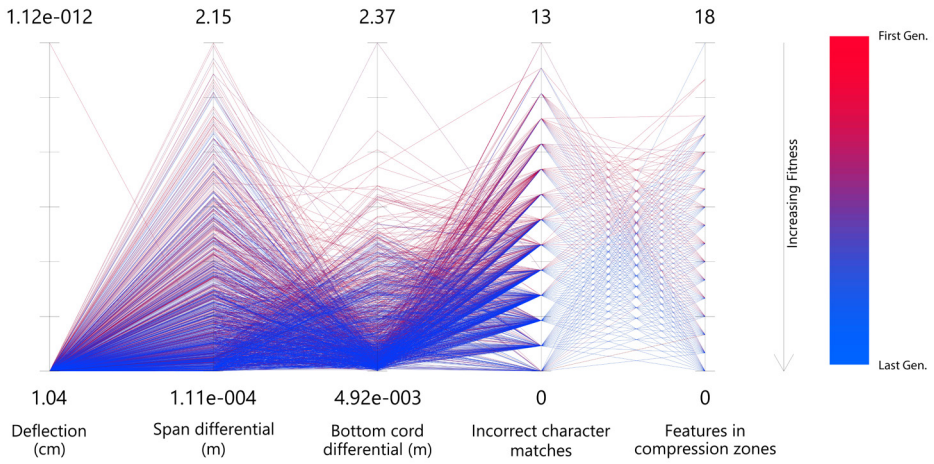

Figure 5.24 Parallel co-ordinate plot of valid solutions, categorised by Fitness Objective on the X-axis

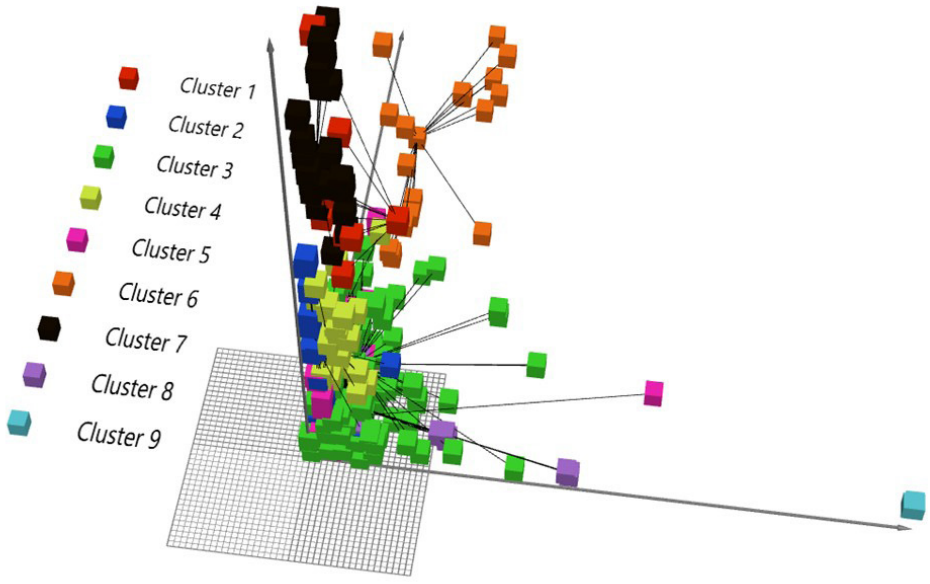

Figure 5.25 K-means clustering of Pareto solutions into nine groups

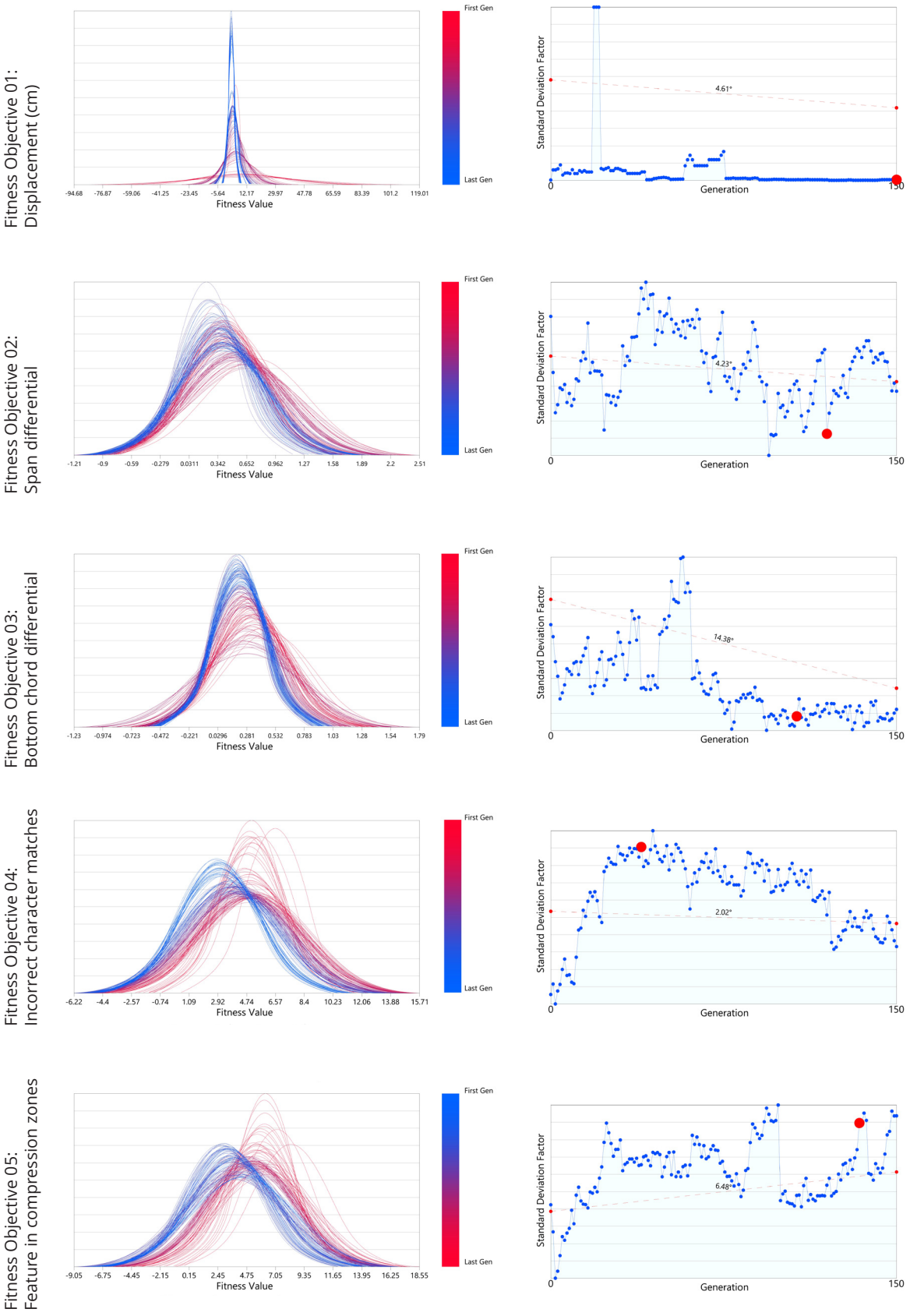

Figure 5.26 Statistical analysis of each Fitness Objective

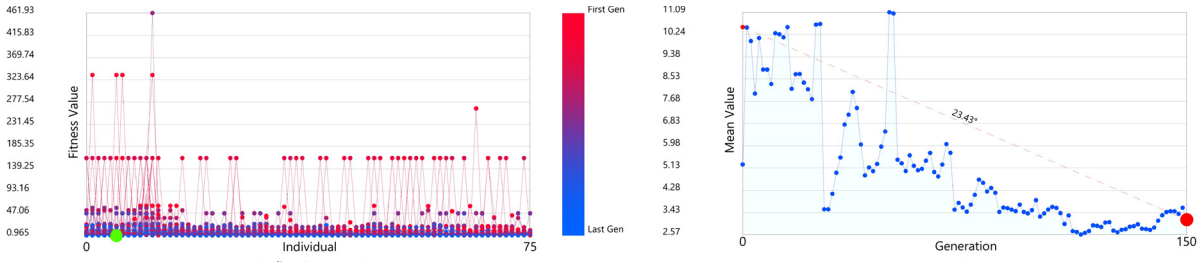

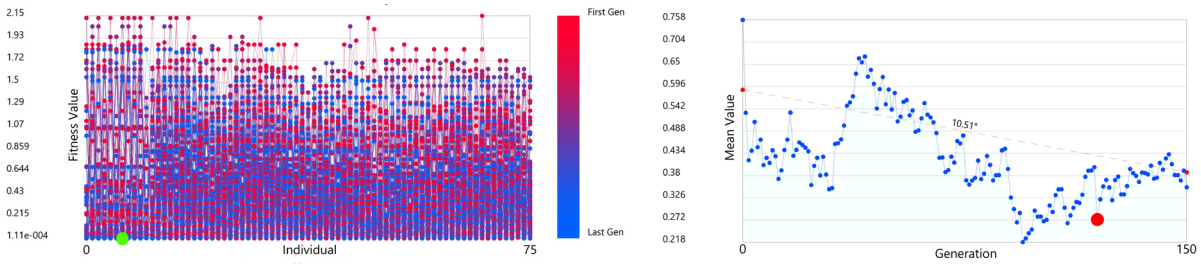

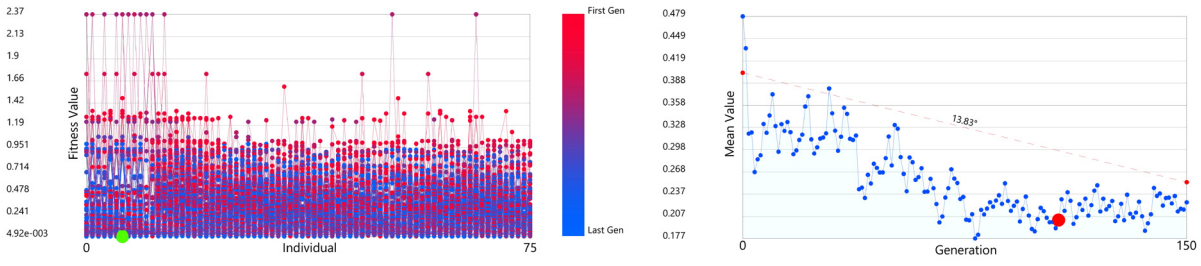

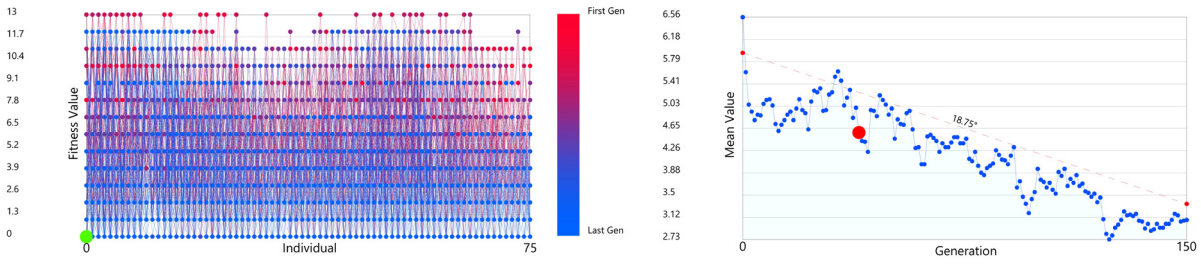

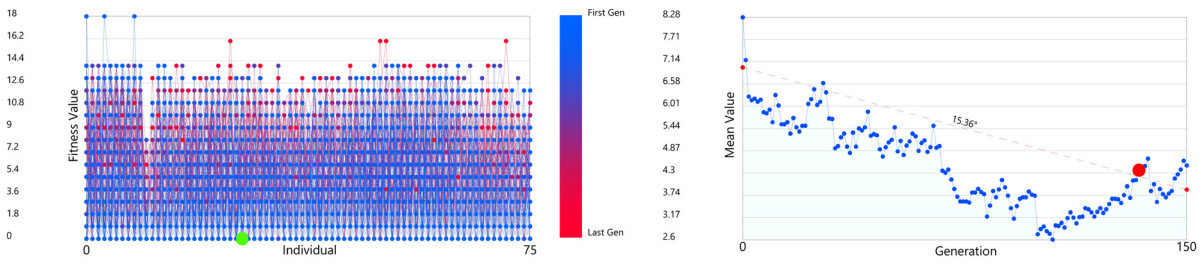

Fitness Values Graph

Mean Values Trendline

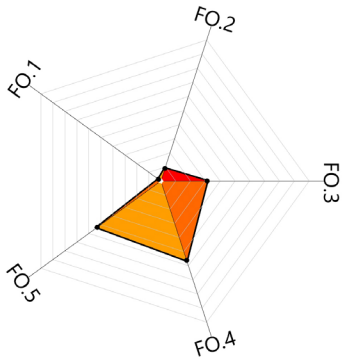

FO.1
Rank 0

Generation 149 // Ind. 5

FO.1
Rank: 0 / 11250
Fitness Value: 0.965371

FO.2
Rank: 791 / 11250
Fitness Value: 0.007447

FO.3
Rank: 3348 / 11250
Fitness Value: 0.054654

FO.4
Rank: 6218 / 11250
Fitness Value: 4

FO.5
Rank: 5855 / 11250
Fitness Value: 4

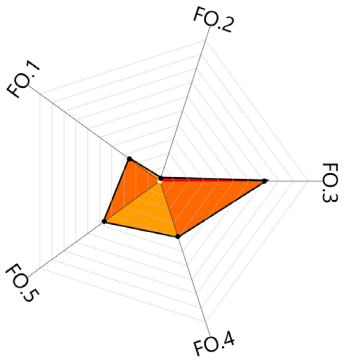

FO.2
Rank 0

Generation 119 // Ind. 6

FO.1
Rank: 2677 / 11250
Fitness Value: 1.801703

FO.2
Rank: 0 / 11250
Fitness Value: 0.000111

FO.3
Rank: 7873 / 11250
Fitness Value: 0.303662

FO.4
Rank: 4275 / 11250
Fitness Value: 3

FO.5
Rank: 5084 / 11250
Fitness Value: 3

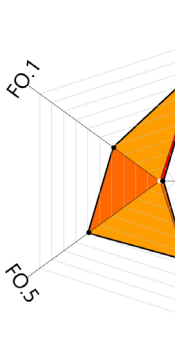

FO.3
Rank 0

Generation 106 //

FO.1
Rank: 4159 / 1125
Fitness Value: 2.15

FO.2
Rank: 8650 / 1125
Fitness Value: 0.68

FO.3
Rank: 0 / 11250
Fitness Value: 0.00

FO.4
Rank: 6117 / 1125
Fitness Value: 4

FO.5
Rank: 6545 / 1125
Fitness Value: 5

Figure 5.27 Five Evolutionary Objectives, ranked by fittest solution

Ind. 6

0
1693

0
9106

4916

0

0

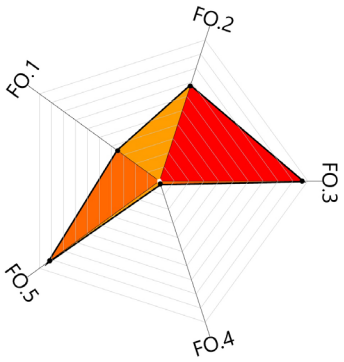

FO.4
Rank 0

Generation 39 // Ind. 0

FO.1
Rank: 3758 / 11250
Fitness Value: 2.078709

FO.2
Rank: 7498 / 11250
Fitness Value: 0.456824

FO.3
Rank: 10808 / 11250
Fitness Value: 0.926309

FO.4
Rank: 0 / 11250
Fitness Value: 0

FO.5
Rank: 10266 / 11250
Fitness Value: 10

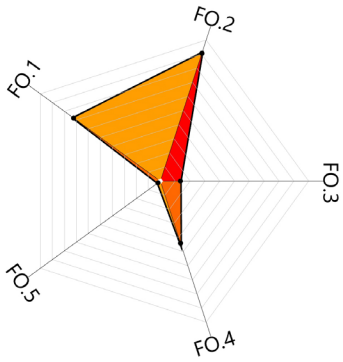

FO.5
Rank 0

Generation 133 // Ind. 26

FO.1
Rank: 8066 / 11250
Fitness Value: 4.252684

FO.2
Rank: 10165 / 11250
Fitness Value: 1.230582

FO.3
Rank: 1315 / 11250
Fitness Value: 0.025665

FO.4
Rank: 4819 / 11250
Fitness Value: 3

FO.5
Rank: 0 / 11250
Fitness Value: 0

5.3.3 Stage 3: Selection of Fittest Solution

The interrogation method employed a series of filters to reduce the set of evolutionary solutions to a manageable range of options (see Figure 5.28).

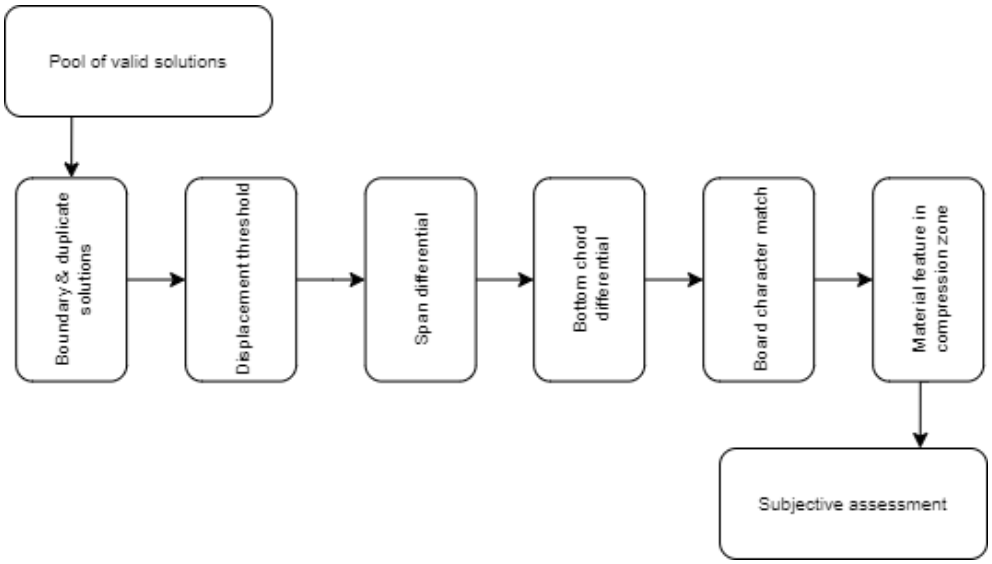

Figure 5.28 Selection filter interrogation workflow

The first filter culled erroneous and duplicate results within the solution set. The subsequent five filters disregarded threshold solutions related to displacement range, span objective differential, bottom chord differential, board character distribution, and features distributed within critical compression zones, as outlined in the following sections.

These filters significantly narrowed the field of valid options, allowing a final visual based interrogation to be employed. The output from this stage was a single materially optimised truss solution that performed within the specified range of acceptable conditions.

5.3.3.1 Boundary and Duplicate Solutions

A significant volume of erroneous boundary results was generated by the MOEA. This was particularly evident in the Fitness Objective 01: Truss Displacement (FO1). Figure 5.29 visualise this anomaly by plotting each of the 11,250 solutions, with the X-axis, representing the 75 solutions within each generation, the Y-axis showing the calculated displacement of each solution expressed in centimetres (smaller values are better); the colour gradient from red to blue depicts the first to last of the 150 generations, respectively. As noted in Table 5.9, the displacement range was calculated between 0.96 and 8.9031^{e+11}cm. It is evident that at least

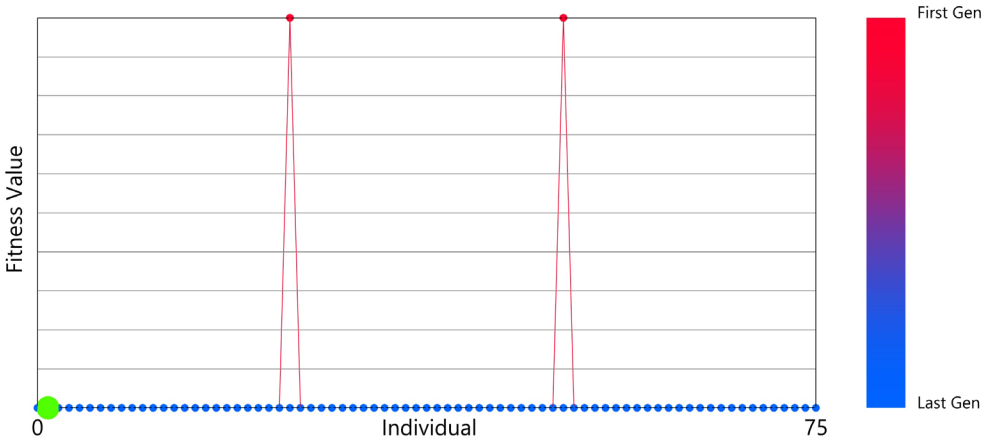

Figure 5.29 Truss displacement fitness value plot FO1:

two of the solutions represented calculation errors within the structural simulation environment.

The two invalid results were found to be solutions 1;50 and 0;24, representing simulation results early in the MOEA calculation process. To better visualise the simulation results, these two solutions were culled from the dataset, resulting in a replotted graph (shown in Figure 5.30). While this process reduced the scale distortion of the Y-axis, it still indicated that several invalid results were still present in the dataset, with six solutions found to have a displacement of approximately 53m, well outside the design expectations.

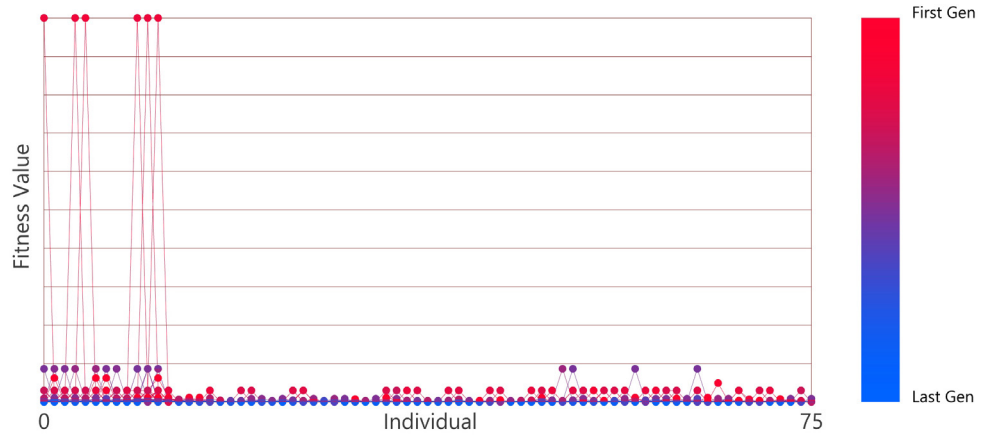

Figure 5.30 Truss displacement fitness value plot with two invalid solutions culled

Further investigation of the evolutionary dataset found many solutions that were outside of the expected displacement range. Figure 5.31 illustrates the dataset with 200 solutions culled from the FO1 results, encapsulating a displacement range of 0.96cm – 53.2cm. As a result, the dataset was

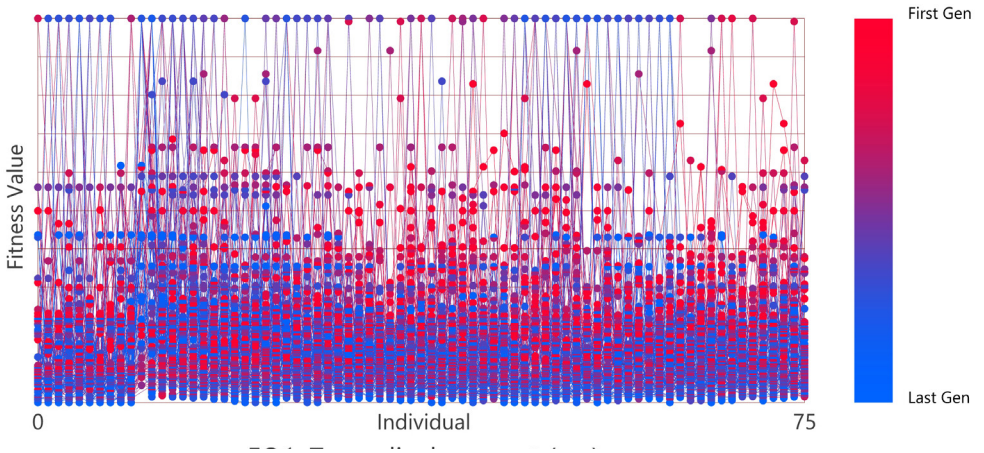

Figure 5.31 FO1: Truss displacement fitness value plot with 200 invalid solutions culled

reduced in size to 11,050 valid solutions, which were within a range more appropriate for further interrogation.

Culling 200 solutions from the dataset, based on the value of FO1, had an impact across the other four Fitness Objectives; however, it was considered necessary as similar extreme boundary results are not present in the other Fitness Objectives. Figure 5.32 illustrates each of the Fitness Objectives plotted against each other. It is evident that there are solutions that have FO2 and FO3 differentials of more than 2m, with instances of 13 elements being placed incorrectly against the material character, and up to 18 features being present within compression sensitive zones. While these represented a wider range than expected within each of the objectives, it was not to the same magnitude of distortion as the boundary results for FO1. Allowing them to remain within the dataset at this stage provided a greater comprehension of the phenomena generated.

Due to the generational nature of MOEA, it was probable that duplicate solutions were created. The final component of rationalising the solution set was the removal of duplicate solutions, and the employed method

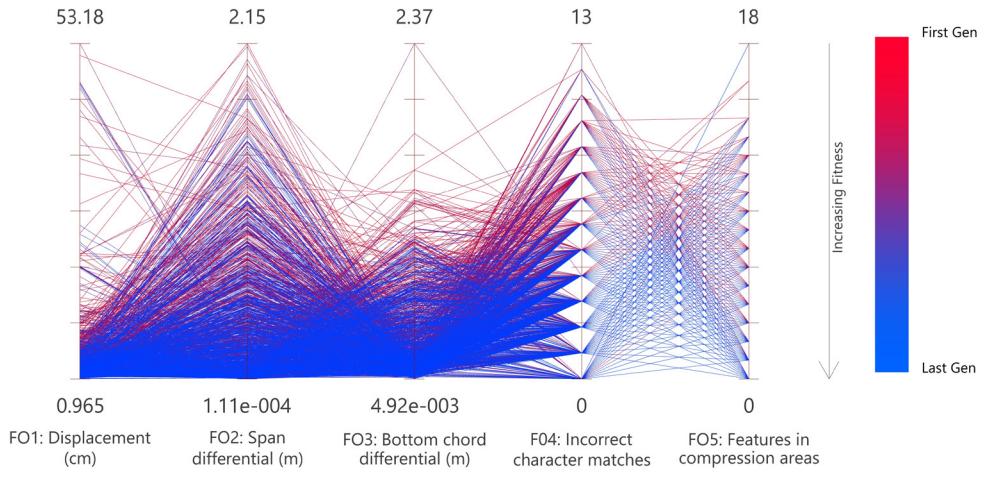

Figure 5.32 Parallel coordinate plot of 11,050 valid evolutionary solutions

considered value of truss displacement, as contained within FO1. It was anticipated that the volume of solutions, and the precision of calculation in FO1, FO2, and FO3, would lend itself to a relatively small volume of duplicates being found; however, this process determined there were 9,392 duplicates within the dataset, leaving 1,658 unique solutions. This presented an unexpected outcome and warranted further investigation of the solution dataset.

The interrogation of duplication was undertaken by extracting the *genotypes* of a set of duplicates and analysing the genes of each. Solution 0;1 of the dataset was found to have the same FO1 result in 26 instances across the solution set and was selected as a duplicate value for investigation. Each genotype contained three chromosomes, which comprised the genes that specified a board's first connection point, corresponding connection length, and the board shuffle order (as discussed in Stage 2, Section 5.3.2).

In all 26 duplication instances the 450 genes were found to be identical sets. Translating this to each solutions' phenotype meant that the same collection of boards from the material inventory, with identical connection points and lengths, were utilised in each. Extrapolating this across all instances of FO1 duplication confirms that only 1,658 unique existed within the 11,250 solutions.

5.3.3.2 Displacement Threshold

While FO1 was established to minimise displacement, there was no expectation within this experiment that a truss with a 10m span would achieve nominally zero movement. *AS 1170.1-2002: Structural design actions, Part 1: Permanent, imposed and other actions* (Standards Australia, 2002) stipulates that a floor truss is required to have a displacement of no greater than *span/300.* As the span objective within this experiment was 10m, a maximum displacement of 3.33cm was deemed acceptable. This value was established as a maximum threshold for FO1, the results of which are plotted in Figure 5.33.

As a result of this process, all solutions with a displacement above the 3.33cm threshold were removed from further consideration. In total, 519 solutions were determined to be above the threshold, leaving 1,139 truss solutions in the pool for consideration.

5.3.3.3 Span Differential

As discussed in Stage 2 (See Section 5.3.2.2), the span differential is determined by the difference between the span objective and the length of the truss top chord in each evolutionary iteration. As the material distribution and connection point locations were iterated within the MOEA,

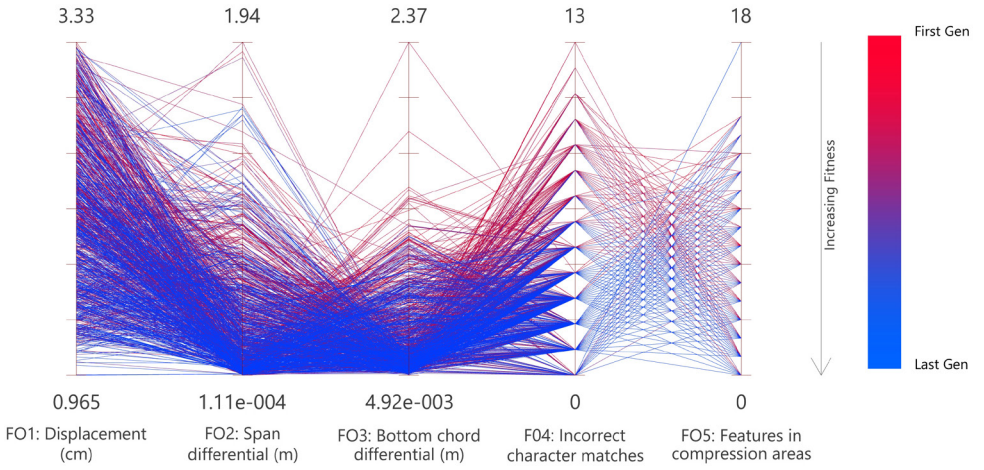

Figure 5.33 Solutions remaining after displacement filter

each solution typically presented a unique span differential. A threshold of 10cm was established as the maximum differential permitted within this filtering process (see Figure 5.34). This threshold was derived from the feature zone buffer encompassing the connection point location and material tolerances (see Section 5.3.1.3.2). This filter determined 728 solutions to be beyond the threshold, leaving 411 truss options to be assessed by their bottom chord differential.

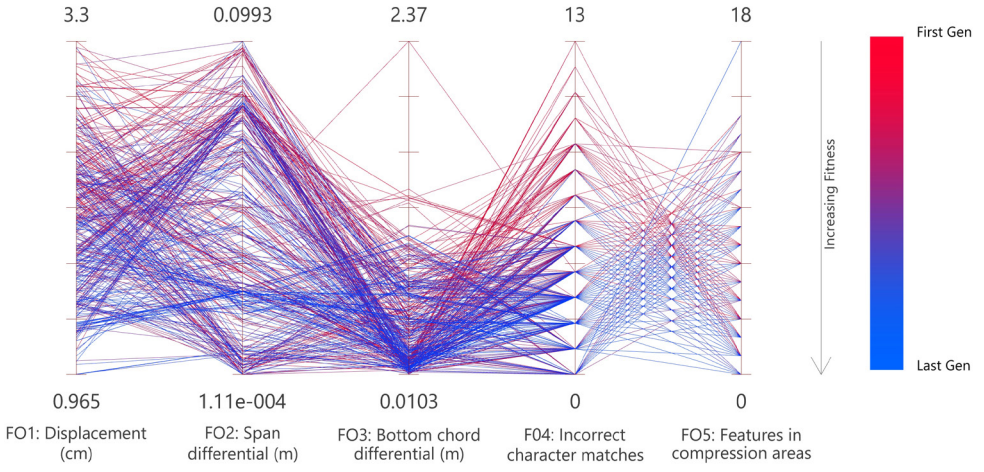

Figure 5.34 Solutions remaining after span differential filtering

5.3.3.4 Bottom Chord Differential

The same material tolerances outlined in Section 5.3.3 influenced the filtering method when assessing the remaining solutions bottom chord differential. Subsequently, an identical threshold of 10cm was set as the maximum permitted differential. This resulted in 304 solutions being culled, leaving 107 viable truss options (see Figure 5.35). The minimum and maximum differentials were determined to be 1.0cm and 9.9cm,

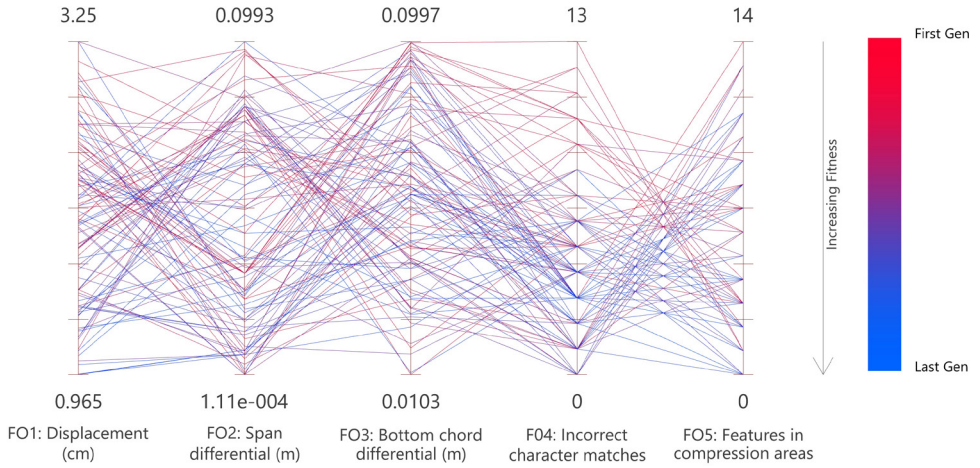

Figure 5.35 Solutions remaining after bottom chord differential assessment

respectively, correlating to an acceptable range considering the previously established material tolerances.

5.3.3.5 Board Character Matching

The material discretisation process (see Section 5.3.1) classified boards based on their suitability for placement within compression, tension, or hybrid load scenarios. Established as a Fitness Objective, the MOEA optimised towards eliminating instances of incorrectly placed boards, based on the internal axial stress present within each truss segment. A character matching filter was established that accommodated up to two boards to be incorrectly placed within a given solution (see Figure 5.36).

Although the number of mismatched boards would ideally be zero, it is evident at this stage of the global selection process that further reduction of this threshold would adversely impact the capacity of FO5 to consider optimised solutions. A mismatch threshold of two was considered appropriate, as it was unlikely to impact the structural integrity of the truss overall, when considered as a system.

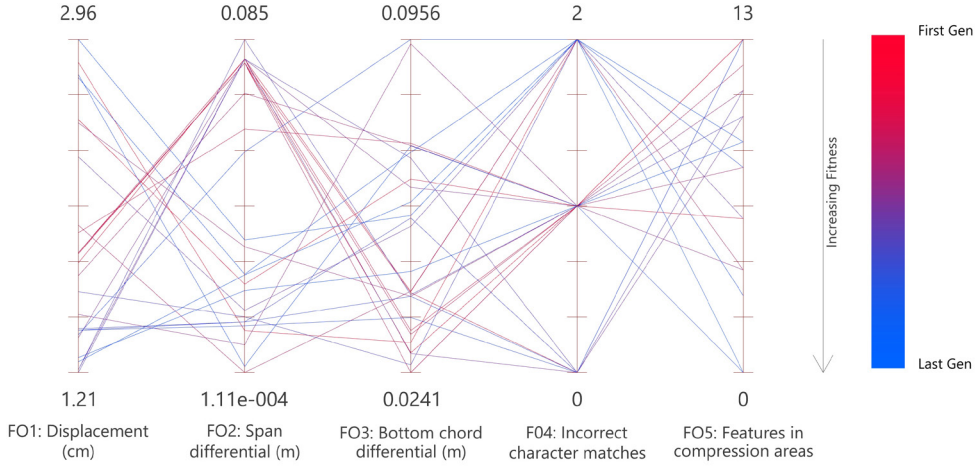

Figure 5.36 Solutions remaining after material character match assessment

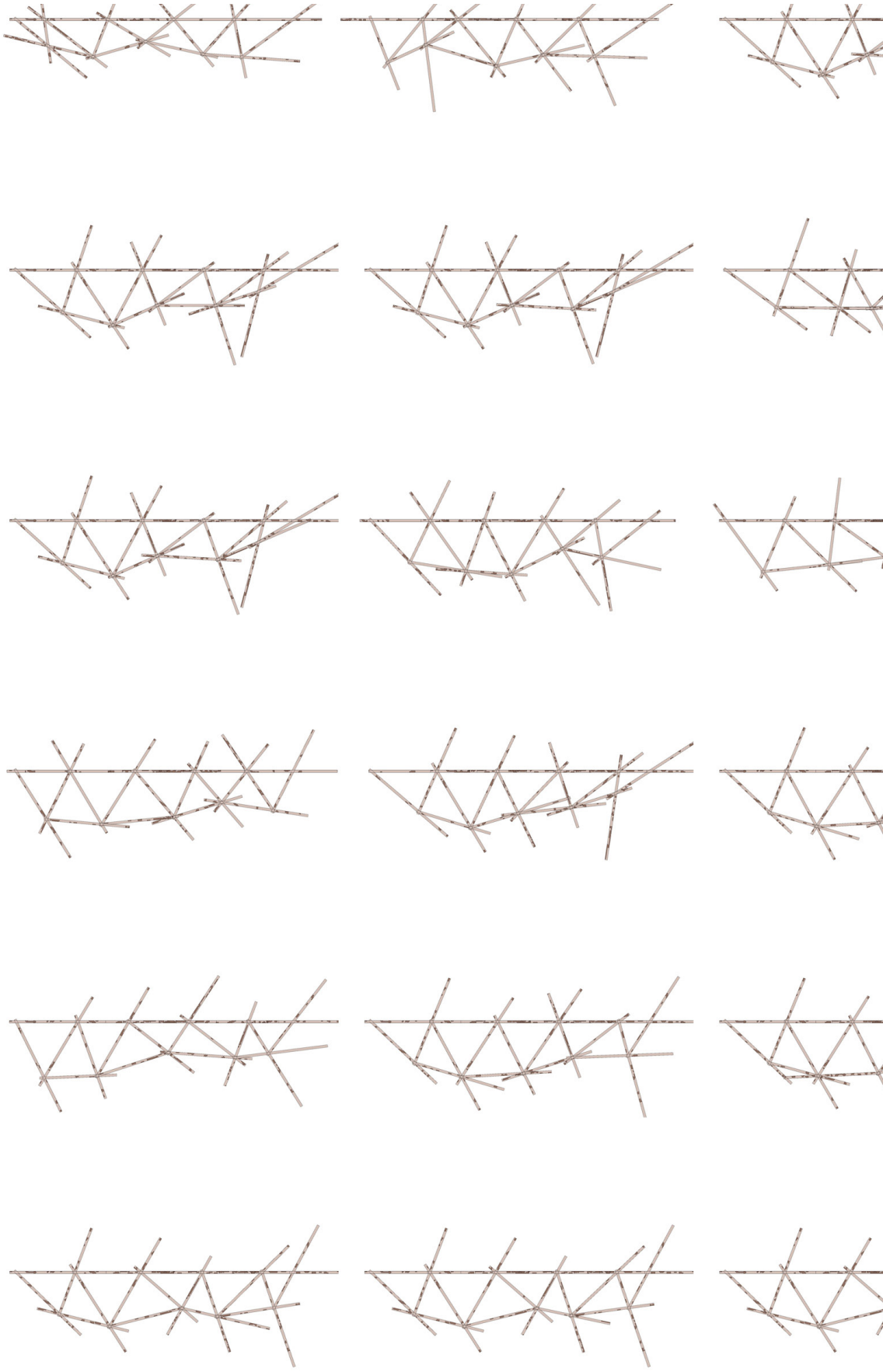

Figure 5.37 Geometric manifestation of 29 solutions remaining after implementation of five levels of selection filtering

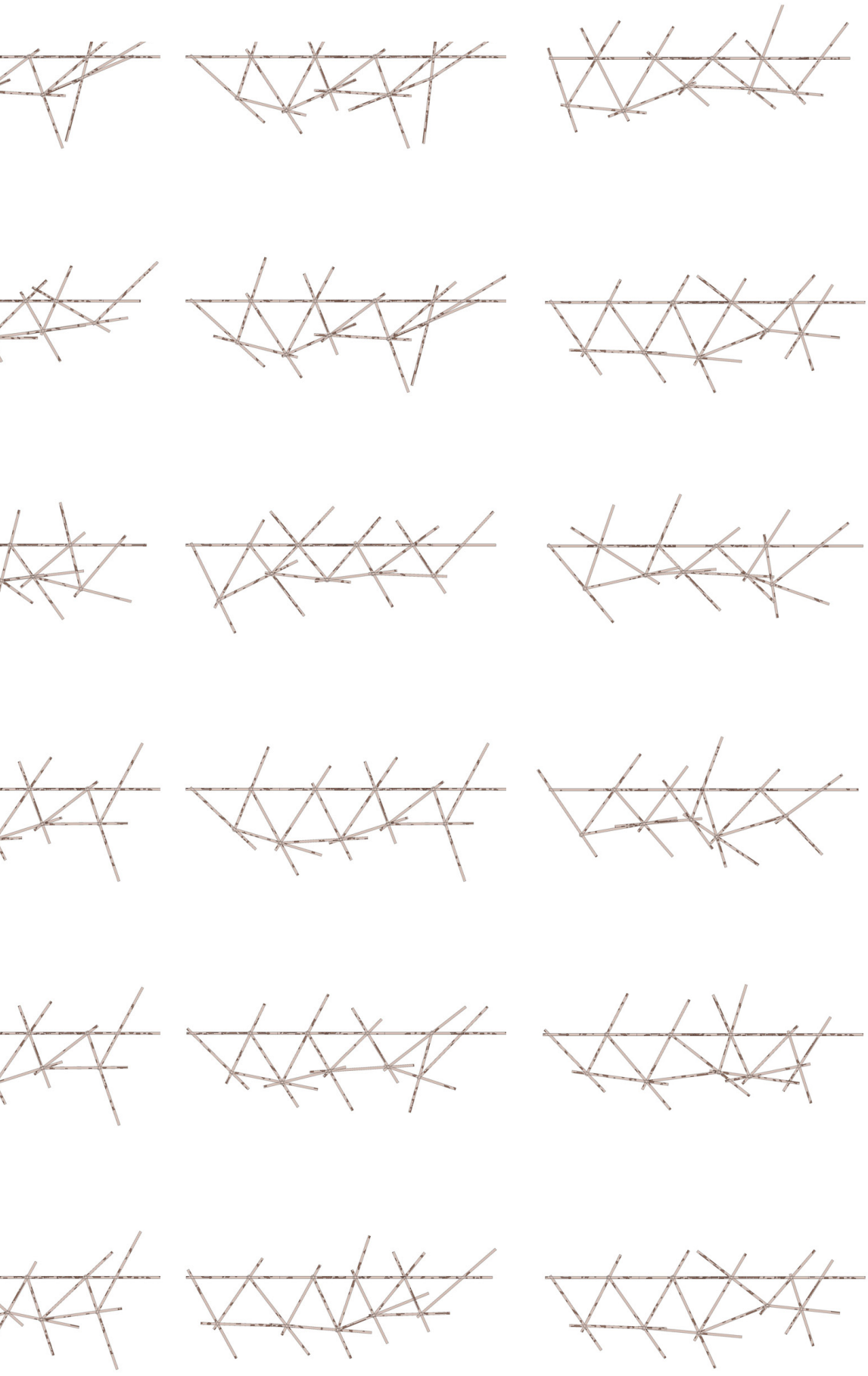

Further, FO4 was interlinked with FO5, as it sought to remove material features from critical compression zones within the truss. Considering this, a mismatched board at FO4 was likely to eliminate solutions that would be deemed invalid when assessed against F05.

A viable alternate solution in a production environment would be to simply replace the mismatched board with a different board from the inventory, if it met the character classification and connection length specification. Setting the filtering threshold to two resulted in 29 solutions being passed to the last objective filtering stage. The geometric manifestation of these truss solutions is illustrated in Figure 5.37.

5.3.3.6 Material Features in Compression Zones

The final objective selection filter considered the distribution of material features located within compression-active truss segments. To ensure that valid truss solutions were available after this filter, a threshold of two incorrectly distributed material features within compression segments was specified. This tolerance allowed the reconciliation of misplaced features to be undertaken in the visual interrogation (see Section 5.3.3.7).

Using this threshold value resulted in two solutions in which there were no occurrences of material features being within compression zones (see Figure 5.38). These solutions (122;68 and 133;2) represented a balanced approach to obtaining an optimised result for FO5. It was evident from Figure 5.39 that a single valid solution could not be selected at this stage, due to the variation found in FO3 and FO4. As there were no remaining

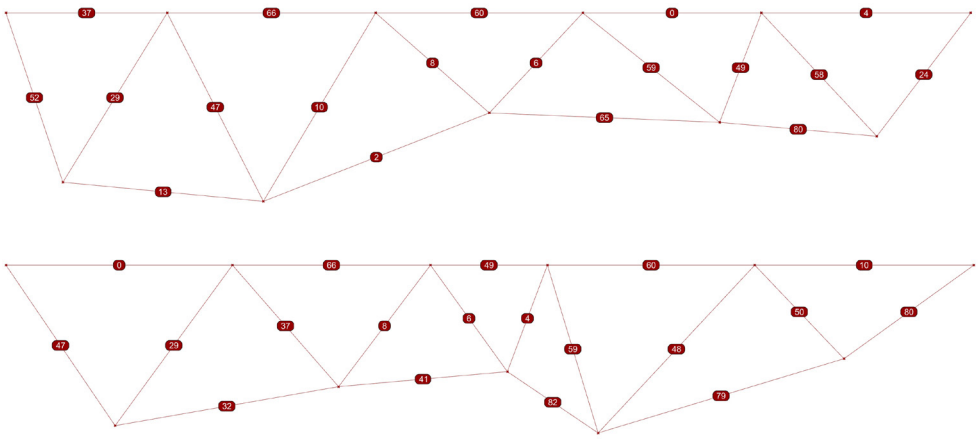

Figure 5.38 Geometric representation of truss solutions 122;68 (above) and 133;02 (below)

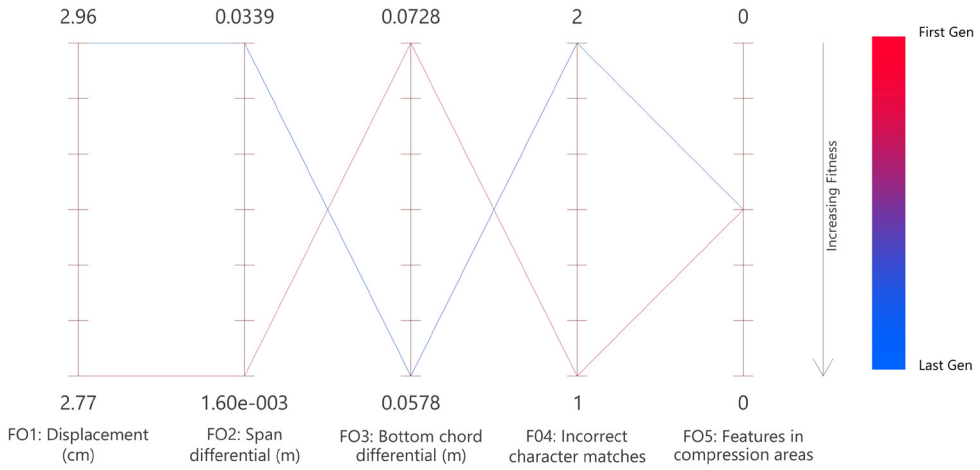

Figure 5.39 Solutions remaining after assessment of features within compression sensitive truss segments

Fitness Objectives to assess, a final subjective assessment was required to differentiate between the two options.

5.3.3.7 Subjective Assessment and Results

The selection filters within the workflow discussed thus far in this Chapter applied objective-based analysis of the solution set, in that they were based on numerical validation of datasets. The final selection method applied the use of a subjective filter that required the designer to interrogate the remaining solutions and specify which solution presented the best overall result and geometry characteristics. The Fitness Objective values of the remaining solutions are detailed in Table 5.10.

It is evident that both solutions presented a set of optimised results that

Fitness Objective	Solution 122;68	Solution 133;02
1: Displacement (cm)	2.772828	2.957646
2: Span differential (mm)	1.601	33.865
3: Bottom chord differential (mm)	72.788	57.807
4: Incorrect character matches	1	2
5: Features in compression zones	0	0

Table 5.10 Fitness objective values of remaining truss iterations

were very closely matched when considering the primary displacement objective, particularly as both results were within the permitted range set by the relevant Australian Standards (see Section 5.3.2.3 and Section 5.3.3.2).

Truss solution 122;68 offered a higher level of optimisation, in terms of the span differential, and a marginally stronger optimisation of material placement, as depicted by FO4 and FO5. Additionally, from a visual

perspective, truss solution 122;68 presented a comparatively higher level of regularity in its segment configuration (see Figure 5.40).

On the other hand, solution 133;02 exhibited a 1.737m truss depth in comparison with 1.951m in solution 122;68. Similarly, solution 133;02 had a greater material efficiency, using nominally 34.989lm of timber, compared with 36.373lm.

While both solutions offered extremely close results across their Fitness Objectives, the truss presented by solution 122;68 was ultimately selected for further investigation, due to its higher level of optimisation in displacement represented by FO1, a closer match to the span objective represented in FO2, and a higher level of optimised material placement, as seen with FO4 and FO5.

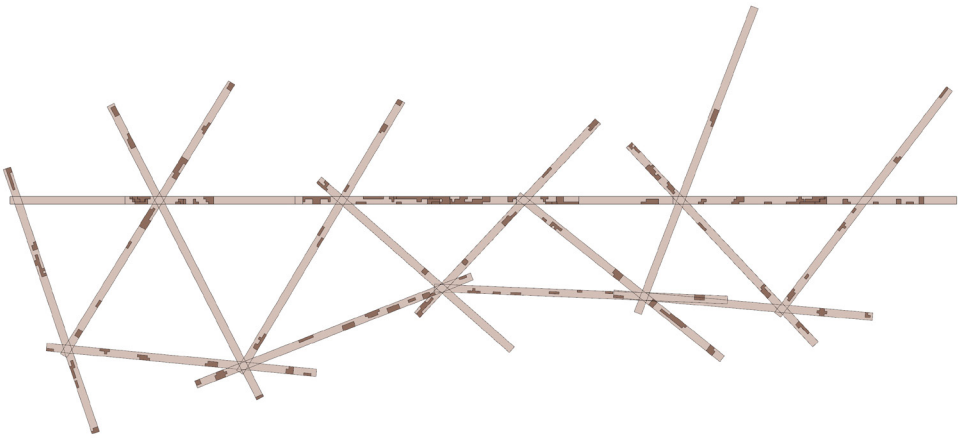

Figure 5.40 Geometric representation of truss solution 122;68 to be considered for material recovery and fabrication

5.3.4 Stage 4: Material Recovery and Inventory Consolidation

Stage 3 of the computational workflow marked the end of the evolutionary approach to material specific truss generation in the experiment; however, in industry it is uncommon for a single truss to be generated in isolation, as they are usually part of larger structural system. While the MOEA discussed in Stage 3 has potential scope to be expanded to accommodate multiple trusses, its capacity to distribute material efficiently would be hindered by the diminishing volume of elements within the constrained material inventory.

Potentially, this could be resolved by significantly increasing the volume of material inventory available for consideration; however, this would require designers and fabricators to have vast quantities of catalogued material in storage, available at any time. While this could be resolved more broadly within industry through a digitally connected supply chain that allows for material stock to be decentralised, the design experimentation within

this study had a prescribed material stock available and working within the constraints of this inventory allowed methods to be explored that maximised material utilisation.

Second, the MOEA workflow did not consider the recovery of material produced from board offcuts after a truss had been generated. Each board within a truss was cut to length as a part of the fabrication process (see Figure 5.39), leaving an off cut with potential viability for reuse. The re-introduction of these offcuts into the material inventory could not occur in a currently active algorithmic process.

As discussed in Stage 2 (see Section 5.3.2), the size of the gene pool or the number of Fitness Objectives within the MOEA could not be varied while the algorithm was running: both the material inventory and the number of trusses were required to be pre-determined before the MOEA processes. As such, material recovery and inventory re-introduction must occur *after* the MOEA selection processes is complete and *prior* to the next truss being calculated. Subsequently, an additional workflow was required undertake this process, as described in Section 5.3.4.1.

5.3.4.1 Offcut Generation

The generation of offcuts was processed by removing the portion of each distributed board that correlated to the corresponding truss segment, as prescribed by the geometric relationship of the connection points. This process could utilise a truss's geometric representation (see Figure 5.39), after it had been processed for fabrication (see Section 5.3.5). However, the likelihood of the complexity (of undertaking the required geometric transformations in this arrangement) to generate waste is increased significantly. It also coupled the waste recovery and generation of additional trusses with a successful fabrication process, creating a 'bottle neck' in the overall digital workflow.

The alternative option for waste recovery was to implement it in association with the constrained material inventory. Two benefits arose from this arrangement.

a) The calculations were undertaken on simpler geometric dataset; and

b) It increased the ease of reintroducing recovered material into the inventory.

The data required to calculate material recovery comprised the ID of each board used in the truss, and their corresponding connections points (Point

A and Point B). This data was encoded as numerical values and, as such, is more easily inserted into the waste recovery workflow.

This data was then used to extract the relevant boards form the material inventory and position the connection points in relation to the corresponding segment length (Figure 5.41). This allowed the generation of an overlay (indicated as a black outlined rectangle) that showed the extent of the web segment requirements in relation to the overall board. The overlay incorporated a buffer of 100mm beyond each connection point, ensuring that material required for physical overlap in fabrication and assembly was accommodated. The resulting material available for recovery sat outside of usage overlay. Of the 19 boards used, 30 offcuts were generated, ranging in length from 124mm to 2353mm.

Each of the available offcuts were interrogated to test their length against a minimum threshold of 1200mm. While the threshold length was adaptable to suit different material scenarios, a length of 1200mm was specified for two reasons.

a) It represented a board length that had a higher suitability for future trusses.

b) Increased potential for valid connection points to be found above the set threshold.

Offcuts found to be shorter than the threshold were deemed unsuitable for reintroduction into the material inventory. While considered a waste

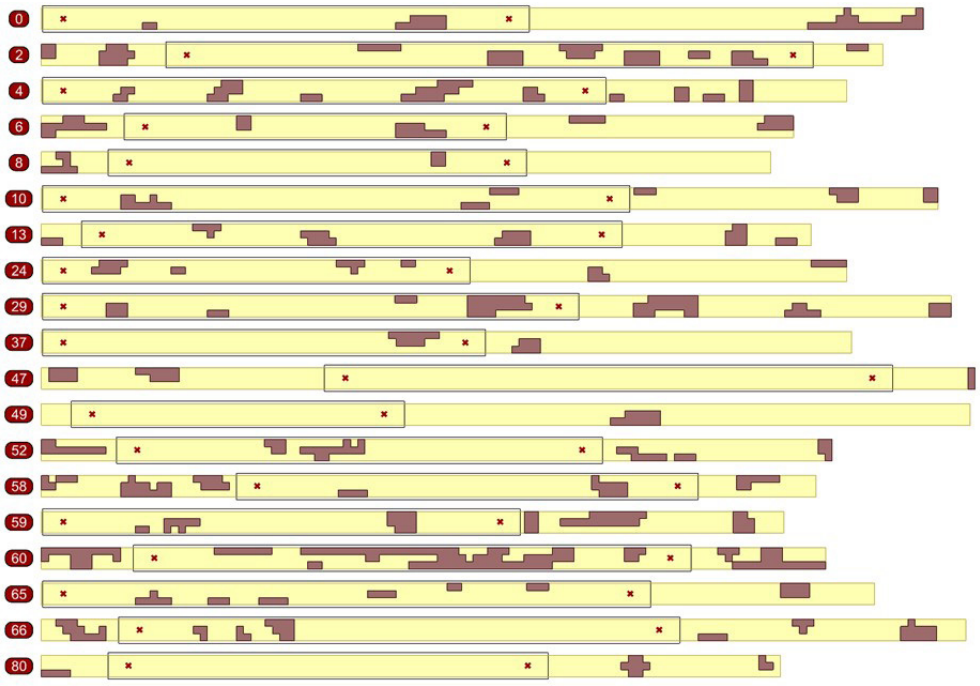

Figure 5.41 Overlay of connection points and board utilisation within truss solution 122;68

by-product, many applications in industry currently exist that repurpose this type of material (Taylor et al., 2005; Taylor & Warnken, 2008).

In different scenarios, the threshold value could be altered to suit varying reuse conditions. If the material being used had less naturally occurring features, shorter offcuts would have a higher potential for containing valid connection points. Likewise, the design requirements of subsequent trusses would vary, potentially equating to small span requirements and varying load conditions. These design changes suggest that shallower trusses and shorter board segments would be more desirable.

Each of the viable offcuts was required to have a unique identification tag assigned to it as they were being re-introduced to the material inventory. Duplication of the origin board ID was an unsuitable option as there was potential for the generation of multiple offcuts from a single board. Consequently, new offcuts were numbered sequentially, commencing from the highest numbered existing board in the inventory.

5.3.4.2 Results

Of the nineteen boards interrogated from the selected truss solution, six offcuts were found to be viable. These recovered offcuts equate to 9.9lm with an average of 1.65lm, which represented a recovery yield of 38.9%. Each of the offcuts was indexed from 84-89 and re-introduced into the constrained inventory for the next truss generation. Thereafter, the material inventory comprised 68 elements (inclusive of the new offcuts) from an original 81 at the commencement of the experiment.

To ensure that subsequent truss MOEA processes were considering the re-introduced offcuts as viable elements a validation was required. The validation process consisted of re-running the truss MOEA workflow with the new material inventory, allowing the generation of a new population of truss solutions. For consistency, the same 10m span goal was employed, and all MOEA settings and selection filters were also replicated. The workflow determined 1,408 trusses to be unique within its solution pool.

Further investigation revealed that of these solutions 464 contained at least one segment within the truss configuration that correlated to a reclaimed offcut from the inventory; however, after running the pool of unique solutions through the selection filters (see Section 5.3.3), only one solution was found to be within the specified range. Truss solution 133;51 (see Figure 5.42) was found to have a displacement of 22mm. This solution

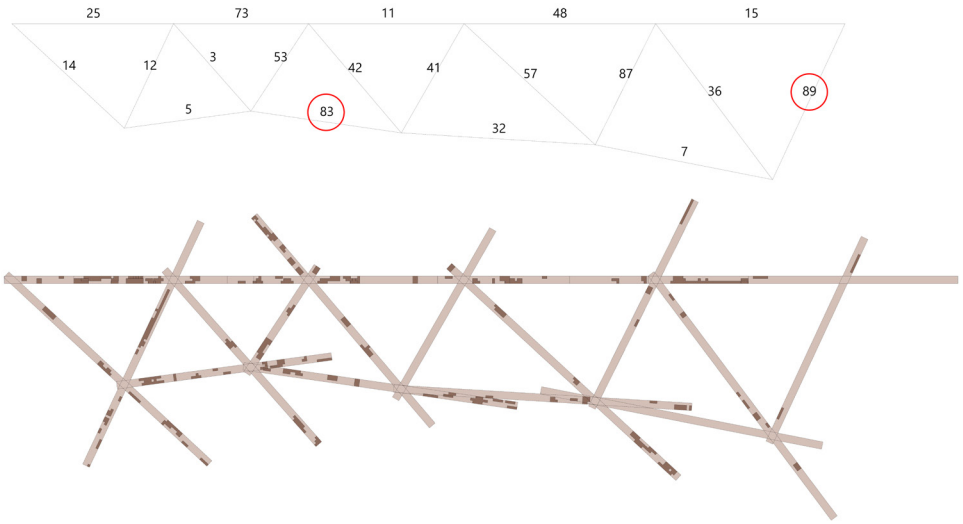

Figure 5.42 Geometric representation of truss 2 solution 133;51, geometric representation (top), and board representation (bottom)

contained two reclaimed offcuts from the inventory (elements 83 and 89), both of which were allocated to web diagonal segments.

The material recovery method was applied to the validation truss (solution 133;51) and resulted in four offcuts being deemed viable. These were reintroduced to the material inventory as boards 90-93, respectively, after which material inventory comprised 53 boards, of which 44 originated from the initial inventory and nine were reclaimed offcuts.

A second validation truss simulation was generated to observe how the MOEA would perform when in a scenario where the material inventory became smaller and contained a larger selection of reclaimed boards to be considered for distribution.

The third truss validation generated 1,862 unique solutions, 960 of which were within the structural displacement threshold. Solution 119;05 was found to have the highest-ranking displacement value of 11mm; however, after processing the solutions with the selection filters, there were no solutions that met the specified selection filter criteria. All solutions either had, or had a combination of, FO2 and FO3 differentials that were too large, or had too many F03 and F04 material character and material feature placement results.

Although the utilisation of reclaimed offcuts was observed to be immediate, there was a significant condition that influenced this, which should be noted. After each truss was generated, the pool of original full-length boards decreased, while the number of reclaimed offcuts increased. The first validation truss had approximately 60 original boards to distribute from; however, the third truss had nominally 50 to choose from, and so on,

until a point was reached where there were no original boards remaining in the inventory.

It was also evident that the inventory had become exhausted after a given set of trusses were generated. To address this issue, the material inventory would need to be re-populated with new, discretised full-length boards to generate more trusses, due to a more wider population of boards from which to select.

5.3.5 Stage 5: Physical Demonstrator

The methods developed within this experiment were intended to situate the design workflow at the intersection of the constrained material inventory, truss generation and fabrication. As opposed to the experiment detailed in Chapter 4 (where fabrication was necessary to visualise the design outcome of the workflow), the truss solutions generated in Chapter 5 could be visualised digitally. This was enabled by a combination of three factors:

c) a simpler geometric and material distribution outcome of the MOEA;

d) the use of whole timber boards, rather than small segment; and

e) a discretisation resolution that presented coarser material representation.

However, as the translation to physical object was embedded within a fully integrated computation workflow, a physical realisation of the workflow was required to demonstrate that its capacity could be implemented within an industry environment.

Within the scope of this study, the objective of a physical demonstrator was not intended to realise fully engineered solutions; rather, it facilitated the realisation of a digital workflow within a physical environment that interlinks material irregularities with physical material outcomes. As such, the workflow detailed in Section 5.3.5 focuses on the processes in preparing a truss for physical demonstration that considers material irregularities as a primary part of the fabrication process, in addition to

employing 5-axis CNC sawing as the primary mode of fabrication. The computational workflow developed is discussed following in three parts.

1. Truss detailing
2. Geometry processing
3. Fabrication process

5.3.5.1 Truss Detailing

Within the Australian construction industry (at the time of writing), a common method of connecting timber elements within a truss is the use of a metal nail plate. This connection system allows for fast and efficient pre-fabrication methods, which reduce the complexity of timber carpentry required at each of the truss connection vertices. The nail plates also act as gussets, allowing the transfer of structural loads to be effectively distributed across the whole system. While they provide a highly optimised solution for trusses that employ regular geometries and lineal span directionality, their application in complex, irregular and three-dimensional truss configurations is limited. Further, given their utilitarian approach to connection detailing, gang-nail connected trusses are typically unsuitable for applications where the truss is exposed, or the visual quality of the truss is critical.

In shifting the truss generation and fabrication within this experiment towards a custom design/fabricator, the machinery and equipment used to affix nail plates to timber are not available. Without this equipment, the connection of a planar geometric arrangement of multiple timber elements at an intersection node, is increasingly difficult to execute effectively. Additionally, the geometric irregularity of the trusses generated within Stage 2 and Stage 3 establish scenarios in which other traditional methods of timber fixing were not viable options.

Many examples of solid connections (based on traditional notions of timber carpentry) are employed in contemporary complex geometric arrangements (Ahmadian, 2020; Amtsberg et al., 2022; Baber et al., 2020; González Böhme et al., 2017; Søndergaard et al., 2016; Svilans et al., 2017). These methods commonly utilise digital fabrication processes that

generate complex three dimensionally-unique joints across an irregular geometric system. The requirement for this complexity is twofold:

- it allows capacity to negotiate the physical geometric conditions at each connection node; and
- it increases the contact surface area between elements, allowing for improved equalisation of forces within a structure, and adequate space for secondary mechanical fixing methods.

However, these connection types result in longer fabrication times due to the material removal methods required. Additionally, the three-dimensional complexity of the element and joints has a significant impact on the assembly logistics of the truss. The requirement for unique joints across irregular geometric systems often necessitates the implementation of robotic modes of fabrication and assembly, resulting in workflows that are not yet applicable to common industry capacities.

The trusses generated in this experiment are two dimensionally planar in their base topology. As such, the geometric complexity afforded by robotic fabrication and assembly methods are beyond the requirements of this experiment. Accordingly, an alternative material arrangement and connection method was sought that enabled consistent detailing of a wide range of two-dimensional geometric scenarios presented by irregular truss structures. The selected method had two objectives:

1. it ensures face-to-face material connections were available, and
2. it positions the truss segments in a close to planar arrangement.

Face-to-face connections of timber elements within a truss offer several advantages within the scope of this experiment. By arranging elements in this manner, the capacity for simple mechanical fixings options including screws or nails is increased. As each truss element is required to be docked to length at the required angle and positioned correctly, the developed workflow can be easily integrated within an automated production process. Additionally, this method removes time consuming CNC machining operations associated with the complex removal of solid timber through subtractive processes Apolinarska (2018). However, as face-to-face connections necessitate the layering of timber elements within the configuration, the physical width of the truss is increased, becoming detrimental to its performance.

A planar arrangement of elements ensures that forces can be distributed vertically within the truss, minimising opportunity for lateral or rotational deformation to occur when placed under load. The staggering of elements required by face-to-face connections is contrary to this condition, as it

widens the truss to accommodate overlap between elements. To counter this, the positioning of elements within the top and bottom chords, in addition to the diagonal segments, were located centrally around a vertical plane (Figure 5.43). The staggering of diagonal segments is intended to balance the transfer of loads evenly to either side of the central plane, reducing opportunity for lateral twisting.

It was apparent that the staggering of elements within the top and bottom chords, along with the diagonal segments, resulted in the width of the truss increasing significantly. With four layers of elements, a truss width of 140mm was generated. For a single truss, this thickness was undesirable as it prevented the use of common mechanical fasteners and required a staged assembly process. For this reason, a lapped shoulder joint was applied (see Figure 5.44).

This configuration presents four advantages.

a) It reduces the overall with of the truss, promoting a greater planarity of elements.

b) It provides adaptability to a greater range of irregular truss geometries.

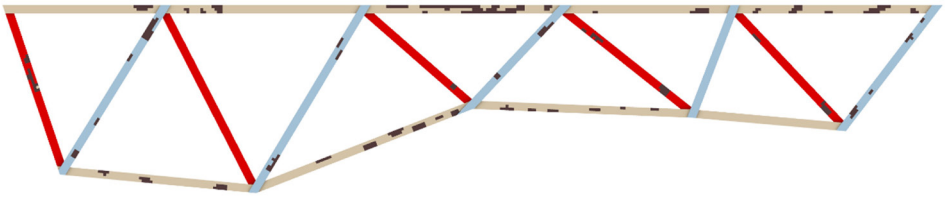

Figure 5.43 Staggering of truss web diagonals to minimise thickness. Blue elements are on front face of top and bottom chords, red elements are positioned at the rear

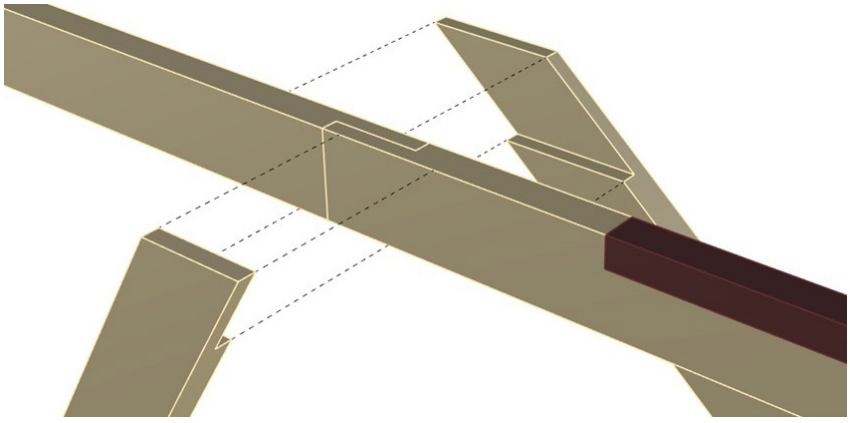

Figure 5.44 Assembly logic of top chord intersection with web truss diagonals

c) It accommodates the use of shorter standard fixings.

d) It allows for greater overlap of elements within the joint configuration.

This process has two disadvantages.

a) As each truss segment requires four cuts rather than two, there is a slight increase in fabrication time.

b) It increases the complexity of assembly, as segments need to be stacked on top of each other prior to fixing.

5.3.5.2 Fabrication Process

The truss solution selected for fabrication was 10m long, 2.1m deep and contained 18 board segments. The size presented logistical complications, as a physical space large enough was not available for the assembly of fabricated elements. It was subsequently decided that a portion of the truss would be fabricated, offering a partial representation of the digital solution. Eight elements were fabricated and assembled, providing a 3.8x 1.9m truss portion.

The fabrication workflow developed for the truss elements employed the SCM Accord 40 5-axis CNC router (as used in *Design Prototype 1: Acousti-Sim* – see Section 4.3.5). However, the fabrication parameters in this experiment differed substantially from those employed *Design Prototype 1*. In *Design Prototype 1,* 3-axis curve-based machining was utilised, requiring the translation of three-dimensional fabrication geometry to be processed within VisualCAM, a third-party CAM platform situated between the digital design files and the CNC g-code. In this method, the generated g-code was not natively generated, requiring several manual adjustments to the CNC configuration prior to fabrication.

While this was an acceptable solution in a scenario where an individual file was associated with single panel with longer fabrication times, it was not suitable for a workflow that required multiple processes to be undertaken on a series of unique parts with significantly shorter fabrication times. As such, a more immediate geometry to fabrication translation was sought.

The SCM router had close integration with its proprietary CAM platform Maestro (SCM Group, 2022). As discussed in Section 4.3.5, the platform provided considerable flexibility implementing fabrication workflow management; however, its unintuitive control interface is often restrictive to the generation of complex fabricated outcomes. Nevertheless, its

capacity to natively generate 5-axis g-code for a circular blade cutting tool offered a significant advantage within the context of this experiment.

The fabrication of each element in the truss was limited to the ends of each board, planar in nature and had a maximum 90mm depth of cut. These conditions were well matched to the 350mm diameter blade available. As a result, test cuts showed that a circular blade produced an average 76% faster fabrication time, in comparison with router based cutting tools.

The programming of the circular blade within Maestro required the provision of two-dimensional curve geometry that correlated to the specification of each truss element. While this seemed contrary to the geometric complexity available within the design model, the specification of tool path strategies was set through a series of parameters within Maestro. Subsequently, this necessitated the extraction of core two-dimensional geometry for each truss element from the digital design model. The translation extracted five sets of geometry for each of the truss elements.

1. Board outline.
2. Board ID.
3. End docking angles and location.
4. Shoulder angles and location.
5. Fixing location.

The board outline and ID were obtained from the original discretisation dataset detailed in Section 5.3.1. They were re-oriented onto the origin of the XY-coordinate plane, and subsequently used as a basis for all geometry transfers. End docking angles and locations were transcribed from the external intersections of truss segments. Similarly, shoulder angles and locations were translated from the internal intersections. Finally, fixing locations were generated from the average centre point of the segment overlap at each truss node.

Each set of geometry was placed on an individual layer that translated to a 'toolpath technology' within Maestro which allowed for the automated generation of 5-axis tool paths. This was the batch processed for each truss segment, with a corresponding DXF file being generated for each element. The layer-based geometry separation correlated to a different 'toolpath

technology' that specified varying machining configurations which were classified as:

- fixing location;
- end docking; and
- shoulder removal.

A fixing location was specified at each end of the boards used within the truss. They were located at the centralised point of overlap between truss segments at each connection node (see Figure 5.45). The mechanical fixing was specified as a M10 bolt at each node, requiring a 12mm clearance hole to be created in accordance with *AS1720.1: Design Methods for Timber Structures* (Standards Australia, 2015). The clearance hole was created using a 12mm diameter drill tool.

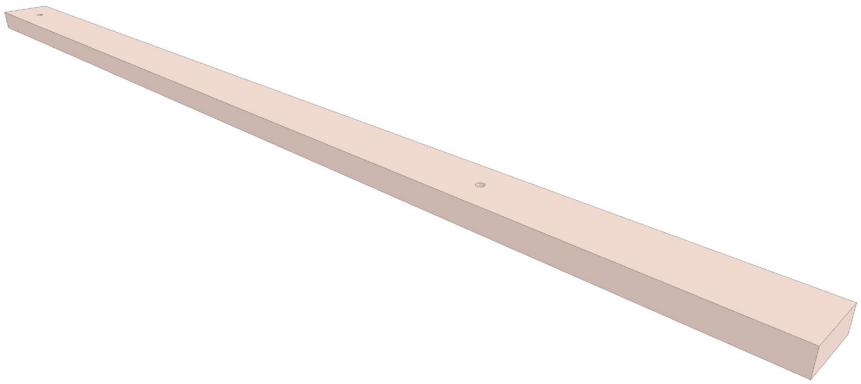

Figure 5.45 Drilling 12mm clearance holes for M10 blot fixing

The end docking of each of truss segment was the first saw blade operation undertaken. This ensured subsequent machine processes would be within the depth range permitted by the saw blade tool (see Figure 5.46). The directionality of curve geometry was normalised to the anti-clockwise guaranteeing consistent placement of toolpaths when compensating for the blade thickness. The toolpath was positioned on the left-hand side of the curve geometry (relative to the start and end points of each curve) specifying that the cut would occur on the 'outside' of the desired board.

The depth of cut was specified within Maestro as 38mm, equating to an additional 3mm beyond the thickness of the timber boards (35mm). While additional depth of cut is common in through-cuts, it was particularly important in this scenario, as it minimised any errors relating to natural board deformation. Finally, a lead-in and lead-out distance of 150mm was

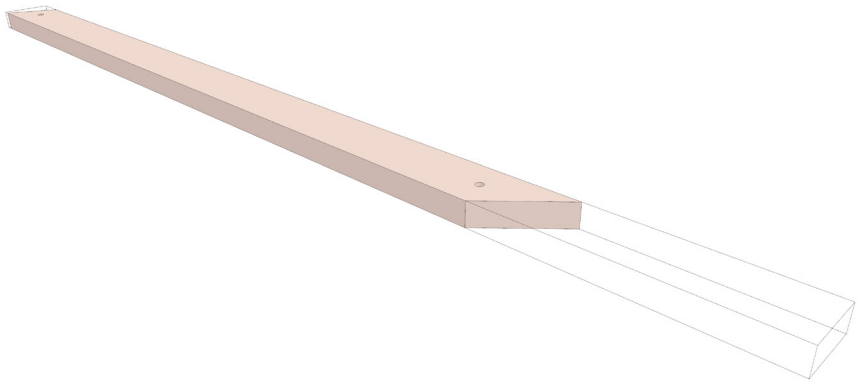

Figure 5.46 Docking of board to required length at specified angle

specified, ensuring that the saw blade would be clear of the remaining material while not directly cutting.

The shoulder removal was specified as a two-part process using the saw blade. The first operation specified the angle and location of the shoulder, with the depth being specified as half of the material thickness. This established the control plane for the 5-axis process of removing the shoulder material. Saw blade operations within Maestro require a control plane for orientation perpendicular to the cutting plane, which was provided by the shoulder location cut (see Figure 5.47). As with the docking cuts, lead in and out dimensions were specified to ensure the saw blade completely disengaged the material prior to undertaking further traversing moves. Figure 5.48 illustrates a sample cut of the two-stage shoulder machining.

With each truss segment correlating to an individual board form the constrained inventory (in addition to unique geometry and machining requirements) the material hold down strategy accordingly was different for each element. Rather than utilising the table-based vacuum previously

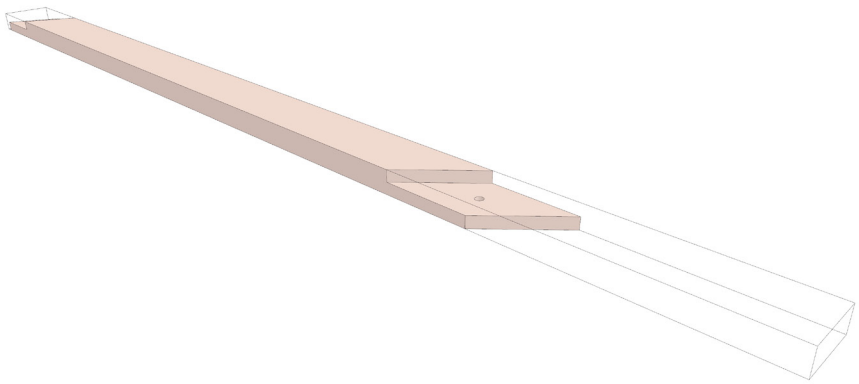

Figure 5.47 Rebating connection shoulder at each end of board

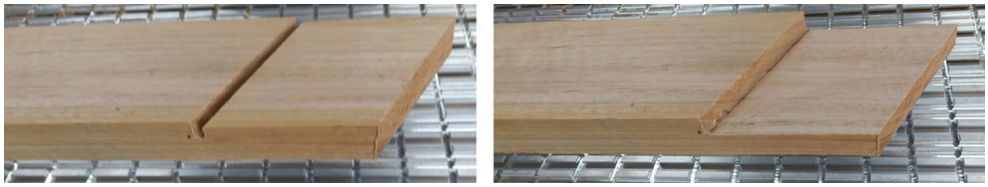

Figure 5.48 Demonstration of shoulder cut stages

used in Section 3.4 and Section 4.3.5, pneumatic clamps were employed to accommodate the clearances required by the 5-axis machining operations.

Subsequently, the pneumatic clamps were required to be re-positioned for each board to ensure that the generated saw blade toolpaths would always be clear of the hold down clamps (see Figure 5.49). This process was somewhat automated by Maestro with the pneumatic clamps being positioned digitally once the toolpaths had been generated. This inserted an additional machine operation within the fabrication processes that used a laser pointer to indicate where the pneumatic clamps were required to be located to eliminate collisions. The pneumatic pneumatic clamp relocation process added considerable manual set for each board; however, it was unavoidable due to the irregular nature of the truss geometry generated.

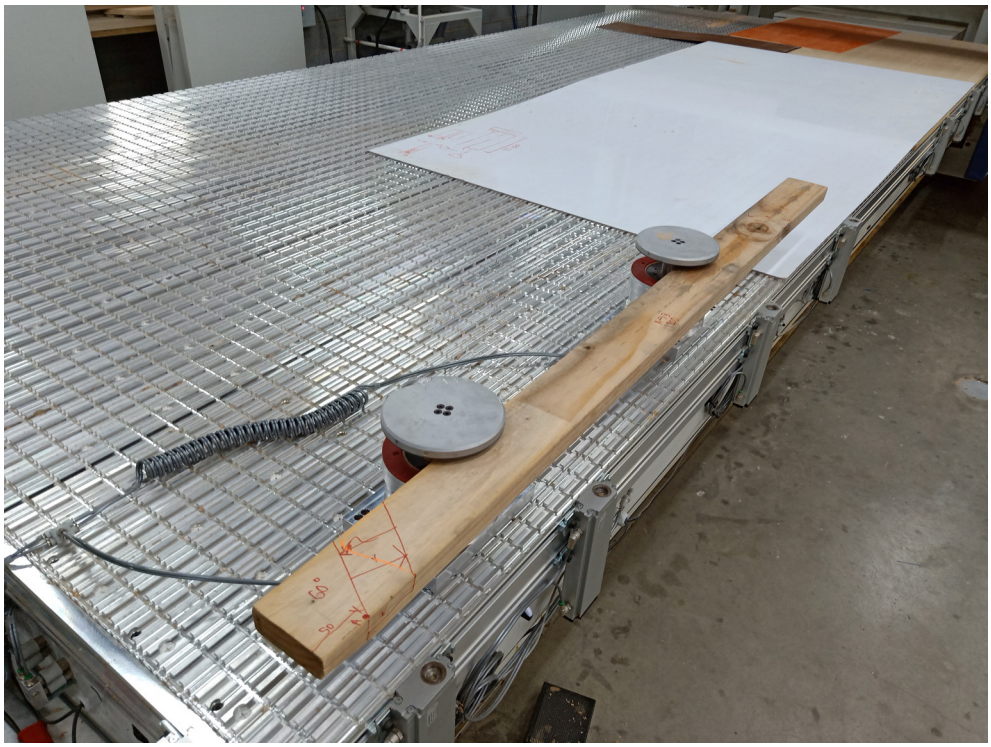

Figure 5.49 Pneumatic clamp arrangement in place for fabrication

5.3.5.3 Results

The eight fabricated segments took a total of 23 minutes 36 seconds to process. On average, the machine time was 72 seconds per board, totalling 9 minutes 36 seconds. The remaining 14 minutes was required to change

the boards over and reposition the clamps after each machining operation, averaging 1 minutes 45 seconds per cycle. While this represented a significant portion of the total fabrication time, there is potential for this to be reduced in an industrial context where more sophisticated CNC machining equipment would be available, in the mass-timber industry.

As the bolt fixing location was encoded within the fabrication workflow, the assembly of truss segments was expected to be a sequential process with the positioning and alignment being embodied within the segments. However, due to an export error from Maestro, the clearance holes that were intended as alignment locations were not processed within the CNC g-code. This issue was not discovered until all parts had been fabricated, removing the opportunity to re-process the files and re-machine the missing holes. As a result, the correct alignment of parts in the assembly process was required to be undertaken manually and a 14-gauge batten screw was used as a fixing alternative, as shown in Figure 5.50.

Figure 5.50 Alternate fixing method at intersection nodes

Despite the alignment points being absent, the positioning of boards in their correct location within the truss proceeded successfully. The precision of machining operations provided each element with a reference angle that correlated with its unique connection condition to other adjoining truss segments. In conjunction with the truss being assembled in a linear manner (that is, left to right), this ensured that each segment could only be positioned and aligned in one location (see Figure 5.51). This embedded

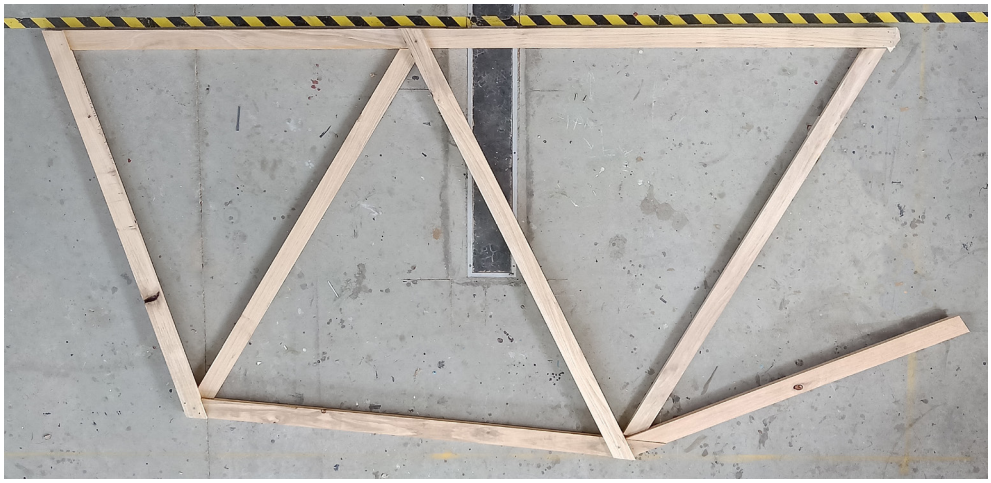

Figure 5.51 Truss layout during assembly process

fail-safe was critical in establishing a fabrication and assembly workflow that allowed the engagement of geometrically irregular trusses.

The assembly of the truss was validated against the digital design model by measuring the planar triangulation of each truss segment within the physical demonstrator and comparing it against the matching triangulation within digital model. It was found that a 7mm discrepancy emerged between the digital and physical representations, with the demonstrator being slightly larger than intended. While this may have been caused by the manual alignment process, there was potential for a minor discrepancy to be present in a workflow that was fabricated correctly. This was due to a 12mm clearance hole being intended for a 10mm bolt at each connection node. The resulting 2mm of play at each node, extrapolated across the entire geometry, would have resulted in a discrepancy of up to ±8mm across the selected truss solution, given its geometric configuration and number of connection nodes.

5.4 Discussion

The experiment detailed in this chapter developed a multi-scalar approach to material engagement, offering a discrete design, material placement, optimisation and fabrication workflow, which is responsive to irregular geometric structural arrangements. It considered the intrinsic character of a constrained material inventory and sought to maximise the opportunity for its utilisation, without defaulting to a standardisation scenario in which irregular material is homogenised into predictable elements. As such, the capacity of the workflow's scalability, in relation to the number of trusses generated, and the specific requirements of varied design problems is constrained only by the material inventory that is made available to it.

It considers the application of the material inventory, as whole timber boards, complete with irregular features and characteristics. Critical to the

success of the experiment was the leveraging of the inventory discretisation at a higher resolution than explored in *Prototype 1*, which revealed new material potentials within a structural system. The classification of the irregularity of feature scale, location and significance within each individual timber board necessitated a MOEA workflow that was directly influenced by the intrinsic nature of each individual board, subsequently generating design solutions, which were a direct result of the material available within the constrained inventory.

The MOEA application and selection method workflows are unique to this experiment for three reasons.

The first relates to the treatment of 'Null' solutions within the MOEA design problem. Within each iteration of the MOEA simulation, multiple scenarios exist that warrant an instance as being deemed invalid. In addition to the 5,000 valid solutions the MOEA generated 22,200 'Null' solutions, the majority of which were geometrical invalid truss configurations. While this increased the computation time for the simulation to execute, it had significant impact on the quality of generated outcomes. As 'Null' solutions are disregarded by the MOEA, they do not influence the generational progression of the simulation; in turn, ensuring that only valid solutions could contribute to the strengthening of the generated solutions. In essence, the 'Null 'solution pool is utilised within this experiment as an embedded quality filter within the MOEA simulation.

The second unique aspect of the developed workflow is in relation to the filtered selection method applied to the valid solutions set. The Fitness Objectives specified within the MOEA comprised five criteria that were conflicting in nature, resulting in the generation of 91 Pareto solutions. While analytical methods of filtration and selection are available within Wallacei, they did not present an acceptable level of optimisation across the objectives. Subsequently, a hybrid approach to solution-selection was required that encompassed all unique solutions within the evolutionary dataset. This method comprised seven assessment criteria that filtered the lesser performing solutions from the pool, ordered according to the performance criteria significance. This approach progressively reduced the number of viable solutions using the first six criteria until two remained, prompting a final selection to be made on a subjective basis. Critically, this technique of selection reinforced the strategy of acceptable optimisation and geometric preference, affording the opportunity for material irregularity to be considered within applications that would otherwise require standardised materials and perfectly optimised performance solutions. Additionally, the selection filtering was parametrically defined, allowing the workflow to have scalable applications in larger inventories

of materials, and more complex material distributions or the generation of multiple trusses within the same workflow. This was demonstrated when recalculating the MOEA process to assess the reintegration of offcut material.

The third application of MOEA and selection methods relates to the classification of waste material from the fabrication process. The offcuts from all truss segments are classified against two interrelated criteria – physical dimension and material character. The relationship between the length of offcut and the location and distribution of material irregularities is used to establish the potential of the board to be re-entered into the material inventory for use in future trusses, with longer offcuts more likely to have connection zones that are applicable to truss geometry.

Similarly, boards with less material features provide greater variation as to how the offcut could be placed within a truss. Through the application of an adaptive threshold, the minimum length and maximum feature coverage were specified to determine the potential of an offcut for reuse within future trusses, with viable offcuts being reintroduced to the constrained material inventory. In the context of this experiment, 38.9% of material offcuts were deemed recoverable for use in future truss iterations. The adaptability and scalability of this method is critical within industry, as it potentially allows capacity for higher material recovery based on material character and future applications. A higher material recovery rate plays a vital role in reducing timber waste that would otherwise be destined for low-value applications, such as solid-fuel generation or fibre markets.

This is significant from a construction standpoint, particularly in relation to utilisation of current material resources across the industry. Within Australia, an average house utilises 14.58m³ timber, with approximately 95% of this being graded plantation softwood in the form structural framing (Forest & Wood Products Australia, 2021). Current roof truss production methods rely upon cutting larger, graded timber boards into many smaller lengths and, as such, the utilisation of shorter plantation hardwood boards is particularly suited to truss manufacture. With roof trusses accounting for nominally 37% (5.43m³) of structural framing in typical residential construction, the opportunity to substitute a estimated 108,000m3 (Forest & Wood Products Australia, 2021) off lower-value plantation hardwood in place of higher value graded softwood within new residential roof frames would see a direct impact on the consumption of softwood structural framing timber using current construction methods.

Figure 5.52 Physical demonstrator of truss fabrication

Figure 5.53 Physical workflow demonstrator overlaid with digital truss representation

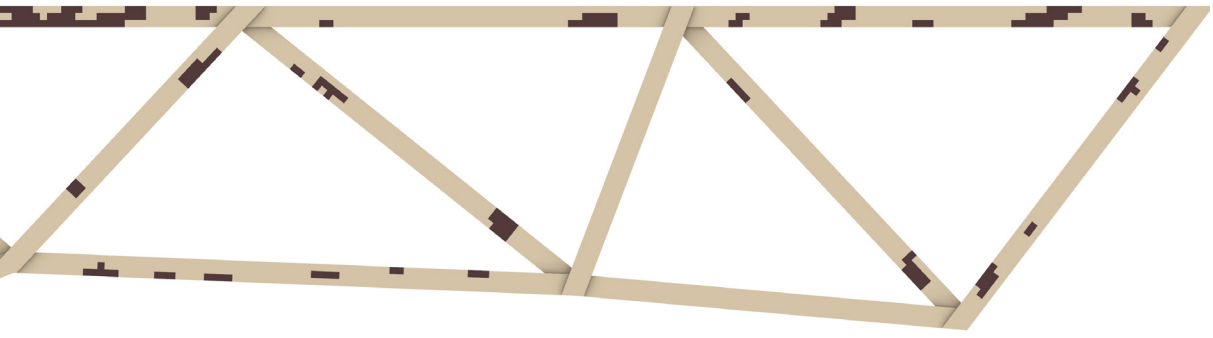

6 CONCLUSION

6.1 Introduction

This chapter concludes the thesis in six sections, including this Introduction.

Section 6.2 restates the aims of the research.

Section 6.3 addresses the research questions, proposed in Section 1.4, and outlines how the study, as expressed in this thesis, addresses each question.

Section 6.4 addresses the contributions of the research in relation to the three domains of investigation:

1. material sustainability;
2. timber as a construction medium; and
3. digitally integrated material practice.

Section 6.5 outlines the limitations of the study, and expands the opportunity for further investigation through a discussion of potential future work.

Section 6.6 provides a concluding statement to the research, positioning its impact and contribution to the future development of the construction sector.

6.2 Restatement of Research Aims

The aim of this study was to develop linkages between architectural design processes and heterogeneous materials that are currently undeveloped within the construction industry. It does this by fostering tailored methods of material engagement within digitally integrated, design-centric workflows. In doing so, it provides opportunity for fibre-managed plantation hardwood to be considered as a valid material for architectural exploration, through the incorporation of innovative methods of design, material interrogation, performance simulation and material optimisation. These methods provide opportunities for scalability within the architecture and construction sectors, by supporting higher levels of material sustainability and consumption than are currently available.

Primarily, the intention of the research was to explore innovative methods of material engagement at the point of design and fabrication, rather than within the timber industry. This establishes scenarios that can exploit the inherent characteristics of an abundant resource, currently disregarded by the forestry and construction industries. While the development of persistent data-rich supply chains from tree through to architect and fabricator would be ideal, it is unlikely to be implemented within fibre-managed plantation hardwood resources, without significant

reconsideration of the supply chain by the forestry industry, due to current logistical and economic factors.

Accordingly, the findings of this study aimed to circumvent the fragmentation of actors within the supply chain by proposing a shift in the onus of material understanding and engagement away from primary producers, by incorporating it within a design and fabrication focused environment, which results in a closer engagement with material character.

As such, this integration provides opportunities for irregular materials to become active participants within architectural design and fabrication processes, fostering greater utilisation of latent materials and a higher level of material sustainability within the construction industry, in general.

By establishing relationships between material interrogation, performance simulation, and computational optimisation within a scalable, design-centric environment, the study pushes forward the notion of material understanding and engagement, within architectural design cycles.

6.3 Answering the Research Questions

The research questions proposed in Chapter 1.4.2 are restated below, accompanied by ways in which the research findings address each one.

1. **To what extent does the intersection of material irregularity and digitally integrated design workflows establish a platform for the engagement of low-value materials within architecture?**

Both the research process and findings demonstrate that the engagement of heterogeneous material irregularities within tailored DIMPs to engage latent material resources, such as fibre-managed plantation hardwood, as valid media of architectural exploration. Three areas of current industry practice were identified as having great potential for augmentation through the adoption of a DIMP; namely, *material understanding*, *material engagement*, and *material fabrication*.

Augmentation of existing modes of *material understanding* facilitates the implementation of the data-enabled practices emerging from the adoption of Industry 4.0 across the forestry, architecture, and construction industries. Undertaking *Probe 1: RGB-D Scanning* (Section 3.3) and *Probe 2: RGB and Constrained inventories* (Section 3.3) demonstrate that digitally integrated methods of material capture and discretisation create a closer connection of irregular materiality with design-centric environments.

Transformation of *material engagement* within architecturally driven workflows was enabled in this study by the coupling of data-driven inventories of irregular materials with innovative computational modes of

simulation and optimisation. The population-based approaches to *material engagement* embedded in *Probe 4: Evolutionary algorithms*, *Prototype 1: Acousti-SIM* (Chapter 4) and *Prototype 2: Mat-Truss* (Chapter 5), provided clear methods of optimisation that negotiate the inherent complexity of unique material irregularity with non-converging design objectives.

The engagement of latent materials, such as fibre-managed plantation hardwood, within material fabrication workflows, is enabled through the adoption of materially-aware methods of digital fabrication. While these processes are emerging in other manufacturing sectors, the construction industry is still hesitant to embrace transformative technologies that have significant labour and financial implications (Section 2.2.2). The materially responsive fabrication processes in *Probe 3: Architectural panel* (Chapter 3.4), *Prototype 1: Acousti-SIM* (Chapter 4) and *Prototype 2: Mat-Truss* (Chapter 5) circumvent these concerns by encoding materially responsive fabrication processes at an elemental level within the DIMP. As such, these Probes and Prototypes demonstrate a scalable approach to material fabrication within tailored design scenarios, which have potential for a lower threshold for adoption within industry with minimal additional infrastructure. This would subsequently decrease the financial risk associated with industry-wide transformation.

2. **How far can the current paradigms within architectural design and fabrication converge to extend beyond the use of standardised materials?**

The study highlights that the siloing of expertise within the construction industry was paralleled by the adoption of standardised materials and processes (which had intensified during the post-Second World War industrialisation period). As the segregation of design thought and realisation continued, the connection between design intent and material understanding diminished, resulting in a reliance on construction materials that are standardised though industrialisation processes. This disconnection also contributes significantly to the carbon footprint of the built environment.

To address this disparity, the digital approaches to material engagement presented in *Probe 1: RGB-D Scanning* (Section 3.2) and *Probe 2: RGB and Constrained inventories* (Section 3.3), supported by the adoption of Industry 4.0 principles, can afford architectural design and fabrication with the capacity to consider non-standardised materials within design-centric workflows Further, this capacity allows the consideration of currently

underdeveloped materials (that offer high levels of sustainability) as valid media of architectural exploration.

The investigation of RGB-D methods of material capture, undertaken in *Probe 1*, provide techniques by which to obtain high resolution 3-dimensional point cloud representations of timber boards that accommodated the detection of board irregularities undetectable by two dimensional methods; although, the complexity of the captured dataset was too computationally demanding to store and interrogate in large inventories of material.

In addressing these issues, *Probe 2* developed a multi-face computer vision method that captured material features at a 1mm scale, generating geometric representations of individual boards and their significant material features. This method of data representation generated larger volumes of timber boards to be contained within a constrained inventory, while maintaining a level of detail suitable for interrogation within design and fabrication workflows.

The digitisation of available material within a constrained inventory provides capacity for the engagement of non-standard materials to be engaged within bespoke design environments. A reliance on standardised materials has led the construction industry to employ materials that are typically over-specified for their application, regardless of being either homogeneous or heterogeneous.

The fabrication methods developed in *Probe 3: Architectural panel* (Section 3.4), *Prototype 1: Acousti-SIM* (Chapter 4) and *Prototype 2: Mat-Truss* (Chapter 5) allow non-standard materials to be utilised as a part of bespoke architectural systems in which fabrication implementation was in conjunction with material features, rather than exclusive to it.

Further, the tailored methods of material utilisation and optimisation established in *Probe 4: Evolutionary optimisation* (Section 3.5), *Prototype 1* and *Prototype 2* provide a level of material specificity within architectural systems that accommodates complex inventories of material, pairing irregular feature with unique design criteria. Subsequently, these experiments bridge the gap between architectural design and material irregularity more closely, by allowing the direct engagement of unique material characteristics within design environments.

3. **To what extent can Australian fibre-managed plantation hardwood be exploited within innovative architectural design environments?**

While current methods of hardwood grading are specifically designed for native timber resources, the material characteristics they identify

as strength-reducing features are shared with timber sourced from both sawlog and fibre-managed plantation forests. *Probe 2: RGB and Constrained inventories* (Section 3.3) established a high-resolution capture and discretisation method of these material features that translated the unique irregularities of individual sawn timber boards into a constrained material inventory for design exploration. While these methods were limited in scale within this study, they have the capacity to be expanded into larger design investigations (as demonstrated by *Prototype 1: Acousti-SIM* and *Prototype 2: Mat-Truss*).

These design-based Prototypes illustrate that the exposure of unique material datasets within workflows can engage fibre-managed plantation hardwood as a valuable material within tailored architectural propositions. This empowers architects to utilise fibre-managed plantation hardwood that provides high levels of sustainability, without the additional logistical and economic factors associated with irregularity and unpredictability.

For these methods to be adopted within the broader industry context, it is apparent that the forestry industry must align its production workflows with persistent data-rich supply chains, and enable the architecture and construction sectors with the capacity to engage unique material datasets throughout the design and construction workflow.

The *Design Probes* (Chapter 3) and *Prototypes* (Chapter 4 and Chapter 5) demonstrate modes of a DIMP that are scalable to larger industry applications in the material grading, design and fabrication. Finally, from the findings, it is recommended that the timber industry address the inadequacies of current methods of material grading through the development of new standards, specifically aligned with the irregularity and performance characteristics of plantation hardwood-based timber products.

4. **What mechanisms within computational design frameworks can mediate material irregularity and notions of precision?**

The findings of this study demonstrates that, while the juxtaposition of material irregularity and notions of precision appear at odds with each other, they are in fact closely interrelated. In contrast with standardised materials with a 'one size fits all' approach to materialisation, an increase in material irregularity requires a higher level of precision in the understanding and communicating of its unique character to maximise its performance potentials.

Probe 2: RGB and Constrained inventories (Section 3.3) indicate that innovative methods of digital material capture and discretisation resolve these issues through the establishment of a data-rich repository of material information.

An increase in material specificity within this repository cultivates material engagement that can be enacted with a level of precision that is unavailable using standardised material and design workflows.

The study findings demonstrates that sustainable methods of timber production can significantly impact the quality and predictability of material character and performance, requiring a shift in design workflow that affords a correlation between design performance and material capacity, which challenges contemporary modes of design ideation. As *Probe 4: Evolutionary Algorithms* (Section 3.5) demonstrated, to maximise the potential of irregular materials within design, the relationship with precision must be specified, and subsequently analysed with regards to its performance. The findings are that the affordances required to accommodate this were two-fold:

1. the establishment of a computational workflow that encompassed material irregularity and its performance in the context of a design problem; and
2. the inclusion of a mechanism that facilitated the consideration of multiple iterations of the design problem.

Both *Prototype 1: Acousti-SIM* (Chapter 4) and *Prototype 2: Mat-Truss* (Chapter 5) address these affordances in the context of design experimentation.

These Prototypes also illustrate that the successful reconciliation of material irregularity and precise engagement is dependent on the specificity of their embedded relationship within the design problem. This requires a negotiation between the design objectives and the capacity of the irregular materials to meet the needs of these objectives, necessitating the introduction of measures of performance and tolerance.

In the case of *Prototype 1*, a constrained inventory of unique timber elements was distributed across a series of hybrid architectural panels, based on their capacity to be physically augmented in accordance with the specified acoustic requirements. *Prototype 2* sought to maximise the structural performance of a truss, based on the distribution of timber boards, in accordance with their individual character and potential performance capacity.

While both design problems could have been resolved by distributing the highest specification material from the constrained inventory, this approach would default to a mode of simplification that ignores an intelligent application of material engagement in accordance with tailored design performance requirements.

However, a constrained inventory contains a potentially infinite number of timber boards, each with its own unique irregularities and performance

capacities. This generates complexity within design problems that must negotiate the infinite number potential design solutions, given the volume of possible iterations available.

Prototype 1 and *Prototype 2* address this complexity through the integration of Multi-objective Evolutionary Algorithms (MOEAs) that apply population-based optimisation methods to negotiate design objectives, material irregularity and material optimisation. While MOEAs have been used extensively as a method of optimisation in architectural design workflows since 2010, they have rarely been employed to reconcile design objectives and elementally specific applications of highly irregular heterogeneous materials (such as fibre-managed plantation hardwood).

The capacity of innovative combinations of data-rich materials inventories and discretisation methods that employ this data, in accordance with specific design problems and MOEA optimisation techniques, is clearly demonstrated in this study. They provide a mechanism to bridge the gap between digital design and industry. This mechanism also engenders a greater number of material applications, which are currently unavailable to the timber industry, and the architecture and construction sectors.

As such, *Prototype 1* and *Prototype 2* demonstrate that the incorporation of materially enabled, population-based optimisation methods afford the capacity to negotiate the scale and complexity of design problems, which contain multiple design objectives and a potentially infinite set of material configurations. Within this mechanism, each Prototype established a MOEA that generated an iterative pool of valid solutions and simulated their performance against each of the design objectives.

While neither design problem aimed to generate a pool of solutions that converged to a single optimised solution, the novel methods of selection afforded the capacity to narrow each field of solutions within a set level of tolerance, and allowed a selection to be made that negotiated material irregularity, performance optimisation and visual preference. This challenges traditional notions of performance optimisation in that it does not seek to obtain a perfect solution. As such, the study presents a 'softer' approach to optimisation and solution selection, which mediates material heterogeneity, performance simulation and valid solutions, and favours

material utilisation and waste minimisation within a field of acceptable performance results.

6.4 Restatement of Contributions

In this section, the contributions of this research are revisited, and divided into two parts:

1. the primary contribution of the study, and
2. the secondary contributions that are mapped against each of the contextual domains; namely, *material sustainability*, *timber in construction*, and *digitally integrated material practice*.

6.4.1 Primary Contribution

The central contribution of this study is a DIMP framework centred on the engagement of material irregularity within design-based computational workflows. As such, it extends material practice beyond current modes of material standardisation and specification, allowing the timber industry, material manufacturers and suppliers, architects and fabricators opportunities to re-evaluate materials currently disregarded due to their perceived defects or unpredictability.

The investigative Probes and Prototypes established the opportunity for abundant renewable resources (specifically fibre-managed plantation hardwood) to be considered as viable options for material exploration within architectural design. The frameworks comprise divergent notions of material engagement within the fields of material capture, material optimisation, and material fabrication.

In the field of material capture, this study contributes innovative digitally enabled methods of capturing irregularities and material characteristics that occur within feature-rich fibre-managed plantation hardwood timbers. Within the context of the investigative Probes and Prototypes, these methods were embedded within architectural and fabrication workflows, providing a persistence of material data throughout the presented bespoke design and fabrication CDFs.

Accordingly, a compelling argument is made for the timber industry to adopt imaging and material testing technology that would enable similar practices. In doing so, the establishment of a persistent data-rich material supply chain (at a scale that is likely to make an positive economic impact on their operations) is created by providing an elemental performance specification for materials, which would otherwise be disregarded within the construction industry. In the context of Design Prototype 2, it is conceivable that the adoption of these methods could facilitate

the utilisation of plantation hardwood (as opposed to softwood) in the manufacture of residential roof trusses, with the potential to increase the value of an estimated 108,000m³ of pulplog grade plantation hardwood annually.

Further, this study establishes innovative methods of material discretisation to aid in the articulation of irregularity within a design workflow. When this is coupled with a data-rich material inventory, architects are afforded this opportunity to utilise unique material properties within bespoke DIMPs, thereby enabling the utilisation of highly sustainable materials that would otherwise be latent due to their incapacity to meet existing grading standards.

In the field of material optimisation, this study contributes methods of computational simulation and optimisation that employ multi-objective evolutionary algorithms to match irregular material characteristics with specific performance requirements, within a design problem. This is especially vital for architects and fabricators, as population-based methods of optimisation allows the evaluation of unique elements sourced from a constrained inventory to be tested in multiple configurations, while not being limited to a static material understanding. The coupling of unique material inventories and specific design problems fosters a higher capacity of material engagement, now very necessary in the consideration of fibre-managed plantation hardwood as a construction material.

Finally, in the field of material fabrication the study contributes computationally augmented modes of digital fabrication that leverage material engagement as an active agent of mediation between performance based design objectives and material manipulation. The methods developed in this study are executed with equipment that is widely available in the construction industry, making a case for greater levels of design and material irregularity in existing fabrication and construction workflows, without significant additional financial burden.

This has a secondary impact for architects in that it should engender confidence in non-standardised design outcomes that incorporate DIMPs and which can be fabricated using existing industry capacity, with minimal additional cost to a construction budget.

6.4.2 Secondary Contributions

The secondary contributions are specific to each of the contextual domains in which the DIMP is situated.

In the *material sustainability* domain, the key contributions are the development of proof-of-concept techniques for material capture (*Probe*

1: RGB-D scanning), and discretisation and cataloguing (*Probe 2: RGB and Constrained Inventories*) that bridge the supply chain data gap between the material suppliers and architecture practice. Subsequently, these provide opportunity for the re-evaluation of out-of-grade and waste materials that present irregular and unpredictable material characteristics and performance, currently latent within higher-value applications within the construction sector.

In the *timber in construction* domain, the main contribution is the establishment of engagement modes that facilitate the consideration of fibre-managed plantation hardwood as a potential material of value within the architecture and construction industries. The techniques extend those developed in the previous domain (that is, to establish fabrication-based workflows, *Probe 3: Architectural panel, Prototype 1: Acousti-SIM*, and *Prototype 2: Mat-Truss*), which are responsive to the naturally occurring material characteristics. Further, the intersection of material character and digital fabrication is executed using commonly available digital fabrication equipment, demonstrating that these methods developed have the capacity to be readily adopted by industry, without financial burden.

In the *digitally integrated material practice* domain, the main contributions comprise innovative methods of material engagement that are present throughout the design workflow, which foster a non-linear approach to the correlation of material, discretisation, design intent, optimisation and fabrication. The material optimisation workflow developed in *Probe 4: Evolutionary Algorithms* investigates both Single and Multi-Objective Evolutionary Algorithms (MOEA) to generate a population-based method of material optimisation that facilitates the of pairing a practically infinite material variation with a complex combination of multiple design objectives.

These methods form the core components of *Prototype 1: Acousti-SIM*, and *Prototype 2: Mat-Truss*, and generate innovative computational means of engaging a constrained material inventory, material distribution,

performance simulation and solution selection, scalable to larger applications within industry.

6.5 Limitations and Future Perspectives

Three key limitations are observed in the conducted study. Each limitation is discussed, with proposed solutions to be potentially undertaken in future research.

6.5.1 Plantation Hardwood Resources

The material engagement within the research comprised the capture, optimisation, deployment, and fabrication of sawn *E. nitens* boards, sourced from a single 16-year-old fibre-managed plantation forest, located in Northern Tasmania, Australia. It is understood that the material characteristics of timber is directly affected by the geographic and environmental conditions in which it was grown. With 72% of Australian plantation hardwood being grown outside Tasmania, in differing climatic and geographic conditions, it is anticipated that sawn boards from other regions, both nationally and internationally, will present different relationships between material character and performance capacity.

As such, future research should endeavour to quantify the degree that plantation timber from different geographical locations would affect the efficiency, resource utilisation, and economic benefit proposed by the developed methods.

6.5.2 Scalability of Probes and Prototypes

The methods developed in this study, using the Design Probes, were limited by the volume of physical material available for experimentation, and a scale of technology and equipment suitable for application within bespoke design and fabrication scenarios. As such, the methods of material capture and discretisation available within the constrained inventory were restricted to 120 boards, approximately 3m in length. This limited the scale of Prototype exploration to relatively small artefacts; however, the workflows within the Probes and Prototypes have the capacity for scalability to significantly larger material and design contexts.

For the developed workflows to be validated within the wider industry context, their scale must be increased to accommodate material systems and design problems that operate at the size of commercial architecture. Subsequently, future research should consider scaling the material engagement methods to include a greater level of automation within the fields of material capture and discretisation to accommodate larger volumes of material. This shift suggests significant opportunity for modes

of material capture and discretisation to be explored in the forestry and primary-production sectors, where the potential for economic, resource and sustainability impacts are significantly greater. This would then necessitate the exploration of persistence within data-enriched supply-chains between material production and design ideation and construction.

While there is significant potential in transforming the supply chain to include persistence of materially enriched data at a larger scale, the complexity of computational optimisation embedded within the Probes and Prototypes poses substantial risk to their adoption by normative design practice. This is particularly significant within Australia where the architecture profession is responsible for an estimated 5% of all residential construction. The accessibility and packaging of material data along supply chains, along with its capacity to be engaged within design processes, is critical to the adoption of plantation hardwood being utilised more broadly within the construction industry.

Subsequently, future research should investigate the adaptation of these innovative workflows into segmented 'platforms of design', which would enable their integration into more common design and construction workflows.

6.5.3 Notions of Material and System Performance

While the Design Prototypes in this study employ modes of either acoustic or structural performance simulation as primary objectives within the relevant design problems, many of the additional objectives relate to more abstract notions of material character and performance. This is due, in part, to the inability to undertake destructive modes of material testing on the limited supply available for experimentation.

Future research should seek to engage a wider range of material testing, such as *Modulus of Rupture* and *Elasticit*y, on a larger pool of materials to enable a greater capacity of performance simulation and validation to be applied to the developed modes of material engagement and design systems.

Further, the integration of more advanced modes of material capture, including Computer Tomography (in addition to the adoption of emerging artificial intelligence platforms) has the potential to advance the understanding of material and system performance within Industry 4.0 enabled workflows relevant to both the forestry and construction industries.

6.6 Concluding Remarks

The architectural profession is undergoing significant technological transformation as it embraces the post-digital information age. Existing modes of digital design and computation are being enriched by emerging modes of data interrogation, artificial intelligence, simulation, optimisation and persistent digital production chains. Coupled with the ubiquity of cheap and readily available computational capacity, these modes will mature into embedded frameworks within architectural practice, giving rise to completely new ways in which architects engage with materiality and sustainability. This opens the potential for as-yet unknown and design potentials when engaging irregular and heterogeneous materials.

Sitting at the intersection of architecture, computational design and the timber and construction industries, this research contributes to the advancement of this technological transformation. It furthers the transformation on two main fronts:

- The development of capture and discretisation methods that promote the persistence of material data between timber production and the built environment.
- The advancement of current approaches to material integration within design frameworks, which readily offer the capacity to engage constrained inventories of irregular materials within advanced computational simulation and optimisation workflows.

Further, the findings of this study have several key implications for the practice and discourse of architecture in the post-digital age. Critically, the first implication offers capacity for architects and designers to address current environmental shortcomings, particularly in the context of environmental sustainability, and material resource renewability and utilisation. Second, the developed methods provide a platform for the persistence of interdisciplinary supply-chain data across existing industry silos. Currently this data-chain only exists in bespoke projects and has little impact on industry-wide practices. The application of the methods developed in the research will contribute to the transformation of the architecture and construction sectors beyond the pre-conceived boundaries of standardised and sustainable material engagement currently employed to mitigate the impact of human-induced climate change within the built environment.

7 REFERENCES

Aagaard, A. K., & Larsen, N. M. (2020). Developing a fabrication workflow for irregular sawlogs. *International Journal of Architectural Computing*, *18*(3), 270–283. https://doi.org/10.1177/1478077120906736

Abdulmawla, A., Bielik, M., Buš, P., Dennemark, M., Fuchkina, E., Miao, Y., Knecht, K., König, R., & Schneider, S. (2017). *DeCodingSpaces Toolbox: Computational analysis and generation of STREET NETWORKS, PLOTS and BUILDINGS*. https://toolbox.decodingspaces.net/

Ackley, D. (1987). *A Connectionist Machine for Genetic Hillclimbing*. Springer New York.

Acuna, M., Strandgard, M., Wiedemann, J., & Mitchell, R. (2017). Impacts of Early Thinning of a *Eucalyptus globulus* Labill. Pulplog Plantation in Western Australia on Economic Profitability and Harvester Productivity. *Forests*, *8*(11), 415–429. https://doi.org/10.3390/f8110415

Adhikari, S., & Ozarska, B. (2018). Minimizing environmental impacts of timber products through the production process "From Sawmill to Final Products". *Environmental Systems Research*, *7*(1), 6. https://doi.org/10.1186/s40068-018-0109-x

AFMG Technologies GmbH. (2022). *EASE 4: Version 4.4 Advanced simulation of electro-acoustics and room acoustics*. https://www.afmg.eu/en/ease-enhanced-acoustic-simulator-engineers

Ahmadian, A. A. (2020). *Computational Design for Cooperative Robotic Assembly of Nonstandard Timber Frame Buildings* [Doctoral Thesis, ETH Zurich]. ETH Zurich Research Collection. https://doi.org/10.3929/ethz-b-000439443

Akanmu, A., Anumba, C., & Messner, J. (2013). Scenarios for cyber-physical systems integration in construction. *Journal of Information Technology in Construction (ITcon)*, *18*(12), 240–260. https://www.itcon.org/papers/2013_12.content.06942.pdf

Amtsberg, F., Mueller, C., & Raspall, F. (2022). Di-terial – Matching Digital Fabrication and Natural Grown Resources for the Development of Resource Efficient Structures. In P. F. Yuan, H. Chai, C. Yan, & N. Leach (Eds.), *Proceedings of the 2021 DigitalFUTURES* (pp. 330–339). Springer. https://doi.org/10.1007/978-981-16-5983-6_30

Ananías, R. A., Sepúlveda-Villarroel, V., Pérez-Peña, N., Leandro-Zuñiga, L., Salvo-Sepúlveda, L., Salinas-Lira, C., Cloutier, A., & Elustondo, D. M. (2014). Collapse of *Eucalyptus nitens* Wood After Drying Depending on the Radial Location Within the Stem. *Drying Technology*, *32*(14), 1699–1705. https://doi.org/10.1080/07373937.2014.924132

Apolinarska, A. A. (2018). *Complex timber structures from simple elements:*

Computational Design of Novel Bar Structures for Robotic Fabrication and Assembly [Doctoral Thesis, ETH Zurich]. ETH Zurich Research Collection. https://doi.org/10.3929/ethz-b-000266723

Apolinarska, A. A., Bärtschi, R., Furrer, R., Gramazio, F., & Kohler, M. (2016). Mastering the "Sequential Roof": Computational Methods for Integrating Design, Structural Analysis, and Robotic Fabrication. *Advances in Architectural Geometry 2016*, 240–258.

Apolinarska, A. A., Knauss, M., Gramazio, F., & Kohler, M. (2016). The Sequential Roof. In A. Menges, T. Schwinn, & O. D. Krieg (Eds.), *Advancing Wood Architecture* (1st ed., pp. 45–59). Routledge. https://doi.org/10.4324/9781315678825-4

Architects Accreditation Council of Australia. (2018). *Industry profile: The profession of architecture in Australia*. https://aaca.org.au/wp-content/uploads/Industry-Profile.pdf

As, N., Goker, Y., & Dundar, T. (2006). Effect of knots on the physical and mechanical properties of Scots pine (*Pinus sylvestris L.*). *Wood Research*, *51*(3), 51–58.

Asa, P., Feghali, C., & Steixner, C. (2022). *Embraced Wood: Building with unprocessed reclaimed timber* [Masters Thesis]. Institute for Computational Design and Construction, University of Stuttgart.

Association of Australasian Acoustical Consultants. (2018). *Guideline for Educational Facilities: Version 2.0*. https://aaac.org.au/resources/Documents/Public/AAAC%20Guideline%20for%20Educational%20Facilities%20Acoustics%20V2.0.pdf

Australian Bureau of Agricultural and Resource Economics and Sciences. (2018). *Australia's State of the Forests Report 2018*.

Australian Bureau of Agricultural and Resource Economics and Sciences. (2022a). *Australian plantation statistics 2022 update*. August 2022. https://daff.ent.sirsidynix.net.au/client/en_AU/search/asset/1033861/0

Australian Bureau of Agricultural and Resource Economics and Sciences. (2022b). *Australian forest and wood product statistics: September and December quarters 2021*. https://daff.ent.sirsidynix.net.au/client/en_AU/ABARES/search/detailnonmodal/ent:$002f$002fSD_ASSET$002f0$002fSD_ASSET:1033683/one

Autodesk. (2021). *DynamoBIM*. https://dynamobim.org/

Baber, K. R., Burry, J. R., Chen, C., Gattas, J. M., & Bukauskas, A. (2019). Inventory constrained funicular modelling. *Proceedings of the IASS Annual Symposium 2019 - Structural Membranes*, 1–10. https://doi.org/10.1007/

s42452-020-03314-9

Baber, K. R., Burry, J. R., Chen, C., Gattas, J. M., & Bukauskas, A. (2020). Inventory constrained design of a timber funicular structure. *SN Applied Sciences*, *2*(9), 1538. https://doi.org/10.1007/s42452-020-03314-9

Balasso, M., Hunt, M., Jacobs, A., & O'Reilly-Wapstra, J. (2021). Development of Non-Destructive-Testing Based Selection and Grading Strategies for Plantation *Eucalyptus nitens* sawn boards. *Forests*, *12*(3), 343. https://doi.org/10.3390/f12030343

Beorkrem, C. (2017). *Material strategies in digital fabrication.* (2nd ed.). Routledge.

Blackburn, D., Vega, M., Yong, R., Britton, D., & Nolan, G. (2018). Factors Influencing the production of structural plywood in Tasmania, Australia from *Eucalyptus nitens* rotary peeled veneer. *Southern Forests: A Journal of Forest Science*, *80*(4), 319–328. https://doi.org/10.2989/20702620.2017.1420730

Booth, P., Maxwell, I., & Schork, T. (2017). Timber 4.0: A Computer-Vision Approach for Visual Grading Low-Grade Plantation Hardwood. In M. A. Schnabel (Ed.), *Back to the Future: The Next 50 Years, (51st International Conference of the Architectural Science Association (ANZAScA)*, 465–474.

Booth, T. H. (2013). Eucalypt plantations and climate change. *Forest Ecology and Management*, *301*, 28–34. https://doi.org/10.1016/j.foreco.2012.04.004

Bradley, J. S. (1986). Speech intelligibility studies in classrooms. *The Journal of the Acoustical Society of America*, *80*(3), 846–854. https://doi.org/10.1121/1.393908

Brouwer, T. (2013). *Low budget ranging for forest management: A Microsoft Kinect study* (Thesis Report GIRS-2013-12) [MSc Thesis]. Wageningen University.

Brugnaro, G. (2021). *Robotic Training for the Integration of Material Performances in Timber Manufacturing* [Doctoral Thesis, The Bartlett School of Architecture].

Brugnaro, G., & Hanna, S. (2018). Adaptive robotic carving: Training methods for the integration of material performances in timber manufacturing. In J. Willmann, P. Block, M. Hutter, K. Byrne, & T. Schork (Eds.), *Robotic Fabrication in Architecture, Art and Design 2018* (pp. 336–348). Springer International Publishing. https://10.1007/978-3-319-92294-2_26

Brütting, J., Desruelle, J., Senatore, G., & Fivet, C. (2019). Design of Truss Structures Through Reuse. *Structures*, *18*, 128–137. https://doi.

org/10.1016/j.istruc.2018.11.006

Brütting, J., Senatore, G., & Fivet, C. (2018). Optimization Formulations for the Design of Low Embodied Energy Structures Made from Reused Elements. In I. F. C. Smith & B. Domer (Eds.), *Advanced Computing Strategies for Engineering* (Vol. 10863, pp. 139–163). Springer International Publishing. https://doi.org/10.1007/978-3-319-91635-4_8

Brütting, J., Senatore, G., & Fivet, C. (2019). Form Follows Availability: Designing Structures Through Reuse. *Journal of the International Association for Shell and Spatial Structures*, *60*(4), 257–265. https://doi.org/10.20898/j.iass.2019.202.033

Brütting, J., Senatore, G., Schevenels, M., & Fivet, C. (2020). Optimum Design of Frame Structures From a Stock of Reclaimed Elements. *Frontiers in Built Environment*, *6*, 57. https://doi.org/10.3389/fbuil.2020.00057

Brütting, J., Vandervaeren, C., Senatore, G., De Temmerman, N., & Fivet, C. (2020). Environmental impact minimization of reticular structures made of reused and new elements through Life Cycle Assessment and Mixed-Integer Linear Programming. *Energy and Buildings*, *215*, 109827. https://doi.org/10.1016/j.enbuild.2020.109827

Bucur, V. (2003). Techniques for high resolution imaging of wood structure: a review. *Measurement Science and Technology*, *14*(12), R91–R98. https://doi.org/10.1088/0957-0233/14/12/R01

Bukauskas, A. (2020). *Inventory-Constrained Structural Design* [Doctoral Thesis]. Bath University. https://researchportal.bath.ac.uk/en/studentTheses/inventory-constrained-structural-design

Bukauskas, A., Mayencourt, P., Shepherd, P., Sharma, B., Mueller, C., Walker, P., & Bregulla, J. (2019). Whole timber construction: A state of the art review. *Construction and Building Materials*, *213*, 748–769. https://doi.org/10.1016/j.conbuildmat.2019.03.043

Bukauskas, A., Shepherd, P., Walker, P., Sharma, B., & Bregulla, J. (2017a). Computational Form-Fitting with Non-Standard Structural Elements. *IABSE Conference, Bath 2017: Creativity and Collaboration – Instilling Imagination and Innovation in Structural Design*, 121–122. https://doi.org/10.2749/222137817821232946

Bukauskas, A., Shepherd, P., Walker, P., Sharma, B., & Bregulla, J. (2017b). Form-Fitting Strategies for Diversity-Tolerant Design. *Proceedings of IASS Annual Symposia*, 1–10. https://researchportal.bath.ac.uk/files/157995605/hamburg_preprint5.pdf

Bureau of Meteorology. (2001). *Map of Climate Zones of Australia*. http://

www.bom.gov.au/climate/how/newproducts/images/zones.shtml

Buri, H., & Weinand, Y. (2011). The tectonics of timber architecture in the digital age. In H. Kaufmann, W. Nerdinger, J. R. O'Donovan, & M. Robinson (Eds.), *Building with Timber: Paths into the Future* (pp. 56–63). Prestel.

Candy, L. (2006). *Practice Based Research: A Guide*. UTS. https://www.creativityandcognition.com/wp-content/uploads/2011/04/PBR-Guide-1.1-2006.pdf

Caneparo, L. (2014). Digital Woodworking. In L. Caneparo, *Digital Fabrication in Architecture, Engineering and Construction* (pp. 163–200). Springer Netherlands. https://doi.org/10.1007/978-94-007-7137-6_6

Cao, Y., Street, J., Li, M., & Lim, H. (2019). Evaluation of the effect of knots on rolling shear strength of cross laminated timber (CLT). *Construction and Building Materials*, *222*, 579–587. https://doi.org/10.1016/j.conbuildmat.2019.06.165

Carpo, M. (2014). Ten years of folding. In R. Oxman & R. Oxman, *Theories of the Digital in Architecture* (pp. 35–46). Routledge.

Carpo, M. (2017). *The Second Digital Turn: Design Beyond Intelligence.* The MIT Press.

Carpo, M. (2019). Particlised: Computational Discretism, or the rise of The Digital Discrete. *Architectural Design*, *89*(2), 86–93. https://doi.org/10.1002/ad.2416

CATT. (2022). *CATT-Acoustic v.9.1*. https://www.catt.se/

Cherry, R., Manalo, A., Karunasena, W., & Stringer, G. (2019). Out-of-grade sawn pine: A state-of-the-art review on challenges and new opportunities in cross laminated timber (CLT). *Construction and Building Materials*, *211*, 858–868. https://doi.org/10.1016/j.conbuildmat.2019.03.293

Chubinskii, A. N., Tambi, A. A., Teppoev, A. V., Anan'eva, N. I., Semishkur, S. O., & Bakhshieva, M. A. (2014). Physical nondestructive methods for the testing and evaluation of the structure of wood-based materials. *Russian Journal of Nondestructive Testing*, *50*(11), 693–700. https://doi.org/10.1134/S1061830914110023

Colella, M., & Fallacara, G. (2019). Towards a 4.0 Mass Customized Wooden Housing in the Mediterranean Area: The Ecodomus Project. In F. Bianconi & M. Filippucci (Eds.), *Digital Wood Design* (Vol. 24, pp. 1201–1228). Springer International Publishing. https://doi.org/10.1007/978-3-030-03676-8_49

Couceiro, J., Hansson, L., Sehlstedt-Persson, M., & Sandberg, D. (2016). The

use of X-ray computed tomography in timber construction research. *New Horizons for the Forest Products Industry: 70th Forest Products Society International Convention, June 26-29, 9, Portland, Oregon, USA, Madison: Forest Products Society, 2016*. https://www.diva-portal.org/smash/get/diva2:1001051/FULLTEXT01.pdf

Cox, T. J., & D'Antonio, P. (2017). *Acoustic Absorbers and Diffusers: Theory, Design and Application* (Third edition). CRC Press.

Craney, R., & Adel, A. (2020). Engrained performance: Performance-driven computational design of a robotically assembled shingle facade system. In B. Slocum, V. Ago, S. Doyle, M. Marcus, M. Yablonina, & M. del Campo (Eds.), *ACADIA 2020: Distributed Proximities* (Vol. 1, pp. 604–613). http://papers.cumincad.org/cgi-bin/works/paper/acadia20_604

Crolla, K. (2018). *Building simplicity: The 'more or less' of post-digital architectural practice* [Doctoral Thesis, RMIT University]. https://researchrepository.rmit.edu.au/esploro/outputs/9921864092901341

Cross, N. (2007). From a Design Science to a Design Discipline: Understanding Designerly Ways of Knowing and Thinking. In R. Michel (Ed.), *Design Research Now* (pp. 41–54). Birkhäuser. https://doi.org/10.1007/978-3-7643-8472-2_3

Cusp. (2022). *Cusp|Building Solutions*. https://cusp.com.au

Davis, D., Patronis, E., Brown, P., & Ballou, G. (2013). *Sound System Engineering* (4th ed.). Focal Press.

Davis, K., Nolan, G., Kotlarewski, N., & Orr, K. (2017). *What is the Potential for Australia's Plantation Hardwoods in Appearance Applications?* IUFRO Division 5 conference 2017, Vancouver, Canada. http://ecite.utas.edu.au/118334

Deb, K., Agrawal, S., Pratap, A., & Meyarivan, T. (2000). A Fast Elitist Non-Dominated Sorting Genetic Algorithm for Multi-Objective Optimization: NSGA-ii. *Lecture Notes in Computer Science*, 849–858. https://doi.org/10.1007/3-540-45356-3_83

Dell'Endice, A., Odaglia, P., & Gramazio, F. (2017). Prefabbricazione robotizzata e innovazione. *MD Journal*, *3*, 42–55.

Department of Industry, Innovation and Science. (2019). *Industry 4.0 Testlabs in Australia*: *Preparing for the future.* https://www.industry.gov.au/funding-and-incentives/manufacturing/industry-40

Deplazes, A. (Ed.). (2005). *Constructing Architecture: Materials, Processes, Structure. A handbook*. Birkhäuser-Publishers for Architecture.

Derikvand, M. (2019). *Optimising laminated high-mass timber components*

assembled from a fibre-grown resource for building applications [Doctoral Thesis, University of Tasmania]. https://eprints.utas.edu.au/34525/

Derikvand, M., Kotlarewski, N., Lee, M., Jiao, H., Chan, A., & Nolan, G. (2018). Visual stress grading of fibre-managed plantation Eucalypt timber for structural building applications. *Construction and Building Materials*, *167*, 688–699. https://doi.org/10.1016/j.conbuildmat.2018.02.090

Derikvand, M., Kotlarewski, N., Lee, M., Jiao, H., & Nolan, G. (2019). Characterisation of Physical and Mechanical Properties of Unthinned and Unpruned Plantation-Grown *Eucalyptus nitens* H. Deane & Maiden Lumber. *Forests*, *10*(2), 194. https://doi.org/10.3390/f10020194

Derikvand, M., Kotlarewski, N., Lee, M., Jiao, H., & Nolan, G. (2020). Flexural and visual characteristics of fibre-managed plantation *Eucalyptus globulus* timber. *Wood Material Science & Engineering*, *15*(3), 172–181. https://doi.org/10.1080/17480272.2018.1542618

Derikvand, M., Nolan, G., Jiao, H., & Kotlarewski, N. (2016). What to do with structurally low-grade wood from Australia's plantation eucalyptus; building application? *BioResources*, *12*(1), 4–7. https://doi.org/10.15376/biores.12.1.4-7

Desch, H. E., & Dinwoodie, J. M. J. M. (1996). *Timber: Structure, Properties, Conversion and Use* (7th ed.). Bloomsbury Publishing.

Dessi-Olive, J., & Hsu, T. (2019). Generating acoustic diffuser arrays with shape grammars. *SimAUD2019*. https://dl.acm.org/doi/pdf/10.5555/3390098.3390135

Devadass, P., Dailami, F., Mollica, Z., & Self, M. (2016). Robotic Fabrication of Non-Standard Material. *Proceedings of the 36th Annual Conference of the Association for Computer Aided Design in Architecture (ACADIA)*, 206–216. https://doi.org/10.52842/conf.acadia.2016.x.g4f

Diaz, M. G., Tombari, F., Rodriguez-Gonzalvez, P., & Gonzalez-Aguilera, D. (2015). Analysis and Evaluation Between the First and the Second Generation of RGB-D Sensors. *IEEE Sensors Journal*, *15*(11), 6507–6516. https://doi.org/10.1109/JSEN.2015.2459139

Dinwoodie, J. (2000). *Timber: Its nature and behaviour* (2nd ed.). CRC Press.

Downton, P. (2003). *Design Research*. RMIT Publishing.

Downton, P. (2004). Studies in Design Research: Ten Epistemological Pavilions. RMIT University Press.

Drigo, M. (1996). The ant system: optimization by a colony of cooperating agents. *IEEE Transactions on Systems, Man, and Cybernetics-Part B*, *26*(1),

1–13. https://doi.org/10.1109/3477.484436

Dunn, N. (2012). *Digital Fabrication in Architecture*. Laurence King Publishing. http://ebookcentral.proquest.com/lib/utas/detail.action?docID=1876132

Encyclopédie méthodique marine: Curved Wood Plate 103 [Print] (1797). In *Encyclopédie méthodique marine*. chez Panckoucke. http://archeologie.culture.fr/epaves-corsaires/en/mediatheque/curved-wood.

England, J. R., May, B., Raison, R. J., & Paul, K. I. (2013). Cradle-to-gate inventory of wood production from Australian softwood plantations and native hardwood forests: Carbon sequestration and greenhouse gas emissions. *Forest Ecology and Management*, *302*, 295–307. https://doi.org/10.1016/j.foreco.2013.03.010

Erboz, G. (2017). *How to define industry 4.0: The main pillars of industry 4.0. 7th International Conference on Management. Managerial Trends in the Development of Enterprises in Globalization Era*. Slovak University of Agriculture in Nitra, Slovaki. https://www.researchgate.net/publication/326557388_How_To_Define_Industry_40_Main_Pillars_Of_Industry_40

Ermann, M. (2015). *Architectural Acoustics Illustrated*. John Wiley & Sons, Inc.

Ettelaei, A., Taoum, A., & Nolan, G. (2022). Assessment of Different Measurement Methods/Techniques in Predicting Modulus of Elasticity of Plantation *Eucalyptus nitens* Timber for Structural Purposes. *Forests*, *13*(4). https://doi.org/10.3390/f13040607

Ettelaei, A., Taoum, A., Shanks, J., & Nolan, G. (2022). Rolling Shear Properties of Cross-Laminated Timber Made from Australian Plantation *Eucalyptus nitens* under Planar Shear Test. *Forests*, *13*(1), 84. https://doi.org/10.3390/f13010084

Evans, R. (1997). T*ranslations from Drawing to Building*. MIT Press.

Eversmann, P. (2017). Robotic Fabrication Techniques for Material of Unknown Geometry. *Humanizing Digital Reality: Design Modelling Symposium Paris 2017*, 311–322. https://doi.org/10.1007/978-981-10-6611-5_27

Eversmann, P., Gramazio, F., & Kohler, M. (2017). Robotic prefabrication of timber structures: Towards automated large-scale spatial assembly. *Construction Robotics*, *1*(1–4), 49–60. https://doi.org/10.1007/s41693-017-0006-2

Evison, D. C., Kremer, P. D., & Guiver, J. (2018). Mass Timber Construction in Australia and New Zealand—Status, and Economic and Environmental

Influences on Adoption. *Wood and Fiber Science*, *50*, 128–138. https://doi.org/10.22382/wfs-2018-046

Exton, P., & Marshall, H. (2011). The Room Acoustic Design of the Guangzhou Opera House. *Proceedings of the Institute of Acoustics*, *33*(2), 117–124.

Fan, Y., Feng, Z., Mannan, A., Khan, T., Shen, C., & Saeed, S. (2018). Estimating Tree Position, Diameter at Breast Height, and Tree Height in Real-Time Using a Mobile Phone with RGB-D SLAM. *Remote Sensing*, *10*(11), 1845. https://doi.org/10.3390/rs10111845

Farrell, R., Innes, T. C., & Harwood, C. E. (2012). Sorting *Eucalyptus nitens* plantation logs using acoustic wave velocity. *Australian Forestry*, *75*(1), 22–30. https://doi.org/10.1080/00049158.2012.10676382

Ferreira, V., Boyero, L., Calvo, C., Correa, F., Figueroa, R., Gonçalves, J. F., Goyenola, G., Graça, M. A. S., Hepp, L. U., Kariuki, S., López-Rodríguez, A., Mazzeo, N., M'Erimba, C., Monroy, S., Peil, A., Pozo, J., Rezende, R., & Teixeira-de-Mello, F. (2019). A Global Assessment of the Effects of Eucalyptus plantations on Stream Ecosystem Functioning. *Ecosystems*, *22*(3), 629–642. https://doi.org/10.1007/s10021-018-0292-7

Fivet, C., & Brütting, J. (2020). Nothing is lost, nothing is created, everything is reused: Structural design for a circular economy. *The Structural Engineer: Journal of the Institution of Structural Engineer*, *98*(1), 74–81. https://doi.org/10.56330/lxah1188

Foley, C. (2003). *Modeling the Effects of Knots in Structural Timber* [Doctoral Thesis, Lund University]. http://dx.doi.org/10.13140/RG.2.2.30965.22243

Forest & Wood Products Australia. (2021). *How much wood in an average house: 14.58 m3 (not 42)*. https://fwpa.com.au/how-much-wood-in-an-average-house-14-58-m3-not-42/

Forrester, D. I., Medhurst, J. L., Wood, M., Beadle, C. L., & Valencia, J. C. (2010). Growth and physiological responses to silviculture for producing solid-wood products from *Eucalyptus* plantations: An Australian perspective. *Forest Ecology and Management*, *259*(9), 1819–1835. https://doi.org/10.1016/j.foreco.2009.08.029

Fowells, H., & Means, J. (1990). The Tree and Its Environment. In R. Burnes & B. Honkala, *Silvics of North America: Vol. 1: Conifers* (pp. 1–11). United States Department of Agriculture.

Frayling, C. (1993). Research in Art and Design. *Royal College of Art: Research Papers*, *1*(1), 1–5. https://researchonline.rca.ac.uk/384/3/frayling_

research_in_art_and_design_1993.pdf

Fredriksson, M. (2014). Log sawing position optimization using computed tomography scanning. *Wood Material Science & Engineering*, *9*(2), 110–119. https://doi.org/10.1080/17480272.2014.904430

Fure, A. (2011). Digital Materiallurgy: On the productive force of deep codes and vital matter. *Proceedings of the 31st Annual Conference of the Association for Computer Aided Design in Architecture (ACADIA)*, 90–97. https://doi.org/10.52842/conf.acadia.2011.090

Furrer, F., Wermelinger, M., Yoshida, H., Gramazio, F., Kohler, M., Siegwart, R., & Hutter, M. (2017). Autonomous robotic stone stacking with online next best object target pose planning. *2017 IEEE International Conference on Robotics and Automation (ICRA*, 2350–2356. https://doi.org/10.1109/icra.2017.7989272

Füssl, J., Lukacevic, M., Pillwein, S., & Pottmann, H. (2019). Computational Mechanical Modelling of Wood—From Microstructural Characteristics Over Wood-Based Products to Advanced Timber Structures. In F. Bianconi & M. Filippucci (Eds.), *Digital Wood Design* (Vol. 24, pp. 639–673). Springer International Publishing. https://doi.org/10.1007/978-3-030-03676-8_25

Garcia, A. B., Cebeci, I. Y., Calvo, R. V., & Gordon, M. (2021). Material (data) Intelligence: Towards a Circular Building Environment. In *Proceedings of the 26th Conference on Computer Aided Architectural Design Research in Asia (CAADRIA)* (Vol. 1, pp. 361–370). https://doi.org/10.52842/conf.caadria.2021.1.361

Ghavami, K. (2020). 2 - Introduction to nonconventional materials and an historic retrospective of the field. In *Nonconventional and Vernacular Construction Materials* (pp. 37–61). Elsevier. https://doi.org/10.1016/B978-0-08-102704-2.00002-0

Giovannini, J. (2011). Guangzhou Opera House. *Architect*, *100*(5), 217–226.

González Böhme, L. F., Quitral Zapata, F., & Maino Ansaldo, S. (2017). Roboticus tignarius: Robotic reproduction of traditional timber joints for the reconstruction of the architectural heritage of Valparaíso. *Construction Robotics*, *1*(1–4), 61–68. https://doi.org/10.1007/s41693-017-0002-6

Gorgolewski, M. (2008). Designing with reused building components: Some challenges. *Building Research & Information*, *36*(2), 175–188. https://doi.org/10.1080/09613210701559499

Gramazio Kohler Research. (2014). *Acoustic Bricks, ETH Zürich, 2012-2014*: *Non-standard Acoustic Panel System*. https://gramaziokohler.arch.ethz.

ch/web/e/forschung/229.html

Gramazio Kohler Research. (2019). *Augmented Acoustics, Esslingen, 2019: Object-Inertial Tracking for Human Assembly of Acoustic Timber Walls*. https://gramaziokohler.arch.ethz.ch/web/e/projekte/408.html

Gramazio Kohler Research. (2021). *Acoustic Diffusor Panels, Immersive Design Lab, ETH Zurich, 2020-2021.* https://gramaziokohler.arch.ethz.ch/web/e/projekte/429.html

Guindos, P., & Ortiz, J. (2013). The utility of low-cost photogrammetry for stiffness analysis and finite-element validation of wood with knots in bending. *Biosystems Engineering*, *114*(2), 86–96. https://doi.org/10.1016/j.biosystemseng.2012.11.002

Guo, X., Liu, Q., Sharma, R. P., Chen, Q., Ye, Q., Tang, S., & Fu, L. (2021). Tree Recognition on the Plantation Using UAV Images with Ultrahigh Spatial Resolution in a Complex Environment. *Remote Sensing*, *13*(20), 4122. https://doi.org/10.3390/rs13204122

Gürsoy, B., & Özkar, M. (2015). Visualizing making: Shapes, materials, and actions. *Design Studies*, *41*, 29–50. https://doi.org/10.1016/j.destud.2015.08.007

Hannouch, A. (2019). Acoustic Simulation and Conditioning in Vaulted Structures. Proceedings of the 24th International Conference of the Association for Computer-Aided Architectural Design Research in Asia (CAADRIA) 2019, 1, 403–412. http://papers.cumincad.org/data/works/att/caadria2019_398.pdf

Harding, J. (2022). *Biomorpher* [Text]. Food4Rhino. https://www.food4rhino.com/en/app/biomorpher

Harper, E. M., Kavlak, G., Burmeister, L., Eckelman, M. J., Erbis, S., Sebastian Espinoza, V., Nuss, P., & Graedel, T. E. (2015). Criticality of the Geological Zinc, Tin, and Lead Family. *Journal of Industrial Ecology*, *19*(4), 628–644. https://doi.org/10.1111/jiec.12213

Hashim, U. R., Hashim, S. Z., & Muda, A. K. (2015). Automated Vision Inspection of Timber Surface Defect: A Review. *Jurnal Teknologi*, *77*(20). https://doi.org/10.11113/jt.v77.6562

Hill, C. A. S. (2019). The Environmental Consequences Concerning the Use of Timber in the Built Environment. *Frontiers in Built Environment*, *5*, 129. https://doi.org/10.3389/fbuil.2019.00129

Hittawe, M. M., Muddamsetty, S. M., Sidibé, D., & Mériaudeau, F. (2015). Multiple features extraction for timber defects detection and classification using SVM. *2015 IEEE International Conference on Image*

Processing (ICIP), 427–431. https://doi.org/10.1109/icip.2015.7350834

Hoadley, B. (2000). *Understanding wood: A craftsman's guide to wood technology*. Taunton Press.

Hodgson, M. (1999). Experimental investigation of the acoustical characteristics of university classrooms. *The Journal of the Acoustical Society of America*, *106*(4), 1810–1819. https://asa.scitation.org/doi/10.1121/1.427931

Holland, J. H. (1962). Outline for a Logical Theory of Adaptive Systems. *Journal of the ACM*, *9*(3), 297–314. https://doi.org/10.1145/321127.321128

Huang, W., Zhang, Y., & Li, L. (2019). Survey on Multi-Objective Evolutionary Algorithms. *Journal of Physics: Conference Series*, *1288*(1), 012057. https://doi.org/10.1088/1742-6596/1288/1/012057

Hyyppä, J., Virtanen, J.-P., Jaakkola, A., Yu, X., Hyyppä, H., & Liang, X. (2017). Feasibility of Google Tango and Kinect for Crowdsourcing Forestry Information. *Forests*, *9*(1). https://doi.org/10.3390/f9010006

International Electrotechnical Commission. (2020). *IEC 60268-16:2020: Sound system equipment—Part 16: Objective rating of speech intelligibility by speech transmission index*. International Electrotechnical Commission.

Iwamoto, L. (2009). *Digital Fabrications: Architectural and Material Techniques*. Princeton Architectural Press.

Jackson, A., & Day, D. A. (2005). *Collins Complete Woodworkers Manual* (Rev. ed.). Collins GB.

Jenny, D., Mayer, H., Aejmelaeus-Lindström, P., Gramazio, F., & Kohler, M. (2022). A pedagogy of digital materiality: Integrated design and robotic fabrication projects of the master of advanced studies in architecture and digital fabrication. *Architecture, Structures and Construction*. https://doi.org/10.1007/s44150-022-00040-1

Johan, R., Chernyavsky, M., Fabbri, A., Gardner, N., Haeusler, M. H., & Zavoleas, Y. (2019). Building intelligence through Generative Design - Structural analysis and optimisation informed by material performance. *Proceedings of the 24th Conference on Computer Aided Architectural Design Research in Asia (CAADRIA)*, 371–380. https://doi.org/10.52842/conf.caadria.2019.1.371

Johns, R. L., & Anderson, J. (2019). Interfaces for adaptive assembly. *Proceedings of the 38th Annual Conference of the Association for Computer Aided Design in Architecture (ACADIA)*, 126–135. https://doi.org/10.52842/conf.acadia.2018.126

Johns, R. L., Wermelinger, M., Mascaro, R., Jud, D., Gramazio, F., Kohler, M.,

Chli, M., & Hutter, M. (2020). Autonomous dry stone: On-site planning and assembly of stone walls with a robotic excavator. *Construction Robotics*, *4*(3–4), 127–140. https://doi.org/10.1007/s41693-020-00037-6

Karmakar, A., & Delhi, V. S. K. (2021). Construction 4.0: What we know and where we are headed? *Journal of Information Technology in Construction*, *26*, 526–545. https://doi.org/10.36680/j.itcon.2021.028

Kennedy, J., & Eberhart, R. (1995). Particle swarm optimization. In *Proceedings of ICNN'95—International Conference on Neural Networks* (Vol. 4, pp. 1942–1948). IEEE. https://doi.org/10.1109/ICNN.1995.488968

King, M. (2017). How Industry 4.0 and BIM are Shaping the Future of the Construction Environment. *GIM International: The Worldwide Magazine for Geomatics*, *31*(3), 24–25. https://www.gim-international.com/content/article/how-industry-4-0-and-bim-are-shaping-the-future-of-the-construction-environment

Kirkpatrick, S., Gelatt Jr, C. D., & Vecchi, M. P. (1983). Optimization by Simulated Annealing. *Science*, *220*(4598), 671–680. https://doi.org/10.1126/science.220.4598.671

Klinger, K. (2007). Information Exchange in Digitally Driven Architecture. In *Proceedings of the 11th Iberoamerican Congress of Digital Graphics* (pp. 300–304). http://papers.cumincad.org/cgi-bin/works/paper/sigradi2007_af53

Klinger, K. (2008). Relations: Information Exchange in Designing and Making Architecture. In B. Kolarevic & K. Klinger (Eds.), *Manufacturing Material Effects: Rethinking Design and Making in Architecture* (pp. 25–36). Routledge.

Kłosak, A. K. (2020). Design, simulations and experimental research in the process of development of sound absorbing perforated ceiling tile. *Applied Acoustics*, *161*, 107185. https://doi.org/10.1016/j.apacoust.2019.107185

Kolarevic, B. (Ed.). (2003a). A*rchitecture in the Digital Age: Design and Manufacturing*. Spon Press.

Kolarevic, B. (2003b). Digital Morphogenesis. In B. Kolarevic (Ed.), *Architecture in the Digital Age: Design and Manufacturing* (pp. 17–45). Spon Press.

Kolarevic, B. (2003c). Information Master Builders. In B. Kolarevic (Ed.), *Architecture in the Digital Age: Design and Manufacturing* (pp. 88–96). Spon Press.

Kolarevic, B., & Klinger, K. R. (2008). Manufacturing / Material / Effects. In B.

Kolarevic & K. R. Klinger (Eds.), *Manufacturing Material Effects: Rethinking Design and Making in Architecture* (pp. 5–24). Routledge.

Koren, B., & Muller, T. (2017). Digital Fabrication of Non-Standard Sound-Diffusing Panels in the Large Hall of the Elbphilharmonie. In A. Menges, B. Sheil, R. Glynn, & M. Skavara (Eds.), *Fabricate 2017: Rethinking design and construction* (pp. 122–129). UCL Press.

Koskinen, I., Zimmerman, J., Binder, T., Redstrom, J., & Wensveen, S. (2013). Design Research Through Practice: From the Lab, Field, and Showroom. *IEEE Transactions on Professional Communication*, *56*(3), 262–263. https://doi.org/10.1109/TPC.2013.2274109

Kotlarewski, N., Derikvnd, M., Lee, M., & Whiteroad, I. (2019). Machinability Study of Australia's Dominate Plantation Timber Resources. *Forests*, *10*(9), 805.

Kretschmann, D. E., & Hernandez, R. (2006). Grading timber and glued structural members. In *Primary Wood Processing* (pp. 339–390). Springer.

Krieg, O. D., Schwinn, T., & Menges, A. (2016). Integrative Design Computation for Local Resource Effectiveness in Architecture. In F. Wang & M. Prominski (Eds.), *Urbanization and locality* (pp. 123–143). Springer. https://doi.org/10.1007/978-3-662-48494-4_7

Krieg, O. D., Schwinn, T., Menges, A., Li, J.-M., Knippers, J., Schmitt, A., & Schwieger, V. (2015). Biomimetic Lightweight Timber Plate Shells: Computational Integration of Robotic Fabrication, Architectural Geometry and Structural Design. In P. Block, J. Knippers, N. J. Mitra, & W. Wang (Eds.), *Advances in Architectural Geometry 2014* (pp. 109–125). Springer International Publishing. https://doi.org/10.1007/978-3-319-11418-7_8

Lachat, E., Macher, H., Landes, T., & Grussenmeyer, P. (2015). Assessment and Calibration of a RGB-D camera (Kinect v2 Sensor) Towards a Potential Use for Close-Range 3D Modeling. *Remote Sensing*, *7*(12), 13070–13097. https://doi.org/10.3390/rs71013070

Langenbach, R. (2020). 1 - What we learn from vernacular construction. In *Nonconventional and Vernacular Construction Materials* (pp. 1–36). Elsevier. https://doi.org/10.1016/B978-0-08-102704-2.00001-9

Larsen, N. M., & Aagaard, A. K. (2020). Robotic processing of crooked sawlogs for use in architectural construction. *Construction Robotics*, *4*(1–2), 75–83. https://doi.org/10.1007/s41693-020-00028-7

Larsen, N. M., Aagaard, A. K., & Kieffer, L. H. (2020). Digital Workflows for Natural Wood in Constructions. In *Proceedings of the 25th Conference on Computer Aided Architectural Design Research in Asia (CAADRIA)* (Vol. 1, pp.

125–134). https://doi.org/10.52842/conf.caadria.2020.1.125

Le Corbusier. (1970). *Towards a new architecture* (F. Etchells, Trans.). Architectural Press.

Leach, N. (2009). Digital Morphogenesis. *Architectural Design*, *79*(1), 32–37. https://doi.org/10.1002/ad.806

Lefsky, M. A., Cohen, W. B., Parker, G. G., & Harding, D. J. (2002). Lidar Remote Sensing for Ecosystem Studies: Lidar, an emerging remote sensing technology that directly measures the three-dimensional description of plant canopies, can accurately estimate vegetation structural attributes and should be of particular interest to forest, landscape, and global ecologists. *BioScience*, *52*(1). https://doi.org/10.1641/0006-3568(2002)052[0019:LRSFES]2.0.CO;2

Legg, P., Frakes, I., & Gavran, M. (2021). *Australian plantation statistics and log availability report 2021*. Australian Bureau of Agricultural and Resource Economics and Sciences.

Liu, Y., Choi, J., & Napp, N. (2021). Planning for Robotic Dry Stacking with Irregular Stones. In G. Ishigami & K. Yoshida (Eds.), *Springer Proceedings in Advanced Robotics* (pp. 321–335). Springer. https://doi.org/10.1007/978-981-15-9460-1_23

Lombardo, A., Shtrepi, L., & Astolfi, A. (2020). Applicability of multi-objective optimization in classroom acoustics design using analytical and geometrical acoustic models. *Forum Acusticum*, 1605–1608. https://doi.org/10.48465/FA.2020.0782

Lu, Y. (2017). Industry 4.0: A survey on technologies, applications and open research issues. *Journal of Industrial Information Integration*, *6*. https://doi.org/10.1016/j.jii.2017.04.005

Lukacevic, M., Füssl, J., & Eberhardsteiner, J. (2015). Discussion of common and new indicating properties for the strength grading of wooden boards. *Wood Science and Technology*, *49*(3), 551–576. https://doi.org/10.1007/s00226-015-0712-1

Lukacevic, M., Kandler, G., Hu, M., Olsson, A., & Füssl, J. (2019). A 3D model for knots and related fiber deviations in sawn timber for prediction of mechanical properties of boards. *Materials & Design*, *166*, 107617. https://doi.org/10.1016/j.matdes.2019.107617

Lynn, G. (1998). *Folds, Bodies & Blobs: Collected Essays*. La Lettre Volée.

Mack, G. (2018). *Herzog & de Meuron: Elbphilharmonie Hamberg*. Birkhäuser Verlag.

Makki, M. (2019). *Urban Variation Through Evolutionary Development:*

Evolutionary Processes in Design and the Impact of Multi-Objective Evolutionary Algorithms Generating Urban Form [Doctoral Thesis, The Open University]. https://doi.org/10.21954/ou.ro.00010b42

Makki, M., Showkatbakhsh, M., & Song, Y. (2022). *Wallacei: Evolutionary Engine for Grasshopper3D*. Wallacei. https://www.wallacei.com

Malki, A. A., Rizk, M. M., El-Shorbagy, M. A., & Mousa, A. A. (2016). Identifying the most significant solutions from pareto front using hybrid genetic k-means approach. *International Journal of Applied Engineering Research*, *11*(14), 8298–8311.

Mans, D. (2017, October 16). *Aviary* [Text]. Food4Rhino. https://www.food4rhino.com/en/app/aviary

Marshall, C. (2010). A Research Design for Studio-Based Research in Art. *Teaching Artist Journal*, *8*(2), 77–87. https://doi.org/10.1080/15411791003618597

Martin, T., Svilans, T., Gatz, S., & Ramsgaard Thomsen, M. (2021). Timber elements with graded performances through digital forest to timber workflows. In *Proceedings of IASS Annual Symposia* (Vol. 2020, pp. 395–407). International Association for Shell and Spatial Structures (IASS).

Maskuriy, R., Selamat, A., Ali, K. N., Maresova, P., & Krejcar, O. (2019). Industry 4.0 for the Construction Industry - How ready is the Industry? *Applied Sciences*, *9*(14), 2819.

McMullin, P. W., & Price, J. S. (2017). *Timber Design*. Routledge.

McPhee, M. J., Walmsley, B. J., Skinner, B., Littler, B., Siddell, J. P., Cafe, L. M., Wilkins, J. F., Oddy, V. H., & Alempijevic, A. (2017). Live animal assessments of rump fat and muscle score in Angus cows and steers using 3-dimensional imaging. *Journal of Animal Science*, 95(4), 1847. https://pubmed.ncbi.nlm.nih.gov/28464097/

Mealings, K. (2016). Classroom acoustic conditions: Understanding what is suitable through a review of national and international standards, recommendations, and live classroom measurements. *2nd Australasian Acoustical Societies Conference, ACOUSTICS 2016*, 1047–1056. https://www.acoustics.asn.au/conference_proceedings/AASNZ2016/papers/p145.pdf

Means, J. E., Acker, S. A., Fitt, B. J., Renslow, M., Emerson, L., & Hendrix, C. J. (2000). Predicting forest stand characteristics with airborne scanning lidar. *Photogrammetric Engineering and Remote Sensing*, *66*(11), 1367–

1372.

MechSoft. (2021). *VisualCAD/CAM*. https://mecsoft.com/visualcadcam/

Menges, A. (2008). Integral formation and materialisation: Computational form and material gestalt. In B. Kolarevic & K. R. Klinger (Eds.), *Manufacturing material effects: Rethinking design and making in architecture* (pp. 195–210). Routledge.

Menges, A. (2015). Fusing the Computational and the Physical: Towards a Novel Material Culture. *Architectural Design*, *85*(5), 8–15. https://doi.org/10.1002/ad.1947

Menges, A. (2016). Computational Material Culture. *Architectural Design*, *86*(2), 76–83. https://doi.org/10.1002/ad.2027

Menges, A., Schwinn, T., & Krieg, O. D. (Eds.). (2017). *Advancing Wood Architecture: A Computational Approach*. Routledge.

Microsoft. (2022). *Kinect for Windows*. https://learn.microsoft.com/en-us/windows/apps/design/devices/kinect-for-windows

Migayrou, F. (2014). The orders of the non-standard: Towards a critical structuralism. In R. Oxman & R. Oxman, *Theories of the digital in architecture* (pp. 17–34). Routledge.

Miller, R. B. (2012). Structure and function of wood. In R. Rowell (Ed.), *Handbook of Wood Chemistry and Wood Composites* (2nd ed., pp. 10–32).

Mishra, A., Humpenöder, F., Churkina, G., Reyer, C. P. O., Beier, F., Bodirsky, B. L., Schellnhuber, H. J., Lotze-Campen, H., & Popp, A. (2022). Land use change and carbon emissions of a transformation to timber cities. *Nature Communications*, *13*(1), 4889. https://doi.org/10.1038/s41467-022-32244-w

Mitsuhashi, K., Poussa, M., & Puttonen, J. (2008). Method for predicting tension capacity of sawn timber considering slope of grain around knots. *Journal of Wood Science*, *54*(3), 189–195. https://doi.org/10.1007/s10086-007-0941-5

Mollica, Z. (2016). *Tree Fork Truss: An Architecture of Inherent Forms* [Masters Thesis, Architecture Association]. https://zacharymolli.ca/assets/download/Mollica-DMThesis-Tree-Fork-Truss-an-Architecture-of-Inherent-Forms.pdf

Mollica, Z., & Self, M. (2016). Tree Fork Truss: Geometric Strategies for Exploiting Inherent Material Form. *Advances in Architectural Geometry 2015*, 138–153. https://doi.org/10.3218/3778-4_11

Monier, V., Bignon, J. C., & Duchanois, G. (2013). Use of Irregular Wood Components to Design Non-Standard Structures. *Advanced Materials*

Research, *671–674*, 2337–2343. https://doi.org/10.4028/www.scientific.net/AMR.671-674.2337

Morel, P. (2019). The Origins of Discretism: Thinking Unthinkable Architecture. *Architectural Design*, *89*(2), 14–21. https://doi.org/10.1002/ad.2407

Mork, J. H., Luczkowski, M., Dyvik, S. H., Manum, B., & Rønnquist, A. (2016). Generating timber truss bridges – Examining the potential of an interdisciplinary parametric framework for architectural engineering. In *IABSE Congress Reports* (pp. 368–376). https://doi.org/10.2749/stockholm.2016.0345

Muratovski, G. (2021). *Research for Designers: A Guide to Methods and Practice*. SAGE.

Nedjah, N., & Mourelle, L. de M. (2015). Evolutionary multi-objective optimisation: a survey. *International Journal of Bio-Inspired Computation*, *7*(1), 1. https://doi.org/10.1504/IJBIC.2015.067991

Negro, F., Cremonini, C., Properzi, M., & Zanuttini, R. (2010). Sound absorption coefficient of perforated plywood: An experimental case study. *Negro, F., Cremonini, C., Properzi, M., & Zanuttini, R. (2010). Sound Absorption Coefficiet of Perforated Plywood: An Experimental Case Study. In 11th World Conference on Timber Engineering-WCTE 2010*, *3*, 587–588.

Ness, D. A., & Xing, K. (2017). Toward a Resource-Efficient Built Environment: A Literature Review and Conceptual Model. *Journal of Industrial Ecology*, *21*(3), 572–592. https://doi.org/10.1111/jiec.12586

Newman, C. (2019). *Tarsier* [Text]. Food4Rhino. https://www.food4rhino.com/en/app/tarsier

Newnham, G. J., Armston, J. D., Calders, K., Disney, M. I., Lovell, J. L., Schaaf, C. B., Strahler, A. H., & Danson, F. M. (2015). Terrestrial Laser Scanning for Plot-Scale Forest Measurement. *Current Forestry Reports*, *1*(4), 239–251. https://link.springer.com/article/10.1007/s40725-015-0025-5

Nolan, G., Greaves, B., Washusen, R., Jennings, S., & Parsons, M. (2005). *Eucalypt plantations for solid wood products in Australia—A review. 'If you don't prune it, we can't use it'* (PN04.3002). Forest & Wood Products Research and Development Corporation.

Nordmark, U. (2002). Knot Identification from CT Images of Young Pinus sylvestris Sawlogs Using Artificial Neural Networks. *Scandinavian Journal of Forest Research*, *17*(1), 72–78. https://doi.org/10.1080/028275802317221109

Odeon A/S. (2022). *Odeon: Room Acoustic Software*. Odeon: Room Acoustics

Software. https://odeon.dk/

Pangh, H., Hosseinabadi, H. Z., Kotlarewski, N., Moradpour, P., Lee, M., & Nolan, G. (2019). Flexural performance of cross-laminated timber constructed from fibre-managed plantation eucalyptus. *Construction and Building Materials*, *208*, 535–542. https://doi.org/10.1016/j.conbuildmat.2019.03.010

Parigi, D., Svidt, K., Molin, E., & Bard, D. (2017). Parametric Room Acoustic Workflows: Review and future perspectives. *Proceedings of the 35th Annual Conference of the Association for Computer Aided Design in Architecture*, *2*, 603–609. https://doi.org/10.52842/conf.ecaade.2017.2.603

Patel, P. (2020). *Architectural Acoustics: A guide to integrated thinking.* RIBA.

Peters, B., Burry, J., Williams, N., & Davis, D. (2013). Hubpod: Integrating Acoustic Simulation in Architectural Design Workflows. *Proceedings of the Symposium on Simulation for Architecture & Urban Design*, 1–9. https://www.researchgate.net/publication/262236839_HubPod_Integrating_Acoustic_Simulation_in_Architectural_Design_Workflows

Pfeiffer, S. (Ed.). (2017). *Interlocking Digital and Material Cultures*. AADR (Spurbuchverlag).

Pickin, J., Wardle, C., O'Farrell, K., Nyunt, P., & Donovan, S. (2020). *National Waste Report 2020*. Department of Agriculture, Water and the Environment.

Piter, J. C., Zerbino, R. L., & Blaß, H. J. (2004). Machine strength grading of Argentinean *Eucalyptus grandis*. *Holz Als Roh- Und Werkstoff*, *62*(1), 9–15. https://doi.org/10.1007/s00107-003-0434-1

Pölzleitner, W., & Schwingshakl, G. (1992). Real-time surface grading of profiled wooden boards. *Industrial Metrology*, *2*(3–4), 283–298. https://doi.org/10.1016/0921-5956(92)80008-H

Preisinger, C. (2013). Linking Structure and Parametric Geometry. *Architectural Design*, *83*(2), 110–113. https://doi.org/10.1002/ad.1564

Preisinger, C. (2022). *The official guide to using Karamba3D 2.2.0*. https://manual.karamba3d.com/

Preisinger, C., & Heimrath, M. (2014). Karamba: A Toolkit for Parametric Structural Design. *Structural Engineering International*, *24*(2), 217–221. https://doi.org/10.2749/101686614X13830790993483

Pryda. (2022). *Pryda Flooring Systems*. Pryda. https://pryda.com.au/for-builders/flooring-systems/

Rainer, H. (2014). Introduction. In S. Jeska & K. S. Pascha (Eds.), *Emergent Timber Technologies: Materials, Structures, Engineering, Projects* (pp. 6–7).

Birkhäuser.

Rais, A., Ursella, E., Vicario, E., & Giudiceandrea, F. (2017). The use of the first industrial x-ray CT scanner increases the lumber recovery value: Case study on visually strength-graded Douglas-fir timber. *Annals of Forest Science*, *74*(2). https://doi.org/10.1007/s13595-017-0630-5

Ramsgaard Thomsen, M., Nicholas, P., Tamke, M., Gatz, S., & Sinke, Y. (2019). Predicting and steering performance in architectural materials. In *ECAADe: Architecture in the Age of the 4th Industrial Revolution* (pp. 485–494). https://doi.org/10.5151/proceedings-ecaadesigradi2019_150

Ramsgaard Thomsen, M., Nicholas, P., Tamke, M., Gatz, S., Sinke, Y., & Rossi, G. (2020). Towards machine learning for architectural fabrication in the age of industry 4.0. *International Journal of Architectural Computing*, *18*(4), 335–352. https://doi.org/10.1177/1478077120948000

Ramsgaard Thomsen, M., Nicholas, P., Tamke, M., & Svilans, T. (2021). A New Material Vision. In F. Melendez, N. Diniz, & M. Del Signore, *Data, Matter, Design: Strategies in Computational Design* (1st ed., pp. 121–129). Routledge. https://doi.org/10.4324/9780367369156-54

Ramsgaard Thomsen, M., & Tamke, M. (2022). Towards a transformational eco-metabolistic bio-based design framework in architecture. *Bioinspiration & Biomimetics*, *17*(4), 045005. https://doi.org/10.1088/1748-3190/ac62e2

Rastrigin, L. (1963). The convergence of the random search method in the external control of a many parameter system. *Automaton & Remote Control*, *24*, 1337–1342. https://doi.org/10.1007/978-1-4939-1384-8_10

Rechenberg, I. (1965). Cybernetic Solution Path of an Experimental Problem [Technical Report Library Translation No. 1122]. *Royal Aircraft Establishment Library*.

Robeller, C., & Von Haaren, N. (2020). Recycleshell: Wood-Only Shell Structures Made From Cross-Laminated Timber (CLT) Production Waste. *Journal of the International Association for Shell and Spatial Structures*, *61*(2), 125–139. https://doi.org/10.20898/j.iass.2020.204.045

Robert McNeel & Associates. (2021). *Rhinoceros*. www.Rhino3d.Com. https://www.rhino3d.com

Robert McNeel & Associates. (2022). *Grasshopper*. https://www.grasshopper3d.com/

Royal Danish Academy. (2022, April 27). *RawLam*. https://royaldanishacademy.com/case/rawlam

Ruan, G., Filz, G. H., & Fink, G. (2021). An integrated architectural and

structural design concept by using local, salvaged timber. *IASS Annual Symposium 2020/21 & The 7th International Conference on Spatial Structures: Inspiring the Next Generation Guilford, UK*. https://www.researchgate.net/publication/354096064_An_integrated_architectural_and_structural_design_concept_by_using_local_salvaged_timber

Rust, R., Xydis, A., Frick, C., Strauss, J., Junk, C., Feringa, J., Gramazio, F., & Kohler, M. (2021). Computational Design and Evaluation of Acoustic Diffusion Panels for the Immersive Design Lab—An acoustic design case study. In *Proceedings of the 39th International Conference on Education and Research in Computer Aided Architectural Design in Europe (eCAADe)* (pp. 515–52410). https://doi.org/10.52842/conf.ecaade.2021.1.515

Rust, R., Xydis, A., Heutschi, K., Casas, G., Du, C., Strauss, J., Eggenschwiler, K., Perez-Cruz, F., Gramazio, F., & Kohler, M. (2021). A data acquisition setup for data driven acoustic design. *Building Acoustics*, *28*(4), 345–360. https://doi.org/10.1177/1351010X20986901

Sakagami, K., Kobatake, S., Kano, K., Morimoto, M., & Yairi, M. (2011). Sound absorption characteristics of a single microperforated panel absorber backed by a porous absorbent layer. *Acoustics Australia*, *39*(3), 95–100. http://www.acoustics.asn.au/journal/2011/2011_39_3_Sakagami.pdf

Satheesh Kumar Reddy, P., & Nagaraju, C. (2019). Structural Optimization of Different Truss Members Using Finite Element Analysis for Minimum Weight. *International Journal of Mechanical and Production Engineering Research and Development*, *9*(4), 99–110. https://doi.org/10.24247/ijmperdaug201911

Sawhney, A., Riley, M., & Irizarry, J. (Eds.). (2020). *Construction 4.0: An Innovation Platform for the Built Environment*. Routledge.

Schwinn, T., Krieg, O. D., & Menges, A. (2013). Robotically Fabricated Wood Plate Morphologies. In S. Brell-Çokcan & J. Braumann (Eds.), *Rob|Arch 2012* (pp. 48–61). Springer Vienna. https://doi.org/10.1007/978-3-7091-1465-0_4

Schwinn, T., & Menges, A. (2015). Fabrication Agency: Landesgartenschau Exhibition Hall. *Architectural Design*, *85*(5), 92–99. https://doi.org/10.1002/ad.1960

SCM Group. (2022). *Maestro Digital System*. https://www.scmgroup.com/en/scmwood/products/maestro-digital-systems

Self, M. (2017). Hooke Park: Application for Timber in its Natural Form. In A. Menges, T. Schwinn, & O. D. Krieg (Eds.), *Advancing Wood Architecture: A Computational Approach* (pp. 141–153). Routledge.

Self, M., & Vercruysse, M. (2017). Infinite Variations, Radical Strategies. In A.

Menges, B. Sheil, R. Glynn, & M. Skavara (Eds.), *Fabricate 2017: Rethinking Design and Construction* (pp. 30–35). UCL Press.

Sheil, B., & Ramsgaard Thomsen, M. (2020). Perspectives: Transactions and Trajectories. In B. Sheil, M. Ramsgaard Thomsen, M. Tamke, & S. Hanna (Eds.), *Design Transactions: Rethinking Information Modelling for a New Material Age* (pp. 30–39). UCL Press.

Sheil, B., Thomsen, M. R., Tamke, M., & Hanna, S. (Eds.). (2020). *Design Transactions: Rethinking Information Modelling for a New Material Age*. UCL Press. https://doi.org/10.2307/j.ctv13xprf6

Shelbourne, C. J. A., Nicholas, I. D., McKinley, R. B., Low, C. B., McConnochie, R. M., & Lausberg, M. J. F. (2002). Wood density and internal checking of young Eucalyptus nitens in New Zealand as affected by site and height up the tree. *New Zealand Journal of Forestry Science*, *32*(3), 357–385. https://www.scionresearch.com/__data/assets/pdf_file/0006/59253/nzjfs-323-2002-shelbourne-357-385.pdf

Shooshtarian, S., Maqsood, T., Caldera, S., & Ryley, T. (2022). Transformation towards a circular economy in the Australian construction and demolition waste management system. *Sustainable Production and Consumption*, *30*, 89–106. https://doi.org/10.1016/j.spc.2021.11.032

Showkatbakhsh, M., & Makki, M. (2022). Multi-Objective Optimisation of Urban Form: A Framework for Selecting the Optimal Solution. *Buildings*, *12*(9), 1473. https://doi.org/10.3390/buildings12091473

Siebein, G. W., Gold, M. A., Siebein, G. W., & Ermann, M. G. (2000). Ten Ways to Provide a High-Quality Acoustical Environment in Schools. *Language, Speech, and Hearing Services in Schools*, *31*(4), 376–384. https://doi.org/10.1044/0161-1461.3104.376

Søndergaard, A., Amir, O., Eversmann, P., Piskorec, L., Stan, F., Gramazio, F., & Kohler, M. (2016). Topology Optimization and Robotic Fabrication of Advanced Timber Space-Frame Structures. In D. Reinhardt, R. Saunders, & J. Burry (Eds.), *Robotic Fabrication in Architecture, Art and Design 2016* (pp. 190–203). Springer International Publishing. https://doi.org/10.1007/978-3-319-26378-6_14v

Souza, C. R. (2014). "*Accord.NET Learning Framework*". http://accord-framework.net/

Spoliansky, R., Edan, Y., Parmet, Y., & Halachmi, I. (2016). Development of automatic body condition scoring using a low-cost 3-dimensional Kinect camera. *Journal of Dairy Science*, *99*(9), 7714–7725. https://doi.org/10.3168/jds.2015-10607

Standards Australia. (1997). *AS/NZS 4491: Timber - Glossary of terms in*

timber-related standards. Standards Australia.

Standards Australia. (A002). *AS/NZS 1170.1-2002: Structural design actions permanent, imposed and other actions*. Standards Australia International.

Standards Australia. (2006). *AS 1720.2: Timber structures and properties*. Standards Australia.

Standards Australia. (2007). *AS 2082-2007: Timber Hardwood - Visually stress-graded for structural purposes*. Standards Australia.

Standards Australia. (2010). *AS/NZS 4063: Characterisation of structural timber*. Standards Australia.

Standards Australia. (2015). *AS 1720.1 Timber structures. Part 1: Design methods*. http://digital-library.canterbury.ac.nz/resources/campus/AS-1720_1-2010-Standard/FC000000460.pdf

Standards Australia. (2016). *AS/NZS 2460-2002: R2016 Acoustics - Measurement of the reverberation time in rooms*. Standards Australia International; Standards New Zealand.

Stanton, C. (2010). Digitally Mediated Use of Localized Material in Architecture. *Proceedings of the 14th Congress of the Iberoamerican Society of Digital Graphics*, 228–231. http://papers.cumincad.org/data/works/att/sigradi2010_228.content.pdf

Svilans, T. (2020). *Integrated material practice in free-form timber structures* [Doctoral Thesis, Royal Danish Academy]. https://discovery.ucl.ac.uk/id/eprint/10121947

Svilans, T. (2021a). GluLamb: A toolkit for early-stage modelling of free-form glue-laminated timber structures. In *Proceedings of the 2021 European Conference on Computing in Construction* (pp. 373–380). https://doi.org/10.35490/ec3.2021.194

Svilans, T. (2021b). *Umeå 01 (RawLam 3)*. Tom Svilans: Architecture + Computation + Fabrication. http://tomsvilans.com/#umea01

Svilans, T., Poinet, P., Tamke, M., & Ramsgaard Thomsen, M. (2017). A Multi-Scalar Approach for the Modelling and Fabrication of Free-Form Glue-Laminated Timber Structures. In *Humanizing digital reality: Design modelling symposium Paris 2017* (pp. 247–257). https://doi.org/10.1007/978-981-10-6611-5_22

Svilans, T., Runberger, J., & Strehlke, K. (2020). Agency of Material Production Feedback in Architectural Practice. In B. Sheil, M. Ramsgaard Thomsen, M. Tamke, & S. Hanna (Eds.), *Design Transactions: Rethinking Information Modelling for a New Material Age* (pp. 84–91). UCL Press.

Svilans, T., Tamke, M., Ramsgaard Thomsen, M., Runberger, J., Strehlke, K.,

& Antemann, M. (2019). New Workflows for Digital Timber. In F. Bianconi & M. Filippucci (Eds.), *Digital Wood Design* (pp. 93–134). Springer. https://doi.org/10.1007/978-3-030-03676-8_3

Swann, C. (2002). Action Research and the Practice of Design. *Design Issues*, *18*(1), 49–61. https://doi.org/10.1162/07479360252756287

Synge, E. H. (1930). XCI. A method of investigating the higher atmosphere. *The London, Edinburgh, and Dublin Philosophical Magazine and Journal of Science*, *9*(60), 1014–1020. https://doi.org/10.1080/14786443008565070

Talbot, B., & Astrup, R. (2021). A review Of Sensors, Sensor-Platforms and Methods Used in 3D Modelling of Soil Displacement after Timber Harvesting. *Croatian Journal of Forest Engineering*, *42*(1), 149–164. https://crojfe.com/archive/volume-42-no.1/a-review-of-sensors-sensor-platforms-and-methods-used-in-3d-modelling-of-soil-displacement-after-timber-harvesting/

Tam, M., Bergis, L., Naicu, D., De Rycke, K., Orlinski, A., & Jankowska, E. (2017, September 6). Intelligent Fabrication—Digital Bridges. *Footbridge 2017 Berlin - Tell A Story: Conference Proceedings 6-8.9.2017 TU-Berlin*. https://doi.org/10.24904/footbridge2017.10515

Tamke, M., Nicholas, P., Ayres, P., & Thomsen, M. (2013). Investigating a new material practice. In P. Cruz (Ed.), *Structures and Architecture* (pp. 693–703). CRC Press. https://doi.org/10.1201/b15267-98

Tamke, M., Nicholas, P., & Zwierzycki, M. (2018). Machine learning for architectural design: Practices and infrastructure. *International Journal of Architectural Computing*, *16*(2), 123–143. https://doi.org/10.1177/1478077118778580

Tasmanian Timber. (2019). T*imber products use less energy.* https://tasmaniantimber.com.au/wp-content/uploads/2019/09/Timber-Products-Use-Less-Energy-200530.pdf

Taylor, J., Mann, R., Reilly, M., Warnken, M., Pincic, D., & Death, D. (2005). *Recycling and End-of-Life Disposal of Timber Products* (p. 141). Forest and Wood Products Research and Development Corporation.

Taylor, J., & Warnken, M. (2008). *Wood recovery and recycling: A source book for Australia.* Forest and Wood Products Australia.

Terzidis, K. (2006). *Algorithmic Architecture* (1st ed.). Architectural Press.

The Boston Consulting Group. (2015). *Industry 4.0: The Future of Productivity and Growth in Manufacturing Industries*. https://www.bcg.com/publications/2015/engineered_products_project_business_industry_4_

future_productivity_growth_manufacturing_industries

Thomas, K. L. (2007). *Material Matters: Architecture and Material Practice*. Routledge.

United Nations. (2015). *The 17 Goals | Sustainable Development*. https://sdgs.un.org/goals

United Nations: Department of Economic and Social Affairs. (2022). *World population prospects 2022: Summary of results*. United Nations.

United Nations: Environment Program. (2022). *Global Status Report for Buildings and Construction: Towards a Zero-Emissions, Efficient and Resilient Buildings and Construction Sector*. United Nations Environment Program.

United Nations Environment Program. (2014). *Sand, Rarer than One Thinks: UNEP Global Environmental Alert Service (GEAS)*. https://wedocs.unep.org/20.500.11822/8665

United Nations Framework Convention on Climate Change. (2016). *The Paris Agreement - A Publication*. https://unfccc.int/documents/184656

uto. (2020). *Food4Rhino: FlowL*. https://www.food4rhino.com/en/app/flowl

Valero, A., & Valero, A. (2010). Physical geonomics: Combining the exergy and Hubbert peak analysis for predicting mineral resources depletion. *Resources, Conservation and Recycling*, *54*(12), 1074–1083. https://doi.org/10.1016/j.resconrec.2010.02.010

van der Harten, A. (2013). Pachyderm Acoustical Simulation: Towards Open-Source Sound Analysis. *Architectural Design*, *83*(2), 138–139. https://doi.org/10.1002/ad.1570

van der Harten, A. (2014, July 26). Food4Rhino: *Pachyderm Acoustical Simulation* [Text]. https://www.food4rhino.com/en/app/pachyderm-acoustical-simulation

van der Harten, A. (2015). *Application of the Transfer Matrix and Finite Surface Size Correction to Room Acoustics Simulation*. 5. https://www.conforg.fr/euronoise2015/proceedings/data/articles/000495.pdf

van der Harten, A. (2020). *Open Research in Acoustical Science and Education*. GitHub. https://github.com/PachydermAcoustic

Vasey, L., & Menges, A. (2020). Potentials of cyber-physical systems in architecture and construction. In A. Sawhney, M. Riley, & J. Irizarry (Eds.), *Construction 4.0* (1st ed., pp. 90–112). Routledge. https://doi.org/10.1201/9780429398100-5

Vierlinger, R. (2018). *Octopus* [Text]. https://www.food4rhino.com/en/app/

octopus

Volz, M. (2004). The Anatomy of Wood: The Material. In T. Herzog, J. Natterer, R. Schweizer, M. Volz, & W. Winter (Eds.), *Timber Construction Manual* (pp. 31–36). Birkhäuser. https://doi.org/10.11129/detail.9783034614634

Vomhof, M., Vasey, L., Aramazio, F., Kohler, M., Bräuer, S., & Eggenschwiler, K. (2014). Robotic Fabrication of acoustic Brick Walls. *Proceedings of the 34th Annual Conference of the Association for Computer Aided Design in Architecture (ACADIA)*. https://doi.org/10.52842/conf.acadia.2014.555

Walker, J. C. F., Butterfield, B. G., Harris, J. M., Langrish, T. A. G., & Uprichard, J. M. (1993). *Primary Wood Processing: Principles and practice*. Springer.

Walker, R. (1990). *The design and application of modular acoustic diffusing elements*. BBC Research Department.

Walton, J. (1990). *Woodwork In Theory And Practice* (2nd ed.). Adult Original - Trade.

Wandinger, U. (2005). Introduction to Lidar. In *Springer Series in Optical Sciences* (pp. 1–18). https://doi.org/10.1007/0-387-25101-4_1

Warmuth, J., Brütting, J., & Fivet, C. (2020). Computational tool for stock-constrained design of structures. In *Proceedings of IASS Annual Symposia*. International Association for Shell and Spatial Structures (IASS). https://www.ingentaconnect.com/contentone/iass/piass/2020/00002020/00000017/art00002

Warmuth, J., Brütting, J., & Fivet, C. (2021). *Phoenix3D*. EPFL. http://sxl.epfl.ch/Phoenix3D

Washusen, R., Harwood, C., Morrow, A., Northway, R., Valencia, J. C., Volker, P., Wood, M., & Farrell, R. (2009). Pruned plantation-grown *Eucalyptus nitens*: Effect of thinning and conventional processing practices on sawn board quality and recovery. *New Zealand Journal of Forestry Science*, *39*(1), 39–55. https://www.scionresearch.com/__data/assets/pdf_file/0007/60487/NZJFS-39200939-55_WASHUSEN.pdf

Weisstein, E. W. (2022). *Runge-Kutta Method* [Text]. MathWorld--A Wolfram Web Resource; Wolfram Research, Inc. https://mathworld.wolfram.com/Runge-KuttaMethod.html

Williams, N. (2017). *Plugin practice: recasting modularity for architects* [Doctoral Thesis, RMIT]. https://researchrepository.rmit.edu.au/esploro/outputs/9921863816301341

Willmann, J., Knauss, M., Bonwetsch, T., Apolinarska, A. A., Gramazio, F., & Kohler, M. (2016). Robotic timber construction—Expanding additive fabrication to new dimensions. *Automation in Construction*, *61*, 16–23.

https://doi.org/10.1016/j.autcon.2015.09.011

Wood Solutions. (2017, August 8). *Visual stress-grading*. Wood Solutions. https://www.woodsolutions.com.au/visual-stress-grading

Wotherspoon, K. P. (2008). Forest health surveillance in Tasmania. *Australian Forestry*, *71*(3), 182–187. https://doi.org/10.1080/00049158.2008.10675033

Wright, O., Perkins, N., Donn, M., & Halstead, M. (2016). Parametric implementation of café acoustics. *Proceedings of Acoustics 2016*, 1–6. https://acoustics.asn.au/conference_proceedings/AASNZ2016/papers/p13.pdf

Wu, K., & Kilian, A. (2016). Developing Architectural Geometry Through Robotic Assembly and Material Sensing. In D. Reinhardt, R. Saunders, & J. Burry (Eds.), *Robotic Fabrication in Architecture, Art and Design 2016* (pp. 240–249). Springer International Publishing. https://doi.org/10.1007/978-3-319-26378-6_18

Wu, K., & Kilian, A. (2018). Designing Natural Wood Log Structures with Stochastic Assembly and Deep Learning. In J. Willmann, P. Block, M. Hutter, K. Byrne, & T. Schork (Eds.), *Robotic Fabrication in Architecture, Art and Design 2018* (pp. 16–30). Springer International Publishing. https://doi.org/10.1007/978-3-319-92294-2_2

Ximenes, F., & Gardner, W. D. (2005). *Production and Use of Forest Products in Australia*. NSW Department of Primary Industries. http://rgdoi.net/10.13140/RG.2.1.1593.5527

Ximenes, F., Kapambwe, M., & Keenan, R. (2008). *Timber Use in Residential Construction and Demolition* (BEDP Environment Design Guide, pp. 1–8). https://www.jstor.org/stable/26148968

Xu, C., Manley, B., & Morgenroth, J. (2018). Evaluation of modelling approaches in predicting forest volume and stand age for small-scale plantation forests in New Zealand with RapidEye and LiDAR. *International Journal of Applied Earth Observation and Geoinformation*, *73*, 386–396. https://doi.org/10.1016/j.jag.2018.06.021

Xu, X., Wang, H., Sun, Y., Han, J., & Huang, R. (2018). Sound absorbing properties of perforated composite panels of recycled rubber, fiberboard sawdust, and high density polyethylene. *Journal of Cleaner Production*, *187*, 215–221. https://doi.org/10.1016/j.jclepro.2018.03.174

Yang, L., & Liu, H. (2018). A review of Eucalyptus wood collapse and its control during drying. *BioResources*, *13*(1), 2171–2181. https://doi.

org/10.15376/biores.13.1.Yang

Zhang, Y. (2021). Geographical spatial distribution and productivity dynamic change of eucalyptus plantations in China. *Scientific Reports*, *11*(1), 1–1515. https://doi.org/10.1038/s41598-021-97089-7